RADC-TR-90-381
Final Technical Report
December 1990

COHERENT FIBER OPTIC LINKS

PCO Inc.

B.T. Debney, J. Hankey, P. Johnson, J. Buus

APPROVED FOR PUBLIC RELEASE; DISTRIBUTION UNLIMITED.

Rome Air Development Center
Air Force Systems Command
Griffiss Air Force Base, NY 13441-5700

This report has been reviewed by the RADC Public Affairs Office (PA) and is releasable to the National Technical Information Service (NTIS). At NTIS it will be releasable to the general public, including foreign nations.

RADC TR-90-381 has been reviewed and is approved for publication.

APPROVED:

Paul Sierak

PAUL SIERAK
Project Engineer

APPROVED:

John A. Graniero

JOHN A. GRANIERO, Technical Director
Directorate of Communications

FOR THE COMMANDER:

B. G. Oaks

BILLY G. OAKS
Directorate of Plans and Programs

If your address has changed or if you wish to be removed from the RADC mailing list, or if the addressee is no longer employed by your organization, please notify RADC (DCLW) Griffiss AFB NY 13441-5700, This will assist us in maintaining a current mailing list.

Do not return copies of this report unless contractual obligations or notices on a specific document requires that it be returned.

REPORT DOCUMENTATION PAGE

Form Approved
OPM No. 0704-0188

1 AGENCY USE ONLY *(Leave Blank)*	2. REPORT DATE	3. REPORT TYPE AND DATES COVERED
	December 1990	Final

4. TITLE AND SUBTITLE
COHERENT FIBER OPTIC LINKS

5. FUNDING NUMBERS
C - F30602-86-C-0004
PE - 62702F
PR - 4519
TA - 21
WU - 65

6. AUTHOR(S)
B.T.Debney
J. Hankey
P. Johnson
J. Buus

7. PERFORMING ORGANIZATION NAME(S) AND ADDRESS(ES)
PCO Inc.
20200 Sunburst St.
Chatsworth CA 91311-6289

8. PERFORMING ORGANIZATION REPORT NUMBER
N/A

9. SPONSORING/MONITORING AGENCY NAME(S) AND ADDRESS(ES)
Rome Air Development Center (DCLW)
Griffiss AFB NY 13441-5700

10. SPONSORING/MONITORING AGENCY REPORT NUMBER
RADC-TR-90-381

11. SUPPLEMENTARY NOTES
RADC Project Engineer: Paul Sierak/(DCLW)/(315) 330-4092

12a. DISTRIBUTION/AVAILABILITY STATEMENT
Approved for public release; distribution unlimited.

12b. DISTRIBUTION CODE

13. ABSTRACT *(Maximum 200 words)*

This report contains the results of the development and testing of a digital coherent fiber optic link and a separate analog coherent fiber optic link. The issues of realizable performance, cost and complexity of implementation and device tolerances are covered for each within a theoretical framework. The digital coherent fiber optic link was one of only two nearly simultaneously appearing 19-inch rack mountable systems in the world. The analog coherent fiber optic link is the first of its kind in the world and new ground is covered in theoretical analysis. In addition, the self heterodyne/homodyne concept is described and experimental results are shown.

14. SUBJECT TERMS
Communications
Fiber Optics
Coherent
Digital
Analog

15. NUMBER OF PAGES
214

16. PRICE CODE

17. SECURITY CLASSIFICATION OF REPORT	18. SECURITY CLASSIFICATION OF THIS PAGE	19. SECURITY CLASSIFICATION OF ABSTRACT	20. LIMITATION OF ABSTRACT
UNCLASSIFIED	UNCLASSIFIED	UNCLASSIFIED	UL

Evaluation

The area of coherent fiber optic communications systems has been evolving recently at a rapid pace. This is no doubt driven by its promise of performance advantage over the conventional intensity modulated direct detection architecture in use today. In the area of digital signal transmission the promise of reducing the amount of power required at the receiver in the 10db range, depending upon modulation/detection format, is significant.

The channel packing or channel density advantage in which one channel is local oscillator selectable at the receiver,is also inherent to these architectures and significant. This implies that digital coherent architectures are serious contenders in the point to point and most significantly high channel capacity network arenas. The work in this contract extended the art in that the coherent system was transitioned from the laboratory optical bench to a engineered 19 inch rack mounted system.

In the analog area the work presented here is a first in theoretical characterization and the RF system delivered is the first of its kind in the world. The very narrow domain of performance advantage for coherent analog over conventional indicates that from the point of view of reduced required power a conventional system is better. The aspects of signal fidelity despite the low realizable signal to noise ratio bear further exploration. In addition direct frequency modulation of the optical source output for extension of analog communication link input signal dynamic range is also left for further exploitation. This is a robust area with much application potential even in non communications areas and the work presented represents a significant step in its evolution.

Paul Sierak

PAUL SIERAK
Program Manager

CONTENTS

1. OBJECTIVE

The objective of the programme 'Coherent Fibre Optic Links' as indicated in the statement of work is to:

"... assess the performance attainable by experimental models of simplex fiber optic communication links which employ coherent demodulation in the optical receiver for both digital and analog modulation formats. The digital binary link will operate towards providing a data transfer rate of 20 Mb/s while the narrow band analog coherent link will operate at a selected input radio frequency carrier signal in the 1 to 10 GHz range."

2. EXECUTIVE SUMMARY

This Final Report is the final deliverable (A002) on the programme 'Coherent Fiber Optic Links'. The project commenced in December 1985 and all technical work was completed in May 1989. The experimental hardware, comprising one digital and one analog system, was delivered and installed at RADC Griffiss in October 1989 at which point the final project presentation was also delivered. PCO Inc. (USA) acted as prime contractor and project manager, whilst all technical work was subcontracted to Plessey Research Caswell (England).

The objective of the programme is as stated in Section 1. To meet this objective the programme activities were organised as shown in Figure 2.1. The work on the analog and digital systems followed similar paths. Both started with an in-depth study and analysis of the architectures and performance, leading to a ranking based on performance, cost and complexity, and resulting in a recommendation for the systems to be realised as experimental models. There then followed the design and hardware realisation of the two systems and the subsequent testing. In both cases the systems were designed to be mounted in 19 inch racks for transportability so that the systems could be delivered and reassembled at RADC Griffiss.

In the case of the digital system the recommendation was to construct an FSK modulated link employing single filter detection and operating at a data rate of 140 Mb/s. This employed 1.55 micron wavelength DFB lasers and the choice of data rate was determined by laser linewidth and FM response issues. As part of the digital system a direct detection link was also installed for comparison purposes. This made use of the same transmitter laser and receiver front-end as the coherent link in order to permit the most meaningful performance comparison. The recommendation for the analog system was to implement a self-homodyne optical PM system, but employing

frequency modulation of the electrical signal in order to reduce overall signal distortion. A signal carrier frequency of 3 GHz was adopted, determined by the bandwidth of commercially available optical phase modulators. This configuration was viewed as offering the best overall balance between performance and complexity. The self-homodyne configuration avoids the need for independent control of transmitter and local oscillator lasers, but more importantly when combined with the matching of the optical path delays between the signal and local oscillator arms permitted the reduction of the effective laser phase noise and hence simulated the use of narrow linewidth transmitter and local oscillator lasers using a conventional DFB laser source.

The digital system was constructed and when tested at Plessey Caswell achieved a receiver sensitivity at the photodetector of -50.6 dBm for a 10^{-9} BER and a data rate of 140 Mb/s. This represented a coherent detection advantage of 7dB compared with the direct detection. Comparing the link budgets for the two techniques coherent transmission yielded a 9.6dB advantage. These figures are in reasonable agreement with the values predicted in the system design. The coherent system was demonstrated at data rates down to 15 Mb/s, though not optimally in these cases. The system employed manual polarisation control using fibre squeezers and the link was completed with ten 1km reels of standard single mode fibre. When tested it remained stable for periods of tens of minutes without the need for polarisation realignment. The analog system was also built and successfully demonstrated the transmission and recovery of a narrow band signal on a 3 GHz carrier using an optically phased modulated link. This link was implemented using the transmitter laser from the digital system. The phase noise suppression effect achieved by optical path matching within the self-homodyne arrangement was demonstrated. The performance of the link in terms of signal to noise ratio and coherent advantage was in good agreement with theoretical predictions.

During the course of this programme the following contract deliverables were successfully completed:

- Digital System Design Plan (July 1987)
- Digital System Test Plan (January 1988)
- Analog System Design Plan (April 1988)
- Analog System Test Plan (October 1988)

The hardware subsequently constructed and tested was delivered to RADC Griffiss and set-up in working order. The digital system as delivered in 19 inch rack form represents at the present time the state-of-the-art in engineered form for coherent systems. Coherent detection of FSK signals is an architecture which is presently being heavily investigated Worldwide in telecommunications for both long span and multichannel systems. Therefore, though no longer representing a novel architecture, with hindsight the choice of this system configuration for the project was well founded as demonstrated by the current level of activity. The level of engineering featured within the delivered system provides it with a high level of uniqueness, as the number of such systems in the World is still few. The analog system delivered to RADC is also similarly unique. Very little attention has been given to coherent analog systems in the World scene and so much of the output from the programme on this topic has broken new ground.

A number of publications have arisen out of this programme, copies of which are appended to this report.

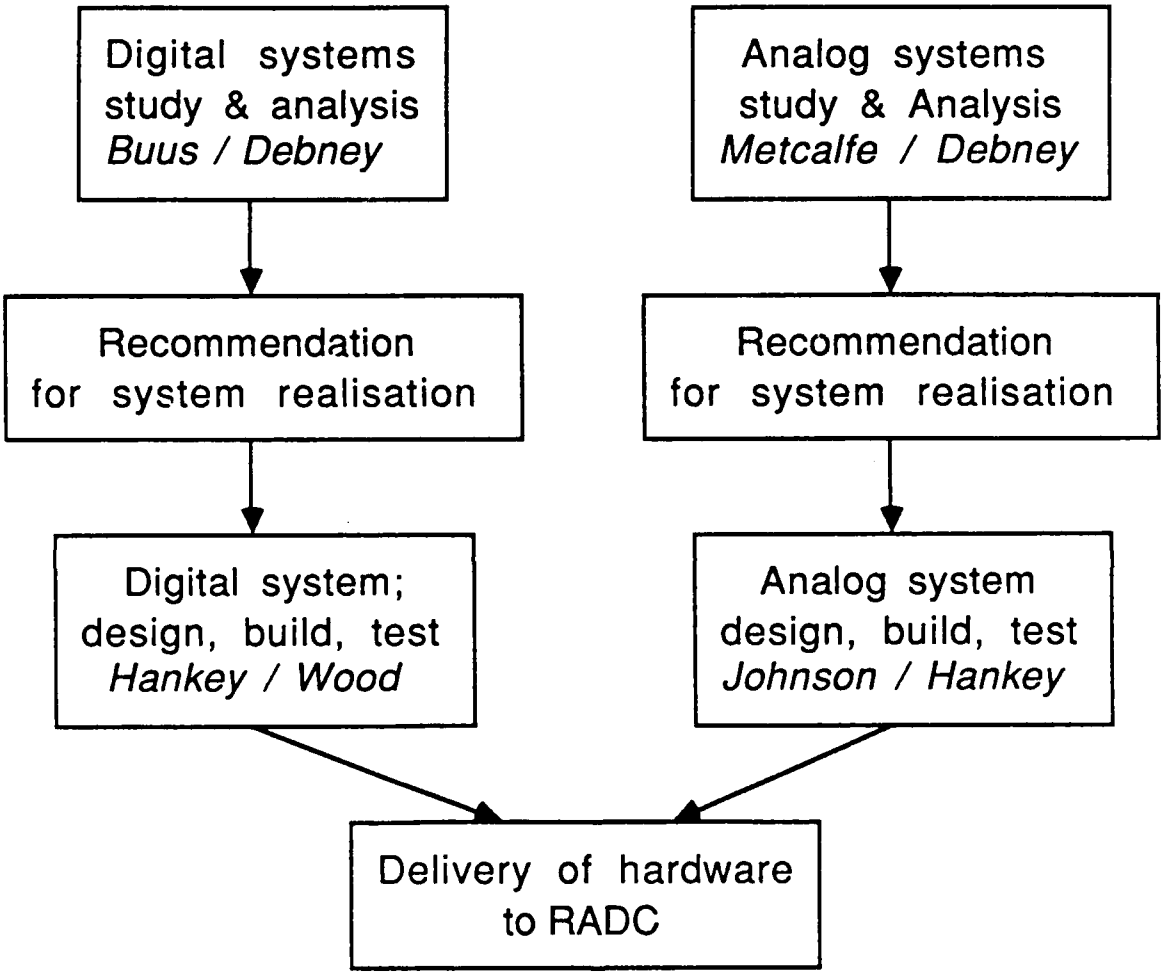

Figure 2.1 Programme Activities

3. DIGITAL COHERENT SYSTEMS STUDY AND ANALYSIS

3.1 DIGITAL SYSTEM CONFIGURATIONS AND THEORETICAL PERFORMANCE LIMITS

This is the basic principle of most present day fibre optic data transmission systems. A laser or LED source is intensity modulated, by modulating the drive current, and a photocurrent is generated at the detector which is directly proportional to the received power P_r (Fig. 3.1).

For this case

$$I_{ph} = MR\ P_r \qquad (3.1.1)$$

where M is the current gain, or multiplication factor in the case of an APD, and R is the detector responsivity defined as

$$R = \eta q / h\nu$$

measured in amps per watt.

The principle of coherent detection in optical systems is precisely that utilised in the superheterodyne radio receiver invented in 1920 by E H Armstrong. The differences are really to be found in the implementation which follows from the fact that the oscillator frequencies are optical rather than rf or microwave. The principle is illustrated in Fig. 3.1. At the detector the field from a modulated signal laser, frequency ω_S, is combined with the field from a local oscillator laser, frequency ω_L. Because the basic detector is a power detector and the optical power is proportional to the square modulus of the combined optical field, then the photocurrent produced is proportional to:

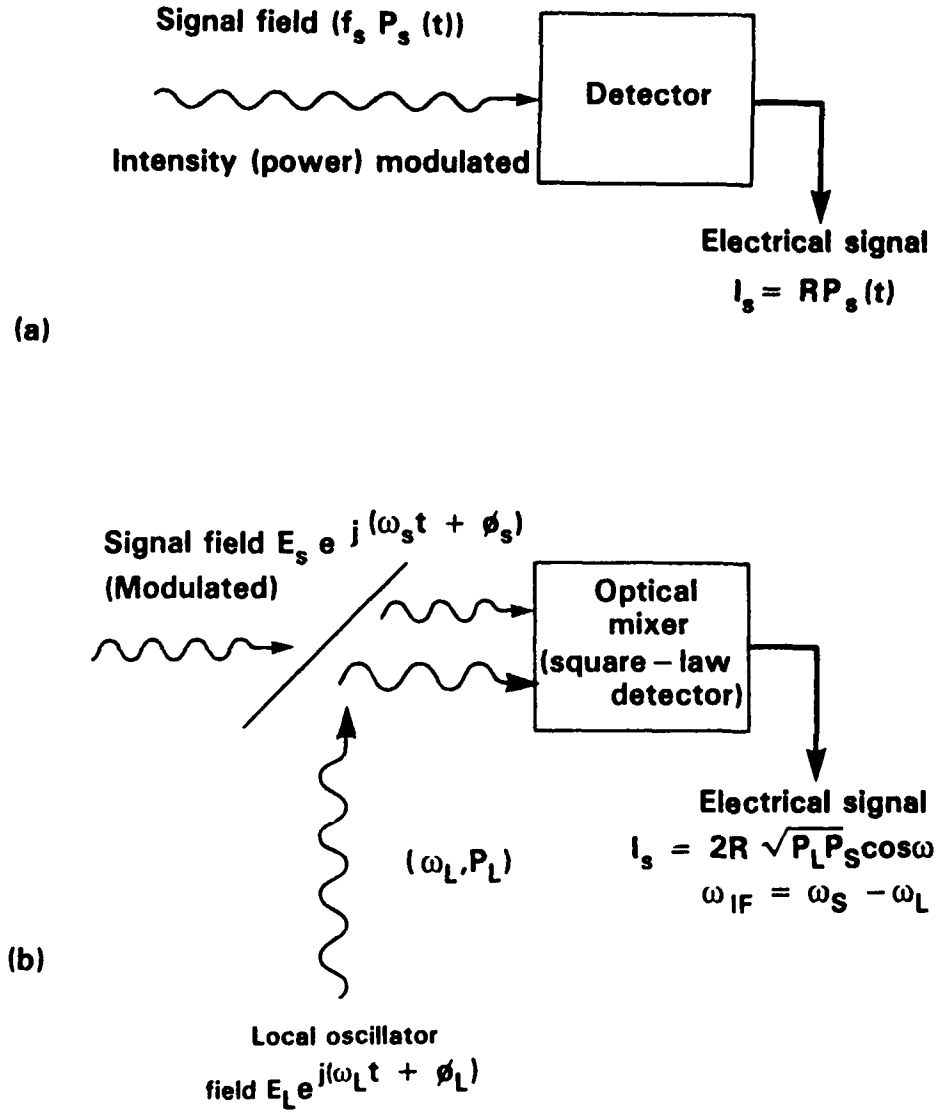

Figure 3.1: (a) The principle of direct detection optical communications. (b) The principle of coherent optical detection. The signal and local oscillator fields with optical frequencies f_S and f_L are 'mixed' and detected to produce an electrical signal at an intermediate frequency f_S-f_L.

$$\left| E_S\, e^{j(\omega_S t + \phi_S)} + E_L\, e^{j(\omega_L t + \phi_L)} \right|^2 \qquad (3.1.2)$$

When time averaged, this yields

$$\frac{E_S^2}{2} + \frac{E_L^2}{2} + E_L E_S \cos(\omega_{IF} t + \Delta\phi) \qquad (3.1.3)$$

where $\omega_{IF} = \omega_S - \omega_L$ is referred to as the intermediate frequency (IF). The resulting photocurrent is then

$$I_{ph} = RP_S + RP_L + 2(P_L P_S)^{\frac{1}{2}} \cos(\omega_{IF} t + \Delta\phi) \qquad (3.1.4)$$

Because the detector is a power detector, or a 'square-law' detector from the point of view of the laser field, it behaves as a mixer and produces an output electrical signal at an intermediate frequency which carries the signal information. The above expression (3.1.4) illustrates the basic principle of coherent detection. The signal modulation appears either in the amplitude (P_S modulated) frequency (ω_S modulated) or phase (ϕ_S modulated) unlike direct detection systems where only amplitude modulation is possible. The IF signal can be made large by increasing the local oscillator (L.O.) power P_L thus improving the receiver signal to noise ratio. The process of detecting the combined signal field and local oscillator laser field at the receiver therefore acts as a mixer and provides gain. The signal to noise ratio cannot be improved indefinitely by increasing the local oscillator power since in the limit of large local oscillator power the detector shot noise which arises from the detector photocurrent associated with the local oscillator laser dominates over all other noise sources and the signal to noise ratio approaches a limiting value, independent of L.O. power P_L.

Fig. 3.2 shows a functional diagram of a coherent optical transmission system based on the heterodyning principle. The transmitter consists of a laser source operating in a single transverse and longitudinal mode possibly coupled to an external modulator in order to impart the amplitude, phase or frequency modulation. At the receiver the weak signal field from the transmitter laser is combined with the field from the L.O. laser in such a way that the wave fronts of the two laser fields are matched for the most efficient detection. In a fibre based system this is usually achieved using a taper fused fibre coupler. The combined signal is fed to a square-law detector and preamplifier to provide the mixing, gain, and low noise amplification. In a heterodyning system the signal modulation appears on an intermediate frequency electrical carrier as indicated by equation 3.1.4. This then passes through an IF filter sufficiently wide to pass the modulated carrier prior to recovery of the modulation.

Fig. 3.2 indicates the provision of an automatic frequency control (AFC) loop in order to maintain a stable intermediate frequency. The intermediate frequency is equal in magnitude to the difference in frequencies of the transmitter and local oscillator lasers so that fluctuations in the frequency of either laser will cause fluctuations in the IF. The demodulation stage will require a certain level of IF stability in order to recover the signal and so the IF must be actively controlled. This is achieved by providing temperature and drive current stabilisation of the lasers to establish a sufficient level of absolute laser frequency stability that the signal can be located within the IF filter and thus permit additional electronic means to lock the IF to its prescribed value. Thermal fluctuations are the main cause of IF drift with semiconductor lasers and this requires temperature stabilisation of the order millidegrees in order to achieve intrinisic IF stability of the order tens of megahertz. At the output of the IF filter the carrier frequency is sampled electronically in order to sense deviations from its prescribed value. A control signal is then fed to the drive current of the local

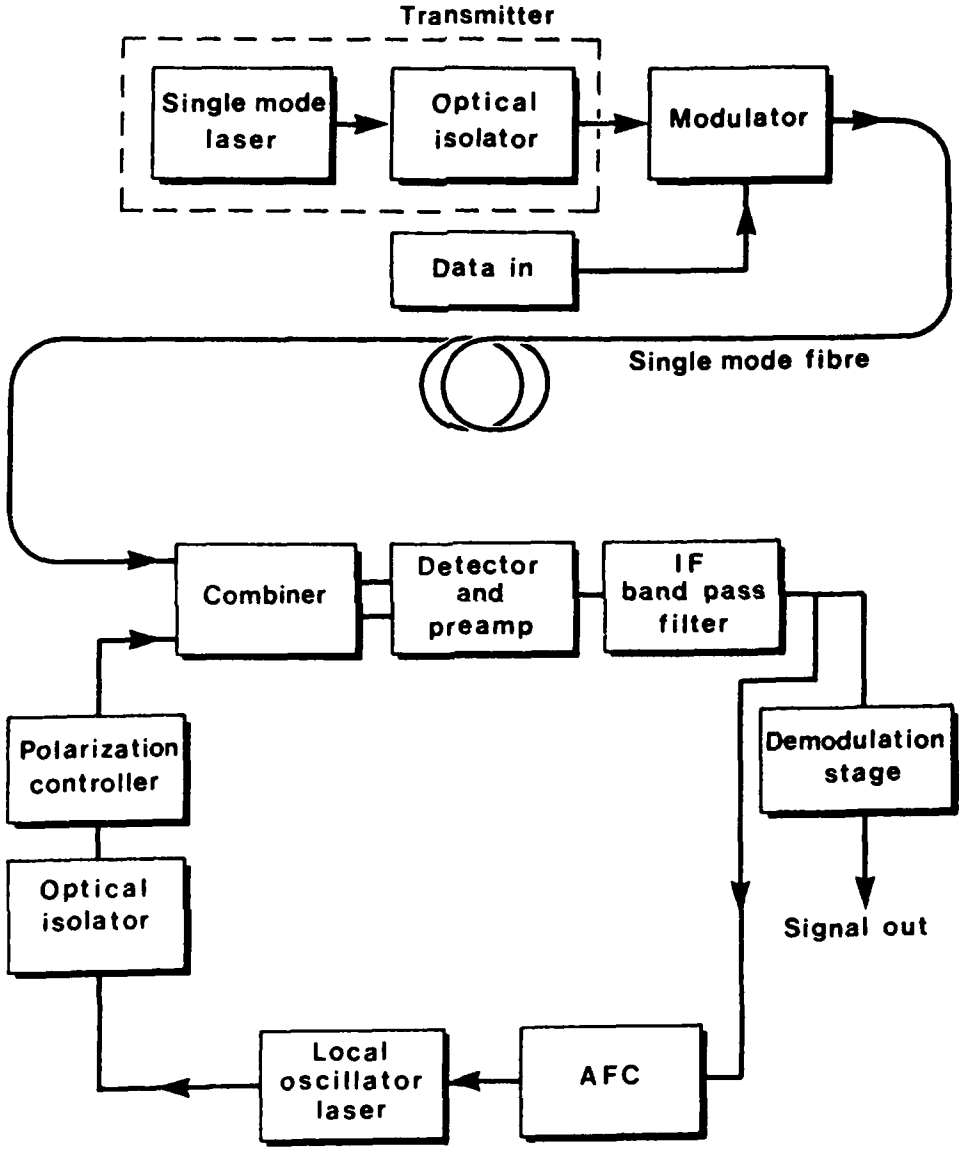

Figure 3.2: An illustration of the functional requirements of a coherent optical fibre optic transmission system using the heterodyning principle.

oscillator laser in order to modify its output frequency and thus bring about a return of the IF to the correct value.

The receiver can be configured in such a way that the IF is zero, referred to as homodyning. In this case it can be seen from equation 3.1.4 that the modulation at the output of the preamplifier appears at baseband and no further demodulation is necessary. The system is completed by suitable low pass filtering. This receiver architecture is particularly efficient in the use of receiver electrical bandwidth, but demands that not only the frequency between the transmitter and local oscillator laser is controlled, but also the phase. The design and implementation of the optical phase lock loop is particularly demanding and to date has resulted in only limited investigations of homodyne detection systems.

In some experiments, and indeed in many sensor applications, the self- or pseudo-heterodyning, or homodyning configuration is adopted where the signal and local oscillator sources are derived from the same laser. This arrangement avoids the need for the stringent laser stability and frequency tracking required in communications systems employing independent transmitter and local oscillator lasers.

In order to maximise the magnitude of the received signal a coherent system requires that the polarisation states of the signal field and local oscillator field at the detector be identical. In a fibre based system this could be achieved through the use of polarisation maintaining fibre. In systems employing standard single mode fibre the polarisation state of the signal field at the detector can be arbitrary and changing with time due to the birefringence of the fibre. The receiver therefore requires that some means be introduced to actively control the polarisation of the local oscillator laser in order to match that of the signal field, or alternatively adopt a receiver configuration which can operate passively and is insensitive to the states of polarisation of the lasers. The latter

is referred to as polarisation diversity and various schemes have been proposed for achieving this. Active polarisation control is potentially more efficient but requires electro-mechanical or electro-optic polarisation transformers and the associated control electronics.

The exact form of the demodulation circuit depends on the modulation format employed. As already indicated amplitude, phase, and frequency modulation are possible which in the case of digital modulation are referred to as amplitude shift keying (ASK), phase shift keying (PSK), and frequency shift keying (FSK). The first two formats are best implemented using external modulators whereas FSK is normally achieved through direct current modulation of the laser. The different modulation formats achieve varying levels of performance in terms of receiver sensitivity. Phase shift keying systems offer the greatest sensitivity and ASK the least. (Homodyning provides 3dB better sensitivity than heterodyning for the same modulation format.)

The systems studied and analysed in this programme have included:

- ASK heterodyning/synchronous demodulation
- ASK heterodyning/envelope detection
- ASK homodyning
- FSK heterodyning/synchronous demodulation
- FSK heterodyning/dual filter and envelope detection
- FSK heterodyning/single filter and envelope detection
- PSK heterodyning/synchronous demodulation
- PSK homodyning
- DPSK heterodyning
- MSK heterodyning

Of these systems MSK, or minimum shift keying, is less well known and so we will give a brief description.

With normal FSK there is the implicit assumption that the signal is coherent within a bit, but switching to another frequency causes a loss of phase coherence. This yields a frequency spectrum for the pulse train which requires the mark and space frequencies (f_1 and f_2) to be separated by a minimum of the data rate B, or in other words a modulation index $h=f_2-f_1/B)$ of unity. MSK assumes phase coherence between bits and this gives rise to a more compact spectrum of frequencies for the pulse train. The narrower frequency spectrum enables a smaller value for the frequency deviation to be used and narrower filters to be employed. In an optimal MSK receiver a frequency deviation of half the data rate is employed (h=0.5) and the phase, rather than the frequency, is measured to determine whether a mark or space has been transmitted. Moreover, the decision is made over two bit periods rather than one.

If we consider an MSK pulse train in which phase coherence is maintained between bits, then it can be shown that, relative to the nominal IF of $(f_1+f_2)/2$, the phase decreases by πh over a bit period for a mark and increases by πh for a space. The receiver therefore measures the phase at the beginning and end of a bit period whose character is to be determined. For h=0.5, transmitting a mark causes the phase to decrease by $\pi/2$.

The receiver requires synchronous demodulation and a complexity comparable with PSK. A performance comparable with PSK is achievable, not surprisingly. The advantage of MSK compared with PSK is that it would appear to avoid the need for an external phase modulator, with its associated loss, provided that direct current modulation of a laser yields FSK with the required degree of phase coherent between bits. There is evidence from an MSK experiment performed by British Telecom that this is the case. In this work the IF spectrum reported was indeed much narrower than would be expected for FSK and the receiver employed used a delay line discriminator, as adopted in DPSK, in order to measure the phase. The theoretical frameworks for the calculation of signal to noise ratio and BER

has been established for all the above systems. The signal to noise ratio at the output of the coherent receiver can in general be expressed in the form

$$\xi = \frac{\alpha R^2 M^2 P_L P_S}{eRP_L M^2 F(M) I_2 B + \overline{I_C^2}} \qquad (3.1.5)$$

in the case of a digital receiver. In this expression P_s refers to the average received power per bit time and I_C^2 represents the mean square noise current arising from the preamplifier circuit. The probability of a bit error corresponding to the signal to noise ratio ξ for each modulation format is shown in Table 3.1.

In expression 3.1.5 α represents a numerical parameter whose value is shown in Table 3.1 for the modulation formats indicated. The first term in the denominator of equation 3.1.5 is described explicitly because in the limit of large local oscillator power P_L this noise contribution dominates. It represents the shot noise in the detector current associated with the detected local oscillator laser power. As the local oscillator power increases the signal to noise ratio approaches a limiting value and is referred to as the local oscillator shot noise limit. Because the L.O. laser essentially provides signal gain it can be seen from equation 3.1.5 that in the limit of large L.O. power the unity gain PIN diode is the optimum form of detector. There is little to be achieved from the use of avalanche photodiodes with their additional gain and associated noise, except perhaps in the case where the L.O. power is sufficiently weak that the signal to noise ratio is considerably degraded relative to the L.O. shot noise limit.

Table 3.2 illustrates the theoretical performance which can be attained in the L.O. shot noise limit. The Table expresses the receiver sensitivity for digital systems in terms of the minimum number of received photons per

transmitted mark required to achieve a bit error rate of 10^{-9}. This is a useful way of presenting the sensitivity because for coherent receivers this quantity is independent of data rate. For comparison, present day direct detection telecommunication systems require around 1000 photons per mark over the data rate range 34 Mb/s to 565 Mb/s. Thus it can be seen that there is the potential for between 10 and 20 dB improvement in receiver sensitivity over direct detection.

Expression 3.1.5 and Table 3.1 can be used to relate the received optical power P_S for a given BER to the data rate B. This is illustrated in Figure 3.3 for a BER of 10^{-9} and a wavelength of 1.55μm.

FORMAT	BER	α
ASK HET SYNC	$\frac{1}{2}\ \mathrm{erfc}\ (\xi^{\frac{1}{2}}/2)$	2
ASK HET ENV. DET	$\frac{e^{-\xi/4}}{2}\ \{\frac{1}{e} + \frac{e}{(2\pi\xi)^{\frac{1}{2}}}\}$	2
ASK HOMO.	$\frac{1}{2}\ \mathrm{erfc}\ (\xi^{\frac{1}{2}}/2\sqrt{2})$	8
FSK HET SYNC	$\frac{1}{2}\ \mathrm{erfc}\ (\xi^{\frac{1}{2}}/\sqrt{2})$	1
FSK HET DUAL FILTER/ENV.	$\frac{1}{2}\ e^{-\xi/2}$	1
FSK SINGLE FILTER ENV.	$\frac{e^{-\xi/4}}{2}\ \{\frac{1}{e} + \frac{e}{(2\pi\xi)^{\frac{1}{2}}}\}$	1
PSK HET.	$\frac{1}{2}\ \mathrm{erfc}\ (\xi^{\frac{1}{2}})$	1
PSK HOMO	$\frac{1}{2}\ \mathrm{erfc}\ (\xi^{\frac{1}{2}}/\sqrt{2})$	4
DPSK	$\frac{1}{2}\ e^{-\xi}$	1

TABLE 3.1

Theoretical expressions for BER as a function of the SNR ξ given in equation 3.1.5.

MODULATION FORMAT	RECEIVER TYPE/DEMODULATION TECHNIQUE		
ASK	Heterodyne/Envelope 87	Heterodyne/Synchronous 81	Homodyne 41
FSK	Heterodyne/Envelope Single Filter Dual Filter 87 45	Heterodyne/Synchronous 41	
PSK	Heterodyne/Differential (DPSK) 22	Heterodyne/Synchronous 20	Homodyne 10

TABLE 3.2

The theoretical limits for receiver sensitivity of coherent detection systems. The numbers in the table indicate the number of photons which must be detected for a transmitted mark order to achieve a bit error of 10^{-9}.

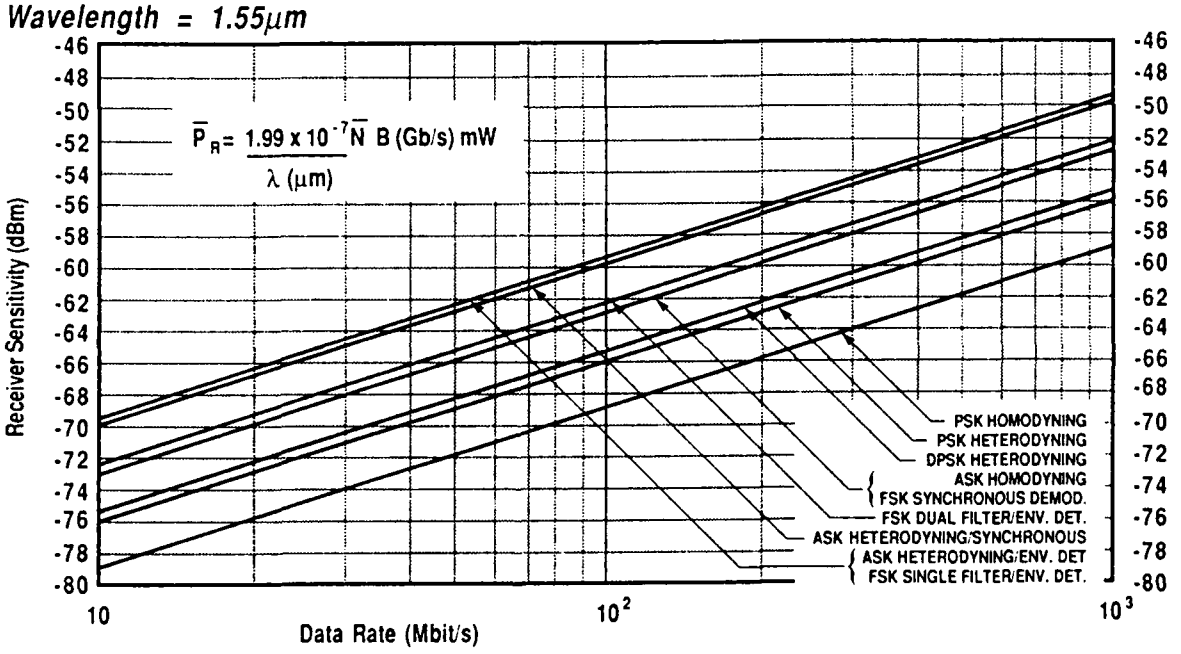

Figure 3.3: Theoretical limits for receiver sensitivity of coherent transmission systems evaluated on the basis of average power per transmitted mark.

3.2 LINK PERFORMANCE CONSTRAINTS

The calculations described on the previous section refer to the situation of the local oscillator shot noise limit when ideal modulation, detection, and demodulation are employed. The results represent the idealised theoretical performance limits which in a practical situation are difficult to realise. A number of factors have been identified which represent practical constraints and which will degrade the system sensitivity below the theoretical limiting value. The major degradation factors are:

- External modulator insertion loss
- Non-linear FM response of laser and unwanted AM (for FSK, derived by direct current modulation)
- Extinction ratio penalty, non-optimum threshold setting, and unwanted FM (for ASK)
- Coupler insertion loss and splitting ratio
- Polarisation controller insertion loss
- Detector quantum efficiency
- Finite local oscillator power
- Local oscillator excess noise
- Finite laser linewidth of transmitter and local oscillator
- Non-ideal filtering (shape and bandwidth)

These will now be described in more detail and the data generated provide input to the calculations of realisable performance in section 3.3.

Coupler Insertion Loss and Splitting Ratio

For the case of the use of a single detector at the output of one port of the coupler for combining signal and local oscillator the detected signal and L.O. power depends on the coupler splitting ratio. Consequently, the signal to noise ratio depends on the splitting ratio with the result that

there exists an optimum value of this parameter which maximises the signal to noise ratio.

Configuration:

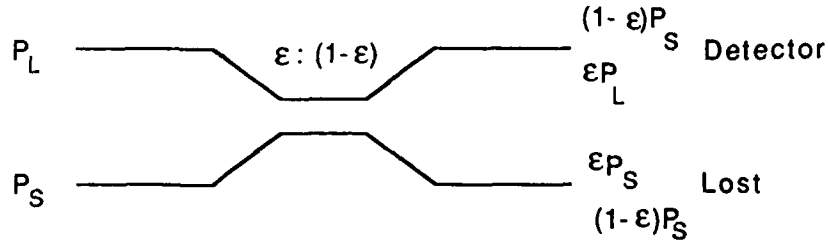

For the configuration above the signal to noise ratio can be written as

$$SNR = \gamma \frac{(1-\varepsilon)\ P_S}{1 + P_{D/\varepsilon P_L}} \qquad (3.2.1)$$

where γ is a constant and P_D is an effective noise term due to the receiver. By writing

$$SNR = \gamma P_S \frac{(1-\varepsilon)\varepsilon}{\varepsilon + P_{D/P_L}} \qquad (3.2.2)$$

we find the optimum value of ε, which maximises the SNR as

$$\varepsilon_{opt} = \sqrt{\left(\frac{P_D}{P_L}\right)^2 + \frac{P_D}{P_L}} - \frac{P_D}{P_L} \qquad (3.2.3)$$

In the hypothetical case where all signal and LO power is detected we have

$$SNR_h = \gamma \frac{P_S}{1+P_{D/P_L}} \qquad (3.2.4)$$

we therefore introduce a splitting penalty given by

$$10 \log \frac{P_S}{1+P_{D/P_L}} \frac{(1+P_{D/\varepsilon P_L})}{(1-\varepsilon)P_S} \text{ dB} \qquad (3.2.5)$$

Selecting $\varepsilon = \varepsilon_{opt}$ this penalty becomes

$$-20 \log \left(1 + \frac{P_D}{P_L} - \sqrt{1 + \frac{P_D}{P_L}} \sqrt{\frac{P_D}{P_L}}\right) \text{ dB} \qquad (3.2.6)$$

Numerical Results

P_D and P_L	ε_{opt} (relative to total Ps detected)	Penalty in dB (relative to total Ps noise limit)	Penalty in dB PL (relative to shot
0	0	0	0
10^{-2}	0.090	0.82	0.87
10^{-1}	0.232	2.29	2.70
0.25	0.309	3.21	4.18
0.5	0.366	3.96	5.72
1	0.414	4.65	7.65
2	0.449	5.18	9.95
∞	0.5	6	∞

Note that P_L is the LO power entering the splitter, not the LO power at the detector. The splitter is assumed lossless in these calculations.

For a fixed $\varepsilon = 0.5$ we find

$\frac{PD}{PL}$	Penalty in dB (relative to shot noise limit)
10^{-2}	3.1
10^{-1}	3.8
0.25	4.8
0.5	6.0
1	7.8

for $\varepsilon = 0.2$

$\frac{PD}{PL}$	Penalty
10^{-2}	1.2
10^{-1}	2.7
0.25	4.5
0.5	6.4
1	8.8

These calculations illustrate well the losses that can be incurred through the use of a single detector receiver and the non-optimum choice of splitting ratio.

Local Oscillator Excess Noise

Local oscillator excess noise represents an intensity noise on the L.O. output which manifests itself as an electrical noise within the receiver after detection. Because it depends on the L.O. power level it does not diminish in the L.O. shot noise limit but instead degrades the SNR as the L.O. power is increased. The dual detector receiver has the merit of suppressing the L.O. excess noise through the antiphase connection of the two detectors to a common preamplifier. In addition, it makes use of all of the available signal and L.O. power. An extensive analysis of the dual detector receiver has been reported in the literature by Abbas et al (JLT, 1985, LT3, pp 1110-1122). In order to make contact with this work it is necessary to provide a suitable characterisation of the local oscillator excess noise. This is described as follows:

The local oscillator power P_L gives a dc current according to

$$I_{dc} = \frac{\eta q}{h\nu} P_L \qquad (3.2.7)$$

The corresponding shot noise in a bandwidth B is

$$\langle I_n^2 \rangle_s = q \frac{\eta q}{h\nu} P_L B \qquad (3.2.8)$$

We now define the relative intensity noise per unit bandwidth, for shot noise limited operation, by

$$RIN_s = \frac{\langle I_n^2 s}{B(I_{dc})^2} = \eta P \frac{h\nu}{L} \qquad (3.2.9)$$

For $h\nu$ = 0.8eV and ηP_L=1mW we have $RIN_s \approx$ -160dB Hz^{-1}.

Laser noise is often characterised by the RIN value, typically one finds $-120dBHz^{-1} > RIN > -140dBHz^{-1}$ (>>RINs).

For a given RIN the L.O. noise spectral density is simply

$$RIN\ (I_{dc})^2 \qquad (3.2.10)$$

We can now make use of the dual detector analysis by Abbas et al by noting that their parameter γ is simply given by

$$\gamma = \frac{RIN}{q} \qquad (3.2.11)$$

q being the electronic charge. RIN = $-120dBHz^{-1}$ gives $\gamma = 6.3 \times 10^6\ A^{-1}$ and RIN = $-140dBHz^{-1}$ gives $\gamma = 6.3 \times 10^4\ A^{-1}$.

Extinction Ratio Penalty

In the case of ASK systems the effect of finite extinction ratio has been considered. This is found to be much more severe in coherent systems than in direct detection systems. Defining ε to be the ratio of transmitted powers for a 'zero' and a 'one' the receiver sensitivity penalty is given by the factor

$$\frac{(1 + \varepsilon)}{(1 - \varepsilon^{\frac{1}{2}})^2} \qquad (3.2.12)$$

For an extinction ratio of 0.1 this yields a receiver sensitivity penalty of 3.7dB, compared with 0.9dB in a direct detection system. This is a potentially serious source of system impairment using ASK modulation.

Non-Optimum Threshold Setting

In the case of ASK systems the penalty for a relative threshold a_{th} below 0.5 is given by

$$20 \log \frac{0.5}{a_{th}} \text{ dB} \qquad (3.2.13)$$

Polarisation Controller Insertion Loss

The polarisation controller is best located between the local oscillator laser and the coupler so that the received signal is not attenuated. The effect is therefore to attenuate the L.O. power and thus gives rise to a modification to the effective L.O. power when quantifying the finite L.O. power penalty.

Detector Quantum Efficiency (η)

This enters through the detector responsivity

$$R = \frac{\eta q}{h\nu} \qquad (3.2.14)$$

The receiver sensitivity penalty relative to unity quantum efficiency is

$$10 \log 1/\eta \text{ dB} \qquad (3.2.15)$$

External Modulator Insertion Loss

The effect of this component is to reduce the link budget by the magnitude of the insertion loss. Since it is the link budget as a whole rather than the receiver sensitivity which is used in comparing link architectures, this factor can erode the difference between PSK and FSK systems, and further degrade ASK. The present performance of fibred components for phase and intensity modulators fabricated in lithium niobate gives a fibre-to-fibre insertion loss of between 3 and 6dB. In later calculations we have assumed 3dB, representing either current state of the art or a figure representative of future commercial components.

Finite Local Osillator Power Penalty

As indicated in equation 3.1.5, the SNR depends on the L.O. power level and only in the limit of being infinitely large does the SNR become independent of P_L; referred to as the L.O. shot noise limit. For finite values of L.O. power the SNR and hence receiver sensitivity is degraded by a factor which depends on the receiver noise. The receiver sensitivity degradation factor χ for a PIN/FET receiver front-end is given by

$$\chi = 1 + \frac{S_I}{S_{LO}} + \frac{S_E}{S_{LO}R_T^2} + \frac{4\pi^2 C_T^2 S_E}{S_{LO}T^2} \left\{ \frac{I_3}{I_2} + U_{IF}^2 \right\} \qquad (3.2.16)$$

The corresponding receiver sensitivity penalty is then 10 log χ dB. In the above expression:

$$S_{LO} = qRP_L$$
$$S_I = qI_o + 2KT/R_L \qquad (3.2.17)$$
$$S_E = \frac{2KT\Gamma}{g_m}$$

and the noise integrals I_3 and I_2 take the values 0.17364 and 1.1277 respectively. U_{IF} is the IF frequency normalised to the data rate, which for the homodyning case is zero.

For most practical cases equation 3.2.16 simplifies to

$$\chi = 1 + \frac{4\pi^2 C_T{}^2 2KT\Gamma}{g_m qRP_L} \left(\frac{I_3}{I_2} + U_{IF}{}^2\right) \frac{1}{T^2} \qquad (3.2.18)$$

Calculations have been performed as a function of L.O. power, IF frequency, and data rate for parameters representative of a typical PIN/FET receiver ($C_{T=}$1pF), g_m=20mS, R=1 A/W). These results are shown in Figures 3.4-7 which are indicative of the magnitudes of penalty which can be encountered though a calculation based on the equations above is advisable for specific cases.

Finite Laser Linewidth

For coherent detection both the transmitter and the local oscillator laser must emit in a single traverse and longitudinal mode and exhibit a high level of temporal coherence. The degree of laser coherence is reflected in the spectral width of the single mode; the narrower the linewidth, the greater the coherence. The linewidth represents the range over which the instantaneous frequency of the laser changes due to the phase noise generated by the spontaneous emission process. Errors occur in ASK and FSK systems as a consequence of laser frequency fluctuations causing the IF

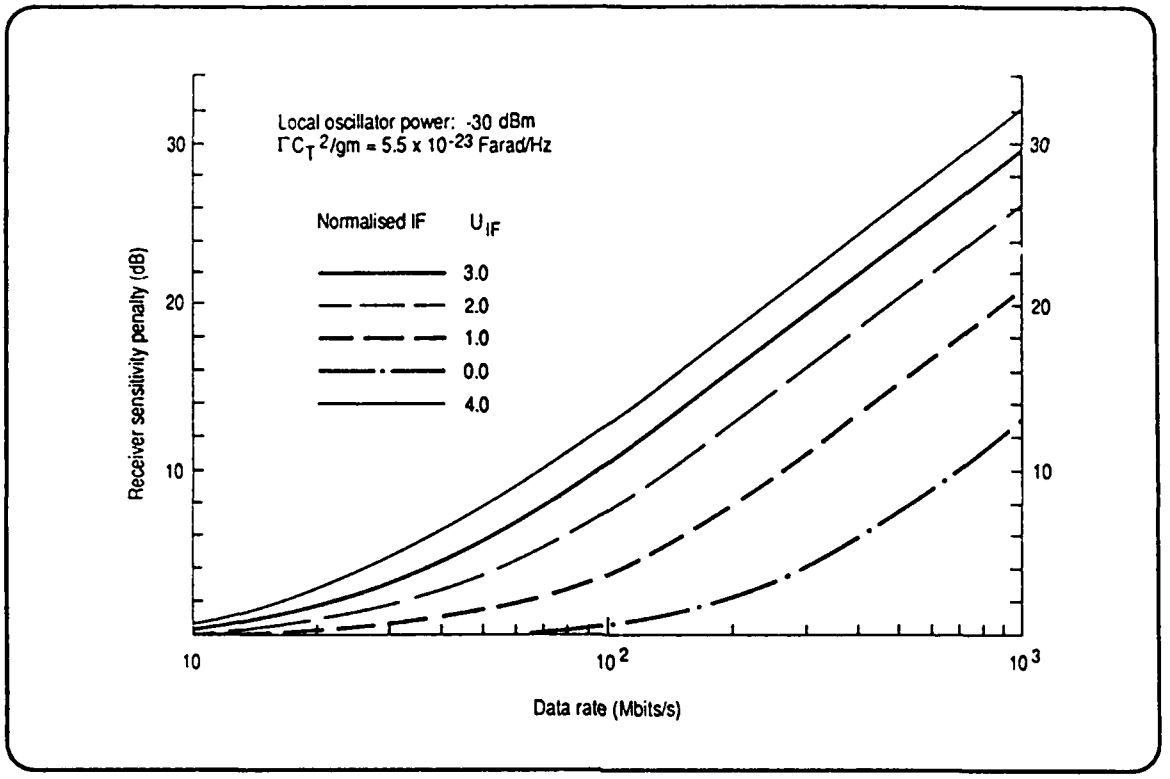
Local oscillator power: -30 dBm
$\Gamma C_T^2/gm = 5.5 \times 10^{-23}$ Farad/Hz
Normalised IF U_{IF}
3.0
2.0
1.0
0.0
4.0
Receiver sensitivity penalty (dB)
Data rate (Mbits/s)
10
10^2
10^3
30
20
10

Fig. 3.4

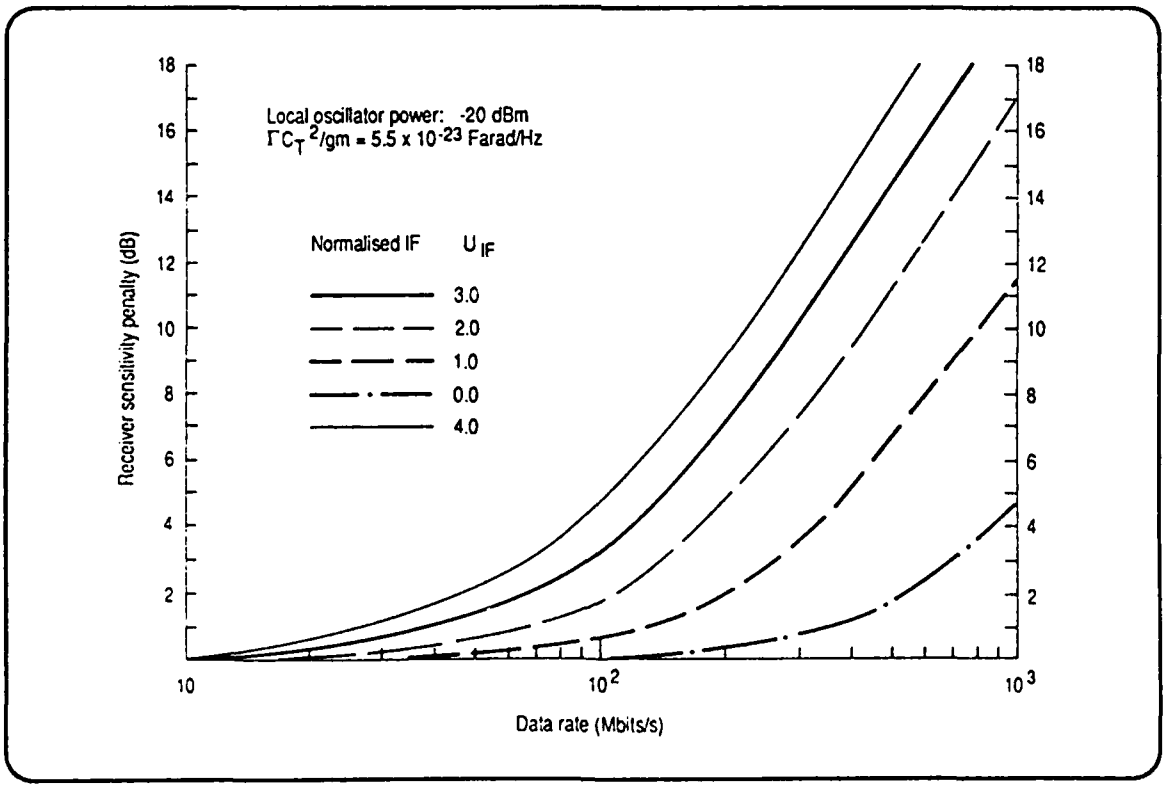
Local oscillator power: -20 dBm
$\Gamma C_T^2/gm = 5.5 \times 10^{-23}$ Farad/Hz
Normalised IF U_{IF}
3.0
2.0
1.0
0.0
4.0
Receiver sensitivity penalty (dB)
Data rate (Mbits/s)
10
10^2
10^3
18
16
14
12
10
8
6
4
2

Fig. 3.5

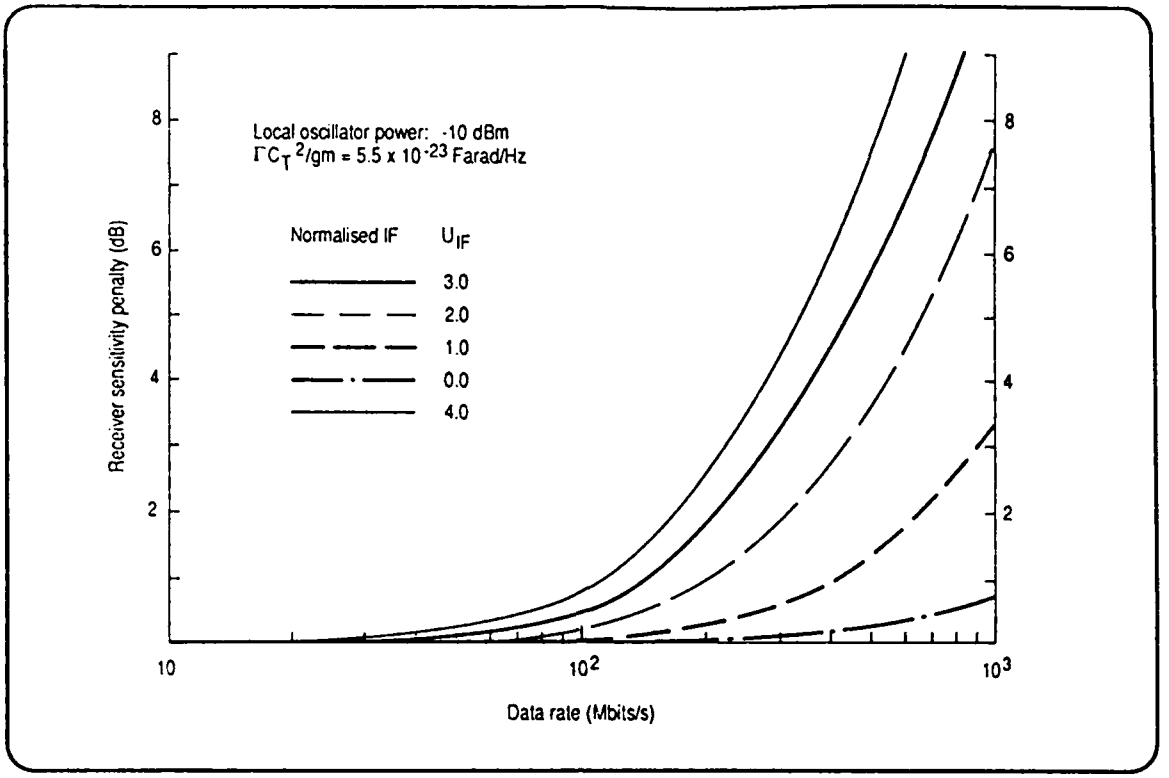
Local oscillator power: -10 dBm
$\Gamma C_T^2/gm = 5.5 \times 10^{-23}$ Farad/Hz
Normalised IF U_{IF}
3.0
2.0
1.0
0.0
4.0
Receiver sensitivity penalty (dB)
8
6
4
2
10
10^2
10^3
Data rate (Mbits/s)

Fig. 3.6

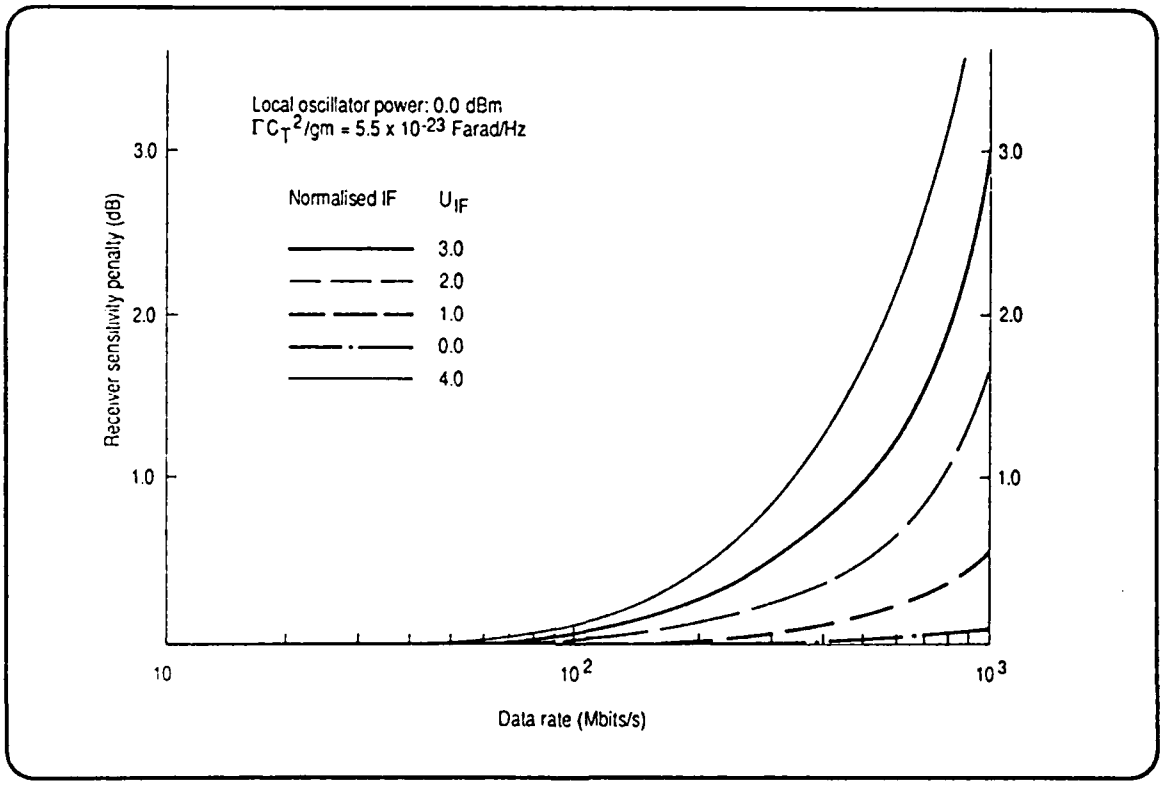
Local oscillator power: 0.0 dBm
$\Gamma C_T^2/gm = 5.5 \times 10^{-23}$ Farad/Hz
Normalised IF U_{IF}
3.0
2.0
1.0
0.0
4.0
Receiver sensitivity penalty (dB)
3.0
2.0
1.0
10
10^2
10^3
Data rate (Mbits/s)

Fig. 3.7

signal to fall outside the passband of the filters employed in the receiver. In PSK systems the phase noise in the laser output impacts directly on the phase information encoded on the transmitter source and thus causes bit errors. Single mode behaviour can be achieved through the use of a multi-longitudinal mode laser with an external cavity, which incorporates a mode selective element such as a grating. Alternatively the Distributed Feedback laser (DFB) also provides a single longitudinal mode through the presence of the internal diffraction grating.

An extensive literature now exists on the analysis of the laser linewidth requirements for coherent detection techniques. Table 3.2 gives a summary of the requirements for these systems expressed as a percentage of the data rate. ASK and FSK heterodyning systems differ from the rest in that the laser linewidth requirement is not so rigidly defined. For these systems the effect of the frequency fluctuations as represented by the spectral width of the laser can be accommodated in the receiver design through the use of broader IF filters. However, this results in the need for wider bandwidth receivers, and the larger noise bandwidth either requires higher levels of L.O. power to achieve L.O. shot noise limited performance or results in a large L.O. power penalty. The figures given in Table 3.3 are generally regarded as a sensible compromise of all these factors.

Because the linewidth requirement is a fixed fraction of the data rate, then generally the lower the data rate the narrower the laser linewidth requirement which can present difficulties in finding suitable laser sources. At the present time the only semiconductor laser source suitable for coherent transmission is based on the DFB laser which generally have linewidths of 30 MHz or more from commercial sources. Laboratory results have indicated that linewidths down to a few MHz are possible with the basic DFB laser structure for some operating conditions. For linewidths narrower than this some form of external cavity laser is required. Linewidths down to a few kHz have been demonstrated for long external cavities either in air or fibre together with a grating for mode selection.

MODULATION/RECEIVER	LASER LINEWIDTH (% OF DATA RATE)	REFERENCE
ASK HETERODYNE	20*	1
ASK HOMODYNE	0.025	2
FSK HETERODYNE	20*	3
MSK HETERODYNE	0.17	4
PSK HETERODYNE	0.25	2
DPSK HETERODYNE	0.17	5
PSK HOMODYNE	0.025	2

TABLE 3.3: Laser linewidth requirements for transmitter and local oscillator to achieve a receiver penalty of 1dB at a BER of 10^{-9}.

REFERENCES

[1] G Jacobsen and I Garrett:
"Theory for heterodyne optical ASK receivers using square-law detection and postdetection filtering",
IEE Proceedings, Vol. 134, Pt. J, No. 5, October 1987, pp.303-312.

[2] T G Hodgkinson:
"Costas loop analysis for coherent optical receivers",
Electronics Letters, 1986, Vol. 22, pp.394-396.

[3] I Garrett and G Jacobsen:
"Theoretical analysis of heterodyne optical receivers for transmission systems using (semiconductor) lasers with non-negligible linewidth",
J. Lightware Technol., Vol. LT-4, No. 3, March 1986, pp.323-334.

[4] K Iwashita, T Matsumoto, C Tanaka and G Motosugi:
"Linewidth requirement evaluation and 290km transmission experiment for optical CPFSK differential detection",
Electronics Letters, 1986, Vol. 22, pp.791-792.

[5] G Nicholson:
"Probability of error for optical heterodyne DPSK system with quantum phase noise",
Electronics Letters, 1984, Vol. 20, pp. 1005-1007.

3.3 REALISABLE PERFORMANCE

Coherent Links

The realisable performance of various coherent systems has been analysed and for comparison also that for direct detection systems.

The following general assumptions have been made:

- The error rate is 10^{-9} and the various penalties are assumed to be completely separable.
- A penalty $P_{\Delta\nu}$ of 1 dB due to a finite laser linewidth is allowed, the corresponding linewidth requirement is stated.
- The detector is assumed to have a quantum efficiency of $\eta = 0.8$ giving a penalty of $P_\eta = 0.97$ dB.
- For a PIN-FET receiver we assume the effective receiver noise to be

$$P_D = \begin{cases} 1.2.10^{-8}(\text{Watt}) + 4.2.10^{-23}\,\frac{\chi_2}{T}\ (\text{Watt.sec}^2) & \text{for } \lambda = 1.3\mu m \\ 1.0.10^{-8}(\text{Watt}) + 3.5.10^{-23}\,\frac{\chi_2}{T}\ (\text{Watt.sec}^2) & \text{for } \lambda = 1.5\mu m \end{cases} \qquad (3.3.1)$$

T is the bit period, the parameter χ is

$$\chi = \begin{cases} \left(\frac{I_3}{I_2}\right)_{bb} = 0.15 \text{ for ideal filtering) for homodyne systems} \\ (f_{IF}T)^2 + (BT)^2 \left(\frac{I_3}{I_2}\right)_{bb} \text{ for heterodyne systems} \\ (f_{IF,0}T)^2 + 2(BT)\,(f_{IF,0}T) + 2(BT)^2 + (BT)^2 \left(\frac{I_3}{I_2}\right)_{bb} \end{cases} \qquad (3.3.2)$$

for dual filter FSK with a modulation index $M = 2BT$

f_{IF} is the intermediate frequency and B the IF bandwidth.

For a single detector system the optimum coupler ratio is

$$\varepsilon \text{ opt} = \sqrt{\left(\frac{P_D}{P_L}\right)^2 + \frac{P_D}{P_L}} - \frac{P_D}{P_L} \qquad (3.3.3)$$

P_L being the local oscillator power. The penalty relative to the performance for infite P_L is then

$$P_C = 10 \log \left(1 + 2\frac{P_D}{P_L} - 2\sqrt{\left(\frac{P_D}{P_L}\right)^2 + \frac{P_D}{P_L}}\right)^{-1} \qquad (3.3.4)$$
$$= 10 \log(1-2\ \varepsilon \text{ opt})^{-1}$$

Local oscillat[illegible]xcess noise has been neglected.

For a dual detector system, for equal splitting in the coupler, we get

$$P_C = 10 \log \left(1 + 2\frac{P_D}{P_L}\right) \qquad (3.3.5)$$

- Penalties due to coupler insertion loss, nonideal filtering and polarization control imperfection are lumped together as a combined penalty P_F.

Direct Detection Links

For direct detection we assume that the average output power coupled to the fibre is $\frac{0.4\ mW}{2}$ = -7dBm and that the (realizable) required average power (receiver sensitivity) is given in the following Table:

data rate (f_B) in Mbit/s	20		100		300	
λ in μm	1.3	1.55	1.3	1.55	1.3	1.55
P_{req} in dBm	-51	-51.8	-47	-47.8	-41	-41.8
Available P_{out}-P_{req} dd in dB	44	44.8	40	40.8	34	34.8

The values for 1.55μm are found from the 1.3μm values by correcting for the detector responsivity.

Figure 3.8 shows these assumptions in relation to PIN/FET and APD based receiver performance. The figures are generally better than is achieved from commercially available PIN/FET receivers and should be representative of a reasonably good APD receiver or a very good PIN/FET.

ASK Homodyne

Assumptions:

Required number of photons per mark in an ideal system N = 36xI_2, I_2 = 1.128, external modulator used, extinction ratio ε = 0.03, maximum linewidth (per laser) 0.2% of data rate.

The coupler penalty is low, therefore only the single detector case is considered.

In all cases the L.O. shot noise is dominating, therefore there is no advantage in using APD's.

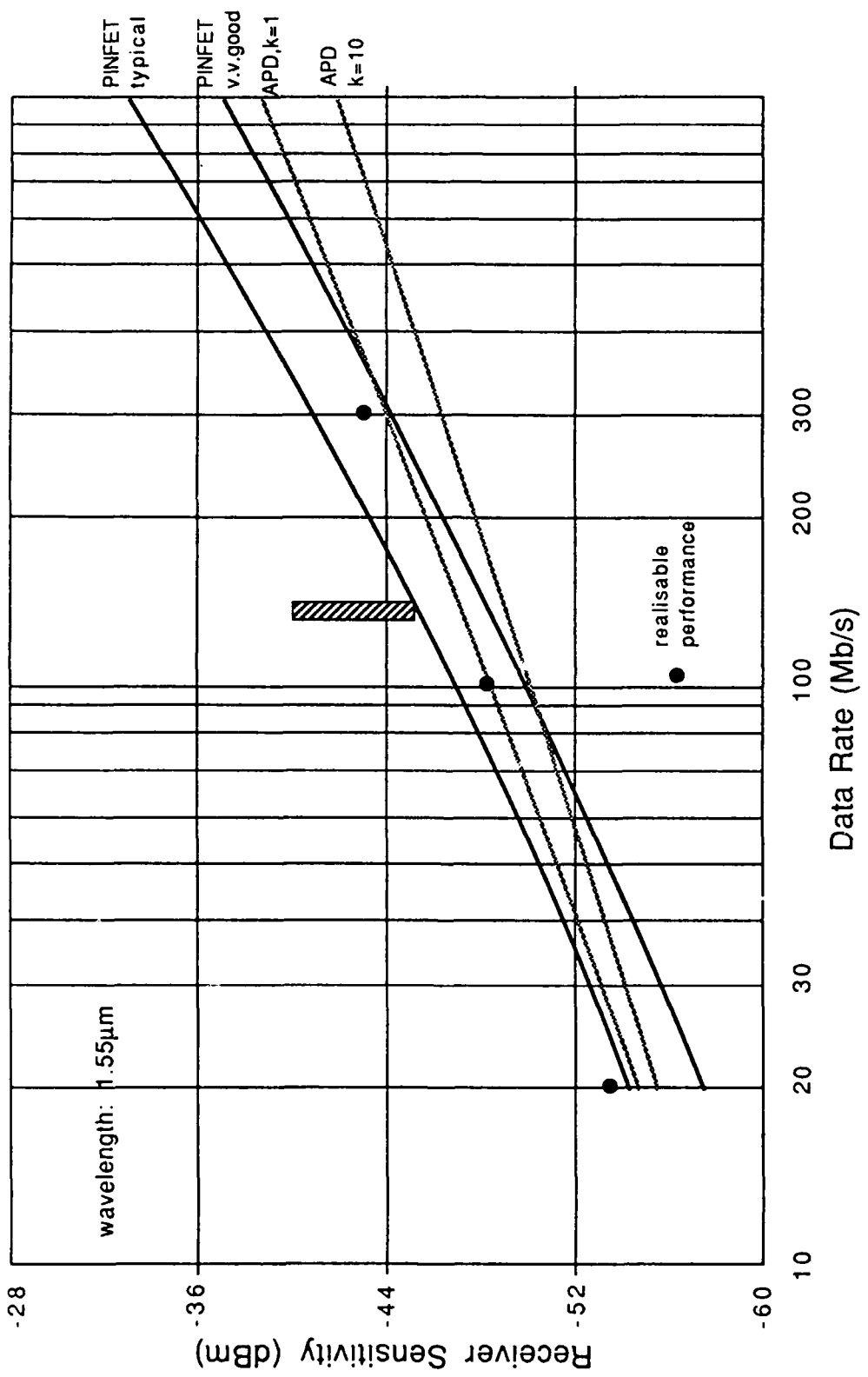

Figure 3.8 Direct Detection Receiver Sensitivity

ASK Homodyne System Budget

f_B in Mbit/s	20		100		300	
λ in μm	1.3	1.55	1.3	1.55	1.3	1.55
P_{out} (in fiber) in dBm	-4		-4		-4	
Modulator insertion loss in dB, P_M	3		3		3	
Extinction penalty in dB, P_ε	1.8		1.8		1.8	
Max. linewidth in kHz	40		200		600	
Linewidth penalty in dB, $P_{\Delta\nu}$	1		1		1	
P_L (in coupler) in dBm	-4		-4		-4	
P_D in nW	14.5	12.2	75	63	582	488
$\frac{P_D}{P_L} \cdot 10^5$	3.63	3.05	18.7	15.7	145	122
Optimum splitting ε opt	0.0060	0.0055	0.0135	0.0124	0.037	0.034
Coupler/finite P_L penalty in dB, P_C	~0.05		0.12	0.11	0.33	0.30
P_F in dB	3		3		3	
Total penalty $P_\varepsilon + P_{\Delta\nu} + P_\eta + P_C + P_F$ in dB	6.8		6.9		7.1	
P_{req}^1 (ideal, per mark) in dBm	-69.1	-69.9	-62.1	-62.9	-57.3	-58.1
P_{req}^1 (realizable) in dBm	-62.3	-63.1	-55.2	-56.0	-50.2	-51.0
Available $(P_{out}-P_M) - P_{req}^1$ in dB	55.3	56.1	48.2	49.0	43.2	44.0
Coherent advantage in dB	11.3		8.2		9.2	

ASK Heterodyne, Envelope Detection

Assumptions:

Required number of photons per mark in an ideal system $N=77.I_2$, $I_2=1.128$

External modulator used, extinction ratio 0.03.
IF frequency equal to 2 times data rate.
IF filter width equal to 2 times data rate, gives a penalty of P_B=3dB.
Threshold setting a_{th} = 0.5, max. linewidth (per laser) 7.5% of data rate.
The penalty for finite local oscillator power is small, the advanatage of using APD's (at optimium gain) is at best marginal.

ASK Heterodyne, Synchronous Detection

This scheme has a potential 0.3 dB advantage over ASK heterodyne envelope in all other aspects the system performance is comparable.

The "price" for this advantage is an increased complexity.

ASK Heterodyne/Envelope Detection Budget

f_B in Mbit/s	20		100		300	
λ in μm	1.3	1.55	1.3	1.55	1.3	1.55
P_{out} (in fiber) in dBm	-4		-4		-4	
Modulator insertion loss in dB, P_M	3		3		3	
Extinction penalty in dB, P_ε	1.8		1.8		1.8	
Max. linewidth in MHz	1.5		7.5		22.5	
IF bandwidth penalty in db, P_B	3		3		3	
Linewidth penalty in dB, $P_{\Delta\nu}$	1		1		1	
P_L (in coupler) in dBm	-4		-4		-4	
P_D in nW	89	74	1944	1630	17400	14600
$\frac{P_D}{P_L}$	$2.23.10^{-4}$	$1.85.10^{-4}$	$4.86.10^{-3}$	$4.08.10^{-3}$	$4.35.10^{-2}$	$3.65.10^{-2}$
Optimum splitting ε opt	0.015	0.013	0.065	0.060	0.170	0.158
Coupler/finite P_L penalty in dB, P_C	0.13	0.11	0.60	0.55	1.80	1.65
P_F in dB	3		3		3	
Total penalty $P_\varepsilon + P_{\Delta\nu} + P_B + P_n + P_C + P_F$	9.9		10.4	10.35	11.6	11.45
P_{req} (ideal, per mark) in dBm	-65.7	-66.5	-58.7	-59.5	-53.9	-54.7
SINGLE DETECTOR						
P_{req}^1 (realizable) in dBm	-55.8	-56.6	-48.3	-49.2	-42.3	-43.3
Available $(P_{out}-P_M) - P_{req}^1$ in dB	48.8	49.6	41.3	42.2	35.3	36.3
Coherent advantage	4.8		1.3	1.4	1.3	1.5
DUAL DETECTOR						
P_C in dB	~0		0.04		0.36	0.31
Total penalty in dB	9.8		9.8		10.1	
P_{req}^1 (realizable) in dBm	-55.9	-56.7	-48.9	-49.7	-43.8	-44.6
Coherent advantage in dB	4.9		1.9		2.8	

FSK Systems

With single filter synchronous detection this resembles ASK heterodyne synchronous. However, the modulator insertion loss P_M and extinction penalty P_ε will be replaced by a penalty due to the non-uniform FM response. This penalty is expected to be smaller than $P_M + P_\varepsilon$ and therefore a better system performance is expected.

Assumptions:

Required number of photons per bit in an ideal system (I_2=1.128).

$$N = \begin{cases} 77.I_2 & \text{for single filter} \\ 40.I_2 & \text{for dual filter} \end{cases}$$

If we take the penalty due to the non ideal frequency modulation to be ~1dB the single filter version will have a 3.8dB advantage over ASK heterodyne envelope with all characteristics being similar. The dual filter version is considered in the following table. In this case we take the IF filter bandwidth to be 2 times the datarate and the difference between the mark and space frequencies to be 4 times the datarate, a linewidth of about 11% (per laser) of the datarate can be tolerated. At high data rates a very large part of the potential 2.84 dB improvement in sensitivity of the dual filter scheme over the single filter scheme is lost due to the finite local oscillator power.

FSK Synchronous Detection

Offers a potential 0.3dB and 0.46dB advantage over envelope detection for the single and dual filter version, respectively. As for ASK systems the price is an increased complexity.

FSK Envelope Detection Budget (Dual Filter)

f_B in Mbit/s	20		100		300	
λ in μm	1.3	1.55	1.3	1.55	1.3	1.55
P_{out} (in fiber) in dBm	-4		-4		-4	
Nonideal modulation penalty in dB, P_{FM}	1		1		1	
Max. linewidth in MHz	2.2		11		33	
IF bandwidth/linewidth penalty in dB, $P_{\Delta\nu}$	4		4		4	
P_L (in coupler) in dBm	-4		-4		-4	
P_D in μW	0.36	0.30	8.66	7.22	77.9	64.9
$\frac{P_D}{P_L}$	$9.0.\ 10^{-4}$	$7.5.\ 10^{-4}$	0.022	0.018	0.195	0.162
Optimum splitting ε opt	0.029	0.027	0.13	0.12	0.29	0.27
Coupler/finite P_L penalty in dB, P_C	0.26	0.24	1.28	1.16	3.7	3.4
P_F in dB	3		3		3	
Total penalty $P_{FM}+(P_B + P_{\Delta\nu})+P_\eta+P_C+P_F$ in db	9.2		10.3	10.1	12.7	12.4
P_{req} (ideal, per bit) in dBm	-68.6	-69.4	-61.6	-62.4	-56.8	-57.6
SINGLE DETECTOR						
P_{req}^1 (realizable) in dBm	-59.4	-60.2	-51.3	-52.3	-44.1	-45.2
Available P_{out}- P_{req}^1 in dB	55.4	56.2	47.3	48.3	40.1	41.2
Coherent advantage	11.4		7.3	7.5	6.1	6.4
DUAL DETECTOR						
P_C in dB	~0		0.19	0.15	1.4	1.2
Total penalty in dB	9.0		9.2	9.1	10.4	10.2
P_{req}^1 (realizable) in dBm	-59.6	-60.4	-52.4	-53.3	-46.4	-47.4
Coherent advantage in dB	11.6		8.4	8.5	8.4	8.6

PSK Homodyne

Required number of photons per bit in an ideal system
$N = 9.I_2$.
Linewidth per laser ~0.2% of datarate.
Optical phase locked loop required. Penalty for nonideal operation = 1dB (added to P_F).
Dual detector advantage marginal because $P_D >> P_L$.

PSK Heterodyne

$N = 18\ I_2$
IF bandwidth = 2 x datarate.
Linewidth ~0.2% of IF bandwidth.
Optical phased locked loop required.
Single and dual detector options considered.

DPSK

$N = 20\ I_2$
IF bandwidth = 2 x datarate.
Linewidth ~0.2% of IF bandwidth.
No phase locked loop required.
Single and dual detector options considered.

PSK Homodyne

f_B in Mbit/s	20		100		300	
λ in μm	1.3	1.55	1.3	1.55	1.3	1.55
P_{out} (in fiber) in dBm	-4		-4		-4	
Modulator insertion loss in dB, P_M	3		3		3	
Max. linewidth in kHz	40		200		600	
Linewidth penalty in $P_{\Delta\nu}$ in dB	1		1		1	
P_L (in coupler) in dBm	-4		-4		-4	
P_D in nW	14.5	12.2	75	63	582	488
$\frac{P_D}{P_L} \cdot 10^5$	3.63	3.05	18.7	15.7	145	122
ε opt	0.0060	0.0055	0.0135	0.0124	0.037	0.034
P_C in dB	~0.05		0.12	0.11	0.33	0.30
P_F in dB	4		4		4	
Total penalty in dB $P_{\Delta\nu} + P_\eta + P_C + P_F$	6		6		6.3	
P_{req} (ideal, per bit) in dBm	-75.1	-75.9	-68.1	-68.9	-63.3	-64.1
P_{req}^1 (realizable) in dBm	-69.1	-69.9	-62.1	-62.9	-57.0	-57.8
Available $(P_{out}-P_M) - P_{req}^1$ in dB	62.1	62.9	55.1	55.9	50.0	50.8
Coherent advantage in dB	18.1		15.1		16.0	

PSK Heterodyne

f_B in Mbit/s	20		100		300	
λ in μm	1.3	1.55	1.3	1.55	1.3	1.55
P_{out} (in fiber) in dBm	-4		-4		-4	
Modulator insertion loss in dB, P_M	3		3		3	
Max. linewidth in kHz	80		400		1200	
Linewidth penalty in dB, $P_{\Delta\nu}$	1		1		1	
IF bandwidth penalty in db, P_B	3		3		3	
P_L (in coupler) in dBm	-4		-4		-4	
P_D in nW	89	74	1944	1630	17400	14600
$\frac{P_D}{P_L}$	$2.23 \cdot 10^{-4}$	$1.85 \cdot 10^{-4}$	$4.86 \cdot 10^{-3}$	$4.08 \cdot 10^{-3}$	$4.35 \cdot 10^{-2}$	$3.65 \cdot 10^{-2}$
ϵ opt	0.015	0.013	0.065	0.060	0.170	0.158
P_C in dB	0.13	0.11	0.60	0.55	1.80	1.65
P_F in dB	4		4		4	
Total penalty in dB $P_B + P_{\Delta\nu} + P_\eta + P_C + P_F$	9.1		9.6	9.55	10.8	10.65
P_{req} (ideal, per bit) in dBm	-72.1	-72.9	-65.1	-65.9	-60.3	-61.1
SINGLE DETECTOR						
P_{req}^1 (realizable) in dBm	-63.0	-63.8	-55.5	-56.4	-49.5	-50.5
Available $(P_{out}-P_M) - P_{req}^1$ in dB	56.0	56.8	48.5	49.4	42.5	43.5
Coherent advantage in dB	12.0		8.5	8.6	8.5	8.7
DUAL DETECTOR						
P_C in dB	~0		0.04		0.36	0.31
Total penalty in dB	9.0		9.0		9.3	
P_{req}^1 (realizable) in dBm	-63.1	-63.9	-56.1	-56.9	-51.0	-51.8
Coherent advantage in dB	12.1		9.1		10.0	

DPSK

f_B in Mbit/s	20		100		300	
λ in μm	1.3	1.55	1.3	1.55	1.3	1.55
P_{out} (in fiber) in dBm	-4		-4		-4	
Modulator insertion loss in dB, P_M	3		3		3	
Max. linewidth in kHz	80		400		1200	
Linewidth penalty in dB, $P_{\Delta\nu}$	1		1		1	
IF bandwidth penalty in db, P_B	3		3		3	
P_L (in coupler) in dBm	-4		-4		-4	
P_D in nW	89	74	1944	1630	17400	14600
$\frac{P_D}{P_L}$	$2.23 \cdot 10^{-4}$	$1.85 \cdot 10^{-4}$	$4.86 \cdot 10^{-3}$	$4.08 \cdot 10^{-3}$	$4.35 \cdot 10^{-2}$	$3.65 \cdot 10^{-2}$
ε opt	0.015	0.013	0.065	0.060	0.170	0.158
P_C in dB	0.13	0.11	0.60	0.55	1.80	1.65
P_F in dB	3		3		3	
Total penalty in dB $P_B + P_{\Delta\nu} + P_\eta + P_C + P_F$	8.1		8.6	8.55	9.8	9.65
P_{req} (ideal, per bit) in dBm	-71.6	-72.4	-64.6	-65.4	-59.8	-60.6
SINGLE DETECTOR						
P_{req}^1 (realizable) in dBm	-63.5	-64.3	-56.0	-56.9	-50.0	-51.0
Available $(P_{out}-P_M) - P_{req}^1$ in dB	56.5	57.3	49.0	49.9	43.0	44.0
Coherent advantage in dB	12.5		9.0	9.1	9.0	9.2
DUAL DETECTOR						
P_C in dB	~0		0.04		0.36	0.31
Total penalty in dB	8.0		8.0		8.3	
P_{req}^1 (realizable) in dBm	-63.6	-64.4	-56.6	-57.4	-51.5	-52.3
Coherent advantage in dB	12.6		9.6		10.5	

3.4 RECOMMENDATION AND RATIONAL FOR EXPERIMENTAL MODEL

The range of system architectures considered in this programme have been investigated with the aim of providing a recommendation for the architecture to be adopted in the design and build of a digital coherent system. The basis on which the options have been assessed are: system performance, complexity and cost of assembly.

System Performance

The realisable performance which we believe can be achieved in implementation of the various architectures has been analysed in detail and results presented in the previous section. A summary of the total system budget impairments for each architecture is presented in Table 3.4. The major penalties which tend to give rise to the distinctions between the architectures are:

External modulator insertion loss (ASK, PSK)	3.0dB
Extinction ratio penalty (ASK)	1.8dB
IF filter bandwidth (Heterodyning)	3.0dB
Single versus dual detector	0-2.2dB

It is found that at the lowest data rate considered there is little advantage in using a dual detector (balanced) receiver, whereas at 300 Mb/s the difference between using a single and dual detector can be as large as 2.2dB.

In assessing the performance attainable with each architecture the parameter which has been chosen to measure system merit is the link margin advantage of the coherent system over a direct detection system - referred to as the 'coherent advantage'. This parameter is a function of the data rate employed and a summary of results obtained for the coherent advantage is presented in Table 3.5.

ARCHITECTURE	TOTAL SYSTEM PENALTIES (dB)		
	DATA RATE (Mb/s)		
	20	100	300
ASK HETERODYNE	12.9	13.4(12.8)	14.5(13.1)
ASK HOMODYNE	9.8	9.9	10.1
FSK SINGLE FILTER	9.1	9.6 (9.0)	10.7 (9.3)
FSK DUAL FILTER	9.2	10.2 (9.1)	12.5(10.3)
PSK HETERODYNE	12.1	12.6(12.0)	13.7(12.3)
PSK HOMODYNE	9.0	9.0	9.3
DPSK	11.1	11.6(11.0)	12.7(11.3)
MFSK	9.1	9.2 (9.0)	10.7 (9.3)

TABLE 3.4

Penalties are an average for 1.3 and 1.55μm wavelength. Figures are for a single detector receiver except where in brackets, corresponding to a dual detector case.

MOD FORMAT	STYLE	DEMODULATION	DETECTORS	20	100	300
ASK	HETERODYNE	ENVELOPE	SINGLE	4.8	1.3/1.4	1.3/1.5
ASK	"	"	DUAL	4.9	1.9	2.8
ASK	"	SYNCHRONOUS	SINGLE	5.1	1.6/1.7	1.6/1.8
ASK	"	"	DUAL	5.2	2.2	3.1
ASK	HOMODYNE			11.3	8.2	9.2
FSK		SINGLE FILTER ENVELOPE	SINGLE	8.6	5.1/5.2	5.1/5.3
FSK		"	DUAL	8.7	5.7	6.6
FSK		DUAL FILTER ENVELOPE	SINGLE	11.4	7.3/7.5	6.1/6.4
FSK		"	DUAL	11.6	8.4/8.5	8.4/8.6
FSK		SINGLE FILTER SYNCHRONOUS	SINGLE	8.9	5.4/5.5	5.4/5.6
FSK		"	DUAL	9.2	6.2	7.1
FSK		DUAL FILTER SYNCHRONOUS	SINGLE	11.7	7.6/7.8	6.4/6.7
FSK		"	DUAL	12.1	8.9/9.0	8.9/9.1
PSK	HETERODYNE	SYNCHRONOUS	SINGLE	12.0	8.5/8.6	8.5/8.7
PSK	"	"	DUAL	12.1	9.1	10.0
PSK	HOMODYNE			18.1	15.1	16.0
DPSK	HETERODYNE	DIFFERENTIAL	SINGLE	12.5	9.0/9.1	9.0/9.2
DPSK	"	"	DUAL	12.6	9.6	10.5
MFSK	"	"	SINGLE	14.5	11.0/11.1	11.0/11.2
MFSK	"	"	DUAL	14.6	11.6	12.4

TABLE 3.5: Coherent Advantage (over Direct Detection) in dB

System Complexity

The basis for the complexity analysis is described by the following criteria:

- Technical difficulty in the design or construction of a particular component.
- Availability of the necessary technology or expertise.
- The technical risk in attempting to develop a component, where the technology/expertise is not readily available.
- Component count.

The approach adopted has been to list the components and system features required for each architecture and exclude those components which are common to all systems, e.g. isolators, polarisation control etc. In this way the complexity of specific components which contrast the different system architectures will be most strongly emphasised.

A complexity factor has been assigned to each component and weighted in such a way that the sum for all components within a given architecture will be representative of that system and can be used to compare different systems.

Below we indicate the components which were considered and where appropriate comment on the technical risk.

Source Linewidth

The homodyne and phase modulated systems all require linewidths of ~1 MHz or below. Therefore a laser (not necessarily a DFB laser) with a long external cavity is required. Such a device is not available at present and a special development program would be required. Both complexity and risk is regarded as large. At low (<100 MHz) datarate ASK heterodyne and FSK

systems require linewidths in the 1-10 MHz range, this can be achieved by using a DFB laser coupled to a coated GRIN rod lens, the complexity and risk is less. For datarates >100 MHz it becomes possible to use DFB lasers without any linenarrowing, such devices are available already.

Modulation

ASK is best performed using external modulation, the problem is that a high extinction ratio is required. Also, PSK requires external modulation. FSK can be performed by direct modulation but equalisation of the nonuniform FM response is needed. The relative difference in both complexity and risk between the various systems is small.

Receiver Bandwidth

This becomes a problem for dual filter FSK systems at high datarates. In the case of a relative bandwidth of two times the data rate and a filter separation of four times the datarate the upper filter will be centered around a frequency of six times the datarate. The required receiver bandwidth may therefore be a problem for dual filter FSK systems at high datarates whereas no particular problems are expected for the other cases.

Splitter

Use of a simple single detector scheme in heterodyne systems may even in the case of optimum splitting ratio lead to a penalty due to finite local oscillator power. This penalty increases drastically with datarate and can be particularly large in dual filter FSK systems. The penalty can be reduced by using a dual detector approach at the cost of added complexity. As an additional benefit of the dual detector scheme excess local oscillator noise is cancelled, the added complexity therefore seems worthwhile, at least for high datarate heterodyne systems.

Filters, etc.

The complexity of the receiver design increases with increasing datarate. When frequencies of ~1 GHz or more are present it may be necessary to go to a stripline approach rather than using lumped elements. This is the case for FSK dual filter systems at moderate and high datarates.

Optical Phase Tracking

The homodyne and PSK heterodyne systems require an optical phase locked loop. Such a device is not available at present and would require a special development program. The added complexity and risk is large.

Demodulation

Synchronous demodulation in ASK heterodyne and FSK systems gives a 0.3dB (0.46 dB for FSK dual filter) advantage over envelope detection. The added complexity, however, does not make this potential improvement attractive.

A complexity factor has been assigned to each component in a system architecture (except those common to all architectures) using the scale:

0 : Baseline against which difficulty/effort is measured
1 : Some effort/difficulty
2 : Significant
3 : Considerable
4 : Very difficult

The assignment of a complexity factor to a component is clearly subjective, though maximum objectivity has been achieved by incorporating a broad spectrum of opinion. The complexity factors for the components in each architecture are shown in Table 3.6. It can be seen that many depend on

the data rate. Whilst we are confident in the assignments given to each component it is questionable as to how meaningful is the quantity derived from summing the complexity factors within a particular architecture. Small differences in the complexity totals are probably not particularly significant. However, we do believe that the trends between architectures and the data rate dependence is a useful guide in comparing overall system complexity.

	LASER LINEWIDTH	RECEIVER BANDWIDTH	SPLITTER DESIGN	FILTER DESIGN	DUAL FILTER COMPONENT COUNT	MODULATOR	TRACKING	DUAL DETECTOR	DEMOD.	TOTAL
ASK HET/ENV/1D	2/1/0	0/0/1	0/0/1	0/0/1		2		0		4/3/5
ASK HET/ENV/2D	2/1/0	0/0/1	0	0/0/1		2		1		5/4/5
ASK HET/SYNC/1D	2/1/0	0/0/1	0/0/1			2		0	2	6/5/7
ASK HET/SYNC/2D	2/1/0	0/0/1	0	0/0/1		2		1	2	7/6/7
ASK HOMODYNING	4/3/3	0	0	0		2	4	0		10/9/9
FSK ENV/IF/1D	2/1/0	0/0/1	0/1/1	0/0/1		0		0		2/2/3
FSK ENV/1F/2D	2/1/0	0/0/1	0	0/0/1		0		1		3/2/3
FSK ENV/2F/1D	2/1/0	0/1/3	0/1/1	0/1/3	1	0		0		3/5/8
FSK ENV/2F/2D	2/1/0	0/1/3	0	0/1/3	1	0		1		4/5/8
FSK SYNC/1F/1D	2/1/0	0/0/1	0/1/1	0/0/1		0		0	2	4/4/5
FSK SYNC/1F/2D	2/1/0	0/0/1	0	0/0/1		0		1	2	5/5/5
FSK SYNC/2F/1D	2/1/0	0/1/3	0/1/1	0/1/3	1	0		0	2	5/7/10
FSK SYNC/2F/2D	2/1/0	0/1/3	0	0/1/3	1	0		1	2	6/7/10
PSK HET/1D	4/3/2	0/0/1	0/0/1	0/0/1		1	4	0	2	11/10/12
PSK HET/2D	4/3/2	0/0/1	0	0/0/1		1	4	1	2	12/11/12
PSK HOMODYNE	4/3/3	0	0	0		1	4	0		9/8/8
DPSK 1D	4/3/2	0/0/1	0/0/1	0/0/1		1		0	1	6/5/7
DPSK 2D	4/3/2	0/0/1	0	0/0/1		1		1	1	7/6/7
MFSK 1D	4/3/2	0/0/1	0/0/1	0/0/1		0		0	1	5/4/6
MFSK 2D	4/3/2	0/0/1	0	0/0/1		0		1	1	6/5/6

TABLE 3.6: Complexity Ranking (20/100/300 Mb/s)

System Cost

A cost ranking has been developed in order to compare the relative cost of assembly for the full range of system architectures. In this case a cost for design, build and testing has been assigned to each component in the system. From this data a cost ranking has been evolved. Where this ranking differs from that for complexity is that all components are considered for each system architecture, together with the cost of final system assembly and testing. The cost ranking is shown in Table 3.7.

Discussion

The realisable coherent advantage is smallest for the ASK based systems as a consequence of ASK being the lowest sensitivity modulation format, and the 3db external amplitude modulator insertion loss. The lowest data rate ASK options yield the greatest coherent advantage (~5db) but the narrow laser linewidth required at a data rate of 20 Mb/s results in a high complexity system. The combination of performance and complexity issues eliminate ASK heterodyning systems from the options for recommendation.

Homodyning systems (ASK, PSK) and PSK heterodyning are eliminated from further consideration because of the high complexity and cost attributed to these system architectures. This is principally due to the requirement for optical phase control, and the high cost and complexity ranking reflects the need to develop an optical phase locked loop. This is technically very difficult to implement and is not a technique presently being investigated at Caswell.

All of the remaining options are ranked approximately the same in terms of cost, and so this criterion does not provide a preference. MFSK and DPSK offer amongst the best figures for coherent advantage, but are rated significantly higher than FSK in terms of complexity. FSK architectures using envelope detection for the demodulation offer the lowest complexity options, particularly when single filter detection (wide deviation FSK) is employed.

MOD. FORMAT	STYLE	DEMODULATION DETECTORS		20	100	200
ASK	HETERODYNE	ENVELOPE	SINGLE	1.1	1.1	1.1
ASK	"	"	DUAL	1.1	1.1	1.1
ASK	"	SYNCHRONOUS	SINGLE	1.1	1.1	1.1
ASK	"	"	DUAL	1.1	1.1	1.1
ASK	HOMODYNE			2.4	2.4	2.4
FSK		SINGLE FILTER ENVELOPE	SINGLE	1.0	1.0	1.0
FSK		"	DUAL	1.0	1.0	1.0
FSK		DUAL FILTER ENVELOPE	SINGLE	1.0	1.0	1.1
FSK		"	DUAL	1.0	1.0	1.1
FSK		SINGLE FILTER SYNCHRONOUS	SINGLE	1.0	1.0	1.0
FSK		"	DUAL	1.0	1.0	1.0
FSK		DUAL FILTER SYNCHRONOUS	SINGLE	1.0	1.1	1.1
FSK		"	DUAL	1.1	1.1	1.1
PSK	HETERODYNE	SYNCHRONOUS	SINGLE	2.4	2.4	2.4
PSK	"	"	DUAL	2.4	2.4	2.4
PSK	HOMODYNE			2.4	2.4	2.4
DPSK	HETERODYNE	DIFFERENTIAL	SINGLE	1.1	1.1	1.1
DPSK	"	"	DUAL	1.1	1.1	1.1
MFSK	"	"	SINGLE	1.0	1.0	1.0
MFSK	"	"	DUAL	1.1	1.1	1.0

TABLE 3.7: Cost Ranking

Recommendation

We conclude that FSK systems, employing envelope detection offer the best overall balance between performance, complexity and cost, and consequently our recommendation was to adopt an architecture based on the FSK modulation format for the system design of the experimental model. The largest coherent advantage could be demonstrated at the lowest data rate, but the demands on the laser linewidth increase the complexity. A data rate of ~100 Mb/s for a system employing single filter detection combines the lowest system complexity and cost together with the prospect of realising a significant coherent advantage. The specific recommendation was:

Modulation Format	:	FSK
Receiver Type	:	Dual detector (balanced receiver) Single filter detection (Wide deviation FSK)
Data Rate	:	140 Mb/s
Wavelength	:	1.55μm

The data rate of 140 Mb/s is recommended for several reasons. Many components developed for direct detection systems are readily available at this data rate and can be employed both in the coherent and direct detection digital system demonstrators. Adopting a data rate much lower than 140 Mb/s significantly increases the technical difficulty in achieving the necessary laser linewidth. Higher data rates require wider bandwidth receiver front ends, ıd this would reduce the prospect of being able to upgrade to a dual filter receiver. 140 Mb/s has the additional merit that it represents the data rate for uncompressed digital video and so the equipment could in the future be used in a demonstration to carry video information. A system design optimised for 140 Mb/s can never the less operate, thought not optimally, at lower data rates and thus permit its performance to be assessed at, say, 20 Mb/s. The reverse situaton would not be true.

4. ANOLOG COHERENT SYSTEMS STUDY AND ANALYSIS

4.1 ANALOG SYSTEM CONFIGURATIONS AND THEORETICAL PERFORMANCE LIMITS

The possibility of carrying analog signals in a coherent fiber optic link has received little attention. The published work is limited[5,6] and relates to the application of CATV distribution. Here the bandwidth advantage of using analog transmission compared with digital is an asset. Within this programme a study has been carried out to assess system architectures, system performance, and technology issues for analogue coherent fibre optic links. This has been compared with the situation for a direct detection implementation for the same analogue signals. These studies have been carried out within the context of the transmission requirements described in the statement of work. These are: analogue signals representing microwave carriers in the range 1 to 10 GHz with modulation bandwidth of ten per cent of the carrier frequency and link distance of 1Km. The short transmission distance has the consequence that the received optical power levels will realistically be up to a few hundred microwatts. The signal spectrum we are considering is shown in Fig. 4.1 but the analysis carried out can be generalised to a baseband system through the transformation $f_{mc}=f_s$.

In a direct detection link only amplitude modulation (AM) is possible, whether implemented by direct modulation of the laser or through an external modulator. The performance of this system architecture has been analysed for receivers featuring both unity gain PIN diode and avalanche photodiode (APD) detectors, with front-end amplifiers based on low noise FET designs (broadband and 'tuned' narrowband) and 50Ω broadband/narrowband microwave amplifiers.

Coherent optical communication techniques offer a wider range of modulation and demodulation techniques, and the component and performance issues are

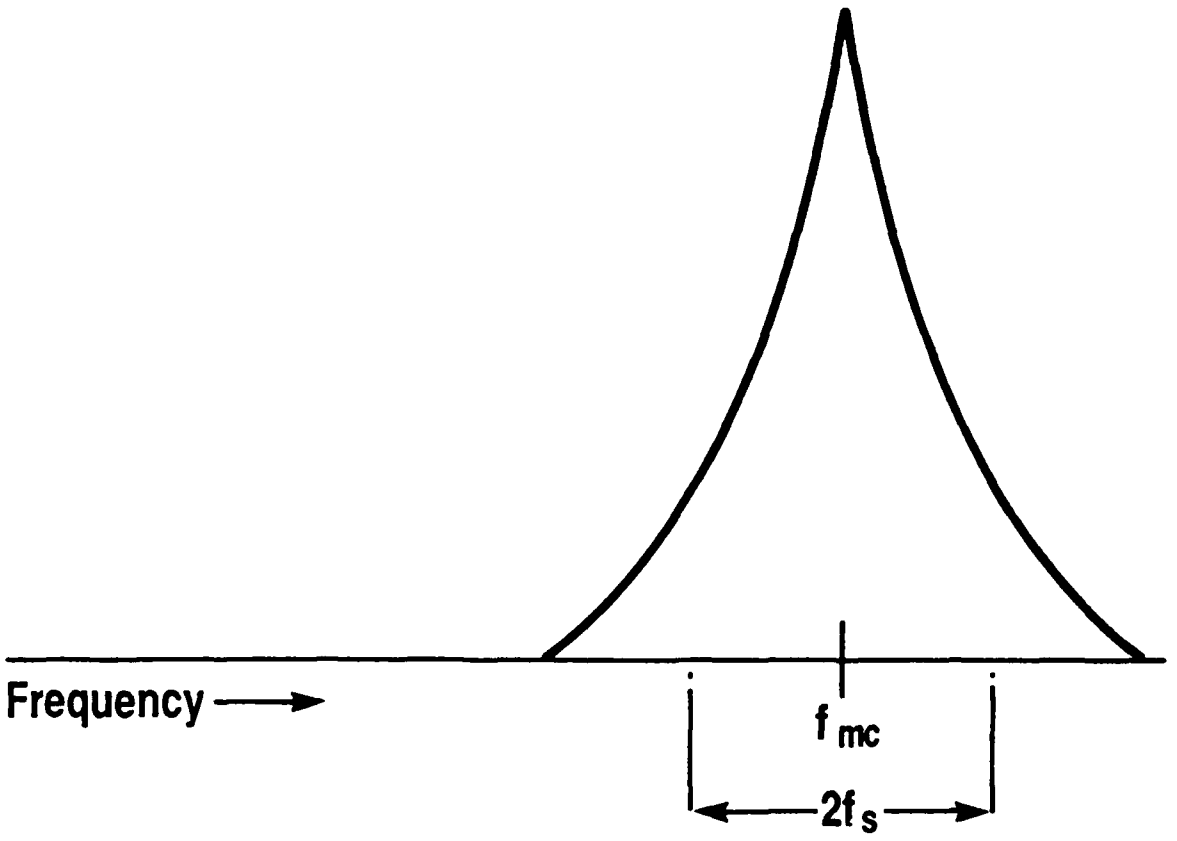

Generalise to baseband signal via: $f_s = f_{mc}$

Figure 4.1: Signal Spectrum for Analog Link SNR Calculations

more complex. The following have been considered in the system analysis for coherent link architectures:

- Modulation formats: AM, PM, and FM
- Heterodyning and homodyning receivers
- Component technology issues for system implementations
- SNR achievable on the local oscillator shot noise limit
- Assessment of receiver penalties
  - finite local oscillator power
  - laser phase noise
- Assessment of theoretical performance limits and realisable performance with present day component technology

Figures 4.2 and 4.3 show functional diagrams of a direct detection and heterodyne coherent detection fibre optic link. In the case of direct detection only intensity modulation is possible and this would normally be carried out using an external amplitude modulator to avoid distortion due to non-linear characteristics of the laser when modulated directly. For this case the received optical power takes the form

$$P(t) = P_r \left(1+K_a m(t)\right) \qquad (4.1.1)$$

Where P_r is the mean received optical power, m(t) the transmitted signal (normalised) and K_a the modulation index (less than unity). For the coherent configuration shown in Figure 4.3 optical AM, FM and PM are possible. For OAM and OPM an external amplitude or phase modulator is necessary, but for OFM it would be possible to modulate the laser directly. Whether direct modulation of the laser is desirable would be dependent on the FM modulation characteristic of the laser, the magnitude of the modulation of the laser drive current (modulation index), the associated AM, and any impact on the stability or linewidth of the source. Equation 4.1.1 also holds in the case of an AM coherent link. For PM and FM the

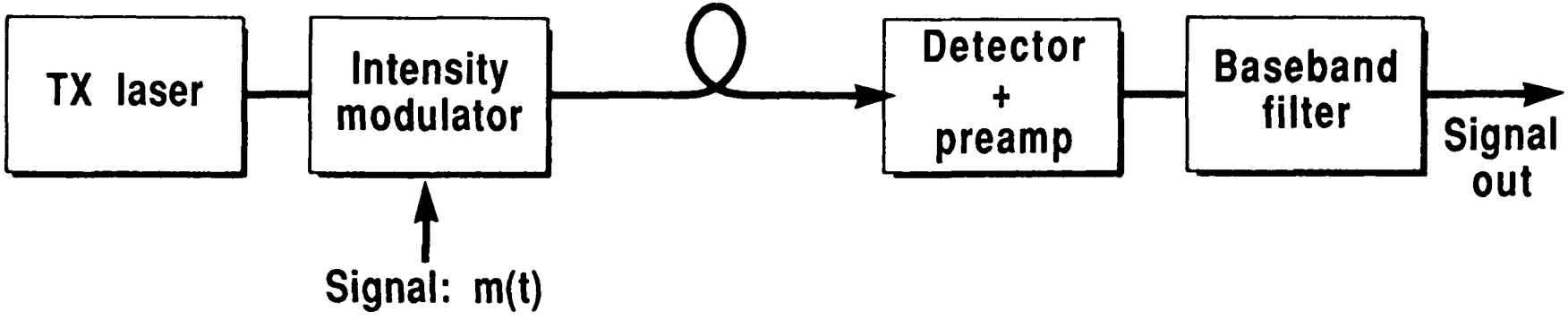

Received signal intensity: $P(t) = P_r\ (1+K_a\ m(t))$

Modulation index K_a limited by linearity of intensity modulator

Figure 4.2: Intensity Modulation and Direct Detection Analog Fiber Optic Link

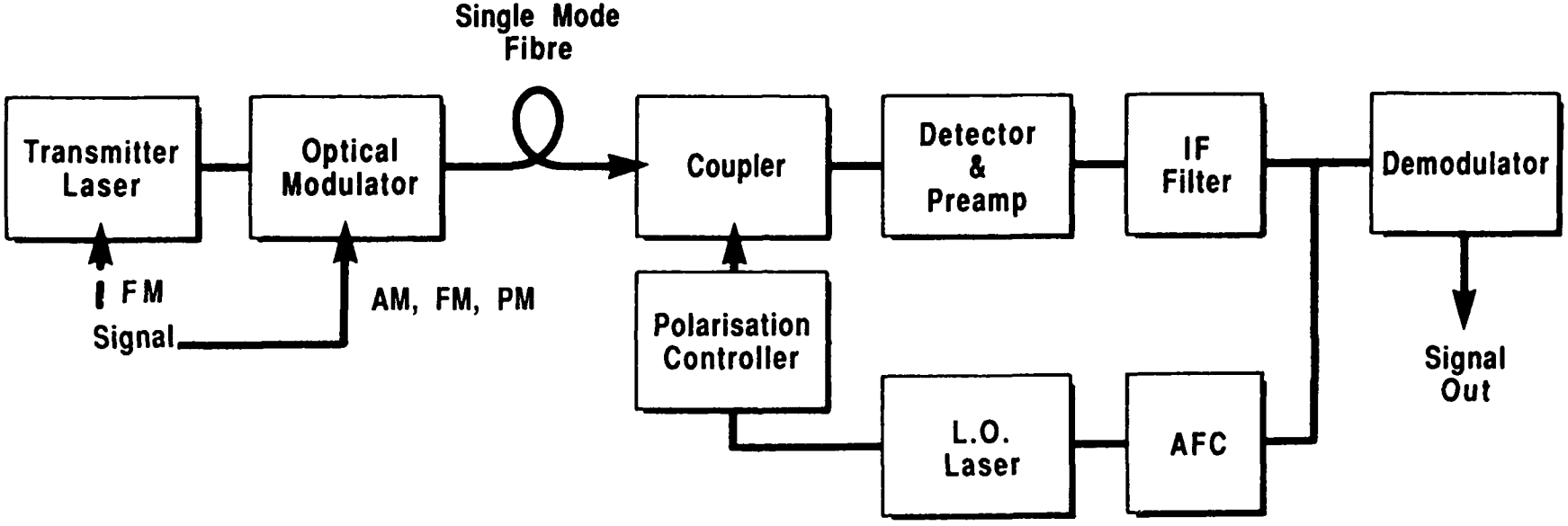

Figure 4.3: Functional Diagram of a Heterodyne Coherent Fiber Optic System (Analog Format)

effect of the modulation can be expressed in terms of the signal field amplitude $E_s(t)$.

$$E_s(t) = E_c \exp\left(j[\omega_c t + \theta(t)]\right) \qquad (4.1.2)$$

and where we have:

$$\theta = K_\theta m(t) \qquad \text{(PM)} \qquad (4.1.3)$$

$$\theta = K_f \int^t m(t')dt' \qquad \text{(FM)} \qquad (4.1.4)$$

K_θ and K_f are the modulation indices, and K_f can be related to the usual form of FM modulation index, β, through the relationship.

$$\beta = \frac{K_f}{2\pi_{fm}} \qquad (4.1.5)$$

fm being the modulation frequency.

Calculations have been carried out for the signal to noise ratio (SNR) of a direct detection link to act as a reference for comparison with coherent systems. The theoretical expressions for SNR are shown in Figure 4.4 and results are illustrated in Figure 4.5. The appropriate way of presenting results for analog transmission is to plot SNR as a function of mean received optical power. The cases considered include both low noise PIN/FET front ends and the combination of a detector and 50Ω microwave amplifier. For the case of a microwave carrier frequency of 10 GHz an amplifier noise figure of 4.5dB is assumed. All the calculations presented here are for an optical wavelength of 1.55μm.

As the starting point for the analysis of the SNR performance of coherent anolog links we have evaluated the SNR of the analog formats in the limit of infinite local oscillator power and neglected any form of system impairment. The expressions for this theoretical limit are shown in Table 4.1.

1. **Broadband low noise PIN/FET**

$$SNR = \frac{R^2 P_r^2 K_a^2 \langle m^2(t) \rangle}{A f_s + B f_s (f_s^2 + 3 f_{mc}^2)}$$

2. **'Tuned' Narrow Band PIN/FET**

$$SNR = \frac{R^2 P_r^2 K_a^2 \langle m^2(t) \rangle}{A f_s + 4 B f_s^3}$$

3. **50Ω microwave amplifier**

$$SNR = \frac{R^2 P_r^2 K_a^2 \langle m^2(t) \rangle}{A f_s + \frac{8kT}{50}(F-1) f_s}$$

F = **amplifier noise figure**

Note: **with APD,** $P_r \rightarrow M P_r$ (signal),

$$A \rightarrow 4q(RP_r + I_D) M^2 F(M) + 8kT/R_L$$

$$A = 4qRP_r + 4qI_D + 8kT/R_L$$

$$B = 32kT\Gamma\pi^2 C_T^2 / 3 g_m$$

Figure 4.4: Signal to Noise Ratio expressions for Direct Detection Analog Receivers

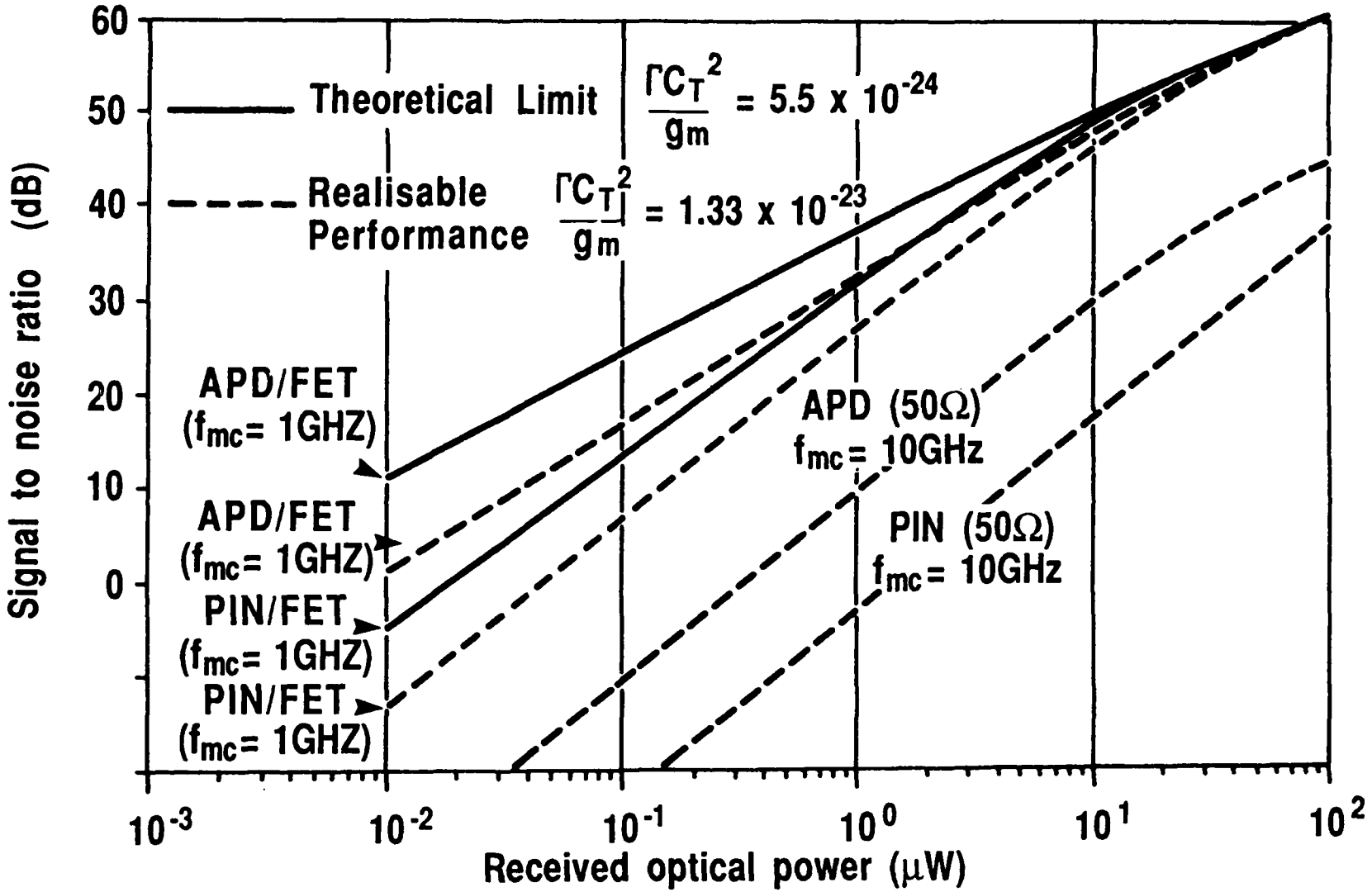

Figure 4.5: Signal to Noise Ratio Calculations for Direct Detection Analog Receivers

Modulation/Receiver Type		*SNR*
AM	Heterodyning	$\mathcal{R} P_r K_a^2 / 8qB$
	Homodyning	$\mathcal{R} P_r K_a^2 / 4qB$
FM	Heterodyning	$3\mathcal{R} P_r \beta^2 (f_{mc} + B/2)^2 / 2qB(3f_{mc}^2 + B^2/4)$
	Homodyning	$3\mathcal{R} P_r \beta^2 (f_{mc} + B/2)^2 / qB(3f_{mc}^2 + B^2/4)$
PM	Heterodyning	$\mathcal{R} P_r K_\theta^2 / 2qB$
	Homodyning	$\mathcal{R} P_r K_\theta^2 / qB$

R: Detector responsivity
Pr: Received optical power
Ka, ß, Ko: Modulation indices

f_{mc} : Carrier frequency
B: Signal bandwidth

Table 4.1: Signal to Noise Ratios for Coherent Detection of Analog Signals in the Local Oscillator Shot Noise Limit

Illustrative calculations are presented in Figures 4.6 and 4.7, for the cases of carrier frequencies of 1 and 10 GHz and a signal bandwidth of ten percent. These results indicate a substantial potential SNR advantage over a direct detection system, particularly at low received optical power. At high received optical power levels the direct detection performance approaches that of AM homodyning since in this limit the shot noise from the received optical signal dominates the noise performance of both systems. Of the analog formats for a coherent link, PM and FM offer the best theoretical performance, with the FM case being strongly dependent on the modulation index β.

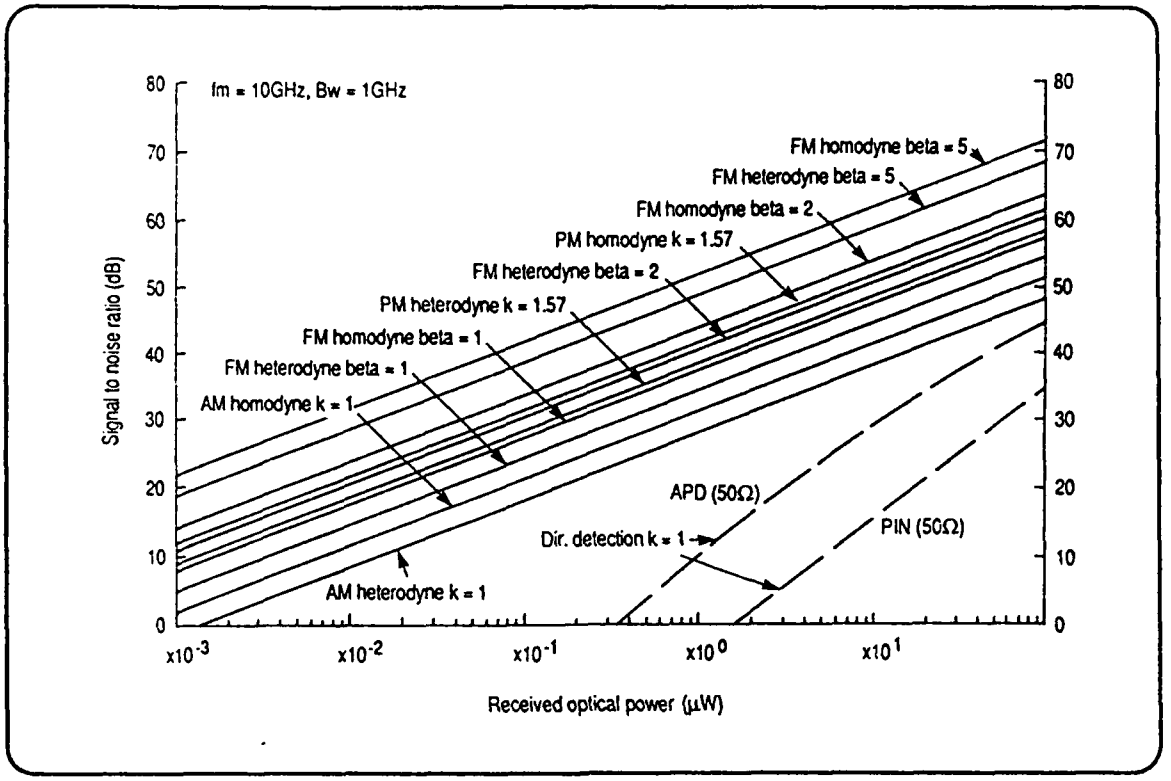

Fig. 4.6 SHOT NOISE LIMITED SNR FOR SINUSOIDAL SIGNAL MODULATION

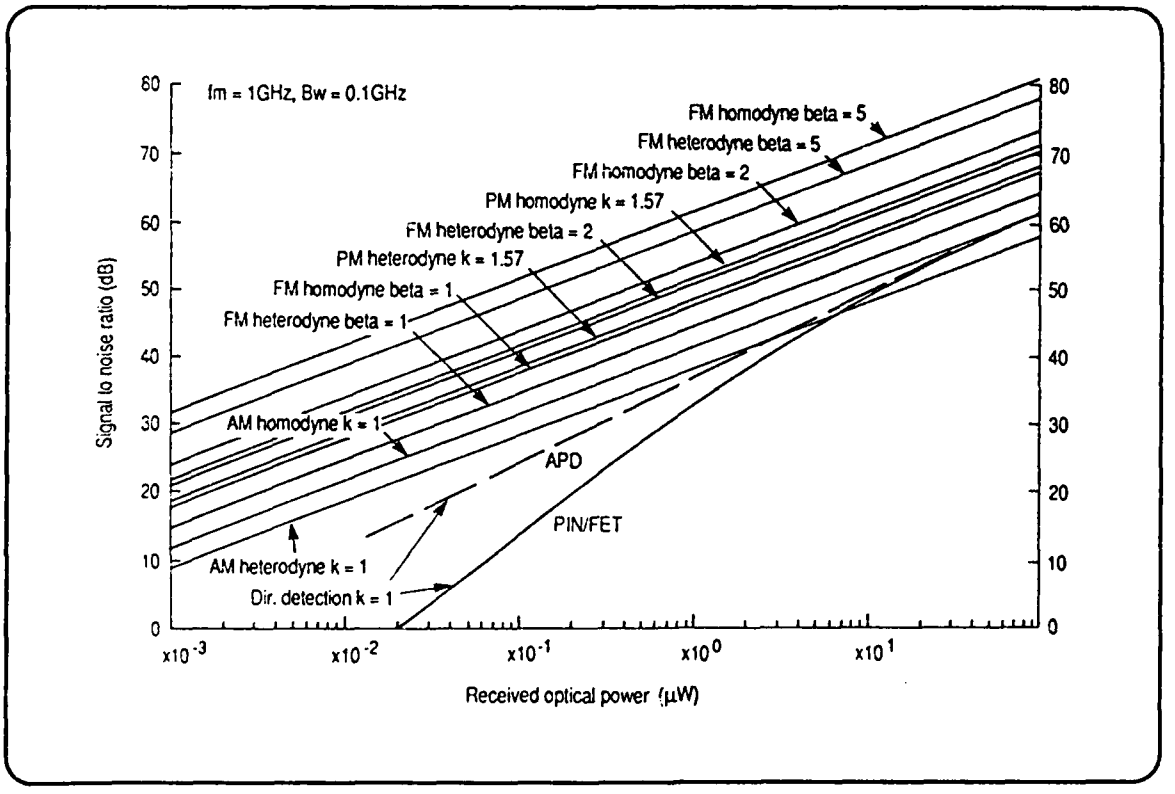

Fig. 4.7 SHOT NOISE LIMITED SNR FOR SINUSOIDAL SIGNAL MODULATION

4.2 ANALOG LINK PERFORMANCE CONSTRAINTS

Many factors can be responsible for degrading the performance of coherent detection links from the theoretical limits. For digital links the relevant factors were discussed in section 3.2, and many of these are equally pertinent for the case of analog systems. However the significance of some of these issues may differ because of the analog nature of the signal, or because of the transmitter and receiver design needed to accommodate the high frequency microwave carrier as shown in Figure 4.1. Issues which require particular study because of these points are:

- Finite local oscillator power
- The influence of laser linewidth (phase noise)
- Distortion due to system non-linearities

These will now be discussed.

Finite Local Oscillator Power

The penalty due to finite L.O. power is essentially the ratio of the front-end amplifier noise to the detector shot noise arising from the L.O. laser. This is clearly a strong function of the available L.O. power and the type of receiver front-end used. The expressions for the degradation factor χ are shown below for various types of receiver, adopting conventional notation.

1. Broadband low noise PIN/FET

$$\chi = 1 + \frac{8\pi^2 \Gamma C_T^2 KT}{qRP_L g_m} \left(f_{IF}^2 + f_{mC}^2\right) \qquad (4.2.1)$$

2. 'Tuned' Front-end (tuned to IF)

$$\chi = 1 + \frac{32\pi^2 \Gamma C_T^2 KT}{qRP_L g_m} f_{mC}^2 \qquad (4.2.2)$$

3. Broadband/Narrowband 50Ω microwave amplifier

$$\chi = 1 + \frac{2KTF}{qRP_L 50} \qquad (4.2.3)$$

The penalty associated with finite L.O. power is obtained in dB by taking 10 log of the expressions above. Figure 4.8 illustrates calculations of this penalty both for a low noise PIN/FET receiver and for a PIN detector with 50Ω microwave amplifiers of various noise figures F. For the latter case the penalties are clearly large for realisable levels of L.O. power.

Laser Phase Noise

Laser phase noise has been shown to be an important consideration in the design of digital coherent links. Much work has been done on the analysis of the influence of laser phase noise in digital systems and the phenomenon is now well understood. However, to date the situation in analog systems has not been addressed, yet intuitively the effect could be similarly dramatic. In terms of a measurable laser parameter, laser phase noise manifests itself through the laser linewidth. In PM and FM systems the phase or frequency fluctuations in the laser spectrum impact directly on the signal information. In an AM system the phase noise causes the laser frequency to fluctuate and this can cause the IF to fluctuate rapidly within the filter. In all cases the laser phase noise introduces a SNR penalty. The penalty can be expressed in two ways in an analog system. The first is to quantify the effect in terms of the magnitude of laser linewidths which can be tolerated such that the SNR is degraded by no more than a given factor relative to the L.O. shot noise limit. The second is to establish the magnitude of the SNR floor which exists when phase noise dominates, for a specified laser linewidth. Analytical expressions have been derived for the laser phase noise penalties in PM and FM systems.

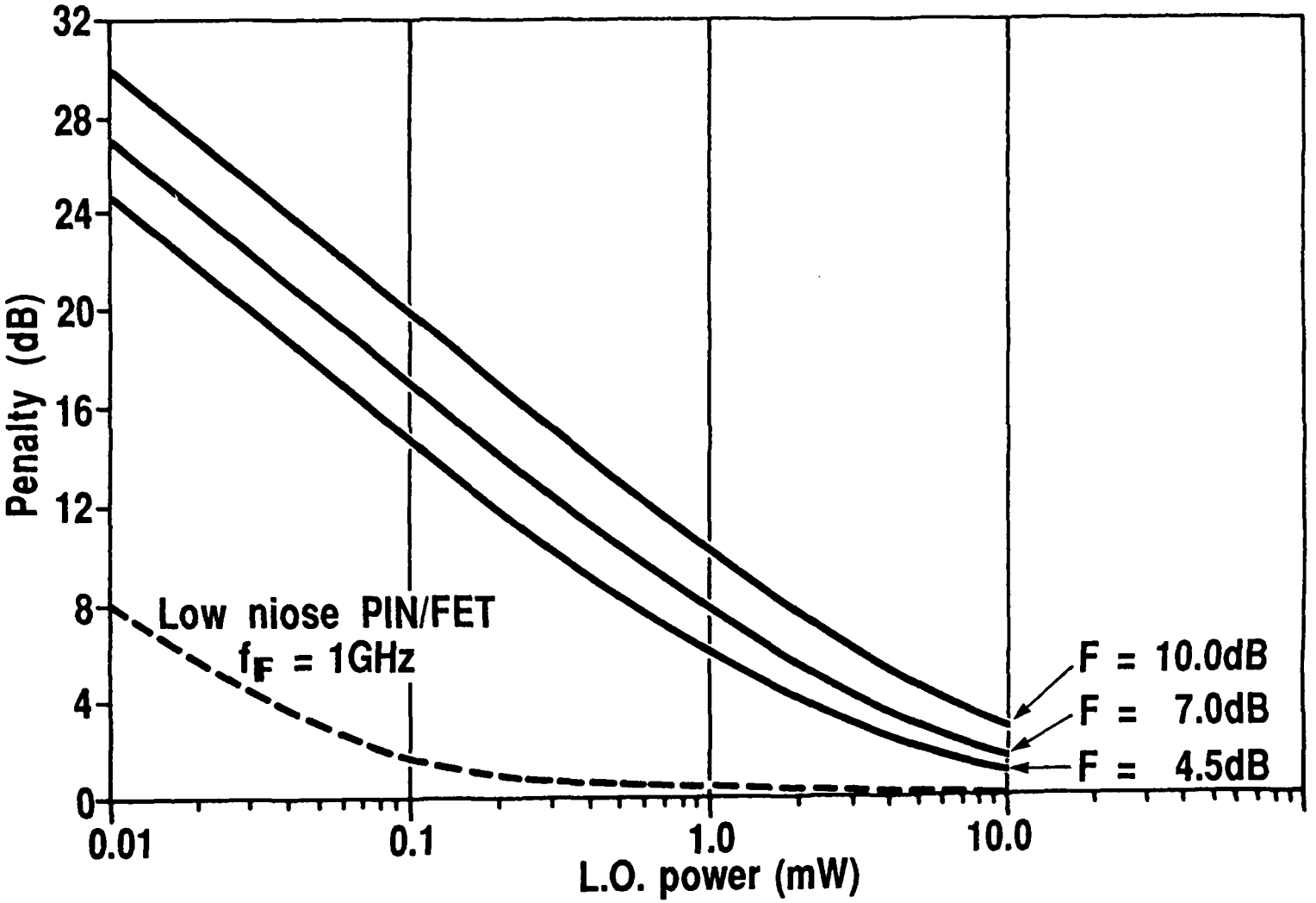

Figure 4.8: Finite Local Oscillator Power Penalty

PM SYSTEMS

The Demodulated signal is proportional to the phase difference between the transmitter and L.O. lasers, which is

$$= K_\phi m(t) + \Delta\phi(t) \text{ (+ receiver noise)} \qquad (4.2.4)$$

where $\Delta 0(t)$ corresponds to the phase fluctuations due to laser phase noise. The analysis treats $\Delta\phi(t)$ as giving rise to an additive noise contribution to the output signal, where it is known that

$$\langle \Delta\phi^2 \rangle = 2\pi\Delta\nu/B \qquad (4.2.5)$$

The effect can be analysed in terms of an equivalent input noise current generator of magnitude

$$\overline{I_n^2}_\phi = \frac{8\pi\Delta\nu R^2 P_r P_L}{B} \qquad (4.2.6)$$

where $\Delta\nu$ = Laser linewidth (assumed identical)
and B = Filter bandwidth (baseband for homodyning)

This enables the effect on SNR to be calculated.

The SNR floor is then easily calculated to be

$$SNR_{FLOOR} = \frac{K_\theta^2 B}{4\pi\Delta\nu_{IF}} \qquad (4.2.7)$$

and for an SNR penalty of $(1 + \xi)$ yields,

$$\Delta\nu_{IF} = \xi \frac{qB^2}{2\pi R P_r} \qquad (4.2.8)$$

where:

$\Delta\nu_{IF}$ = IF spectral width (L.O. + signal laser)
B = filter bandwidth (final lowpass)
ξ = degradation factor (relative to shot noise limit)

Results of calculations based on equations 4.2.7 and 4.2.8 above are shown in Figures 4.9 and 4.10.

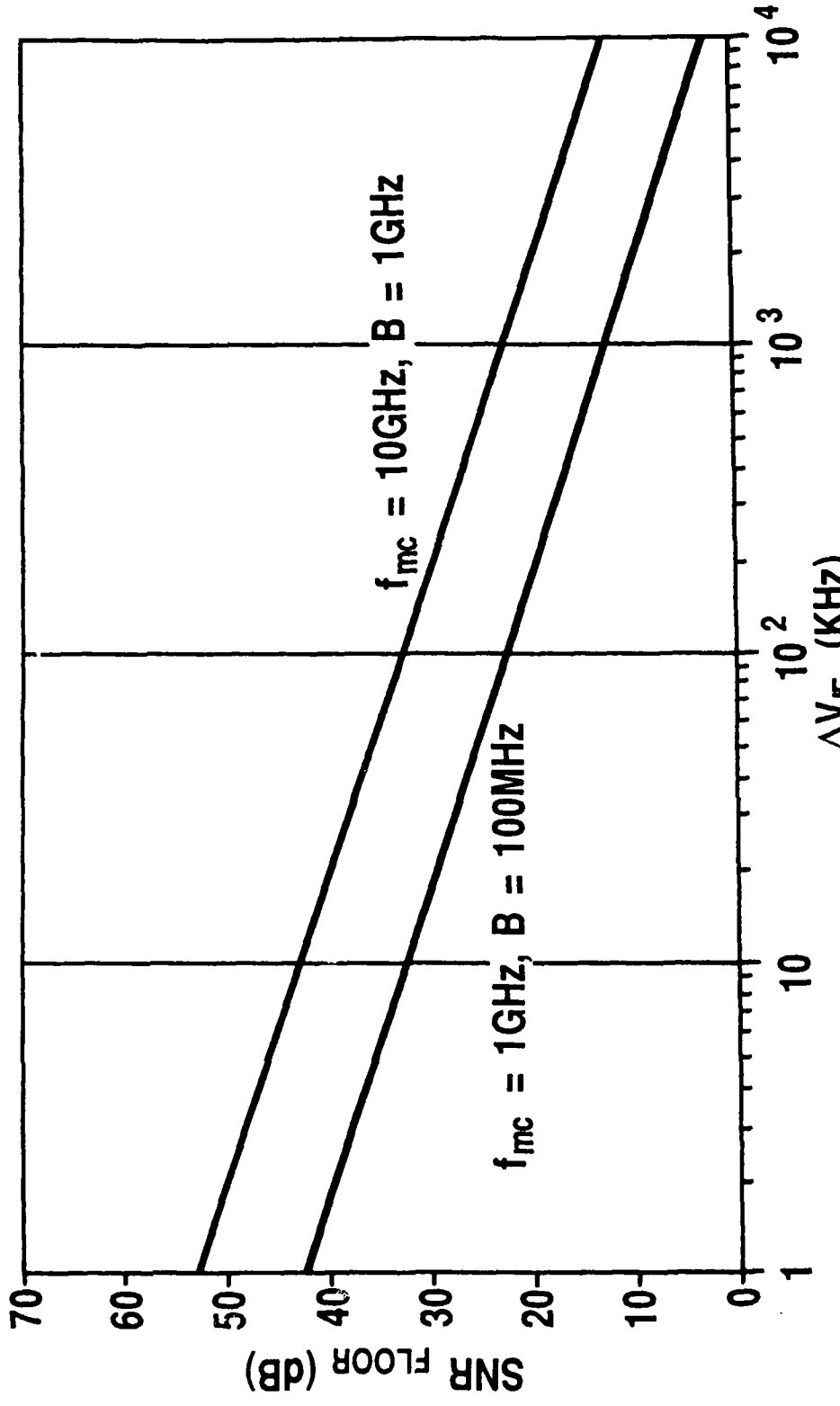

Figure 4.9: SNR Floors due to Laser Phase Noise in PM Systems

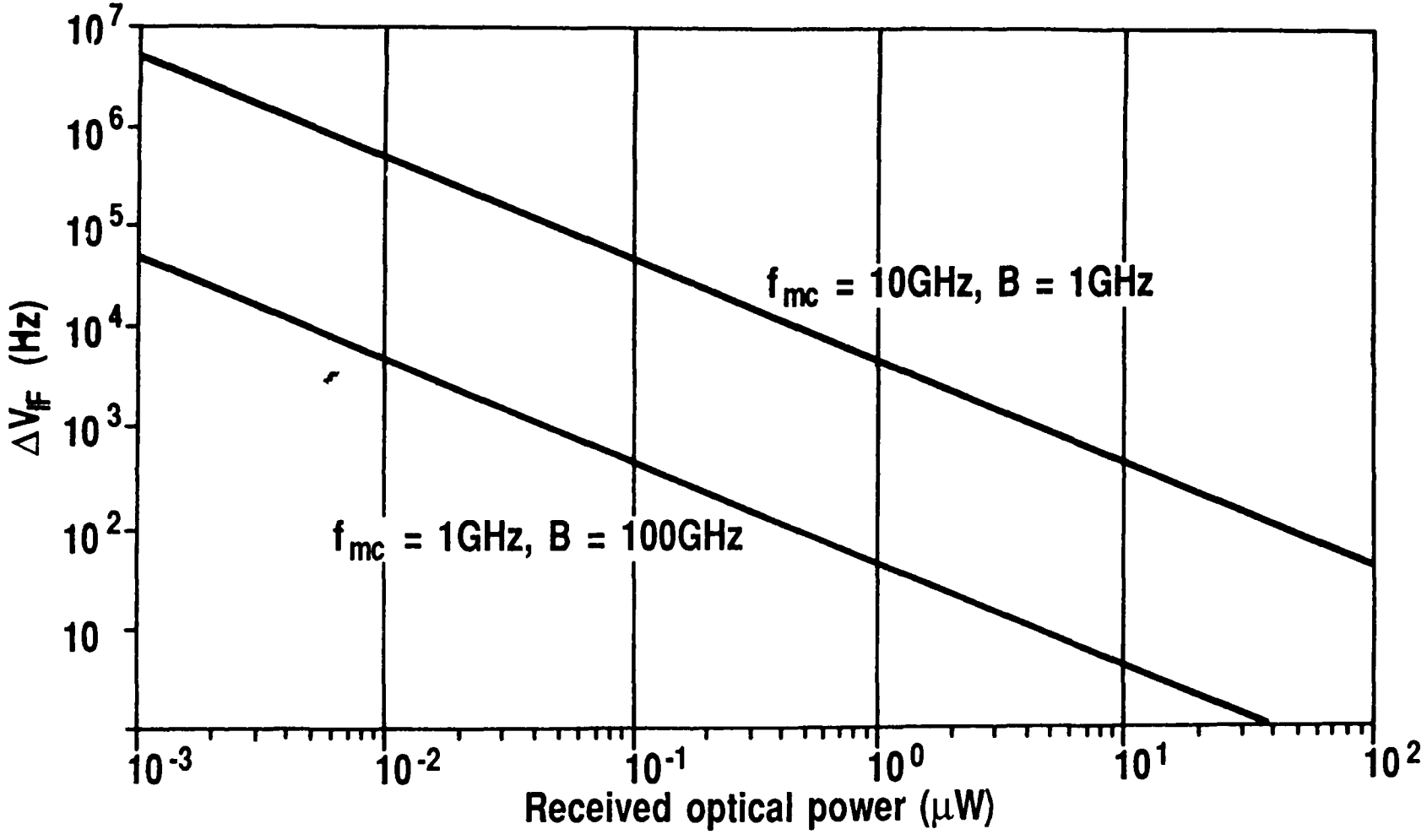

Figure 4.10: IF Spectral Width for 1dB SNR Penalty Relative to L.O. Shot Noise Limit

FM SYSTEMS

In this case the demodulated signal is proportional to the derivative of the phase difference between the transmitter and L.O., which is

$$= 2\pi K_f m(t) + \frac{d\Delta\phi(t)}{dt} \text{ (+ receiver noise)} \qquad (4.2.9)$$

We can again treat phase noise (or strictly its derivative) as an additive noise contribution, and use the known relationship

$$\langle \left(\frac{d\Delta\phi}{dt}\right)^2 \rangle = 4\pi\Delta\nu B \qquad (4.2.10)$$

The equivalent input noise current generator is then

$$\overline{i_{nf}^2} = 16\pi\Delta\nu R^2 P_r P_L B \; / \; f_m^2 \qquad (4.2.11)$$

where f_m is the modulation frequency (sinusoidal input signal).

The SNR floor is then calculated as

$$SNR_{floor} = \frac{\pi\beta^2 f_m^2}{2\Delta\nu_{IF} B} \qquad (4.2.12)$$

and a SNR penalty of $(1 + \xi)$ yields,

$$\Delta\nu_{IF} = \xi \frac{q\pi f_m^2}{RP_r} \qquad (4.2.13)$$

where:

f_m = maximum modulation frequency ($\sim f_{mc}$)

B = filter bandwidth (low pass)

The results of calculations using equations 4.2.12 and 4.2.13 are shown in Figures 4.11 and 4.12 and, as for the case of phase modulation, indicate the severe requirements on laser linewidth, particularly when large SNR is required.

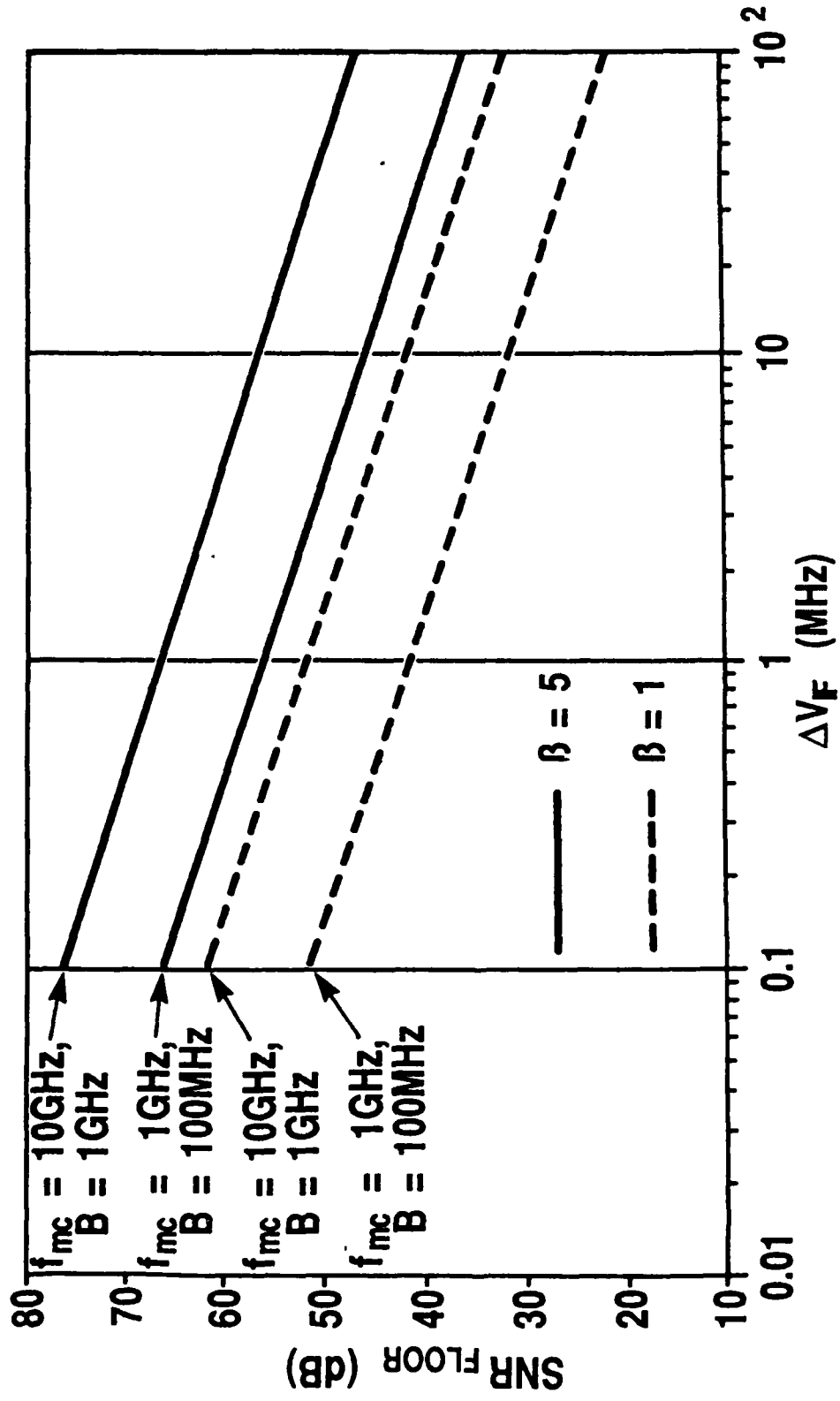

Figure 4.11: SNR Floor due to Laser Phase Noise in FM Systems

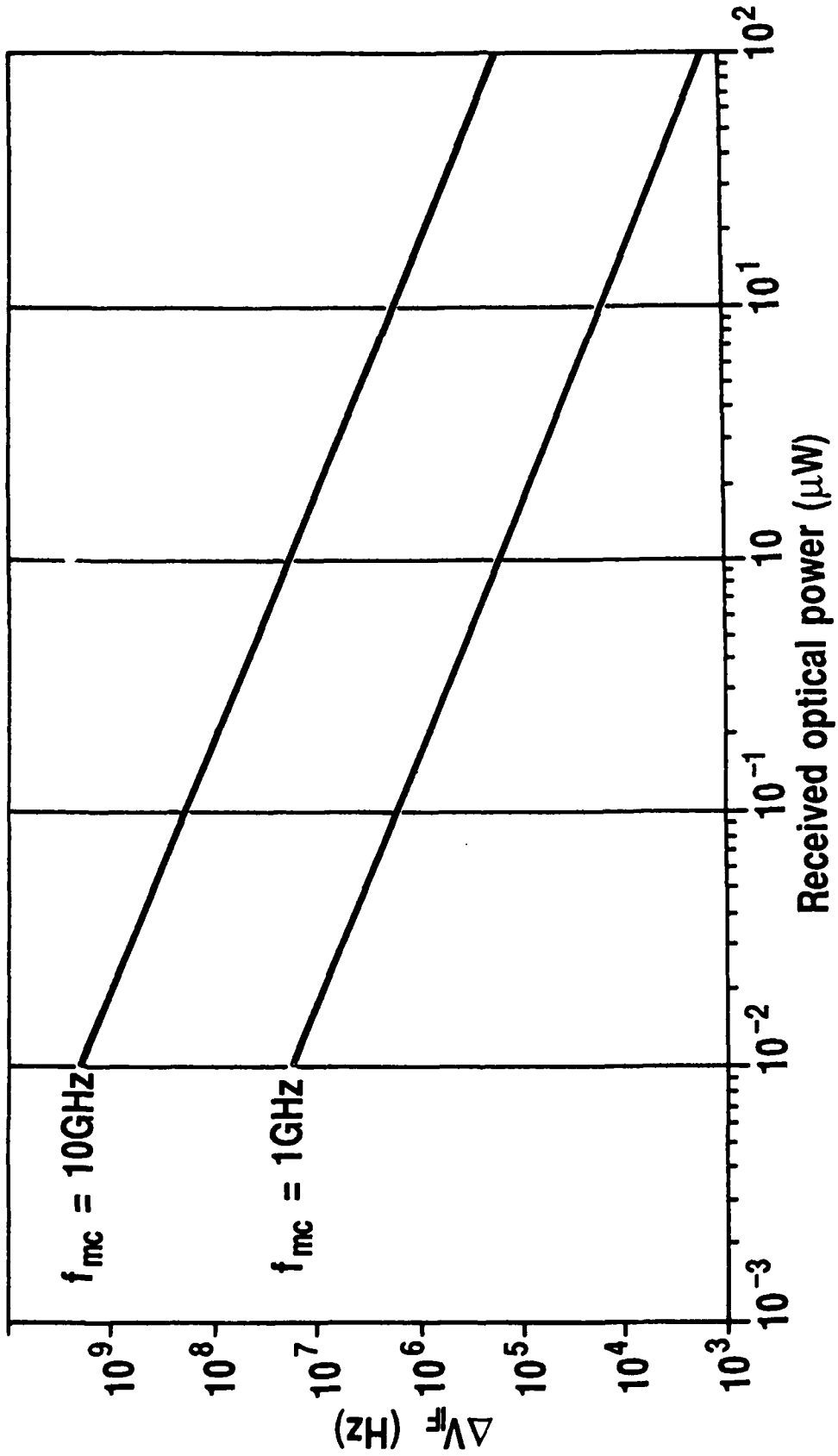

Figure 4.12: IF Spectral Width for 1dB SNR Penalty Relative to L.O. Shot Noise Limit

AM SYSTEMS

The situation in AM systems is different. The laser phase noise causes the IF to fluctuate so that the signal spectrum moves within the IF filter. Under these conditions part of the signal spectrum may fall outside of the filter and introduce distortion. The laser phase noise therefore strictly gives rise to a distortion related penalty. This problem has not proved amenable to analytical solution and so numerical simulation techniques have been adopted in order to quantify the effect. The noise spectral density is evaluated as the difference between the input and output signal spectral densities averaged over the distribution of intermediate frequency fluctuations due to the laser phase noise. The simulations have been used to calculate the SNR floor and the results are shown in Figure 4.13. We have assumed for the purpose of these calculations a flat IF filter with sharp cut-off. The results confirm and quantify what is intuitively expected, that by broadening the IF filter to better contain the signal spectrum, the effect of laser phase noise is reduced. Also evident is that, in common with digital systems, AM is the format which is most tolerant of laser phase noise.

Distortion

The general question of distortion in analog systems leads to consideration of the modulation and demodulation techniques. In AM coherent links, as with direct detection, distortion arises from the non-linear characteristics of the intensity modulator. These systems require the modulation index to be restricted such that the relationship between optical intensity and drive voltage is linear. In a PM system the demodulated signal is also proportional to $\sin K_\theta m(t)$ so that in a similar fashion it is necessary to restrict the modulation index in order to control the level of distortion. In optical FM systems the situation is

more complex and signal distortion is a function of the FM response characteristic of the laser or external modulator, and the linearity of the FM demodulator. It is therefore very difficult to quantify non-linearities and distortion levels in optical FM systems but in principle the use of optical FM does hold the possibility of greater signal fidelity than AM or PM systems.

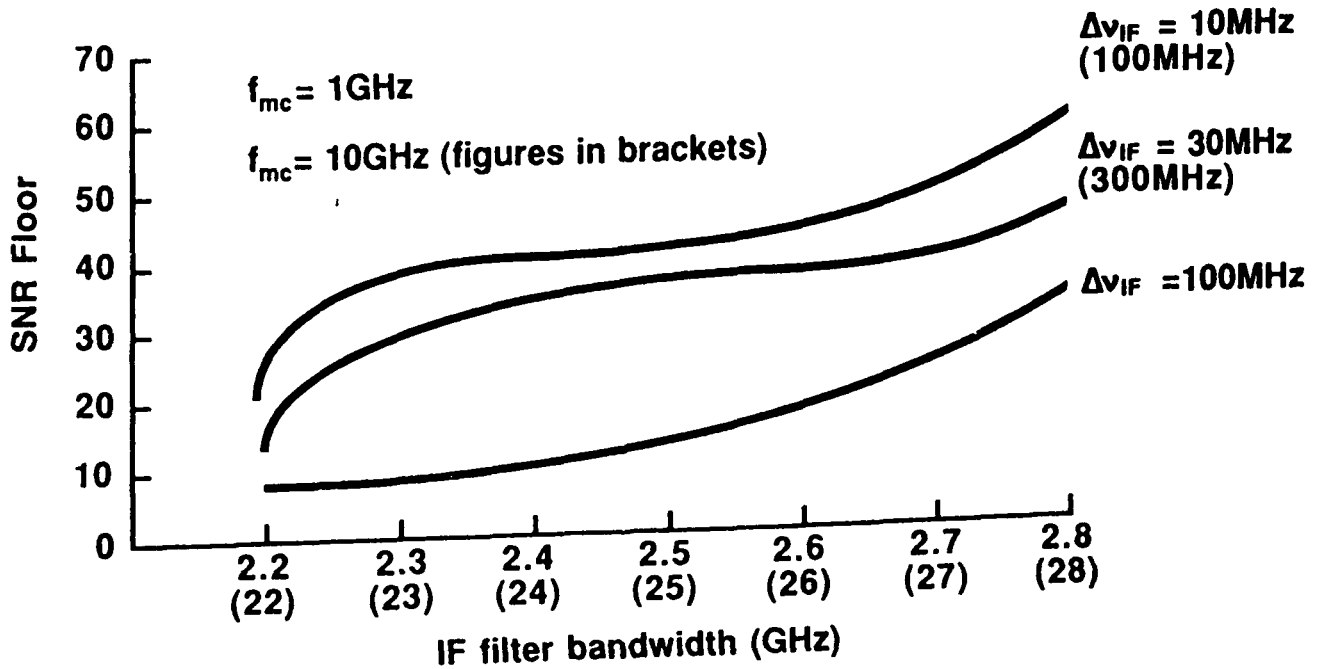

Figure 4.13: Effect of IF Filter Bandwidths on SNR Floor for AM Systems

4.3 REALISABLE PERFORMANCE

In order to assess the performance which could be realisable in an analog link, calculations of SNR have been carried out using parameters for amplifier, detector, and laser technology accessible at the present time. For the purposes of these calculations the following general assumptions are made:

- L.O. power on the detector : 0.5mW
- Laser linewidth : 15 MHz (AM, FM)
  5 kHz (PM)
- Where receiver bandwidth is greater than 3 GHz, the receiver is a 50Ω microwave amplifier with detector. Noise figure 4.5-10dB dependent on bandwidth.

In the case of linewidth we take 15 MHz to be achievable with a very good DFB laser and 5 kHz from a state-of-the-art external cavity laser.

The results of these calculations are shown in Figures 4.14 and 4.15, and specific assumptions relating to these cases are given in Tables 4.2 and 4.3.

The calculations of the SNR for the FM cases assume that the CNR is sufficiently large that the theoretical basis for the FM SNR enhancement is valid, i.e. the signal levels are above those for which the 'threshold effect' is observed. The signal levels for the threshold effect have been estimated and marked in Figures 4.14 and 4.15. Although calculations are indicated for lower signal levels they cannot be relied upon for their accuracy; indeed it should be considered unwise to operate an FM system in this regime.

In analysing the results of Figures 4.14 and 4.15 a few general conclusions are readily drawn. The receiver bandwidth, local oscillator power, and

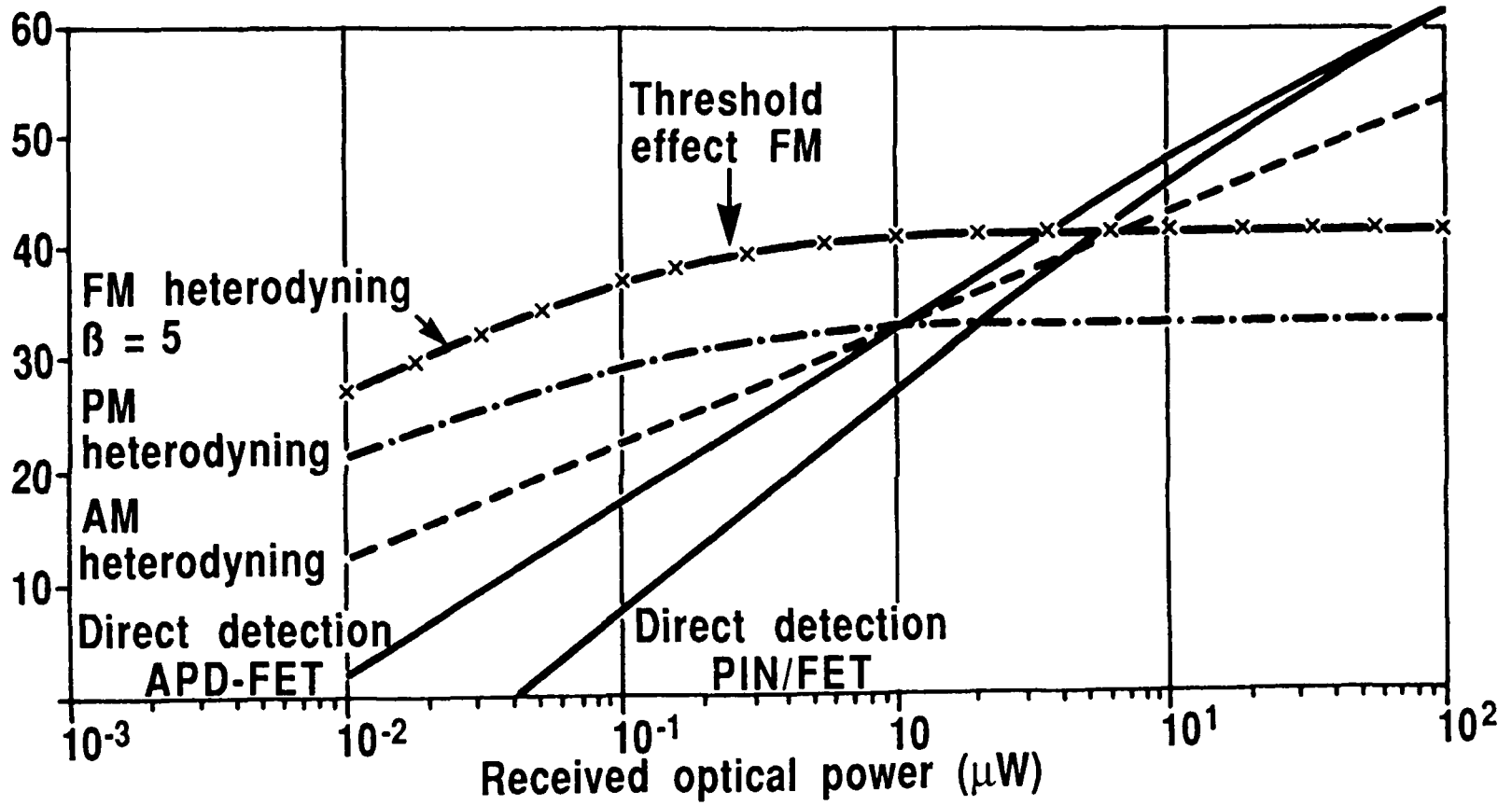

Figure 4.14: Realisable SNR (vertical scale in dB) Performance for case: f_{mc}=1 GHz, B = 100 MHz

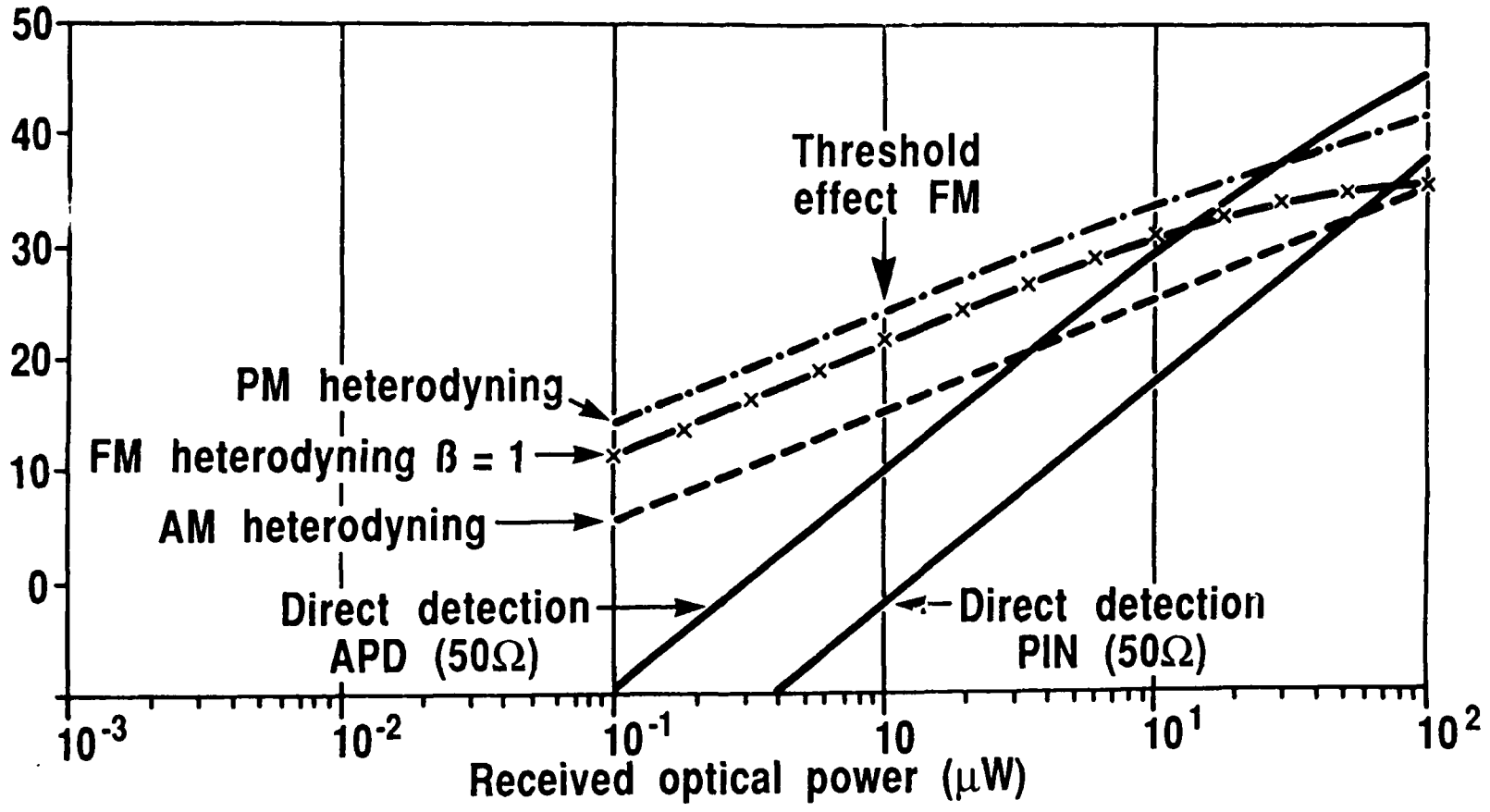

Figure 4.15: Realisable SNR (vertical scale in dB) Performance for the case: f_{mc}= 10 GHz, B = 1 GHz

TABLE 4.2

REALISABLE PERFORMANCE : ASSUMPTIONS

CASE 1 : f_{mc}=1 GHz, B=100 MHz

Direct Detection

PIN and APD with low noise FET preamp.

FET : $\Gamma C_T^2 / g_m = 1.33 \times 10^{-23}$

APD : $M \times B_{3db}$ = 40 GHz

AM Heterodyning

50Ω broadband amplifier : NF = 4.5dB

Finite L.O. power penalty : 6dB (balanced receiver)

No significant linewidth noise floor.

PM Heterodyning

50Ω broadband amplifier : NF = 4.5dB

Finite L.O. power penalty : 6dB

$\Delta\nu_{IF}$=10kHz, SNR_{floor}=33dB

FM Heterodyning

β=5, 50Ω amplifier: NF=7dB

Finite L.O. power penalty: 11dB

$\Delta\nu_{IF}$=30MHz, SNR_{floor}=41dB

β=1, SNR_{floor}=27dB

TABLE 4.3

REALISABLE PERFORMANCE : ASSUMPTIONS

CASE 2 : f_{mc}=10 GHz, B=1 GHz

Direct Detection

PIN and APD with 50Ω amplifier: NF=4.5dB

AM Heterodyning

50Ω broadband amplifier : NF = 10dB
Finite L.O. power penalty : 13dB
No laser linewidth penalty

PM Heterodyning

50Ω broadband amplifier : NF = 10dB
Finite L.O. power penalty : 13dB
$\Delta\nu_{IF}$=10kHz, SNR_{floor}=43dB

FM Heterodyning

β=1, 50Ω amplifier: NF=10dB
Finite L.O. power penalty: 13dB
$\Delta\nu_{IF}$=30MHz, SNR_{floor}=37dB

laser linewidth are all very important considerations in assessing the performance of coherent analog links. The receiver bandwidth requirement is a particularly serious issue for the case of optical FM where the modulation index β is large. Because in general the front-end is a relatively noisy 50Ω amplifier, and a wide bandwidth is required, the local oscillator power penalty is large for accessible laser powers. In both FM and PM cases very narrow linewidth laser sources are required to avoid catastrophic SNR floors.

For signal powers greater than around 10μW direct detection receivers are seen to generally offer better performance than coherent and for very short fibre links this is indeed the domain we are considering. At lower received optical power coherent detection offers improved SNR compared with direct detection with the margin being dependent on the power level and signal bandwidth, however, under these conditions the SNR is generally low.

4.4 RECOMMENDATION AND RATIONAL FOR EXPERIMENTAL MODEL

We now summarise the results and conclusions from the analog systems study and present the recommendations and rational for the experimental system, which was subsequently constructed.

Summary of Systems Analysis

The SNR performance of direct detection links is illustrated in Figure 4.5. The PIN or APD combined with an optimised low noise FET preamplifier front-end design offers the best performance, as would be expected. The APD should offer an advantage over the simple PIN diode based on the gain-bandwidth product realisable with current 1.3/1.55μm GaInAs/InP APD's. However, this may be difficult to realise at the higher carrier frequencies because of the bandwidth limitations of present day commercial devices (1-2 GHz).

At the present time a 50Ω microwave amplifier, coupled to a discrete packaged detector, is the only viable approach for carrier frequencies above ~2 GHz, consequently yielding a poorer performance than would be achievable with an optimised low noise front-end design.

In the limit of large received optical power levels the SNR of a direct detection system approaches the theoretical performance limit for an AM homodyning system configuration.

The analysis of coherent analogue systems leads to the following general results:

AM systems generally offer the poorest performance of all the coherent detection schemes. However they offer the greatest tolerance to laser phase noise so that in principle broad linewidth commercial DFB lasers

could be used to implement such a system. To counter balance this the demodulation electronics are demanding, particularly filter design, which must be extremely flat to limit distortions. The performance that could be realised with an AM system implemented with available component technology would generally offer poorer performance than a direct detection system.

PM systems can offer significantly better-performance than AM. The performance achievable is very dependent on the linewidth of the laser sources. Phase modulation is the most demanding of all the coherent architectures in terms of laser linewidth requirement. Typically laser linewidths of the order ~kHz are needed in order to avoid serious SNR floors due to laser phase noise. In addition, PM systems using either the heterodyning or homodyning receiver approach require an Optical Phase Lock Loop (OPLL) to provide phase and frequency control between transmitter and local oscillator lasers.

FM systems potentially offer the best performance of all the modulation formats, although this is only achievable with large modulation index β which results in the requirement for broad bandwidth detectors and receiver amplifiers. The laser linewidth requirement is also quite demanding, lying between that of AM and PM systems.

The theoretical performance limits of the coherent detection system configurations have been evaluated on this programme and results were indicated in Section 4.1. These results assume infinite local oscillator power, zero bandwidth laser sources and make no concessions to the component technology requirements. Calculations have also been carried out to assess the performance which could be realised in a coherent link using available (commercial or experimental state of the art) component technology. This has been compared with the corresponding situation for direct detection analog links in order to determine the realisable performance improvement. The assumptions made in this analysis, and the

corresponding results, were described in sections 4.3. In conclusion it is found that detector/receiver bandwidth, local oscillator laser power and laser linewidth are all critical issues in assessing the realisable performance of a coherent analog link. Because of the optoelectronic and electronic component limitations at the present time it is found that for signal power levels greater than around 10μW (which is representative of the situation in a 1km link) direct detection receivers offer generally better signal to noise ratio performance than coherent. At lower received optical power levels coherent detection can offer better SNR than direct detection though these power levels are not representative of the situation in a short transmission link. The reasons for these results are many, but can be briefly summarised as follows:

- Large receiver bandwidths are required to accommodate the microwave carrier, particularly in the case of FM, which results in a high receiver noise and insufficient local oscillator power from available lasers to provide significant coherent gain.

- With high levels of received optical power (~100μW) the coherent advantage is fundamentally low due to the dominating effect of the signal shot noise which is common to both direct and coherent detection.

- Narrow linewidth laser sources are required in the case of PM and FM systems to avoid SNR floors. These are not generally available and hence laser phase noise is a major cause of performance degradation.

Component issues which represent a serious limitation to the realisation of coherent analogue links for this specific application have been identified as:

- The availability of narrow-linewidth, high power (local oscillator) laser sources.

- The availability of wideband detectors and microwave amplifiers in some cases (particularly problematic for the high carrier frequency signals and using large β FM systems).

- The availability of suitable wideband phase and amplitude modulators.

- The implementation of an external, wideband, FM modulator.

- Filter design in AM systems.

A study of the complexity and cost issues for coherent analog links has been carried out in order to assess the preferred system configuration for construction and demonstration within this programme. This has been carried out bearing in mind that to be worthwhile such a system must demonstrate an improved performance over direct detection. A discussion of these issues has previously been presented in a Technical Note and is reproduced here in Appendix A.

The results obtained lead to the conclusion that superior performance is only achievable with a sophisticated system implementation involving angle modulation (PM or FM), but this requires component technology with a performance which is not currently commercially available. Experimental laboratory prototype components could in some cases meet the requirements but at relatively high cost and risk.

Concept for Experimental Model

The difficulties encountered with the realisation of a high performance analog link are associated with the lack of available componentry, in particular the laser sources and high frequency wide bandwidth electronics. The activity worldwide in analog coherent optical communication links is extremely small and so the investigations carried out within this programme

are at the forefront of this technical field. This fact in itself suggested that the investigation and demonstration of any aspects of such systems would make a valuable contribution. Following discussions between PCO, Plessey, and RADC it was agreed that a potentially valuable and attractive technical approach to the realisation of an analogue coherent system could be based upon a self-heterodyning or homodyning configuration. This has subsequently formed the basis of the recommended approach which is described in the following. A technical note on the self-heterodyne/homodyne analog link option has previously been presented and is reproduced here for completeness in Appendix B. Below we summarise the most salient features of this technical approach and indicate the performance expected from such a configuration.

The concept of a self-heterodyning and homodyning system configuration relates to the situation where the transmitter source and local oscillator source are derived from the same laser. The output from the laser is split into two, one part of which is modulated and subsequently recombined with the other part, representing the local oscillator, at the receiver. The local oscillator 'source' can be frequency shifted using an acoustic-optic modulator to represent a heterodyning configuration, or remain unshifted in frequency thus simulating a homodyning configuration. The advantage of this approach is that the need to deal with the laser stabilisation and receiver IF tracking issues is removed and system experiments can be performed more readily. Indeed these configurations were adopted in the early coherent optical communications experiments in order to demonstrate basic concepts, advantages and parameter dependencies before the laser source and control electronics development had reached the level to permit experiments with independent transmit and local oscillator lasers.

Other than the points made above a major advantage in adopting the self heterodyning or homodyning configuration for the analog link is that it will permit the capability to control the effective linewidth of the laser

source. This arises out of the ability to match the path lengths between the laser source and receiver for both the transmitter and local oscillator arms and thus correlate the combined signals. In this way laser phase noise levels can be partially cancelled thus reducing the effective IF spectral width. The worst case situation is clearly where the two arms are uncorrelated in which case the IF spectral width will be twice the source laser linewidth. The problem of the degree of phase noise reduction achievable by the technique of path length matching is one which we are not aware of having been addressed in the literature. An anlysis of this problem has been carried out to determine the linewidth reduction achievable in practice in order to assess the type of laser source necessary to implement a self heterodyne/homodyne analog link. The analysis is described in Appendix C.

Calculations indicate that an effective linewidth of approximately 10 KHz should be achievable with a DFB laser as the primary source. This is very encouraging in that it permits a self heterodyning/homodyning configuration to yield results otherwise only achievable with sophisticated external cavity lasers.

The Recommendation

We recommended that a self-homodyning phase modulation system be implemented on this programme. The self-heterodyning configuration requires a frequency shifting element and will be 3dB poorer in SNR than homodyning. The PM system offers good performance and is fairly straightforward to implement using an external lithium niobate phase modulator. The carrier frequency was determined from the bandwidth of available phase modulators and receivers. The available low noise receivers would be marginal in bandwidth for a 1 GHz carrier so that the optimum approach would appear to be to use a detector and 50 ohm amplifier. A survey of commercially available lithium niobate phase modulators

indicated that this component is the limiting factor in the choice of carrier frequency. The bandwidth available suggested a maximum carrier frequency of 3 GHz.

To summarise, the recommended approach was:

- Self-homodyning configuration
- Phase modulation
- DFB laser sources, wavelength 1.55μm
- Carrier frequency 3 GHz

The self-homodyne approach for demonstrating an analog coherent link has a number of interesting features and advantages compared with the use of independent transmit and L.O. lasers. This configuration allows a very narrow effective laser linewidth to be achieved and thus establish a link with a peformance which is not laser phase noise dominated. The real bonus in the aproach is that this situation can be constructed using a standard DFB laser without an external cavity and the concomittant engineering and stability issues.

This link configuration permits the investigation of the PM homodyne system performance as a function of received signal power, local oscillator power, and laser linewidth. In particular the range of laser linewidth accessible through adjusting the path differences is very large and probably represents a unique way of achieving such a broad linewidth range. This approach therefore allows experiments to be made to compare results with the theoretical linewidth analysis carried out on this programme.

The self-homodyning configuration should be regarded as a vehicle for demonstrating a coherent analog link which will permit the investigation of performance as a function of receiver signal power, local oscillator power and laser linewidth. The performance should be compared with an intensity modulation/direct detection link for the same received optical power.

The actual performance which can be achieved with a PM self-homodyning link is highly dependent on the details of the implementation, e.g. received signal power, L.O. power, linewidth, signal bandwidth and receiver type. What we will do here is give an indication of projected performance based on calculations assuming reasonable parameter values. These are described in the Table below.

SNR Calculations for a PM Self Homodyning Analog System Configuration

PR(μW)	PL(μW)	COHERENT SHOT NOISE LIMIT SNR (dB)	FINITE L.O. POWER DEGRADATION FACTOR (dB)	RESULTANT COHERENT SNR (dB)	DIRECT DETECTION SNR (dB)
1	1	39	34	5	-6
1	100	39	14	25	-6
10	10	49	24	25	14
10	100	49	14	35	14
100	100	59	14	45	34

PR : Received signal power
PL : Local oscillator power

Assumptions: Signal carried frequency of 2 GHz
with full recovery at receiver

Modulation index = π /2
Coherent SNR (phase noise floor) = 43dB
Effective laser linewidth = 10 kHz

These results are an example to give an indication of the relative SNR performance demonstrable using the self-homodyning configuration. We have in these calculations assumed an effective laser linewidth of 10 kHz, but clearly this configuration will permit us to evaluate the performance as a function of laser linewidth and confirm our theoretical assessment of signal to noise ratio floors due to laser phase noise.

Up to the present time very little attention has been given to the subject of analogue coherent optical communications. The only work we are aware of has been published by British Telecom Research Labs (1) and Doctor Neher Labs (Research Lab of the Dutch PTT) (2). The work at BTRL has not been presented in the open literature beyond the initial publication in 1985. From discussions with the authors we are aware that the theoretical work on AM system performance contains errors, which have been addressed within our own calculations. Over the past two years the Doctor Neher labs have been engaged in the construction of a phase modulation system to transmit multi-channel video. We have been aware of their progress through contact with their laboratories on a European Collaborative programme. They have encountered major difficulties in the development of suitable linenarrowed external cavity lasers with the stability necessary to implement the system. No results are yet available.

The self-heterodyne/homodyne configuration has been adopted in a number of early experiments in coherent systems (3,4,5), where progress was made possible without the need for sophisticated lasers and, in the case of homodyning (3,4), the optical phase lock loop. The experiments conducted were limited to digital systems, but nevertheless give insight to the advantages and problems which arise with this system configuration.

REFERENCES

[1] D Heatly, Proc. 10OC/ECOC, 1985, pp.343-346.
[2] J P Bekooij et al, Proc. ECOC, 1987, Helsinki, pp.359-362.
[3] T G Hodgkinson et al, 1982, Elec. Lett., Vol. 18, No. 12, p.523-5.
[4] D J Maylon et al, 1983, Elec. Lett., Vol. 19, No. 4, p.144-6.
[5] K Kikuchi et al, 1983, Elec. Lett., Vol. 19, No. 11, p.417-8.

5. DIGITAL SYSTEM

5.1 DESIGN

5.1.1 Design Outline and Key Assumptions

This section will describe the design approach for the digital coherent system and the digital direct detection link. The configuration for the coherent link is summarised in Figure 5.1. The system employs FSK modulation at 140 Mb/s implemented by direct current modulation of a single mode DFB laser. The receiver employs single filter detection (wide deviation FSK single sideband detection) and the local oscillator is a DFB laser similar to that at the transmitter. The detailed design has been covered in the digital design plan CDRL Item A003 (July 1987) and further details will be found in that document. However, since the assumptions made in the system design are relevant to the system performance, these points will be reviewed here.

An evenly coded signal is required to remove any DC signal content. The maximum number of ones and zeros in the data stream must be restricted to remove low frequency compoments and thus allow AC interstage coupling. This encoding can be done electronically, but it removes flexibility from the user, since a complex code can be data rate dependent because of time delays in the encoding and unnecessarily increases the complexity of the transmitter and receiver racks.

The input data is non return to zero (NRZ) at an ECL logic level, and thus permits direct connection to BER test equipment. No clock extract is used on the receiver unit, since this allows some flexibility in data rate permitted to the user. The resonant principle used for clock extract circuit functions gives a narrow range of frequencies over which the system

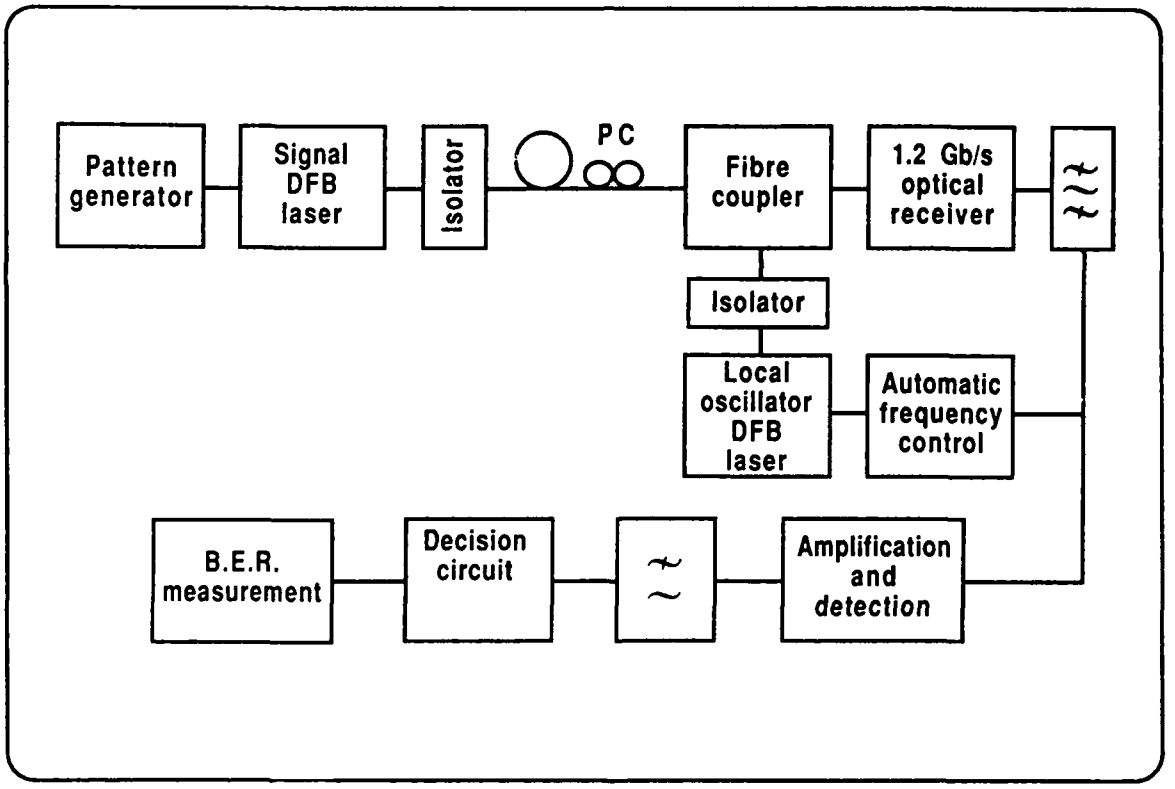

Figure 5.1 CONFIGURATION OF THE COHERENT LINK

could be operated and is unnecessarily restrictive. The nominal data rate chosen for the design is 140Mb/s.

The main aim of the system design is to provide as close a comparison as is possible between coherent and direct detection. This was ensured by using the same optical components, namely source laser and front end receiver for both direct and coherent detection links. Different levels of modulation are required for the laser and this will be discussed in detail in the control circuit section. In the receiver, the LO laser is connected only for coherent detection system. The amplifier and filters are clearly different for the coherent and direct detection, therefore separate IF amplifier and base band amplifier boards have been designed connecting from the common front end.

A single filter system was designed which was determined by available receiver bandwidth and laser linewidth. The minimum modulation index for a

dual filter system is a strong function of laser linewidth. As an engineering approximation, the frequency deviation M required can be taken as (ref 5.1).

$$M = 2f_D + 20\Delta\lambda$$

where f_D is the data rate and $\Delta\lambda$ is the linewidth.

A more exact calculation of the filter width required as a function of laser linewidth is shown in the table below. (ref. 5.2) The modulation index must be at least twice the width of the filter.

Beat Linewidth $\Delta\lambda$ total	Bandpass 10^{-10}	Filter Width for BER Floor 3×10^{-12}
20	230	336
30	345	405
40	460	540
50	575	675
60	691	808
70	806	942

This significance of the 3×10^{-12} BER floor is that will give a 1dB penalty at 10^{-9} BER.

The data demodulation was achieved by a square law detector. This can be considered as self mixing of the IF signal, in that the IF itself is used as the coherent source to mix itself down to baseband. This reduces the complexity compared to first extracting the IF before down mixing.

These assumptions mean the system can be used over a broad range of frequencies even though the post detection filtering will not be optimum. However, the fundamental limit of usable frequency will be the non-flat amplitude and phase response of the laser diode under modulation (Ref 5.3).

5.1.2 Components

The key component in a coherent system is the laser, since it is both the source and local oscillator. For this system, we have chosen to use a 1 55μm distributed feedback (DFB) laser, with no external cavity. (ref. 5.4) The lasers have linewidths typically in the region of 10 to 50MHz with no external feedback. The two lasers must be matched in wavelength at the same temperature to within 2nm in order that tuning with temperature

will ensure exact wavelength matching. A modulation response which is flat over a wide range of frequencies is desirable in order to remove the necessity of extending the passband filters.

A laser packaging technique which has an integral thermocooler and thermistor is required to ensure adequate temperature control. The laser must also be protected from external reflections in order to ensure the facet emission remains stable and single moded. In addition, an efficient method of coupling the light into the fibre must be used to increase the power coupled into the fibre. These requirements are stringent and no commmercially available device met the requirement at the time. Therefore, Plessey DFB lasers were used in a custom designed package. The target specification for these lasers is shown in the table below.

Output power into fibre	$\geq 200\mu W$
Wavelength separation	$<2nm$
Side mode rejection	$\geq 30dB$
FM response flat in range 10-300MHz	$\pm$ 1dB
Linewidth	$<15MHz$

Other components required in the system are fibre connectors of low loss, but mostly critically, low reflection. A low loss fibre coupler with a split ratio of 50-50 in a wavelength region of 1.55μm is required. Both of these components are available commercially. The connectors chosen have been purchased from Dorran Inc and are premoulded with angled facets to give low reflection values. The coupler used was purchased from Gould Inc and is the highest performance on loss and accuracy of split ratio available.

The front end receiver must have a bandwidth of ~1GHz for a single filter system and ~2GHz for a dual filter system. The thermal noise of the front end is critical when assessing the system penalty due to finite local

oscialtes power. Therefore, the receiver design approach which is used for the most sensitive direct detection systems is used, the PIN-FET with an integrating response. (ref. 5.5)

The use of a balanced front end receiver which uses two PINS connected out of phase to give cancellation of any amplitude modulation has an advantage in the system analysis. This removes any coupler split loss, in that both output arms are used and there is no signal loss nor any system penalty due to loss of LO power. This does not give conflicting requirements on couplers splitting ratio compared with a single photodiode receiver where the finite LO penalty offsets the signal loss penalty (Ref 5.6)(Ref 5.7). As the coupler splitting ratio is changed on a single PIN receiver, the loss in sensitivity varies. When the coupler split ratio is biased to the signal on say a 90%/10% coupler the loss of L.O. power leads to a large finite L.O. power penalty. Conversely using a 90%/10% coupler with a bias to the L.O. leads to a large signal loss. The optimum splitting ratio is in the region of 40 to 60% but is dependent on the value of L.O. power available and the receiver front-end thermal noise. Varying the L.O. power in a coherent experiment using the Plessey front end lead to the result that a coupler split ratio of 45%/55% was the optimum. The optimum point was not a sharp minimum in sensitivity penalty, coupler ratios from 30% to 70% were within 1dB of the optimum.

The target performance of a receiver front end was defined in the following table.

Bandwidth	>800Hz
Total input capacitance	>0.5pf
Fet transconductance	>25mS
Low frequency gain	>5V/V
Optical overload level	>-10dBm
Noise	$<1.5 \times 10^{-12} W/\sqrt{Hz}$

The choice of a Plessey design was on the grounds of low thermal noise, high bandwidth and the available option of a balanced PIN design.

To change the state of polarisation in the signal input fibre, fibre squeezers are employed. Pressure was applied by use of a custom design of mount with a hinged arm which was forced onto the fibre by means of a solenoid. This can be seen in a photograph in Figure 5.2.

Power supplies were purchased from a suppliers available range. A high efficiency switched mode supply was chosen, with input voltages of both 240V and 110V to allow ease of set up between the voltage standards.

5.1.3 Control Circuits

To ensure coherent detection, the source and LO laser must be held at the same wavelength and hence frequency, differing only by the IF frequency. A typical DFB laser would have characteristics of 12GHz frequency shift per degree temperature change and 1-2GHz frequency shift per mA of bias current variation. These characteristics mean accurate and stable control circuits are required for both temperature and current. If an IF stability of within 50MHz is taken as the target then this can be translated into requirements of the control loops.

The current board is required to have a noise level of less than 5μA rms and a temperature sensitivity of less than 10μA per degree change in the environment, assuming a change of 10^{0}C. The lasers are roughly an order of magnitude more temperature sensitive and therefore the equivalent requirement in temperature control is 0.2mK rms and 0.4mK per K environmental change. This degree of temperature stability was considered to be impractical so the receiver design assumes the use of an AFC loop.

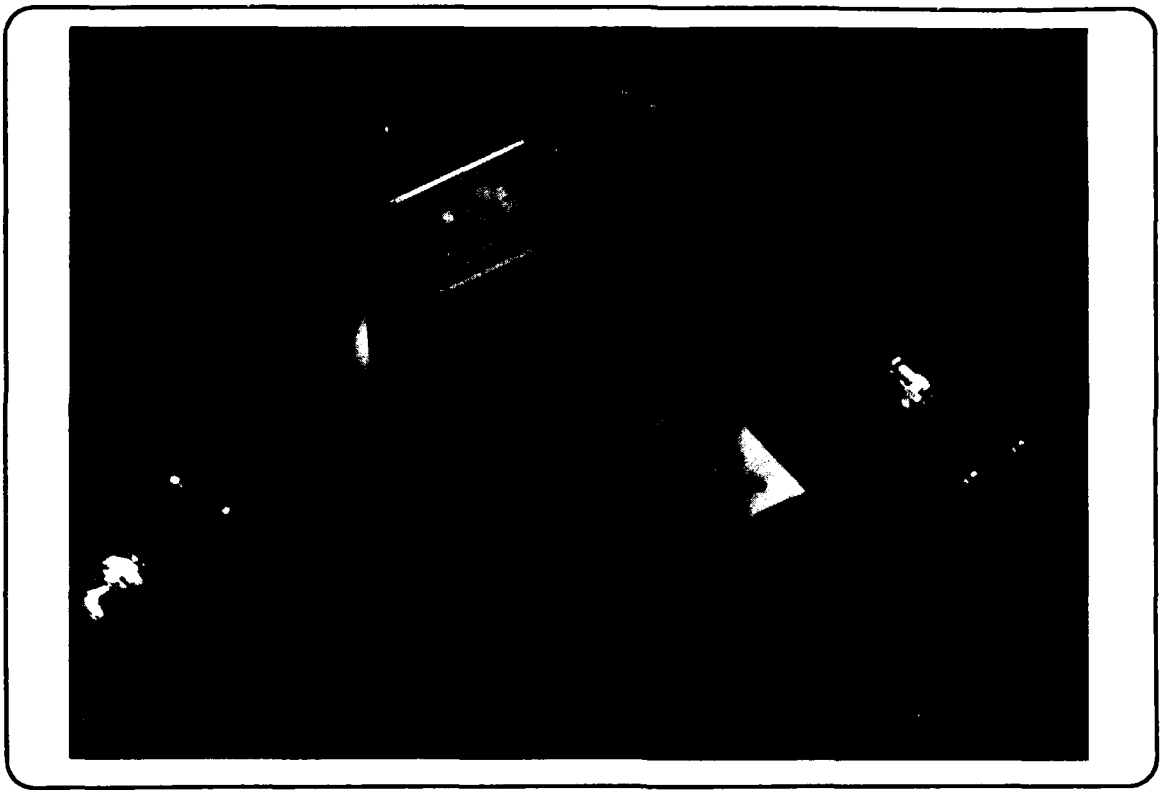

Figure 5.2 PHOTOGRAPH SHOWING THE FIBRE SQUEEZERS USED FOR POLARISATION CONTROL

The temperature control circuit was designed in such a manner that the laser temperature can be set between 10^0C and 40^0C by the user. The circuit takes the change of resistance of the thermistor and provides two drive currents for the external and internal thermocoders in the laser package. The schematic of the thermal control circuit is shown in Figure 5.3. The thermistor and the set temperature potentiometer are biased from the same voltage reference. The voltages on the potentiometer and the thermistor are firstly buffered and then compared. The difference voltage is amplified with different amounts of gain to inner and outer thermocoolers. When the thermistor indicates the required temperature has been achieved, the drive current is reduced. In addition to this basic circuit there is a facility to increment the required temperature from an external control voltage, but this was not used in the system. There is a safety cut out so if the thermistor connection was open circuit no current would flow through the coolers. This is included because in the open circuit condition, the driver would consider the module too cool and hence heat the thermocoolers but the laser module with no feedback signal could be heated to destruction. A monitor point is available on the front panel which indicates the voltage across the thermistor and hence its temperature.

The current control current is a constant current source which drives with respect to earth as shown in Figure 5.4. The current is set by means of a potentiometer adjusted by the user. This voltage is summed with the externally applied voltage from the AFC loop. The combined output of the summing amplifier is applied to another amplifier and drive transistor which provides a voltage to current converter to the laser. The bias current is adjustable between 40mA and 180mA and can be set with an accuracy of 10μA. The bias current is applied to the laser through an inductor and 10Ω and 1Ω series resistors. A voltage monitor from these resistors is available on the front panel to monitor the current.

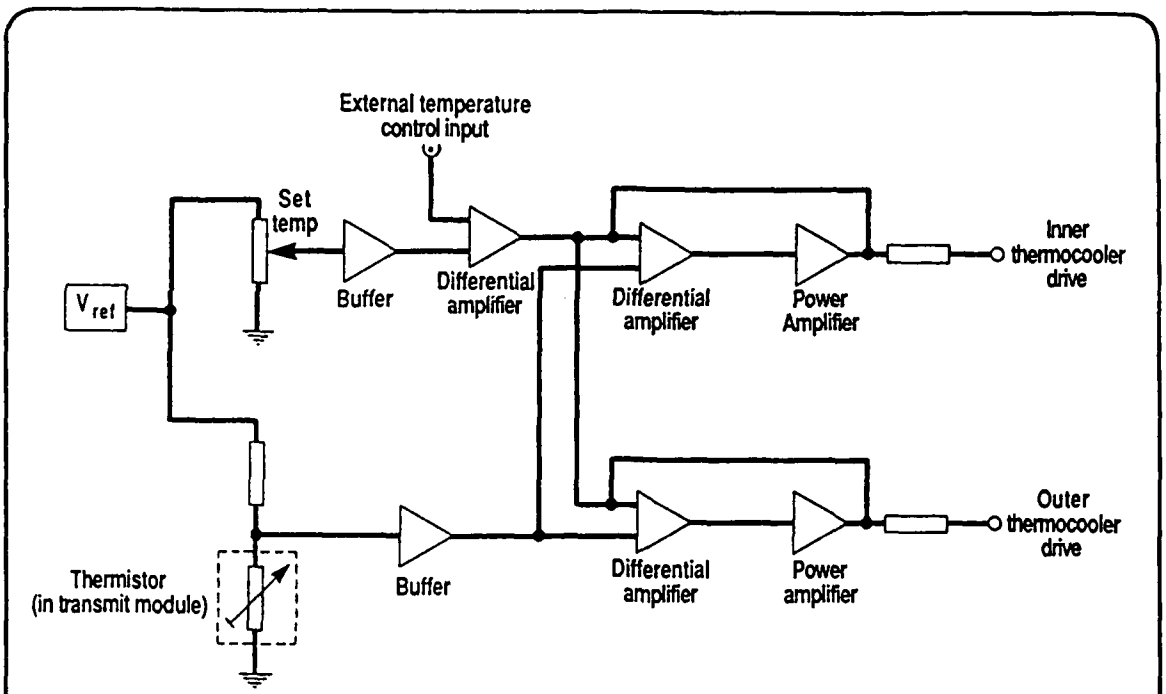

Figure 5.3 LASER TEMPERATURE CONTROLLER

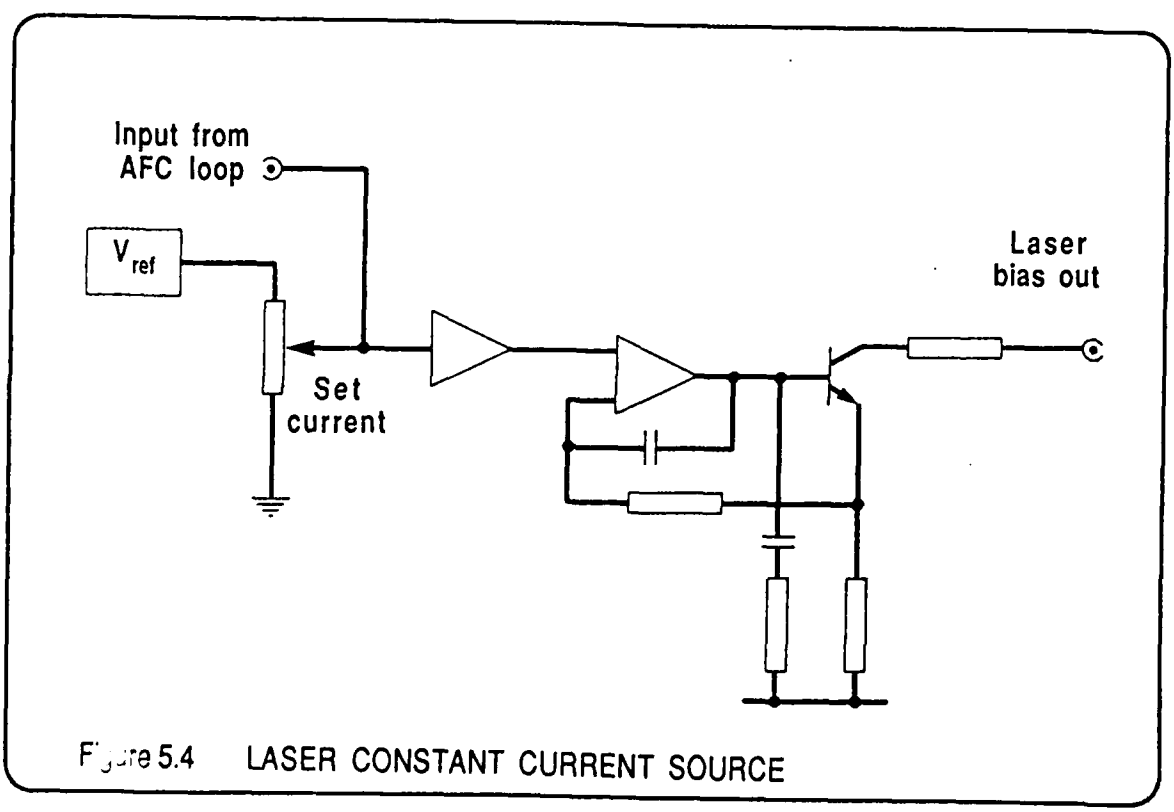

Figure 5.4 LASER CONSTANT CURRENT SOURCE

The modulation circuit is AC coupled onto the laser and is shown in Figure 5.5. A second inductor and a capacitor form a bias T in the laser connector shell. The modulation current is 30mA peak to peak for the direct modulation link and 1-2mA peak to peak for the coherent link. The input stage on the current board is common to both links and is buffeted so that no change in input amplitude will affect the amplitude of the drive signal. If no signal is applied, the circuit may oscillate through switching on the noise. Terminating the input with a 50Ω resistor when no signal is applied will reduce this effect.

The voltage output from the modulation board is either on the direct detection or the coherent lead. The appropriate lead connection is made to the laser connector shell where it is 50Ω terminated. The unused lead must also be 50Ω terminated whilst not in use.

All the connections from the drive circuits are routed through the laser connector shell. It has been designed so it can not be easily connected wrongly. However, the power supplies must be switched off before this connection is broken or made.

The AFC design uses a digital approach, which can be seen in outline in Figure 5.6. The input stage is a limiting amplifier which makes the AFC independent on input level up to 1GHz which is the limit of the saturating amplifier. The signal, now at a digital level, has a frequency which is the mean of the instantaneous frequency due to phase noise and modulation. This is divided by a prescaler which divides by a constant factor of 20. Following this division, the signal is divided by a variable, set by two switches from a hexidecimal 00 to FF, a potential ratio of 256. This output is then digitally compared in an EOR gate phase detector with a constant 60kHz frequency derived from a crystal oscillator. This technique allows the centre of the lower sideband to be set at the optimum IF frequency by a change in the division ratio. The output of the phase

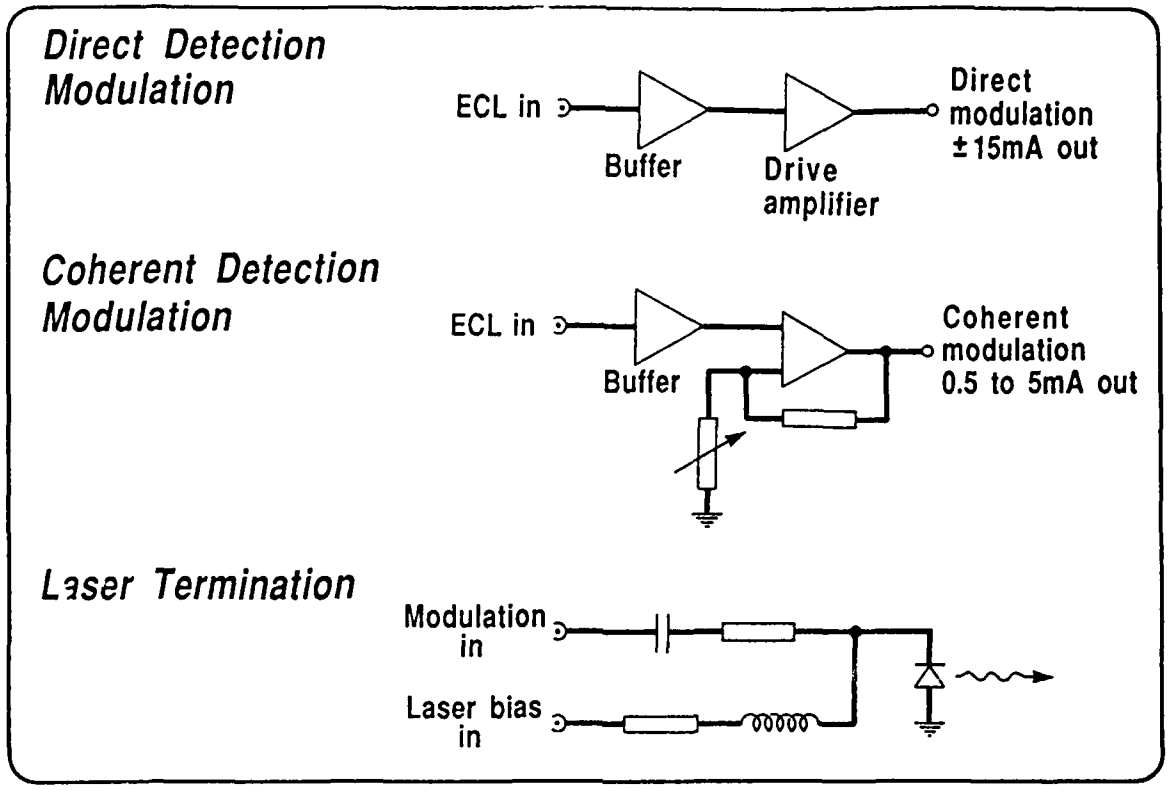

Figure 5.5 MODULATION CIRCUITS

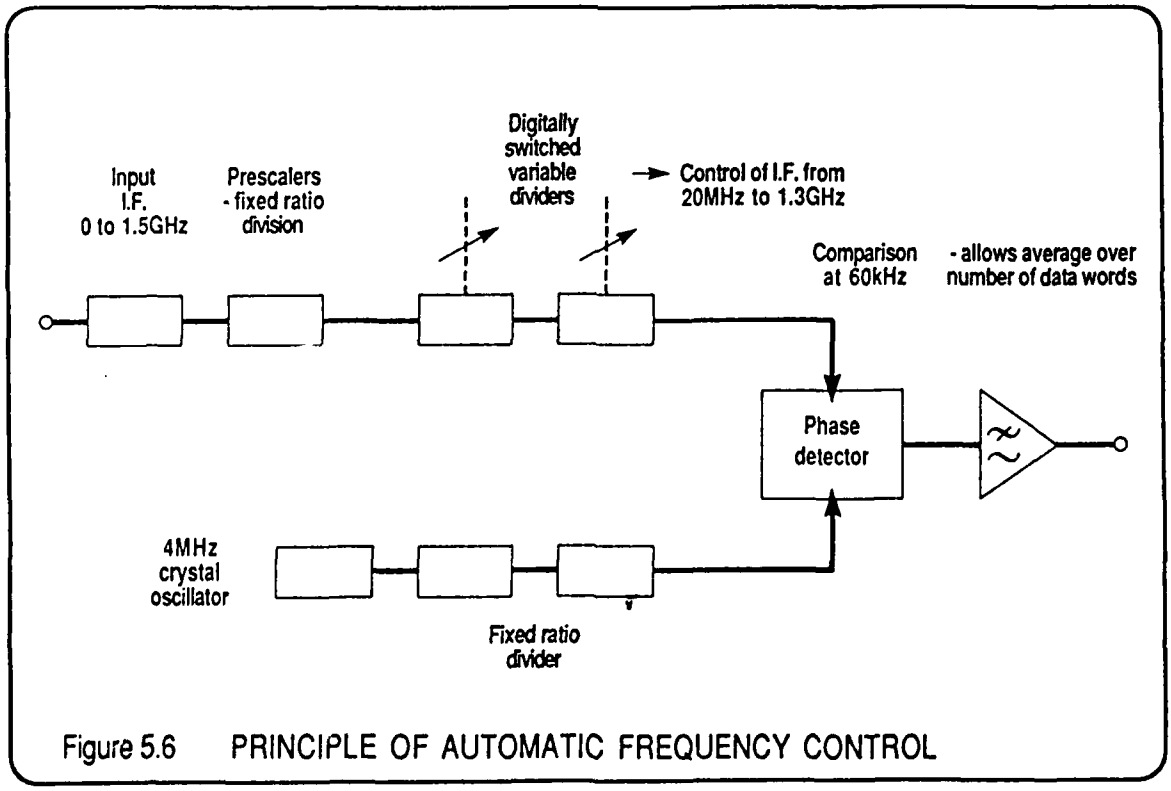

Figure 5.6 PRINCIPLE OF AUTOMATIC FREQUENCY CONTROL

detector is amplified and filtered and then applied to the external input of the current control board to shift the frequency of the LO laser as necessary.

5.1.4 Summary of Design Approach

The decision whether to use an in-house Plessey component or purchase a commercially available item was always taken on the grounds of specification, availability and cost. Where a component was commercially available, it was purchased. The current and temperature controllers and AFC control circuits wee designed in house because of the specific requirements to the project. The direct detection link was also designed in-house because it was simple and straightforward and allowed comparison with the coherent system. Power supplies wre purchased for ease, but they were subsequently found to be too noisy, (see 5.3.5) so replacements were built.

The use of Plessey lasers and the receiver front-end ensured components of adequate specification were used and selection for improved performance was feasible. Use of in-house lasers enabled custom packaging of the chip to give thermal stability and optical isolation.

5.2 CONSTRUCTION

5.2.1 Laser Construction

The laser modules consisted of a Plessey 1.55μm DFB laser of double channel buried heterostructure chip design mounted together with a thermistor onto a ceramic substrate. This laser was aligned through coupling lenses and an isolator into single mode fibre. The temperature was controlled by an inner thermocooler and the assembly was enclosed by a box. This box was mounted in a larger box on another, outer thermocooler. This two cooler

approach ensures the laser is thermally isolated from the environment. The isolator included in these modules can be seen in figure 5.7.

The electrical connections to the laser, thermistor and both thermocoolers were carried through glass to metal seals in the side walls of the inner and outer boxes. A connector shell screws into fittings on the outside of the outer box, through which all the required bias and control voltages were applied.

The outline drawing of the laser module can be seen in Figure 5.8, the complete module photograph can be seen in Figure 5.9 and the electrical connection diagram is shown in Figure 5.10.

5.2.2 Transmitter Rack

The transmitter rack can be seen in Figure 5.11. It consists of the transmt laser mounted on a heatsink, horizontally mounted in the rack. The laser fibre is spliced to a connector tail. The half connector is mounted in the bulkhead uniter on the front panel. Mounted in the rack are the modulation circuit boards, current and temperature control boards.

The modulation board has two coaxial output leads, one of which must be connected to the laser modulation input. The thermal control and laser bias avient lines run to the laser connector at the back of the rack.

The power supplies voltages to the rack run from the rear of the power supply case to the rear of the transmit rack.

Figure 5.7 PHOTOGRAPH OF OPTICAL ISOLATOR

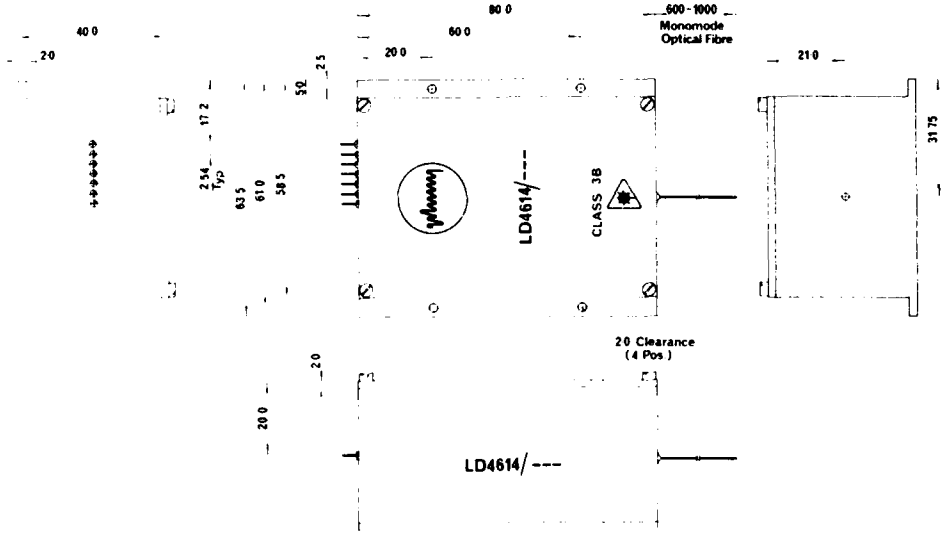

Figure 5.8 OUTLINE DRAWING OF LASER PACKAGE

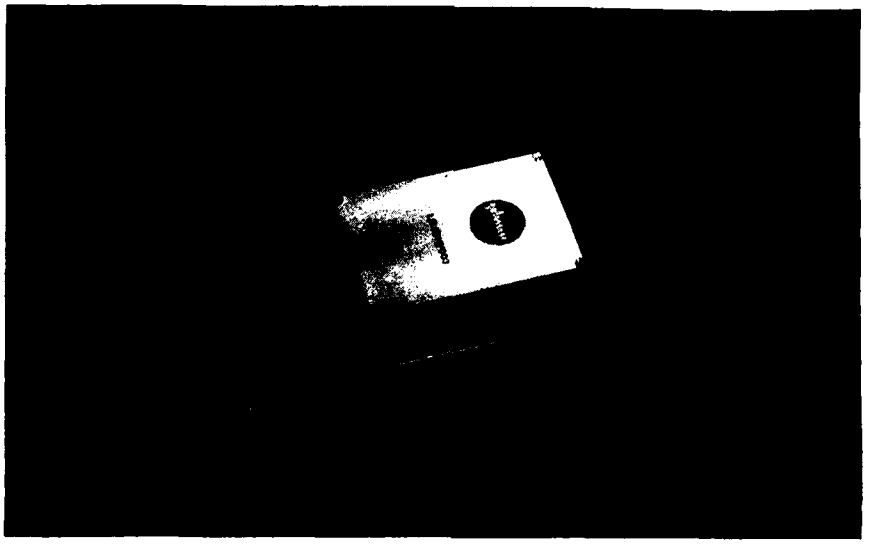

Figure 5.9 PHOTOGRAPH OF THE LASER PACKAGE

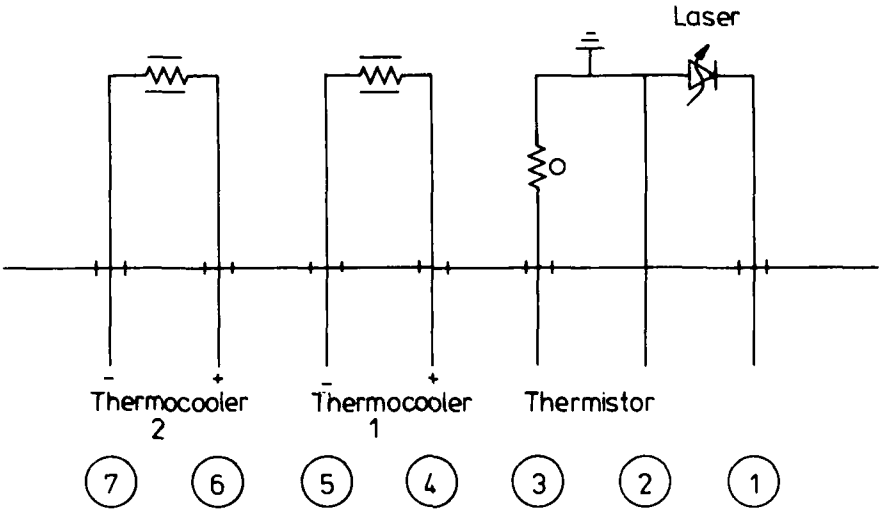

Figure 5.10 CIRCUIT CONNECTIONS TO LASER PACKAGE

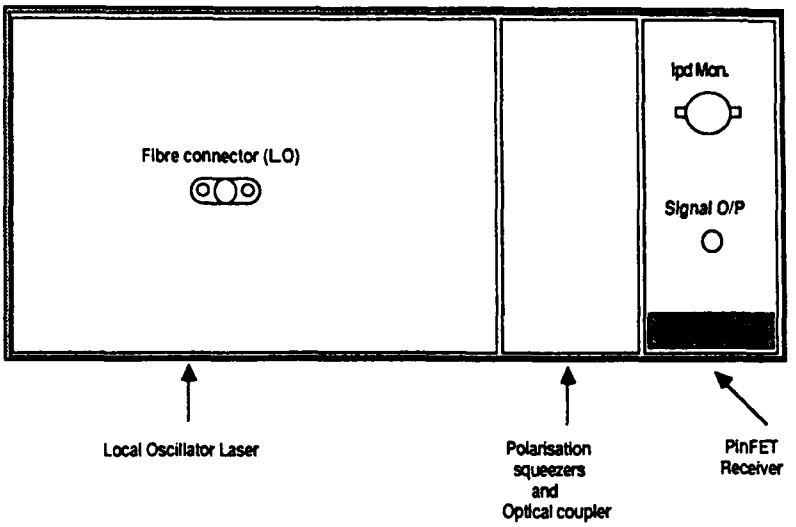

Figure 5.11 TRANSMITTER UNIT

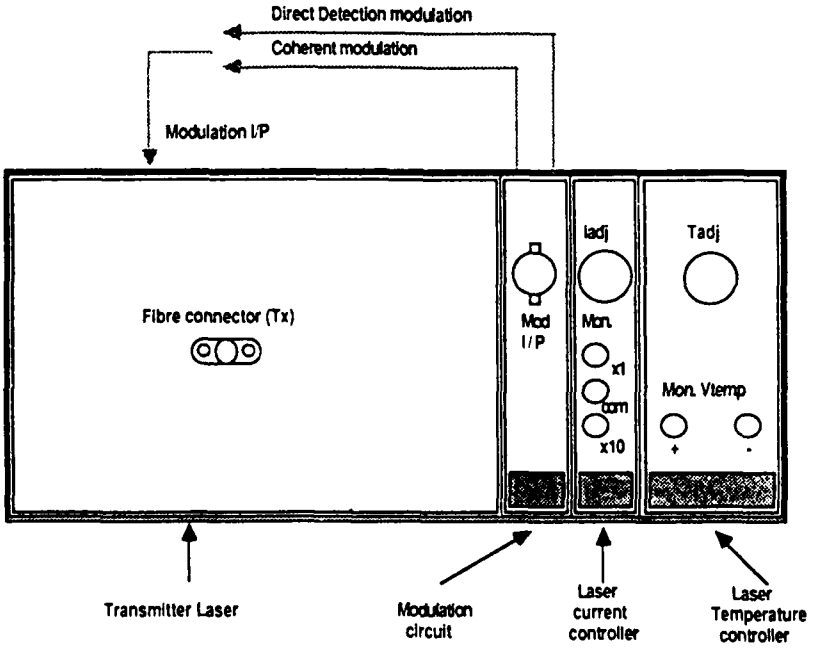

Figure 5.12 RECEIVER OPTICS RACK

5.2.3 Receiver Racks

There are two receiver racks, one contains all the optics and some electrical biassing, shown in Figure 5.12. The other contains the control and signal processing electronics as seen in Figure 5.13.

The optical signal is coupled into the optics rack via a Dorran bulkhead connector. It is then spliced into a length of fibre with 250μm outer coating diameter. This fibre is threaded through the jaws of the fibre squeezer to implement polarisation control. This fibre length is spliced at its far end onto the fibre coupler.

The LO laser is spliced onto the other input arm of the fibre coupler. One output arm of the optical coupler is spliced onto the receiver fibre, the other is available for power monitoring to calibrate the system.

The receiver front-end is of high impedance design giving an integrating electrical response. The photodetector is a reverse biassed PIN photodiode mounted on a silica block. The detector is a substrate entry design, with a GaInAs absorbing region on an InP substrate giving very low capacitance and high quantum efficiency. The amplification is the common source biassed GaAs MESFET with high gm, low gate source capacitance and low gate leakage. This is buffered out of the package and then the integrating response is equalised by a differentiator network. The optical front-end receiver is shown in Figure 5.14, it is in a 14 pin DIL package with 0.3" pitch between pins with a custom fibre optic bush on the sidewall. The photodiode can be seen in the lower right hand side of the photograph.

The signal is amplified and is fed out of the optics rack by a SMC bulkhead connector on the front panel. Also on the front panel is a BNC socket to monitor the photocurrent. This reads the sum of both LO induced current and signal photocurrent. This socket is isolated from the panel because

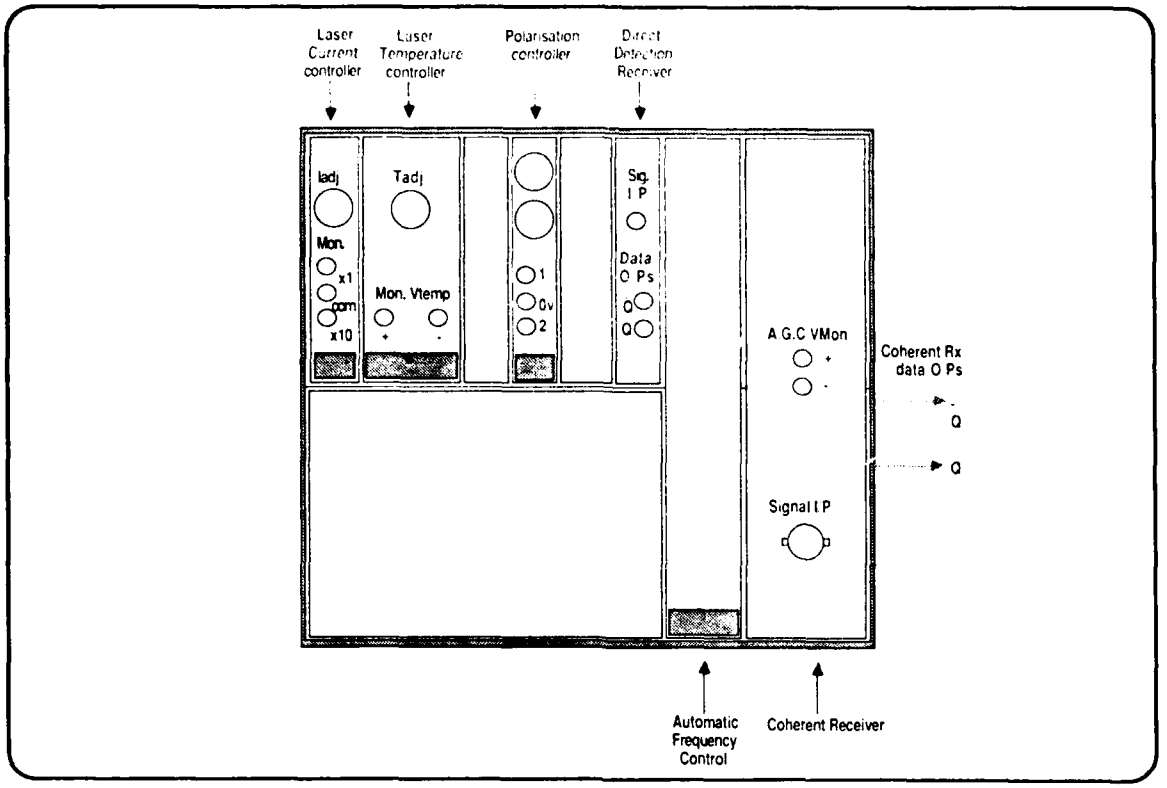

Figure 5.13 RECEIVER ELECTRONICS RACK

Figure 5.14 FRONT END RECEIVER PHOTOGRAPH

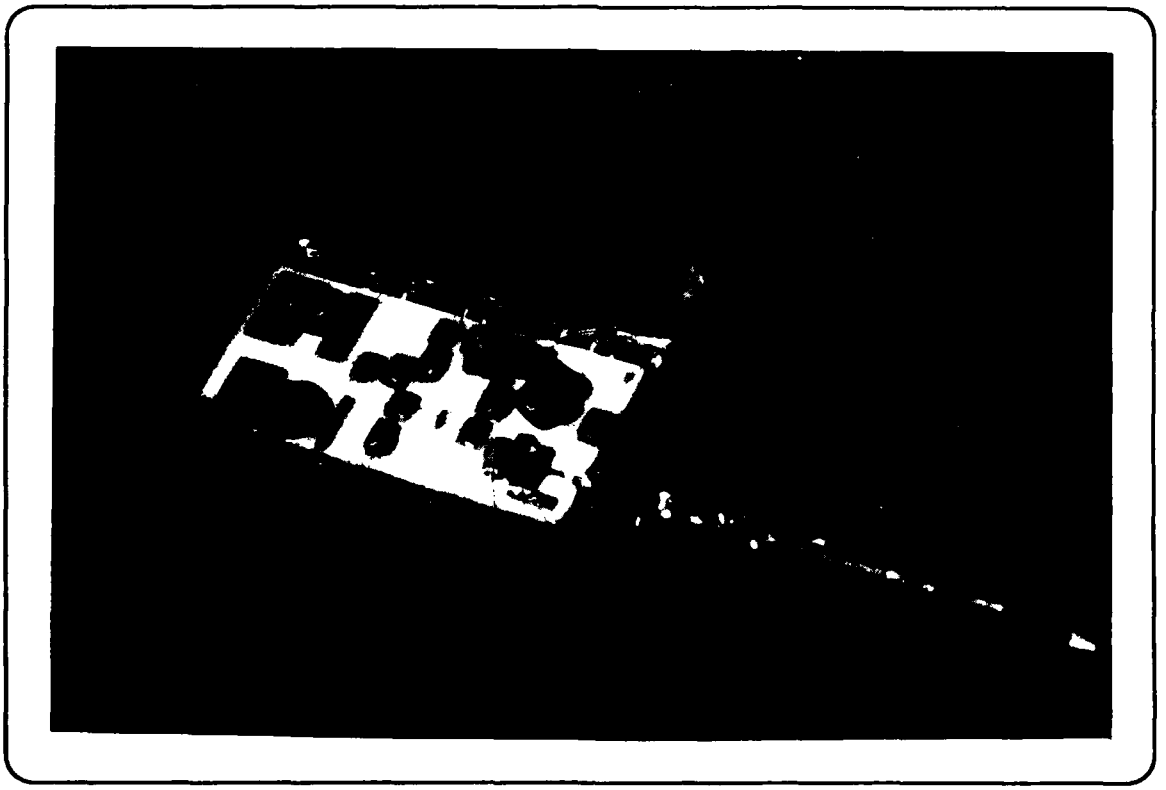

both contacts have a DC bias level. This monitor is a voltage poduced by the photocurrent across a 10kΩ resistor. It is not of use whilst the system is operating but is useful whilst setting up. On no account must this socket be earthed because this will remove the bias from the photodetector.

The connection to the power supply module is at the rear of the optics rack as are the control lines to the fibre squeezers. All the connections to the LO laser run through a cable assembly from the electronics rack to the connector shell on the rear of the LO.

The electronics for the local oscillator, the direct detection amplifier, the IF amplifier, AFC board and the polarisation squeezer controllers are located in the larger electronics rack. The location of all the functions is shown in Figure 5.12. The laser current and temperature control circuits are the same as those used in the transmit rack with the exception that the external input is connected as part of the AFC loop on the current control.

The polarisation control board has two current sources which are varied by the potentiometers mounted on the front panel. These supply up to 400mA on each solenoid coil, this limit prevents excess force being applied to the fibre, cracking the plastic outer coating. The monitor point on the front panel gives a voltage which represents the current through the solenoid. it must be noted that the common point for both these monitor points is not at DC earth and this point must not be earthed if monitoring the solenoid currents. Once biased, the solenoids store considerable energy and if the electrical contact to the solenoid is disconnected whilst they are powered up, a back EMF will be generated and the user will get an electric shock. The maximum voltage to this rack is 18V, but it is still recommended that the power is off and the coil is discharged before disconnection.

The direct detection board consists of 2 stages of amplification and a filter. The filter is a 3 pole Butterworth function and has a low pass 3dB point of 65MHz. This is followed by a comparator. The AFC design approach is described in Section 5.1.3. It is built on a 6U Eurocard and takes up a full height slot in the rack next to the coherent IF board, which is also a 6U Eurocard. All the high frequency components on the IF board were built and separately tested before installation on the board. They are all connectorised with SMA type connectors to ensure ease of assembly. The IF board has two splitting points in the IF to the AFC and a monitor point to a spectrum analyser. The interfaces between the sub-systems is shown in Figure 5.15. If the AFC or the monitor point is not in use then these lines must be 50Ω terminated to prevent reflections dominating the IF frequency response. There are a total of five amplifiers on the IF board in three packages. One is on the AFC line to increase the signal level after it is tapped off. The signal amplifiers shown in Figure 5.15 each consist of one of constant gain and one of variable gain. The gain is varied manually by a potentiometer on the IF board. If the gain is set too high, the BER achieved will not be optimum because the amplifiers will be in overload. The equipment was commissioned at RADC with the optimum setting for a 10^{-9} BER. This is not a critical adjustment unless the amplifiers are beginning to clip.

After detection, the signal is low pass filtered, this used the same design, third order Butterworth with a 3dB point of 65MHz, as the direct detection link. The comparator is mounted on a small board to keep the height level with the amplifier chain. The comparator has two outputs, one has an in-line capacitor to provide a DC block since the output can not drive a 50Ω load when DC coupled. This can be connected to an oscilloscope for monitoring. The other output is DC coupled, at ECL levels which will drive the 75Ω load of ECL compatible BER test sets. However, if a BER test set with a 50Ω load is used then a DC block must be inserted and threshold on the BER set adjusted to zero volts.

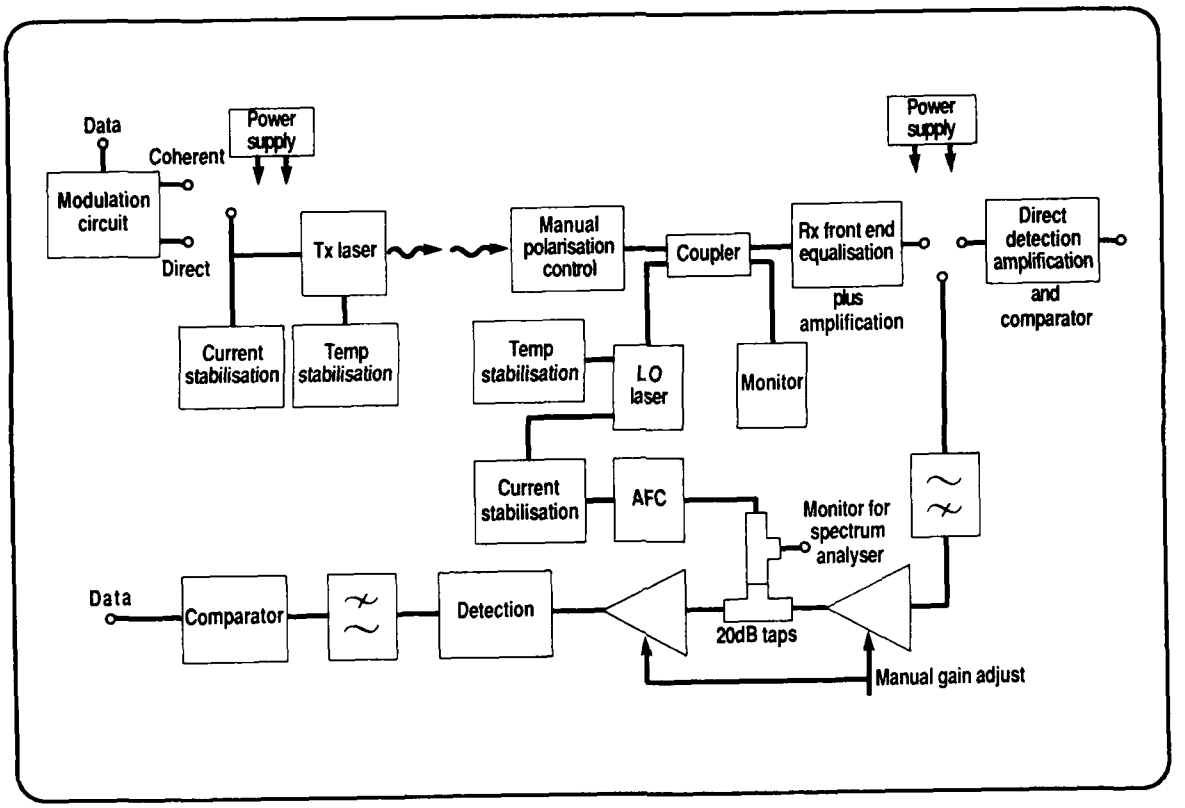

Figure 5.15 BLOCK DIAGRAM OF COHERENT AND DIRECT DETECTION LINKS

Figure 5.16 IF CIRCUIT CHARACTERISTICS WITH FREQUENCY

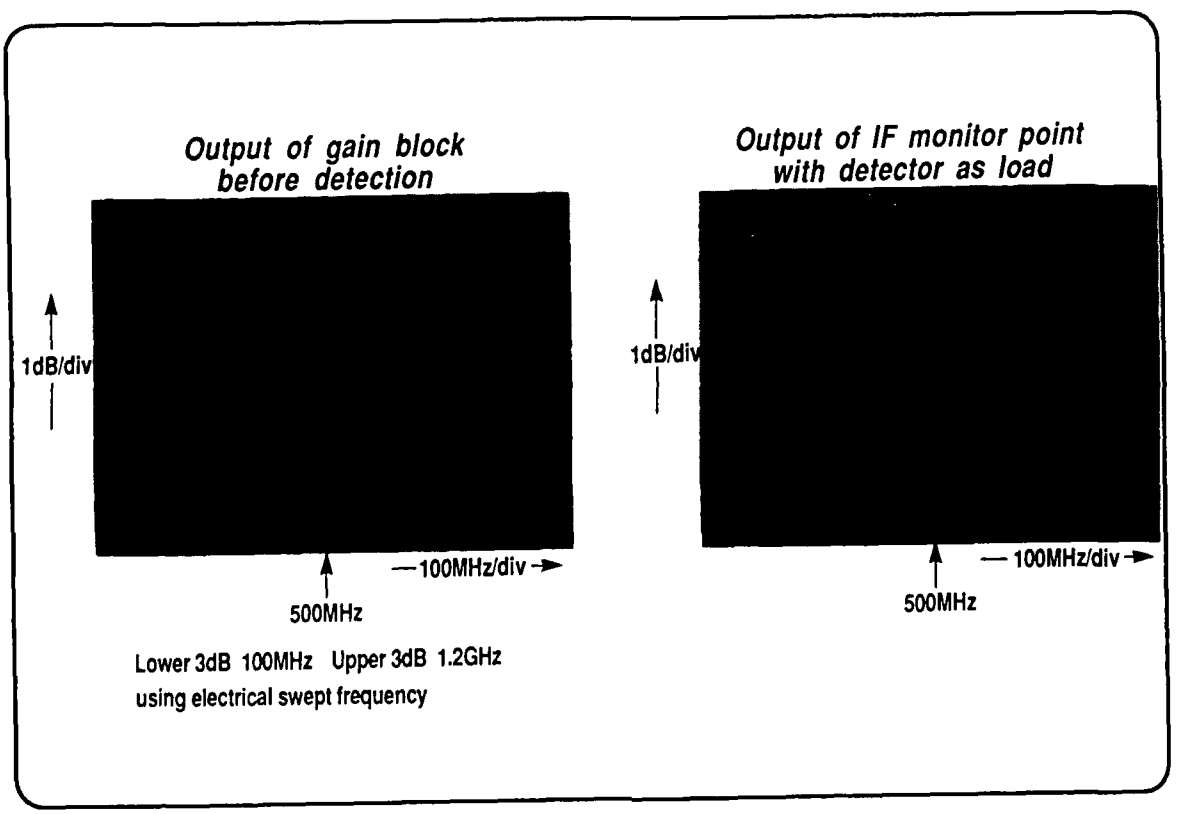

5.2.4 System Optimisation

When all the subsystems and components had been tested, it was realised that that the final system would need optimising for the available components. The most important feature in this regard was the laser linewidth. The system and filters as reported in the design plan were designed for the target specification of laser linewidth of 15MHz. This would require filter widths as calculated in section 5.1.1 of 350 to 400MHz. However, the combined laser linewidth was higher than 30MHz total, since one of the lasers was broad, giving a total of 65MHz. The filter width required is 700 to 800MHz, which centred on 500MHz gives a 3dB bandwidth of the receiver front end and IF amplifiers of 900MHz. The front end used had a bandwidth of 950MHz but the following amplifiers were beginning to add to the roll off. As a result two of the IF amplifiers were changed for ones which have 1dB peak in the transfer response at 1GHz. This was expected to compensate for the roll off, and the resultant IF frequency response is shown in Fig. 5.16a. It can be seen, on the 1dB per division scale, that the gradual roll off from 400MHz has a slight upturn at 700 to 800MHz giving a 3dB bandwidth in excess of 1GHz. Figure 5.16b shows the IF frequency response on the IF monitor point when the IF chain is loaded by the demodulator. This is somewhat reflective in the frequency domain and the resultant is a 2dB dip at ~550MHz together with other ripples.

The sideband centre frequency can be varied by means of a switch on the AFC board. The system was set at a high error count, at 10^{-3} BER and the sideband centre frequency adjusted until the BER showed a minimum. This can be seen in Figure 5.17 and 550MHz was seen to be the optimum. Clearly no penalty is apparent because of the dip in frequency response in the region of 550MHz.

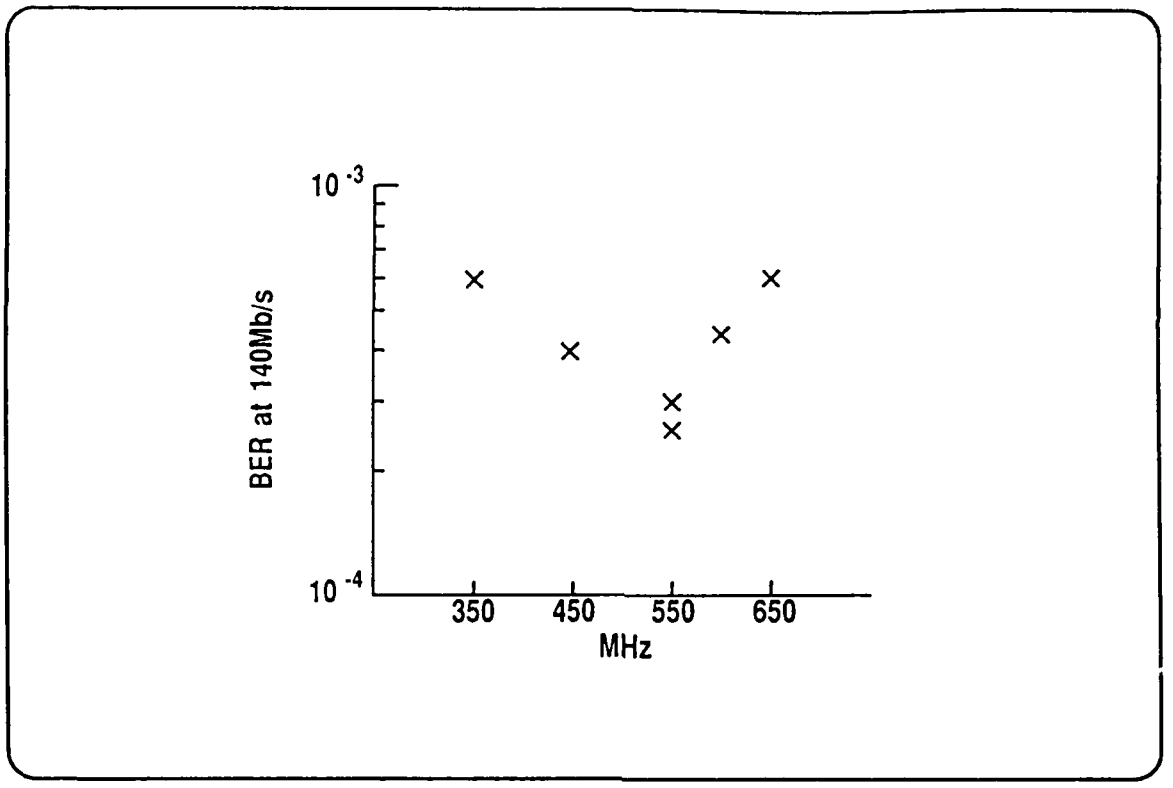

Figure 5.17 EFFECT OF CHANGING IF (LOWER SIDEBAND) CENTRE FREQUENCY

Figure 5.18 BER OF DIGITAL LINK DURING OPTIMISATION STAGE

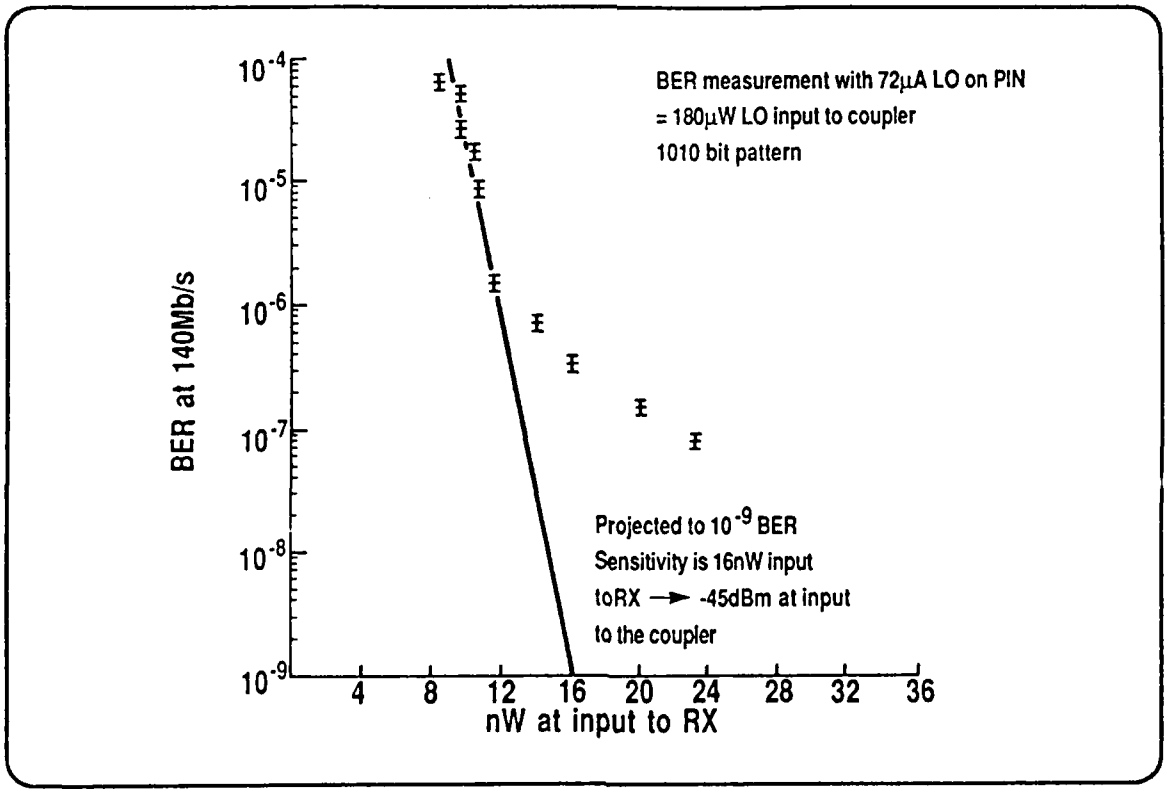

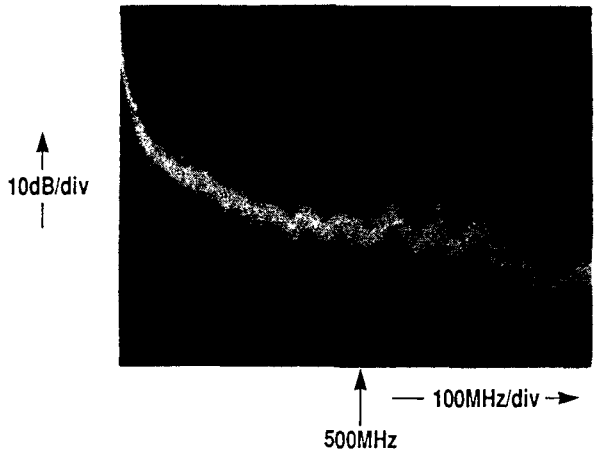

Figure 5.19 IF SPECTRUM SHOWING LOW FREQUENCY EXCESS NOISE

Figure 5.20 POSSIBLE REFLECTION PATHS IN RECEIVER OPTICS

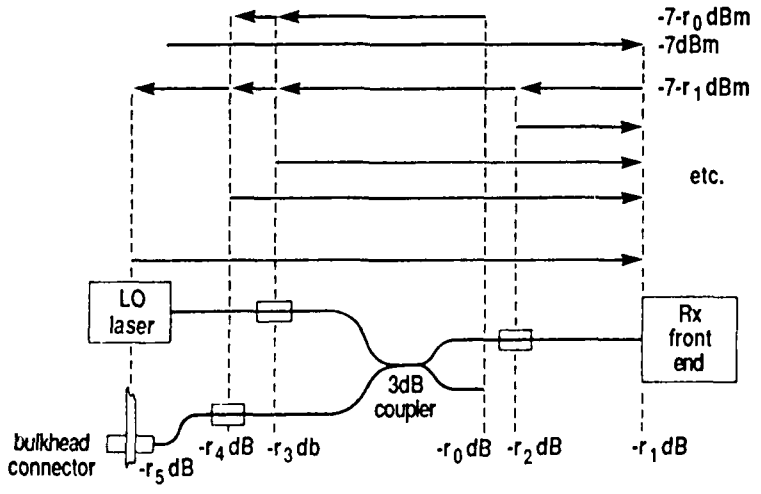

A BER curve was measured against input signal power; the resultant can be seen in Figure 5.18. It shows a strong BER floor becoming apparent below 10^{-6} BER. If the floor was absent the sensitivity would have been 16nW at the input to the receiver. The optical front end in use at this time was the dual PIN receiver, in order to use all the available LO power with no signal loss. However, the shot noise spectrum of the system with no signal present was not flat. A typical shot noise spectrum is shown in figure 5.19, in which the high pass filter of the IF board had been removed. The most notable feature of the spectrum is the high values of noise in the sub 100MHz region giving a resemblance to a 1/f noise spectrum.

After some changing of the optics section of the system it was realised that this low frequency excess noise was due to reflections at optical splices in the system. The LO is reflected back into the system from the cleaved fibre end in the receiver. This reflected signal is then re-reflected at one of many splices, back into the receiver and together with the LO then produce self homodyne components when they are mixed down on the photodetector. The range of possible reflection paths are seen in Figure 5.20. The extent to which the "excess noise" extends into the frequency domain depends on the distance travelled between reflections and hence the degree of coherence between the reflected waves. If the two optical paths were very different in length then a Lorentzian distribution would be seen as in a self homodyne measure of laser linewidth. This would have a distribution which would extend to more than a GHz.

In order to reduce this effect the fibres between the coupler and the receiver were cut as short as was possible to still fit them into the system. It was found that splices from the LO to the coupler and signal input to the coupler had considerably less effect. The major cause of the reflection was considered to be the cleaved fibre end in the front end receiver, although calculations showed the level of reflection was not the 4% that could be expected by a normal facet angle. The dual PIN receivers

were found to be more prone to this excess noise because they have two fibres. As a result the front end receiver was changed to a single PIN receiver since a 3dB penalty at 10^{-9} BER was considered less significant than the error floor seen in Figure 5.18.

After this optimisation a BER of 10^{-9} was achieved and the system was tested to the design plan. The laser sideband of the system can be seen in figure 5.21and shows the modulation centred at 500MHz, the clean shoulders of the shot noise spectrum at 100MHz and 950MHz with no excess low frequency noise breaking through the high pass IF filter.

5.3 TEST RESULTS

5.3.1 Test Plan Summary

The test plan set out to characterise the digital links primarily by measuring the bit error ratio or BER. This is a much more accurate method of determining the sensitivity of the link than signal to noise measurements before a comparator and is the most significant characteristic to the system user. Details of the test conditions and a discussion of each of the results are given in the following sections and the emphasis is on the system measurements. However it was considered necessary to measure the critical components as part of the test plan in addition to a routine test of each component as it was assembled. Detail of the test plan are also given in the document delivered as CDRL item A004, dated January 1988.

Laser characterisation for current and temperature tuning charactistics with wavelengths was carried out. The laser linewidth was measured for a range of temperatures and drive currents for each of the transmit and LO lasers in order to determine the optimum wavelength to mimimise the combined IF linewidth. The laser power variation with current and

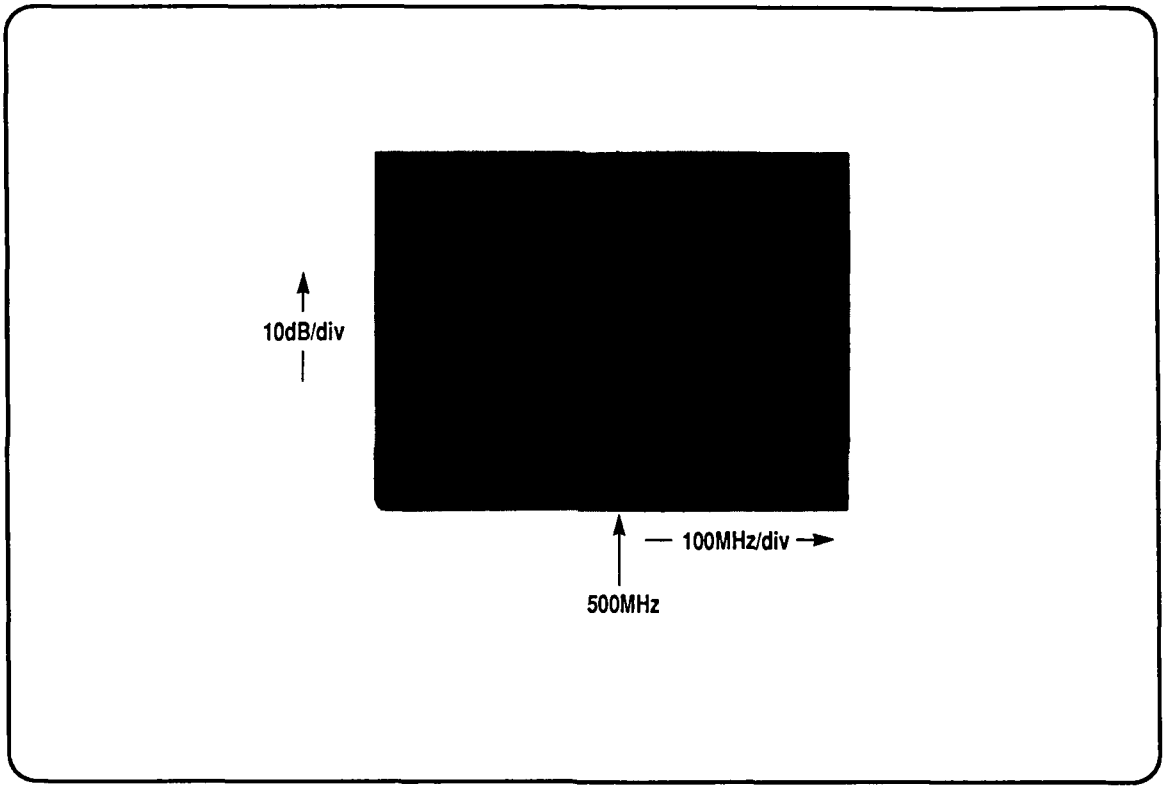

Figure 5.21 LOWER SIDEBAND WITH 140Mb/s MODULATION

temperature was also determined, using a DC measurement technique. The FM response of each laser was measured, in that a varying input frequency of constant amplitude was applied to the laser and the frequency deviation for each applied frequency was measured.

The front-end receiver was measured and the loss parameters of the combining couplers were noted in order that the loss between front-end and bulkhead connector can be determined.

The BER ratio with input optical power was characterised at a frequency of 140Mb/s. The optical power was set in the mid range of the BER curve and the variation of BER with modulation frequency was characterised. The BER was then set at better than 10^{-8} and a stabilisation test was carried out. This was done twice, once with the 10km of fibre between the transmit and receive units, together with optical attenuation, and once with ~ 5m of fibre. This separates out the effects of polarisation drift in the fibre length and drift in the coherent system. The polarisation control settings were not re-adjusted during the stability test with the 10km fibre length.

The dynamic range of the system was established by reduction of the attenuation, which was used in addition to the fibre loss in the link for sensitivity measurements.

All the above measurements were carried out with a 1010 word pattern which gives an input signal of 70MHz square wave using 140Mb/s NRZ modulation. The effect on the link budget was assessed for patterns which included 1100 and 111000 patterns in addition to 1010. This was the effect of simultaneously applying a mix of frequencies to the laser but it is not a completely broad frequency spectrum as generated by a pseudo random bit sequence.

The IF stability was assessed from switch on when the AFC loop was disconnected. The position of the IF was sampled using a spectrum analyser in peak hold mode.

Using the same front-end receiver and first amplifier the system was reconfigured to be a direct detection system. The BER against input power was repeated for the direct detection system and the input optical power at 10^{-9} BER was compared between direct detection and coherent demodulation.

5.3.2 Laser Results

The light output power against current curves for the transmit laser is shown in Figure 5.22. The equivalent curve for the LO laser is shown in Figure 5.23. The output power of the transmit laser at the minimum linewidth condition is 400μW at 93mA. The lasing threshold can be seen to be 35mA. The LO laser has an output power of 260μW at a temperature of 15°C. The minimum linewidth condition occurs at a current of 83mA, any increase or decrease in the current at this temperature increased the linewidth. Other temperatures also show increased linewidths. The minimum line width condition at a wavelength of 1533.7nm, for the transit laser is 25MHz, this is shown in Figure 5.24b. Figure 5.24a shows the spectral response of the transmit DFB, any sidemodes of the laser, with no modulation are greater than 50dB down on the main mode. The minimum linewidth condition for the LO laser is a linewidth of 40MHz, this is shown in Figure 5.25b, it can clearly be seen to be broader than the previous Figure 5.24b. The sidemode suppression is greater than 40dB in the spectral response of Figure 5.25a.

The FM response of both the lasers is shown in Figure 5.26. The dc thermal response is shown on the zero MHz axis and is 1.7GHz per mA and 1.4GHz per mA for each laser. The curve shows the magnitude of the FM response, as the regime changes from thermal to current controlled index changes there

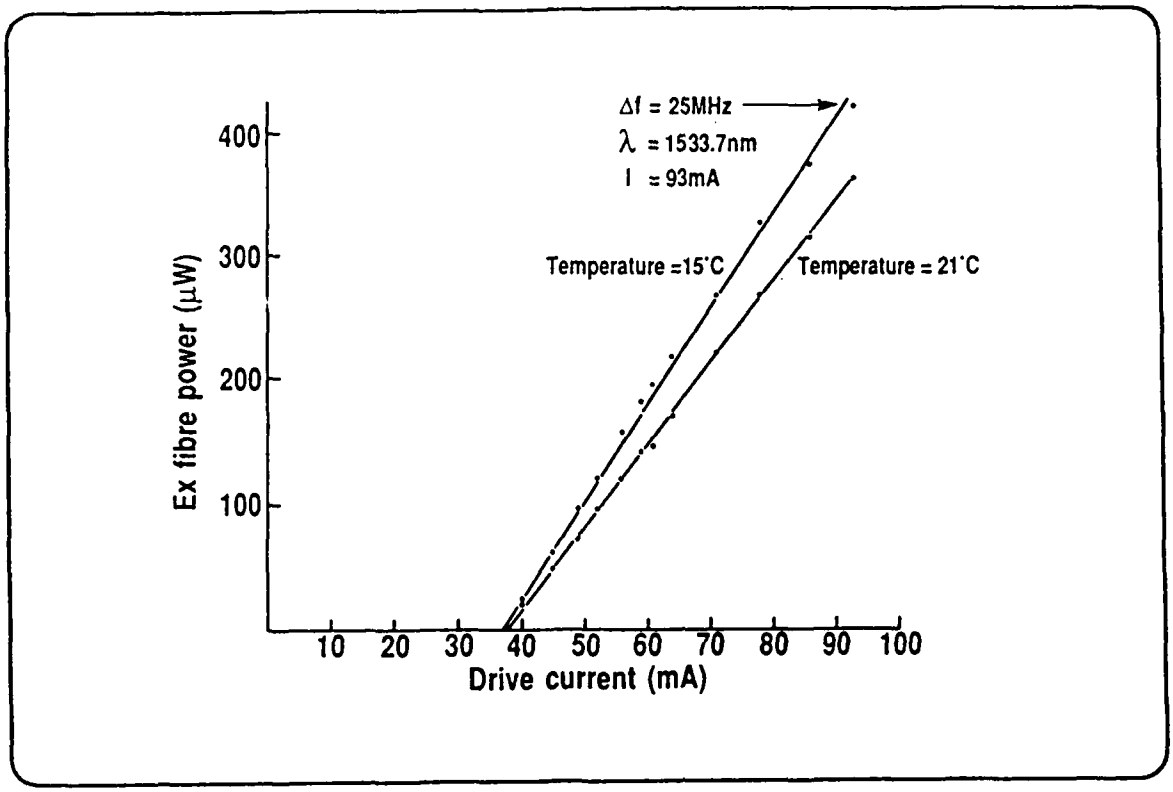

Figure 5.22 POWER CURRENT CHARACTERISTICS OF TRANSMIT LASER

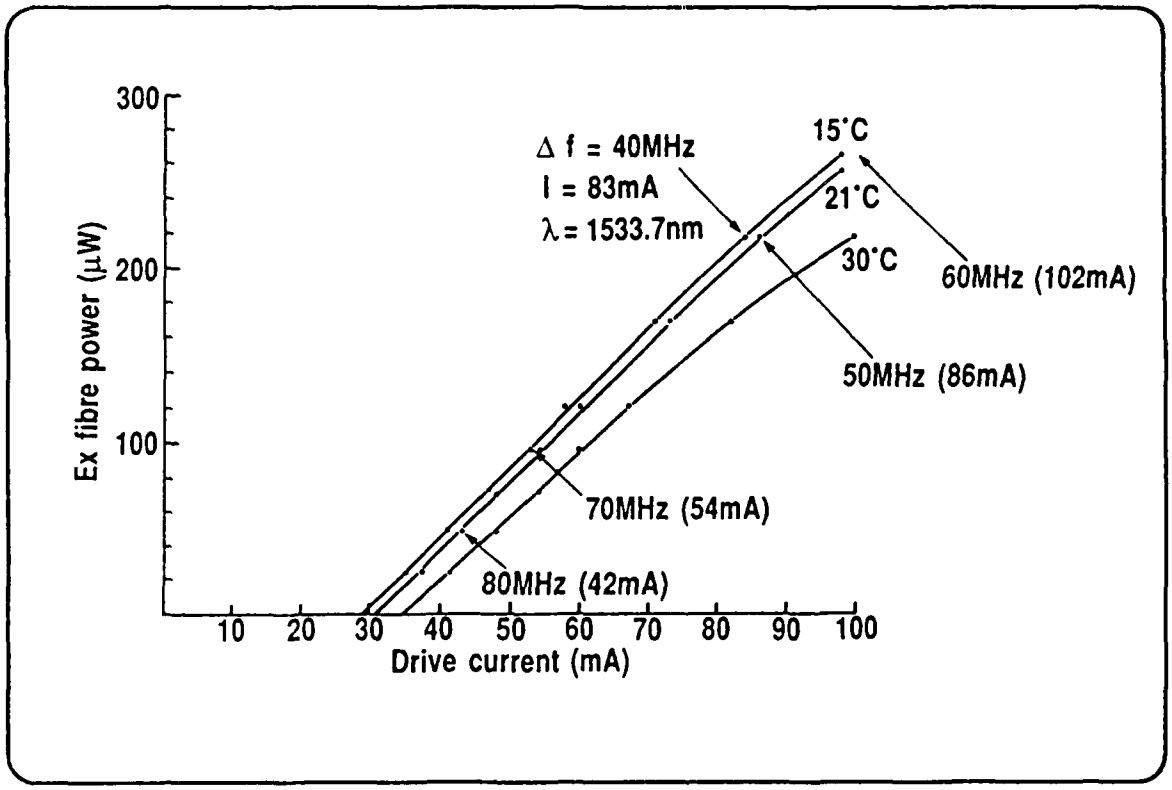

Figure 5.23 POWER CURRENT CHARACTERISTICS OF LOCAL OSCILLATOR LASER

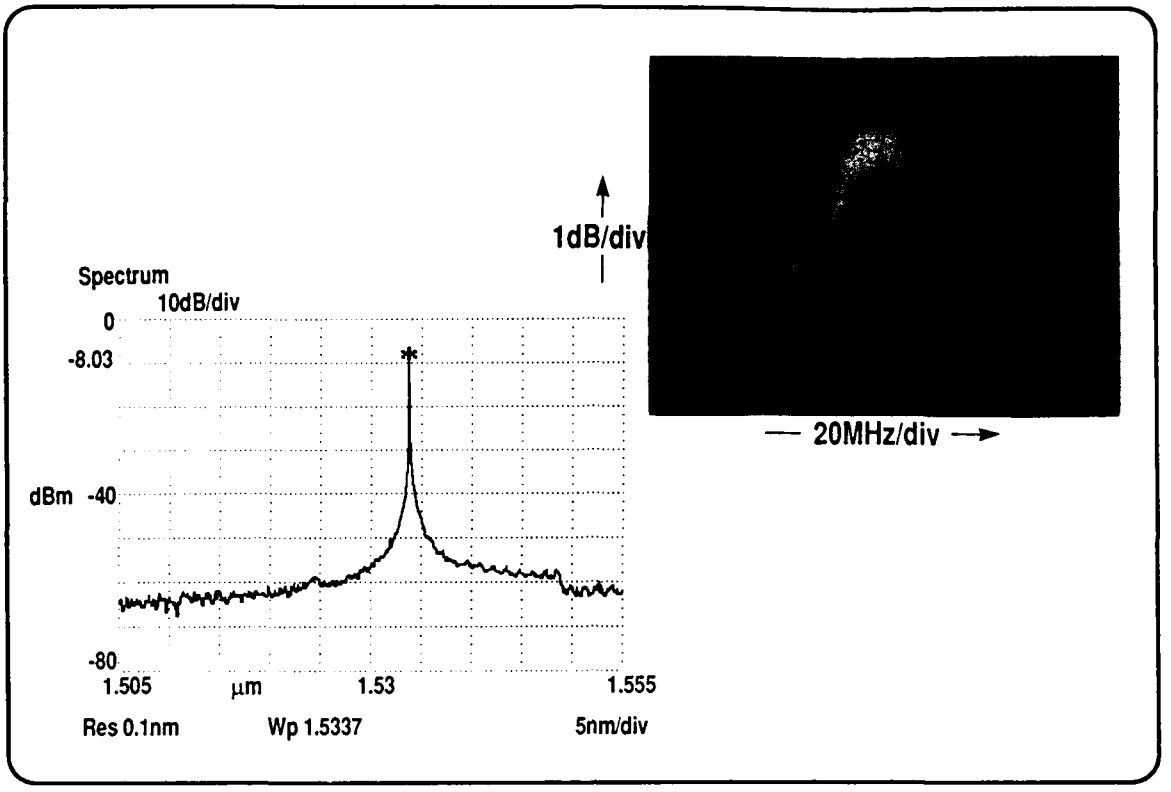

Figure 5.24 SPECTRAL RESPONSE OF THE TRANSMIT LASER

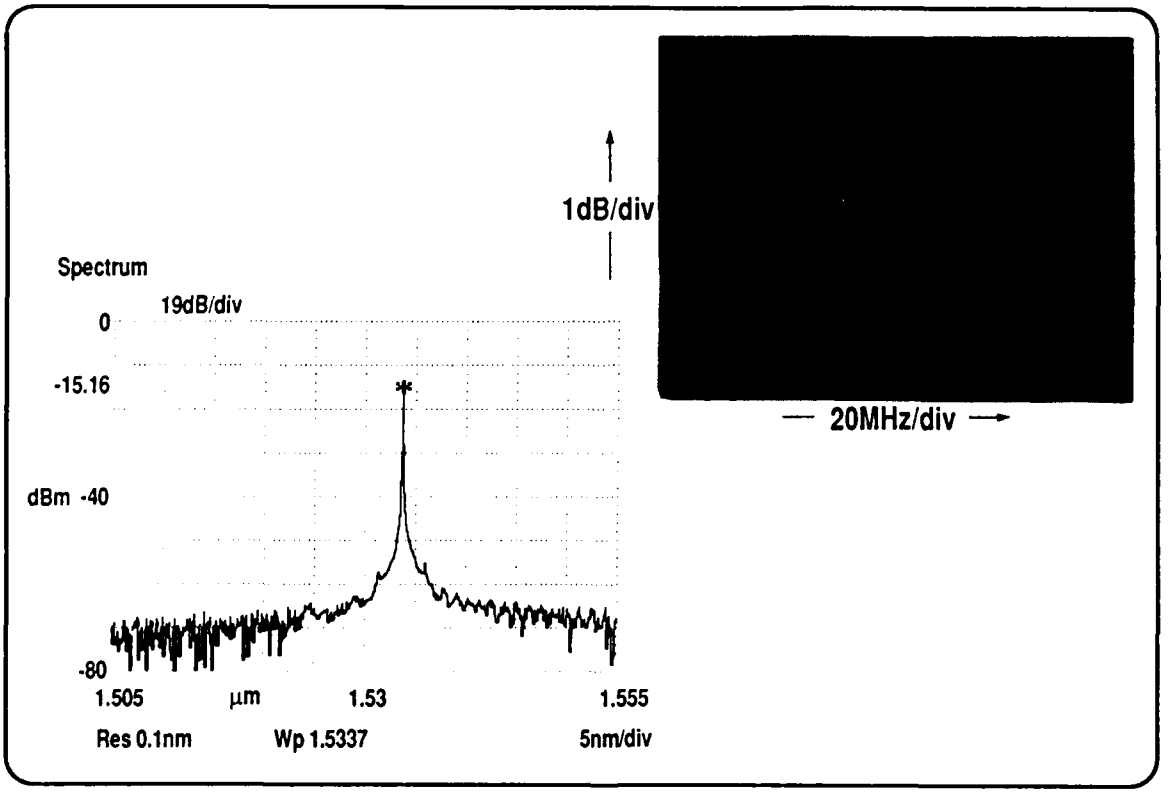

Figure 5.25 SPECTRAL RESPONSE OF THE LOCAL OSCILLATOR

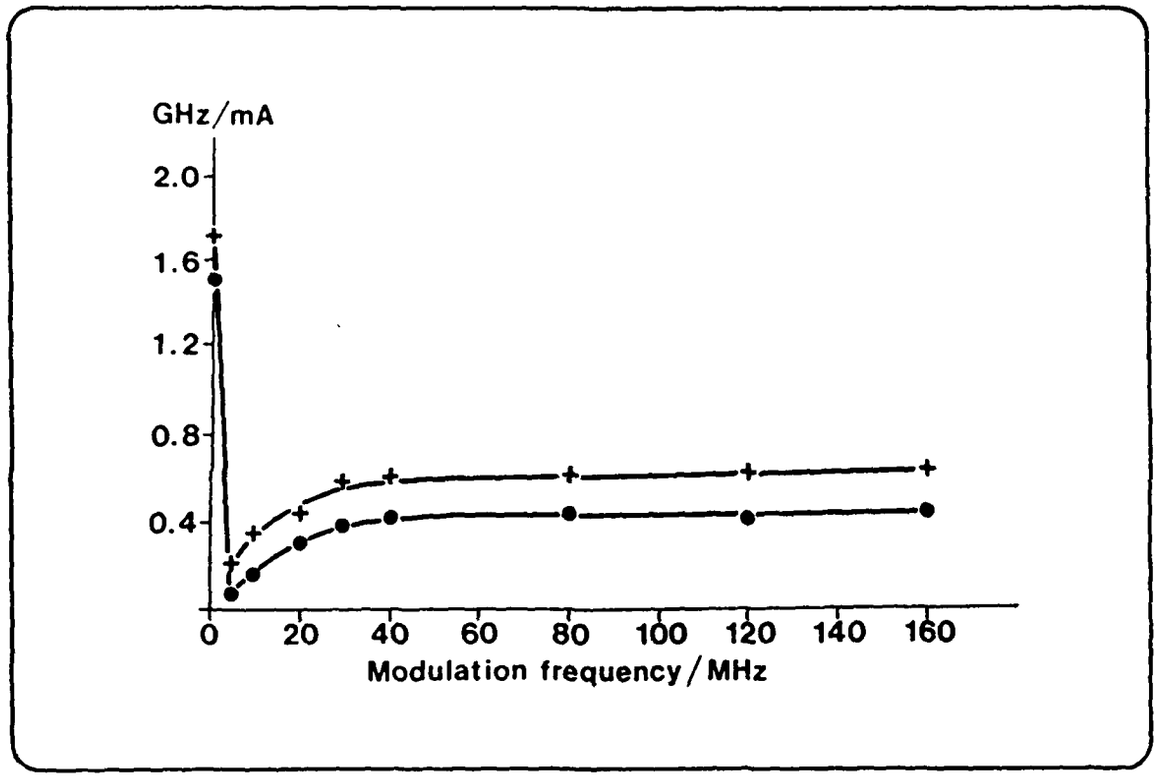

Figure 5.26 FREQUENCY DEVIATION VARIATION WITH MODULATION FREQUENCY

is also a change of phase. In both these lasers this occurs at ~5MHz. It would therefore be impossible to modulate a laser with a broad spectrum of signal in which the frequency went over this virtual null and phase change, because below this frequency the signal would be detected in the "wrong" sideband. The curve has a steady increase in modulated amplitude over the range from 5 to 40MHz and then it appears flat to 160MHz. The 1dB points on the low frequency roll offs are roughly 25MHz and 30MHz clock rate.

When these results are compared with the provisional specification for the lasers it can be seen that the lasers are better than required on both output power and sidemode suppression. The nominal wavelength is 1.55μm and the two lasers were matched at 1.5337μm. The wavelength separation of the two lasers at the same temperature is well within 2nm since they are matched when both are at 15°C. The laser modules include both isolation and thermocoolers for temperature stabilisation. Unfortunately the linewidth of the lasers was higher than that desired. But adaption of the system as discussed in the section of optimisation has removed any penalties that this linewidth would have caused. The FM response was specified to be flat to 1dB from 30MHz to 300MHz. This cannot be exactly measured so the 25MHz 1dB point from the curve is within the error of the curve. The measurements were made beyond 160MHz clock rate as shown on the figure since a 500MHz reading was taken which would be on the same straight line but was not plotted.

5.3.3 Receiver Results

The performance of the front-end receiver can be summarised below.

Responsivity @ 1.55μm	0.95A/W
Gain	7.5 V/V
Input capacitance	0.6 pF
Bandwidth	950MHz
12:1 SNR at 678Mb/s	-37.1dBm
Overload level	> -11dBm

The mean input noise in terms of an input current can be calculated from the SNR measurement knowing the filter bandwidth for the measurement was 470MHz. This gives a total noise of 30nA in the filter or a mean equivalent noise of 1.4pA per root Hz of bandwidth.

The frequency shape of this noise can be seen in Figure 5.27. This was measured on a similar receiver to that used in the system, but because it was a dual PIN receiver, the input capacitance, and hence high frequency noise was higher.

In comparing these results with the requirement specifications the receiver meets the requirement in all the measured parameters other than capacitance where the achieved total input capacitance is 0.6pF compared with required 0.5pF . This is within the ± .1pF measurement accuracy of the method used to determine capacitance.

The results sheet for the optical coupler can be summarised as:

Excess loss	0.04dB	at	1548nm
Coupling ratio	52%	"	1541nm
Directivity	>50dB		

No attempt was made to remeasure the Gould results because the accuracy of the remeasure would not be better than .1dB for excess loss.

In addition to the coupler loss when calibrating the system sensitivity allowance must be made for the splice losses in the system. There are three splices from the bulkhead connector to the receiver front end. From the bulkhead connector the first splice is from the Dorran jump lead to a

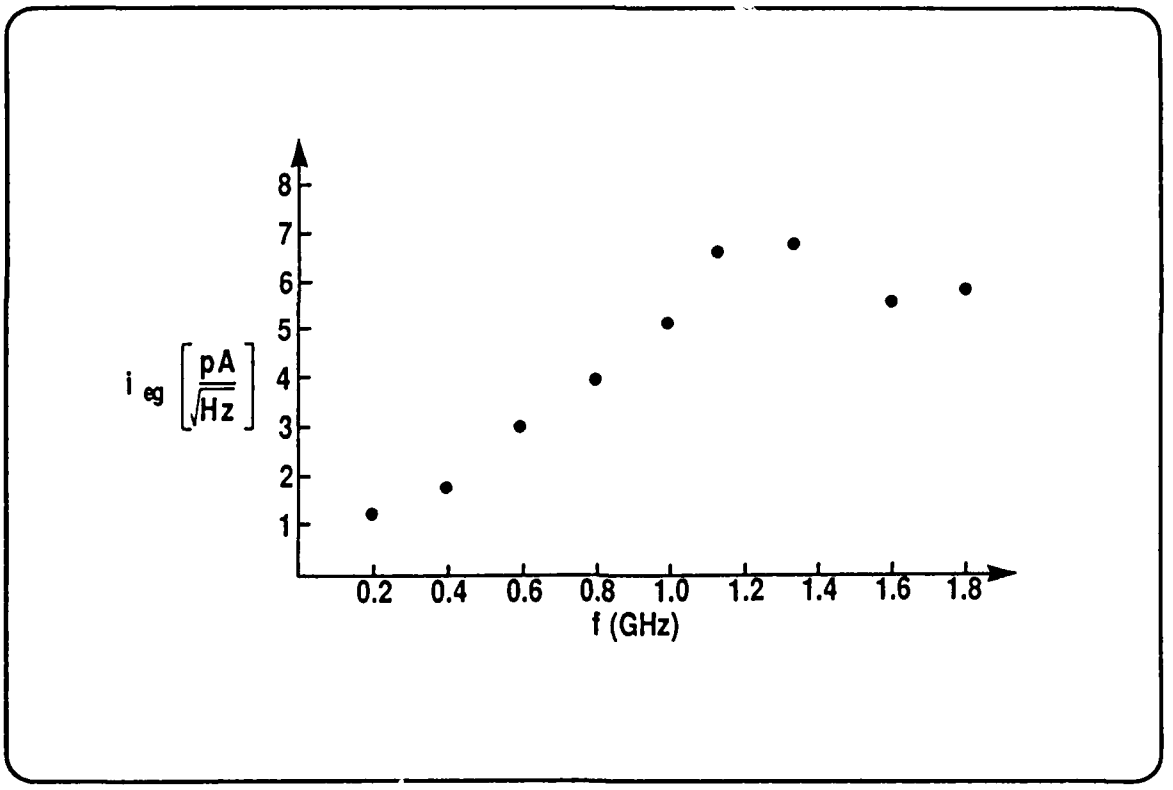

Figure 5.27 EQUIVALENT INPUT NOISE CHARACTERISTICS WITH FREQUENCY OF THE FRONT END RECEIVER

length of 250μm outer diameter fibre. This runs through the polarisation squeezers which have no excess loss to a second splice which connects to the fibre coupler. This extra length was included because if the squeezer was to produce fatigue in the fibre over a long period of time, and hence produce breakages, this length could be replaced. From the ouput of the fibre coupler is a further splice to the receiver front end.

The calibration (at a high optical input level) of the losses through these splices can be seen in Figure 5.28. The input power to the bulkhead connector on the receiver was measured using a jumper lead to fibre end into a calibrated power meter. This gave a reading of 11μW which would include the connector loss which the data sheet claims is 0.7dB maximum. The system fibre is replaced and the 11μW optical power produces a photo-current of 4.54μA. Given the responsivity, measured previously, of 0.95A/W this implies an optical power of 4.78μW at the receiver front end. The splitting loss of the coupler accounts for 3dB of this loss of 3.6dB, which implies the three splices have a mean loss of 0.2dB. This was considered a satisfactory result. As a check on the photocurrent reading a power meter on the other arm of the coupler read -22dBm which agrees to within 1dB.

5.3.4 System Results

Figure 5.28 also shows the available loss budget of the system. The output power from the transmit laser, as measured by a jumper cable with a Dorran connector to free fibre end was 286μW. This power is the transmit laser as measured previously minus one splice and one bulkhead connector loss. The power at the output of the J.D.S variable attenuator when set at 0dBm was 128μW, which gives a total loss of 3.5dB, the total for two splices, insertion loss of the attenuator (given as less than 1.5dB in the data sheet) and a further Dorran connector pair. When operating the system losses up to 38dB could be set on the attenuator giving a total allowable

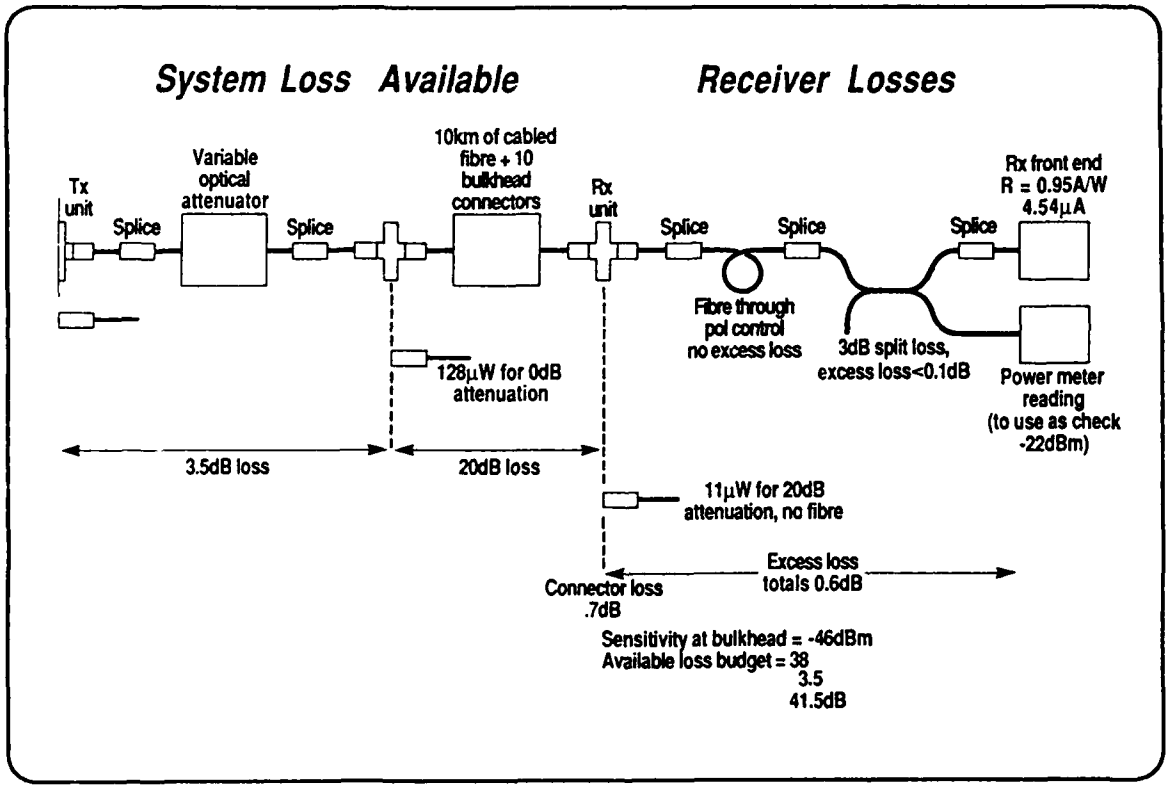

Figure 5.28 SYSTEM LOSS BUDGET AND RECEIVER CALIBRATION

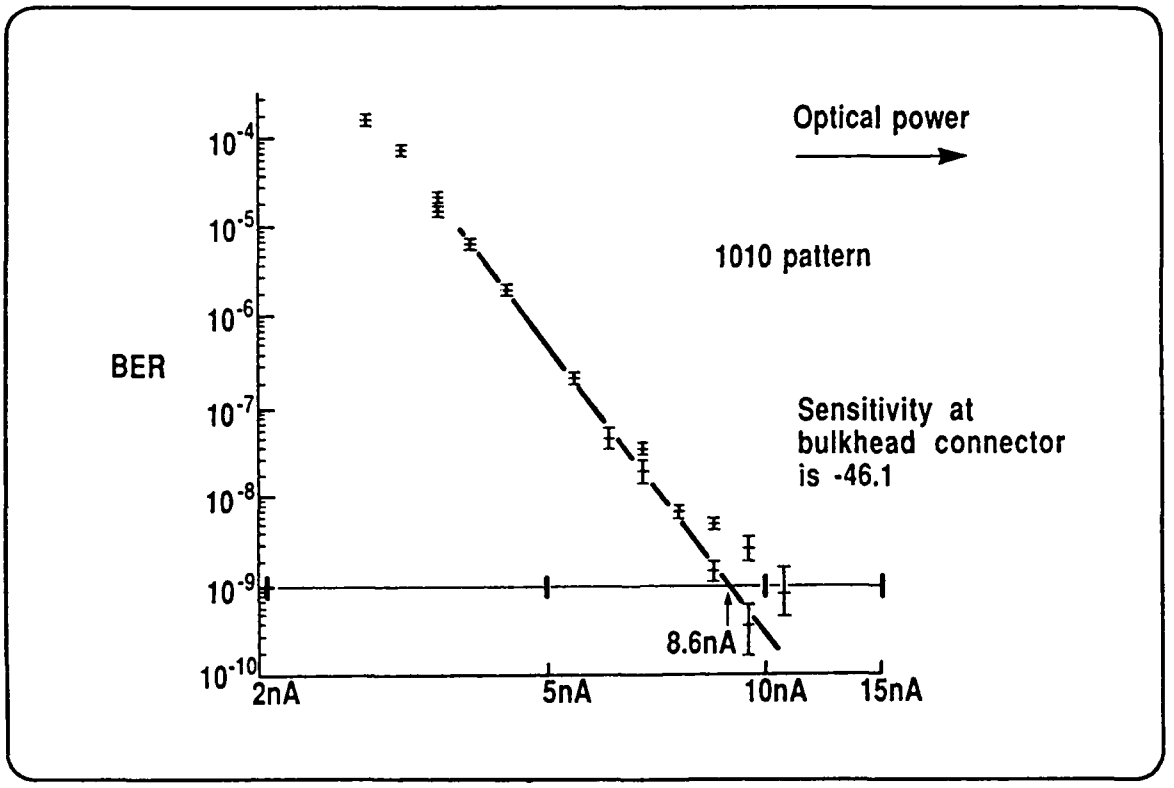

Figure 5.29 BIT ERROR RATION OF 140Mb/s SYSTEM

system loss budget of 41.5dB from the transmit bulkhead to the receiver bulkhead.

The BER curve against input power to the receiver is shown in Figure 5.29. The x axis uses measured photocurrent at the receiver front-end. This was derived from the variable attenuator against photocurrent when no LO power was present. The photocurrent for a BER of 10^{-9} is seen to be 8.6nA. This is a sensitivity of -50.4dBm at the input to the receiver, or, from the calibration at the higher input level of the receiver, -46.8dBm at the bulkhead connector and -46.1dBm in the fibre allowing 0.7dB for the connector loss.

On Figure 5.29 the error bars plotted are the standard error of a distribution of measurements for each power setting. Where two points are plotted for each photocurrent this indicates the optimisation of the polarisation control which was readjusted on four of the data points.

Figure 5.30 shows the stabilisation test of the system with only 5m of fibre. After the initial adjustment no further optimisation of the polarisation setting was made. The BER was put in the middle of the curve by adjusting the attenuator so changes in either direction could be quantified. The equipment was left for a total of three hours with samples of the BER taken during this period. It can be seen from the curve that the BER improved with time by a factor of 10. This is equal to a non optimum start penalty of 1dB which is the accuracy of polarisation alignment obtainable manually.

The BER against time with the 10km of fibre included in the link is shown in two Figures, 5.31 and 5.32. The first curve is for the first 90 minutes of the test with the second curve showing 80 minutes elapsed to 159 minutes. The BER was set at 1×10^{-9} by optimising the polarisation at the sensitivity limit and the equipment was then left with no further adjust-

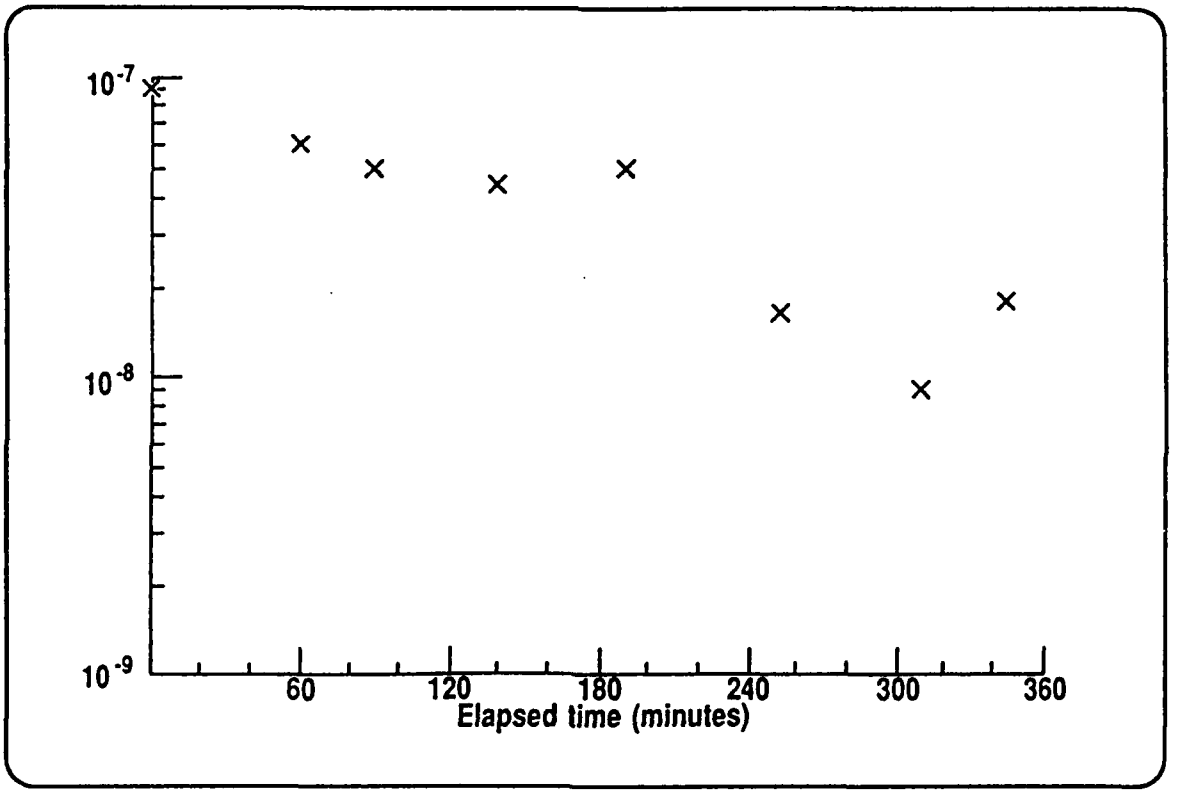

Figure 5.30 STABILISATION TEST WITH 5m OF FIBRE

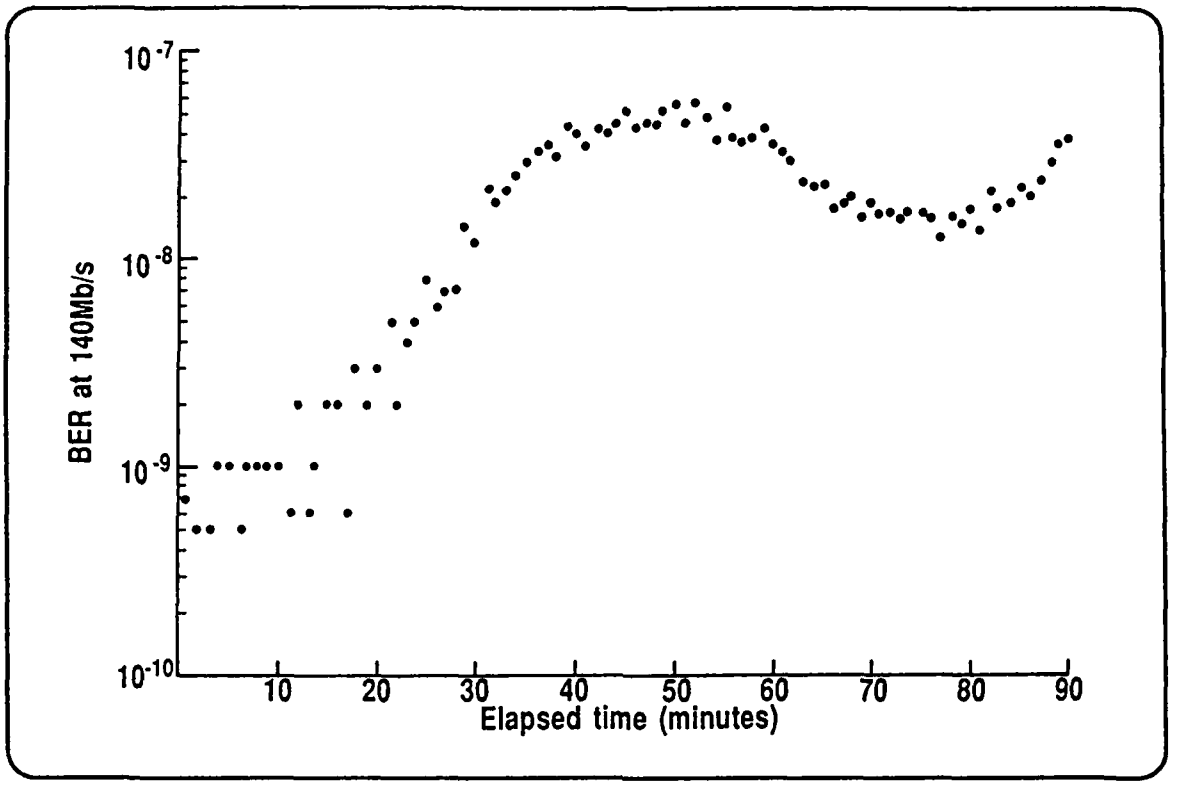

Figure 5.31 STABILITY TEST OF COHERENT LINK WITH 10km OF FIBRE

Figure 5.32 STABILITY TEST CONTINUED

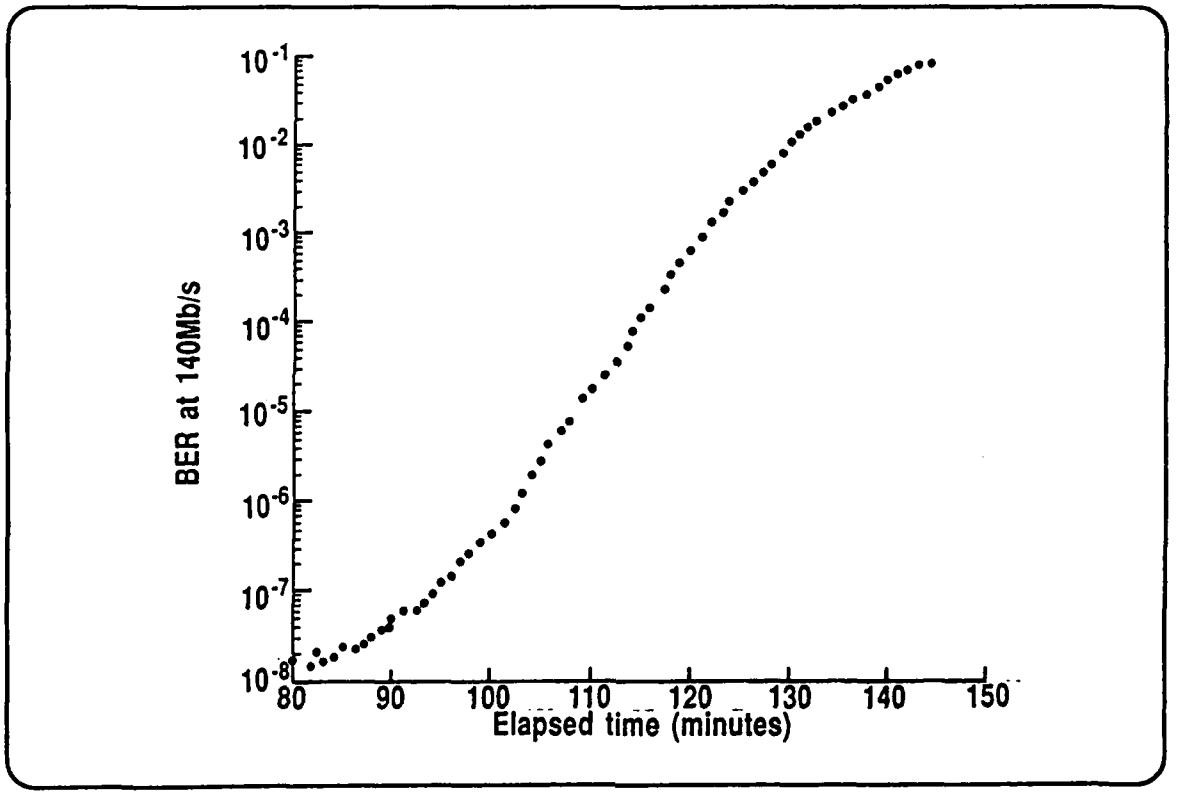

ment for two and a half hours. Again, as the run without fibre, the first change was to improve the BER, to 4 x 10^{-10} indicating an original polarisation inaccuracy of 0.5dB. The polarisation was not readjusted throughout this test so this gives the effective time period of polarisation drift and hence indicates how often the polarisation must be readjusted to keep to a defined BER. To keep to 0.5dB penalty ie; half a decade on BER the polarisation would have to have been readjusted after ten minutes. The link was within 2dB of its original setting for 94 minutes with no polarisation readjustment. Hence if a link margin was greater than 2dB the BER would have been better than 10^{-9} for 90 minutes in a laboratory environment. After 90 minutes had elapsed the polarisation continued to rotate giving an ever worsening BER. When the BER receiver had an overflow on errors and synchronisation was lost the test was finished. At this point the IF spectrum was noted and no sideband could be seen in the LO shot noise spectrum.

The effect of changing the clock frequency on the system was characterised in Figure 5.33. The link budget was adjusted on the attenuator to give 10^{-6} BER at 140Mb/s. This gave shorter sampling times for the BER measurement and allowed the changes with frequency to be quantified. As the clock frequency was increased the number of errors increased to worse than 10^{-3} at 160Mb/s. No further increases were made, since to get sensible results the low pass, post detection filter would have had to have been changed. The reduction of clock frequency below 140Hz clock rate gave less errors down to 110MHz. This implies the post detection filter, which was established previously as optimum for the direct detection link was at too low a frequency to optimise the coherent sensitivity. From the improvement between a 140MHz and 110MHz clock rate, through the same filter it can be deduced that the filter width was too low for optimum at 140Mb/s by 30MHz. The improvement in BER corresponds to a sensitivity improvment (by reference to fig. 5.29) of 3dB. This implies the achieved sensitivity at

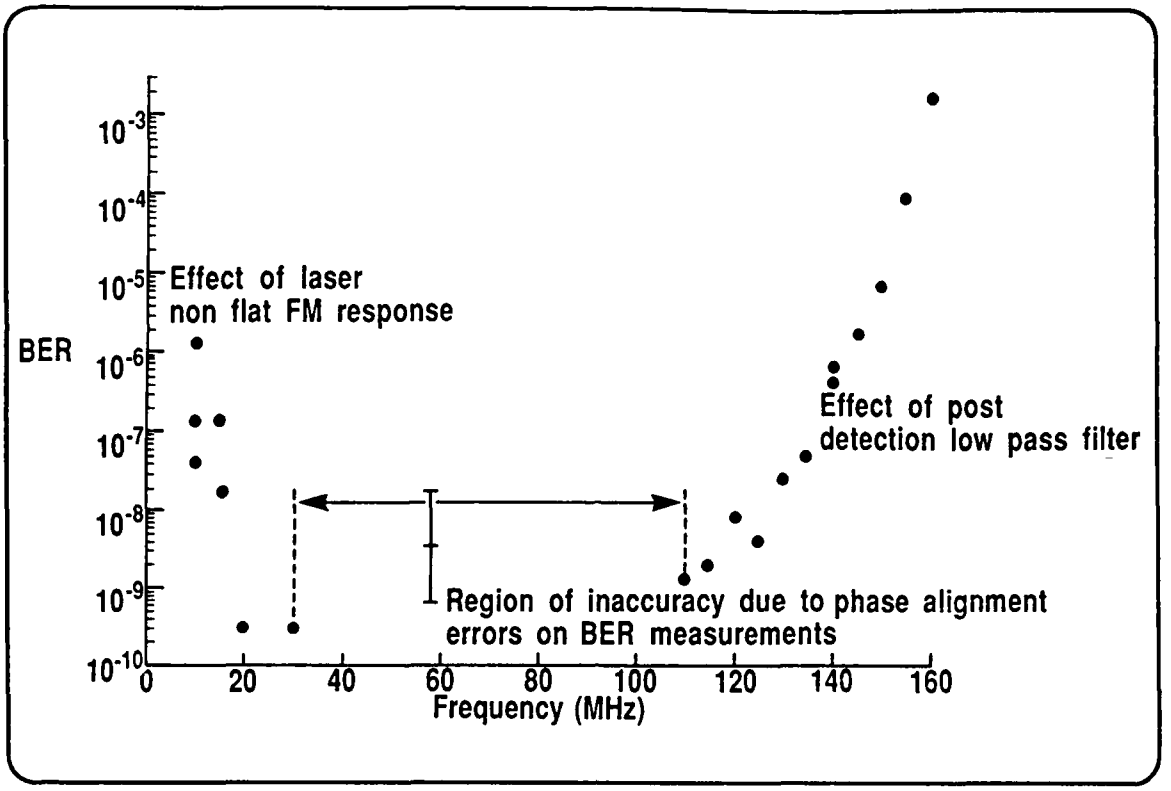

Figure 5.33 EFFECT ON BER IF CHANGING CLOCK FREQUENCY

Figure 5.34 LOWER SIDEBAND SPECTRUM VARIATION WITH MODULATION FREQUENCY

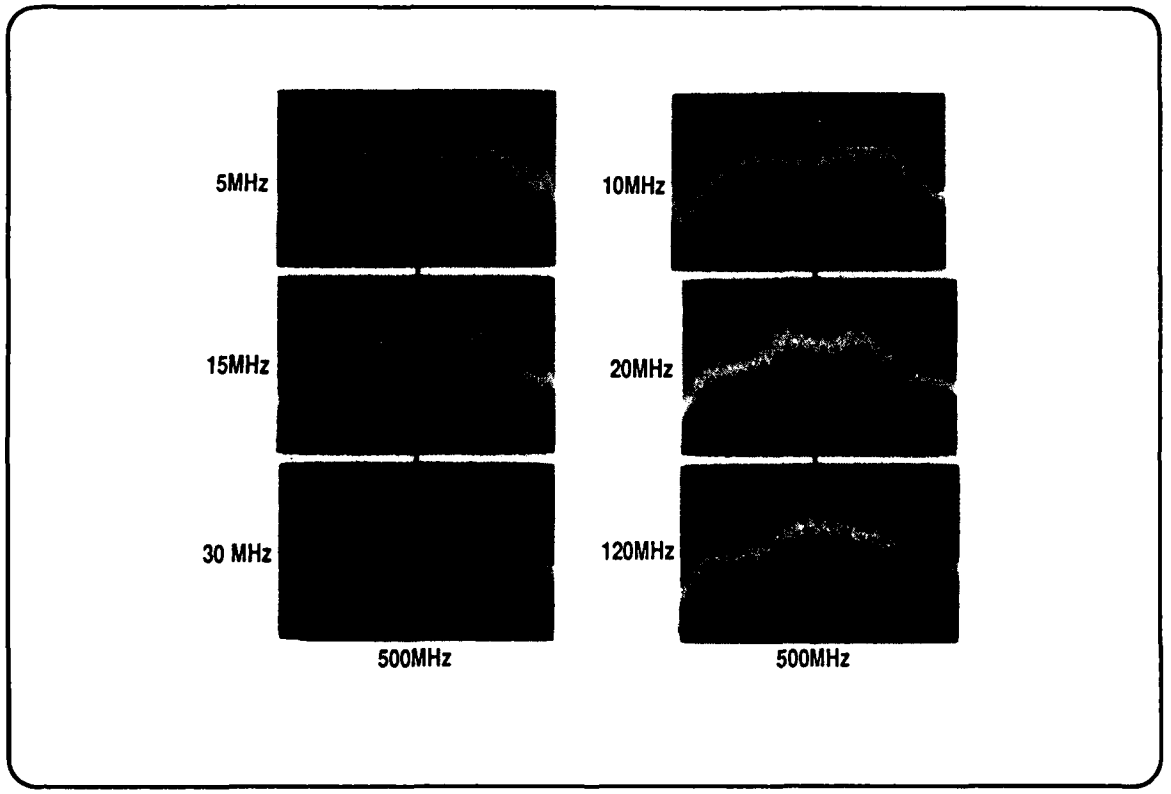

the bulkhead connector can be improved by about 2dB by increasing the post detection filter width from 65MHz to 95MHz, at the date rate of 140Mb/s.

Below 110MHz clock rate it became very difficult to sychronise the clock and data patterns. This was because the delay required on the clock was beyond the delays available on the BER measuring equipment. The clock for the receiver section is not derived from the data it is taken directly from the transmit section. There is a constant delay through the system but this will correspond to a different phase alignment of the data as the date rate is changed. Once the compensating delay required for the clock is beyond that available in the equipment various lengths of coaxial cable have to be used to provide the delay. This is not very accurate and since phase alignment of the clock sampling the data has a sharp optimum of approximately 100ps then adjustment with coaxial cable lengths is not easy.

The results between 110MHz and 30MHz are scattered because of the problems encountered on aligning clock and data. They have not been plotted because it would be confusing, but on a run down in frequency followed by a run up very different BER values were achieved, because of the alignment. Below 30MHz lengths of cable were adequate to set the clock sampling point because the time difference between the crossovers is higher. However below 30MHz more errors are detected as the non flat FM response dominates. Results were obtained at 10MHz clock but not at 5MHz. The lower sideband with varying clock frequency can be seen in Figure 5.34. Starting at the lower right hand side of the photographs with the 120MHz clock the sideband can be seen to be centred about a single frequency with no other features and is 10dB above the shot noise. At 30MHz the sideband width is lower, as would be expected since the data rate is lower and again is a distribution about a single frequency. However at 20MHz the sideband has two clear lobes corresponding to two distinct frequencies. This will be due to the FM response curvature, the fundamental in the square wave will have a

different deviation compared to all its highest harmonics. At 15MHz these lobes are becoming broader, despite the modulation frequency being less and the deviation between the lobes is larger due to the continued and increasing amplitude difference in the FM response giving a much larger bandwidth signal spectrum. By 10MHz the lobes and the separation can just be seen, but it is becoming difficult to distinguish signal from the shot noise spectrum, and by 5MHz any signal present can not be distinguished from shot noise, It is therefore not surprising that the BER worsens with decreasing frequency in the range 30MHz to 5MHz, nor that no result can be obtained for 5MHz.

An alternative characterisation of the link to data rate with frequency is the effect of differing data words. The FM response of the laser is the cause of any such variation and the word pattern is the more sensitive test since the components are present simultaneously. A word pattern was programmed in which the 8 bit word consisted of a 1010 bit stream, the 12 bit also contained 1100 bit sequences and the 24 bit contained 111000 sequences. All the words were evenly coded in that the number of ones and zeros were the same so no DC offset existed in the data streams. At the same settings of the optical attenuator the word pattern was changed and BER measurements made. The clock phase was optimised for the 24bit word which gave a slight penalty (1dB) on the 8 bit pattern. The result of this experiment can be seen in Figure 5.35. It can be seen that the 1010 pattern achieved 10^{-9} BER but longer bit sequences did not and the slope of the curves is such that they would be unlikely to achieve 10^{-9}. These curves were generated with a 140MHz clock rate so the word pattern had components at 70MHz, 38MHz and 23MHz in square wave terms. The results of the BER at each of these three frequencies can be seen in Figure 5.33. Each of the frequencies when applied separately gives a BER of better than 10^{-7} with 20dB of attenuator loss. This correponds to 7nA of received photocurrent on Fig. 5.35. The results with the word pattern at the same setting can be seen to be 10^{-7} for 70MHz and 10^{-4} and 10^{-3} when

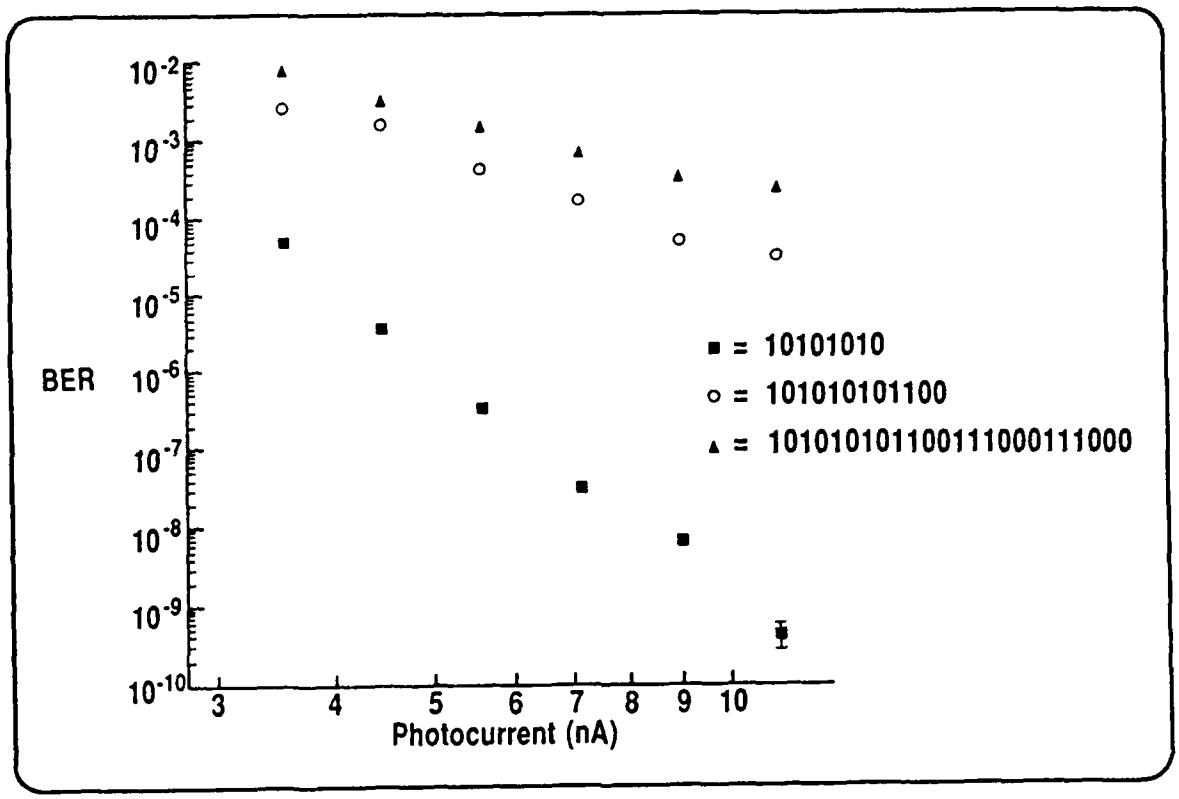

Figure 5.35 EFFECT OF WORD PATTERN ON BER

components of 35MHz and 23MHz are present simultaneously. Although from comparison with the frequency results of 5.33 no such degradation would be expected.

The use of single filter detection has the implication that no matter what shape or spectrum width the signal has, the AFC will lock the centre of the frequency spectrum to its lower sideband reference frequency. This has the implication that if the FM response varied with frequency, whilst only one frequency was present the AFC would lock on no matter how wide the frequency deviation. When several frequencies are applied simultaneously, as in a word pattern, then the AFC locks onto the mean of the deviations. The resultant laser sideband width is then considerably wider than with any one frequency applied. The FM response results of Figure 5.25 also imply the deviation is the same for these frequencies and certainly no tail is expected with 1100 patterns. The reason for this effect is considered to be the FM response is slightly non flat in band and hence the composite sideband of the frequencies is much broader than the 1010 pattern. Since the filter width, ie the IF frequency width is only just broad enough to pass the laser linewidth then the extra sideband width of a non flat response is too broad for the system.

The dynamic range of the link was established whilst the 10km of fibre was in place. The BER curve can be compared to that generated with no fibre in place and the difference in attenuator setting and hence the fibre loss is 19dB. This fibre loss is somewhat variable, on another occasion, perhaps with a different torque on the optical connectors, it was 21dB.

The optical attenuator can be changed fairly quickly so a dynamic range characterisation can be done before the polarisation will have drifted far and hence re-optimisation is easy. The curve in Figure 5.36 shows the results of the dynamic range characterisation. This was achieved without

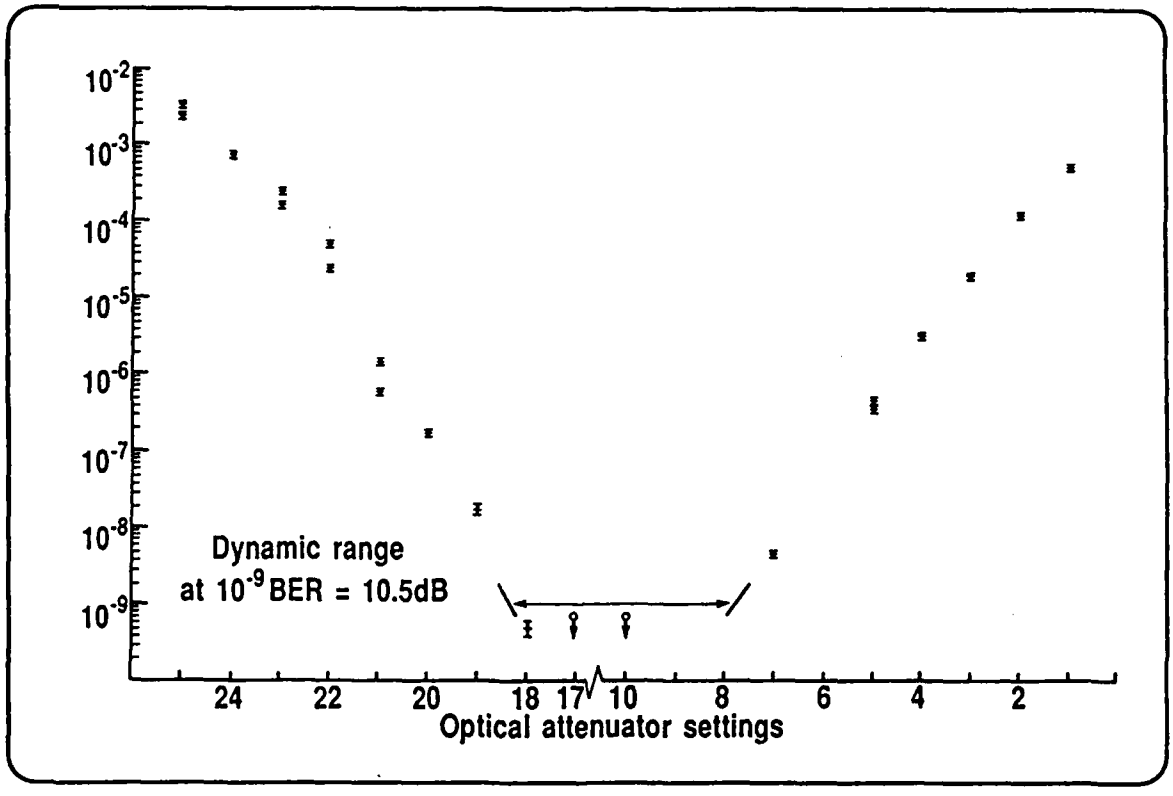

Figure 5.36 DYNAMIC RANGE OF DIGITAL COHERENT LINK WITH 10km OF FIBRE

any change of gain or other electrical adjustment. It shows a dynamic range at 10^{-9} BER of 10.5dB optical power. At a lower BER, such as 10^{-6} BER this dynamic range was 16dB in optical power. The range could be further extended by inclusion of AGC in the IF stage, the gain control was included as a manual control in the optimisation stage but is not self optimising. The overload mechnism appears to be softer than the noise limit and will no doubt be due to an amplifier working at or near its 1dB compression point giving rise to third order and higher intermodulation products.

5.3.5 IF Stability and Warm Up Time

In operation the system has an AFC loop to hold the frequency difference between the lasers constant. This will compensate for drifts including the warm up stabilisation period if the frequency change is not too broad. However to operate the system satisfactorily the AFC must be reset to mid range at the end of the defined warm up period in order to give a full operating range.

In order to establish the appropriate warm up period the AFC was disconnected. The length of time to reach 5GHz, 1GHz and 500MHz from the IF frequency was established. The lasers have very similar operating temperatures, both are cooled from room temperature. Therefore in settling to the final steady state condition the lasers are both following the same source frequency-time curve. The frequency difference between them is therefore stabilised very quickly. (If one laser had been cooled and one heated then this time would have been much longer.) The time to reach all the above frequency differences is under 10s. No more accurate measurements can be made since the sweep time of the spectrum analyser is in the order of seconds and switch-on can not be synchronised with a start of sweep, and by the time the analyser has swept to 5GHz the IF is well below 5GHz.

In order to ascertain the IF stability the IF was tuned to its 500MHz value within seconds of switch-on and then the spectrum analyser was put into maximum hold mode. The IF then swept out an envelope of its position with time on the analyser. No absolute frequency with time information was generated with this method but that is not usually relevant as long as the maximum excursion in a given time is known.

Figure 5.37 shows the results of this experiment, in the period from 30 seconds to 15 minutes the maximum frequency change was +300MHz. In the following 90 minutes the IF drift was ±350MHz about the nominal 500MHz. The lock range of the AFC loop is greater than 1GHz so these drifts would be adequately tracked.

However, if a warm up time is to be defined we would suggest 30 minutes which was used during the test programme. The results however indicate that if the AFC is connected and zeroed in the first few minutes the system should stay in lock for several hours.

5.3.6 Direct Detection Comparison

The procedure for changing from coherent to direct detection is as follows:

1. Switch off power supplies to both Tx and Rx units.
2. Change co-ax connection between modulation board and Tx laser. Put 50 ohms termination on unused lead.
3. Undo connector providing drive current to LO laser and thermocoolers, by unscrewing mounting screws. Place away from laser module.
4. Change co-ax connection from receiver front end from IF board to direct detection.
5. Switch on both Tx and Rx power supplies.
6. Turn Tx current from VMON=93mV to 50mV.
7. Measure direct detection sensitivity.

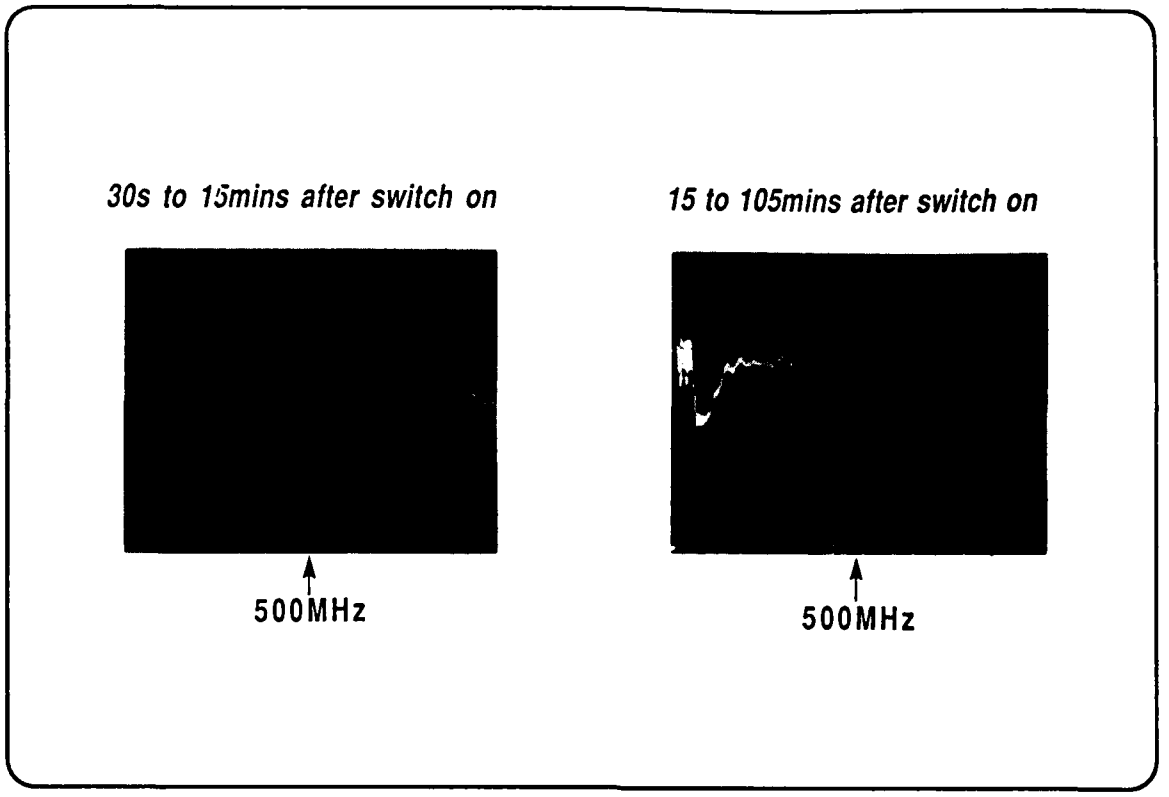

Figure 5.37 IF DRIFT WITH AFC DISCONNECTED

Figure 5.38 BER CURVE OF DIRECT DETECTION SYSTEM

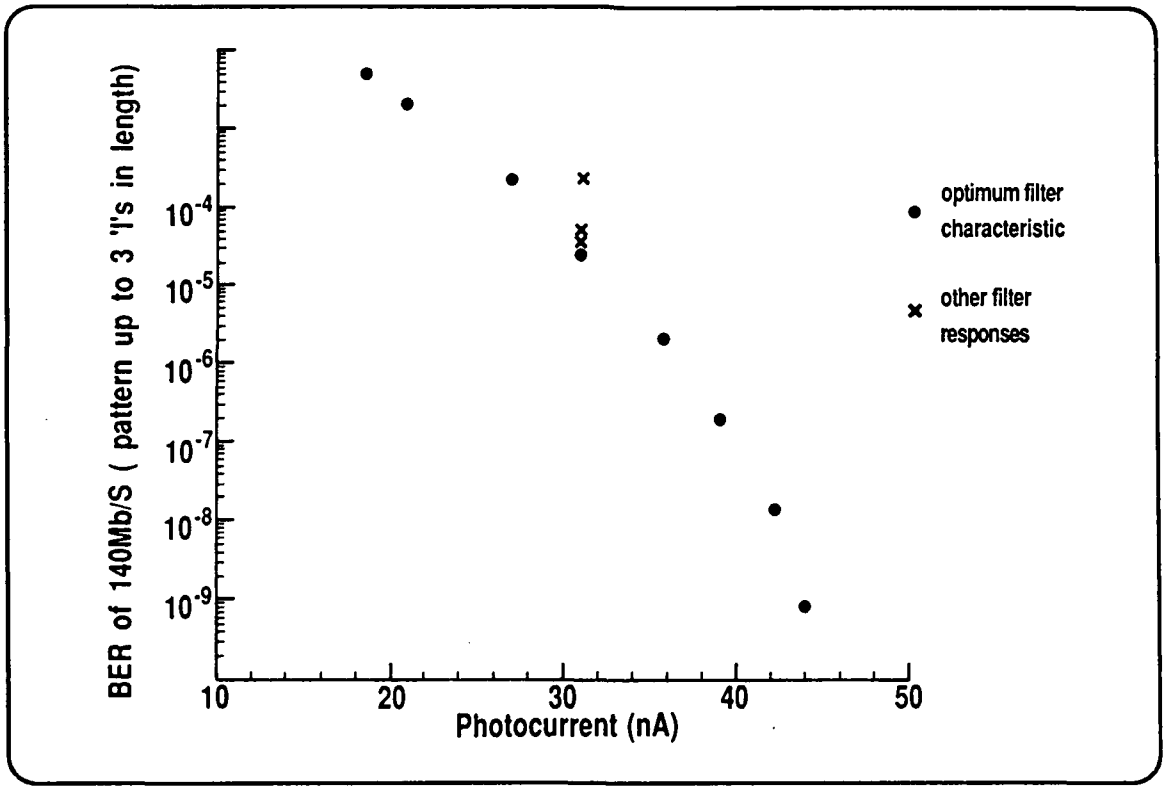

It must be noted that under no circumstances must the current lines be reconnected to the LO laser whilst the power supplies are switched on. This would cause catastrophic damage to the LO.

In direct detection mode the transmit laser is run at a DC current of 50mA which is 15mA above threshold. The modulation applied in the direct link is ±15mA giving as close to a 100% modulation index as possible.

The direct detection sensitivity was measured as photocurrent on the pin photodiodes. The BER curve is shown in Figure 5.38. The effect of changing the filter bandwidth can be seen on this Figure and the value used is the optimum at 65MHz-3dB point. The sensitivity at 10^{-9} BER in terms of mean photocurrent is 44nA. This can be compared with the 8.6nA mean photocurrent at which 10^{-9} BER is achieved on coherent detection.

This is a coherent advantage of 7.1dB at the front-end receiver. However because a single PIN receiver is used there is an extra 3dB loss in the coupler in the coherent case. Of course in this system the coupler is present in the direct detection system too, but would not be in a purely direct detection link. This reduces the coherent advantage, but use of a dual PIN would remove the 3dB loss and hence the 7.1dB advantage is still valid. During all these experiments 80μA of LO power was available therefore there is no extra penalty due to lack of LO power (ref. 5.6).

When comparing the advantage of coherent systems over direct detection systems the total budget advantage must be used. In this case this is the extra loss budget available between the bulkhead connectors of the system and includes some advantage which is a result of the laser characteristics.

To understand this advantage it is best to refer to the current power characteristics of the transmit laser in Fig. 5.22.

When the laser is modulated in the direct detection case it is modulated between 35mA (threshold) and 65mA, with a 50% duty cycle. The mean output power available is that which corresponds to a DC drive level of 50mA. The coherent modulation point is at a mean, DC drive current with a ±1mA modulation. The modulation depth is small giving changes of only .1dB between the peak coherent output power and the mean. The coherent modulation scheme has two output power advantages over the direct modulation scheme. One is the small difference between peak and mean giving a 2.9dB advantage. This is common for all FSK modulation schemes. The other advantage in this system is because of the particular drive currents chosen for the direct modulation scheme. Since an extinction ratio where extinction ratio is the ratio of power in the "zero" state to the "one" state of approximately zero was required, the laser was driven from threshold and the modulation was arbitarily set up at 30mA pp. This has led to a further coherent advantage of 2.8dB because of the higher peak output power of the coherent bias conditions. However, this is a comparison for these particular direct detection modulation conditions and are not a general advantage for a coherent communication link.

During this comparison between coherent and direct detection it was found that the switch frequency of the switch mode power supplies was being picked up by the direct detection receiver. It must be noted that the coherent link was immune to such pick up. As a result the direct detection result was obtained on bench power supplies. More power supplies were built of linear design which would not have any transients in the 400kHz region in order that a comparison can be made on the system power supplies.

5.4 SUMMARY AND DISCUSSION

A coherent fibre optic transmission system employing FSK modulation of 140Mb/s and single filter detection has been designed and constructed. The system is mounted in 19 inch racks and has undergone an agreed programme of testing at Plessey Caswell.

The system can be seen in Figure 5.39, the power supply racks have been omitted and only one 1km reel of fibre is included for clarity. Each part of the transmitter and receiver racks can be compared with figures 5.11, 5.12 and 5.13 to identify each block of the system.

The coherent advantage at the receiver has been shown to be 7dB (at 140Mb/s). The receiver has been characterised with varying frequencies and above 15Mb/s the sensitivity is better than the 140Mb/s value. A further improvement of 2dB in sensitivity at 140Mb/s could be achieved with a higher bandwidth post detection filter, giving a 9dB coherent advantage at the receiver.

When the system was operated with a short length of fibre with little polarisation drift, it was stable for several hours. When 10km of fibre was in place the system operated for ten minutes to within 0.5dB and then would require polarisation re-alignment. However, with no polarisation re-alignment the system operated to within 2dB for greater than 90 minutes.

The system gives a budget improvement of 12.8dB for coherent detection between the bulkhead connectors of this system. However 3dB of this is due to the loss of the coupler which gives an unfair disadvantage to the direct detection link, however, when using a dual PIN receiver it represents a fair comparison. Of this advantage 2.8dB is due to the higher drive current of the coherent system which is not necessarily an advantage as

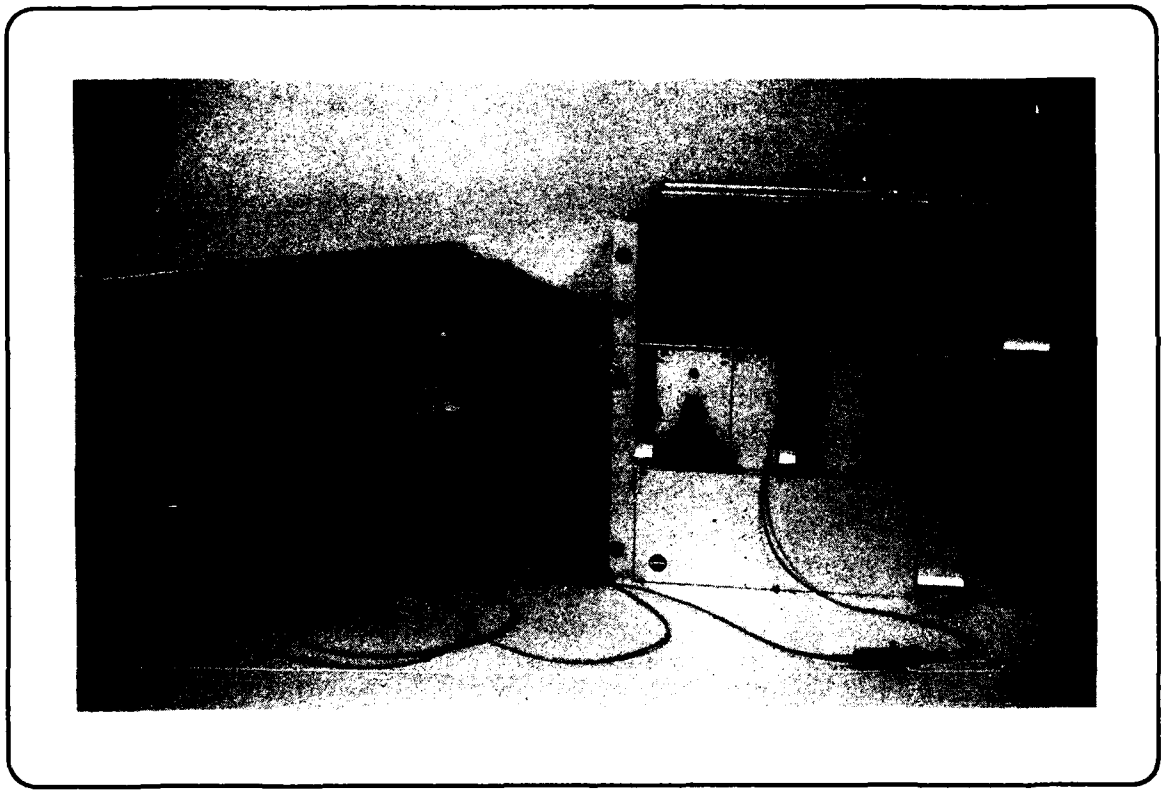

Figure 5.39 PHOTOGRAPH SHOWING COMPLETE DIGITAL SYSTEM

higher direct modulation currents could have been used. Hence the advantage of coherent detection over direct detection is a minumum of 7dB in the detected sensitivity and is demonstrated here to be 12.8dB in the loss budget between front panels.

This can be illustrated by the following summation of advantages:

7.1	sensitivity advantage at the receiver
2.9	mean launch power advantage of coherent FSK modulation
2.8	higher peak bias current level of the laser
12.8 dB	budget improvement

However, for a fair comparison of the two detection methods we should look at a different summation of the figures in which two design changes are assumed. Firstly, use of a dual PIN receiver in order to not lose 3dB in the coupler and no coupler split loss would appear in the direct detection comparison. Secondly the peak modulation current would be increased in the direct modulation scheme in order to achieve the same peak launch power of the transmit laser. This leads to the following summation of advantages.

7.1	sensitivity advantage of the receiver
2.9	mean launch power coherent advantage
10.0	system budget improvement

If further work is undertaken on the system we would recommend certain directions. A polarisation control loop using a microprocessor and 2 more fibre squeezer stages would remove any drift due to polarisation rotation. This would have some penalty due to the applied polarisation dither from which the control signal is derived, but this is usually less than 0.5dB. This was not implemented in this programme because of the constraints of

time and cost. To remove the dependance on word pattern the input word can be encoded [Ref. 5.8 and 5.9] to a biphase signal. The use of analogue decoding in these reported experiments removes the 3dB penalty from increasing the signal bandwidth. This requires a clock frequency of the data in addition to data at the transmitter and to keep the data steady a frequency doubler to reclock the encoded data. The delays in such a circuit are such that it would not work over a wide range of frequencies. However it could be designed for a particular frequency eg 100MHz if desired. The more frequency critical stage is the clock extract required from the data before the analogue decoding. This is usually implemented with resonant devices such as SAW filters. Although different SAW filters could be inserted for differing frequencies it would not have a broad range of operation because of the delay matching in the circuit between clock and data.

This system is engineered and rack mounted and few such systems exist in the world even in research laboratories at the present date.

REFERENCES

5.1 J. Salz, Coherent lightwave communications
AT&T Tech J Vol.54 P.2153-2209

5.2 I. Garrett and G. Jacobsen
The effect of laser linewidth on coherent optical receivers with nonsynchronous demodulation
Journal of Lightwave Technology, Vol. LT5, No. 4, April 1987.

5.3 R.S. Vodhanel, N.K. Cheung, T.L. Koch
Direct frequency modulation of vapour phase transported, distributed feedback semiconductor lasers
App Phys Lett vol.48 p.966-968

5.4 C.A. Park, A.C. Carter, P.J. Williams, P.V. Dennis, J. Buus, M.D. Scott, A.H. Moore
Stable single mode DFB laser
SILA 86, Cardiff 1986.

5.5 J. Hankey, R.H. Lord, A. Hurel
A PINFET receiver for Gb/s optical communication systems
IEE Colloq. High Capacity Fibre Optic Systems, London, Tech. Dig. 1987/23, 6/1-6/5, February 1987.

5.6 J. Hankey, C.A. Park, J. Buus, B.T. Debney
Characterisation of a single filter FSK system
ECOC 87 vol.1 p.457

5.7 T.G. Hodgkinson; Receiver analysis for synchronous coherent optical fiber transmission systems
IEE Lightwave Tech Vol.LT5 p.575-586

5.8 P.W. Hooijmans, M.T. Tomeson, A. Vande Grijp
A linewidth and bit rate flexible FSK heterodyne system using a frequency discriminator and biphase coding.
ThA 21-5, Gothenburg, September 1989. Proc. ECOC '89, p.409.

5.9 R. Noé, H. Rodler, A. Ebberg, G. Gaukel, F. Auracher
Pattern independent FSK heterodyne tranmsmission with endless polarisation control and a 119 photoelectrons/bit receiver sensitivity 100C 89 Kobe, Japan, Paper 18C2-3 Vol. 1 p.44.

6. ANALOG SYSTEM

6.1 DESIGN

6.1.1 Recommendation

The recommendations for the analog system design was described in section 4.4, and a detailed design description can be found in the document "Design plan for a demonstration of a coherent optical communication system carrying analog signal information"; CDRL A003, April 1988. The system is shown in schematic form in Figure 6.1. It represents a self-homodyning configuration in which the laser is run c.w. and split to provide a signal and local oscillator. The signal is optically phase modulated and then recombined with the local oscillator prior to detection.

The interferometer is adjusted for quadrature operation, i.e. for maximum sensitivity and linearity. If the phase modulation is limited to $\pm\pi/10$ then the phase modulation is approximately linear with drive voltage. Any deviation of the operating point from quadrature, or over modulation of phase will degrade the performance of the system. The performance of the lithium- niobate phase modulator determines the highest carrier frequency that can be used. For the phase modulator used in the system, the -3 dB bandwidth was 3.25 GHz. Consequently, a carrier frequency of 3 GHz was used.

The electrical signal used to drive the phase modulator is derived from a VCO, operating with a centre frequency of 3 GHz. The output of the VCO is modulated in frequency, according to the input modulating signal. This input modulating signal is at a nominal frequency of 10 kHz, and is of amplitude sufficient to modulate the frequency of the VCO by ±100 MHz.

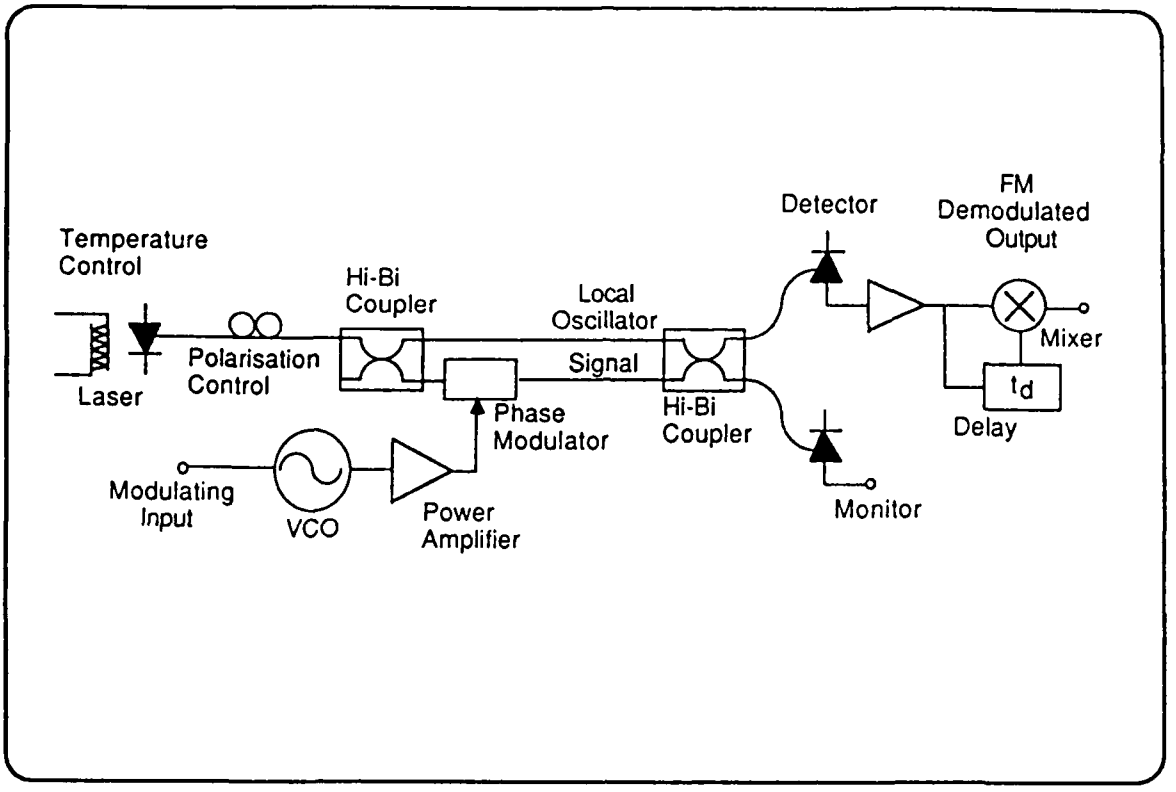

Figure 6.1 SCHEMATIC OF COMPLETE ANALOG TRANSMISSION SYSTEM SHOWING OPTICAL SUBSYSTEMS

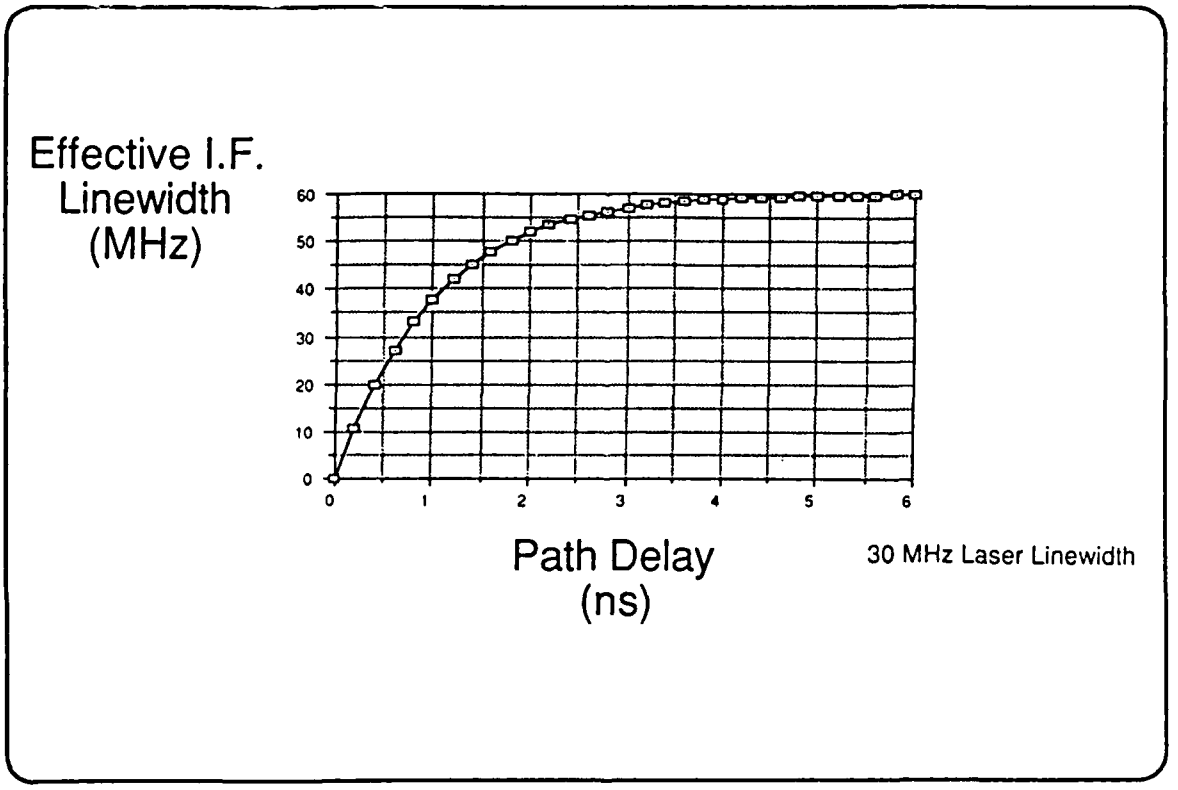

Figure 6.2 EFFECTIVE LINEWIDTH IN COHERENT SELF-HOMODYNE/HETERODYNE AS A FUNCTION OF RELATIVE PATH DELAY

Consequently, though we are optically phase modulating, the electrical system is based on frequency modulation. Consequently FM demodulation techniques are applied to the detected output. The demodulator is based on a delay-line/ mixer combination, the output of which directly represents the input.

In summary, the system adopts a self-homodyning configuration using optical phase modulation for the transmission of analog information. The optical phase is modulated by a frequency modulated microwave carrier of 3 GHz.

6.1.2 Effective linewidth in self-homodyne/heterodyne systems

In a conventional heterodyne/homodyne coherent optical system, two laser sources are used, one as the signal source, and the other as the local oscillator source. The two laser sources are completely uncorrelated. Consequently, the detected I.F. signal has a spectral width equal to the sum of that of the two lasers (for no modulation). In a self-homodyne/ heterodyne system, a single source is used to provide the signal, and the local oscillator. Consequently, the local oscillator and signal may be partially correlated. The degree of correlation depends on the relative path delay between the local oscillator and signal paths. For zero delay, the local oscillator and signal are completely correlated, and the detected I.F. signal has a bandwidth of zero (for no modulation). As the path delay is increased, the correlation between the local oscillator and signal decreases exponentially, and the detected minimum spectral linewidth increases exponentially, approaching the homodyne/heterodyne case for path delays large in relation to the coherence length of the laser used. This is illustrated in Figure 6.2, which shows that the effective linewidth in self-homodyne/heterodyne coherent systems increases exponentially with increasing path delay. Figure 6.2 indicates the general trend of effective linewidth versus path mismatch. In fact the effective linewidth graph does exhibit some substructure.

Figure 6.3 shows the effect of changing the relative path difference between the two arms of the interferometer. The ratio of the signal to noise level (due to laser phase noise) is shown. For small path delays the signal is much larger than the phase noise, this ratio decreasing as path difference increases. This indicates that for maximum signal to noise ratio, minimal path difference between the two arms of the interferometer is necessary.

By using a self-homodyne/heterodyne configuration, the effective linewidth of the laser source can be controlled. This arises from the ability to match the path lengths between the laser source and receiver for both the signal and local oscillator arms, and thus correlate the combined signals. Calculations indicate that an effective linewidth of approximately 500 kHz should be achievable with a DFB laser as the laser source (assuming a laser linewidth of 30 MHz and a path mismatch of 1 cm or 0.05 ns). This is given by:

$$\Delta f_{eff} = 2\Delta f[1-\exp(-2\pi\Delta f\ t_d)] \qquad 6.1$$

where Δf_{eff} is the effective linewidth, Δf is the laser linewidth, and t_d is the time delay equivalent to the path mismatch. In practise, for the short lengths of fibre used in the system, path matching of significantly better than 1 cm can be acheived and an effective linewidth of the order of a few kiloHertz should be possible. This is very encouraging since it permits a self- homodyne/heterodyne configuration to yield results otherwise only acheivable with sophisticated external cavity lasers.

For analog coherent systems, stringent requirements on the effective detected linewidth are placed. To avoid serious SNR floors in phase modulation schemes due to laser phase noise, linewidths of the order of a few tens of kiloHertz are required, as discussed in section 4.2. In addition, phase modulation systems using either the homodyne or heterodyne

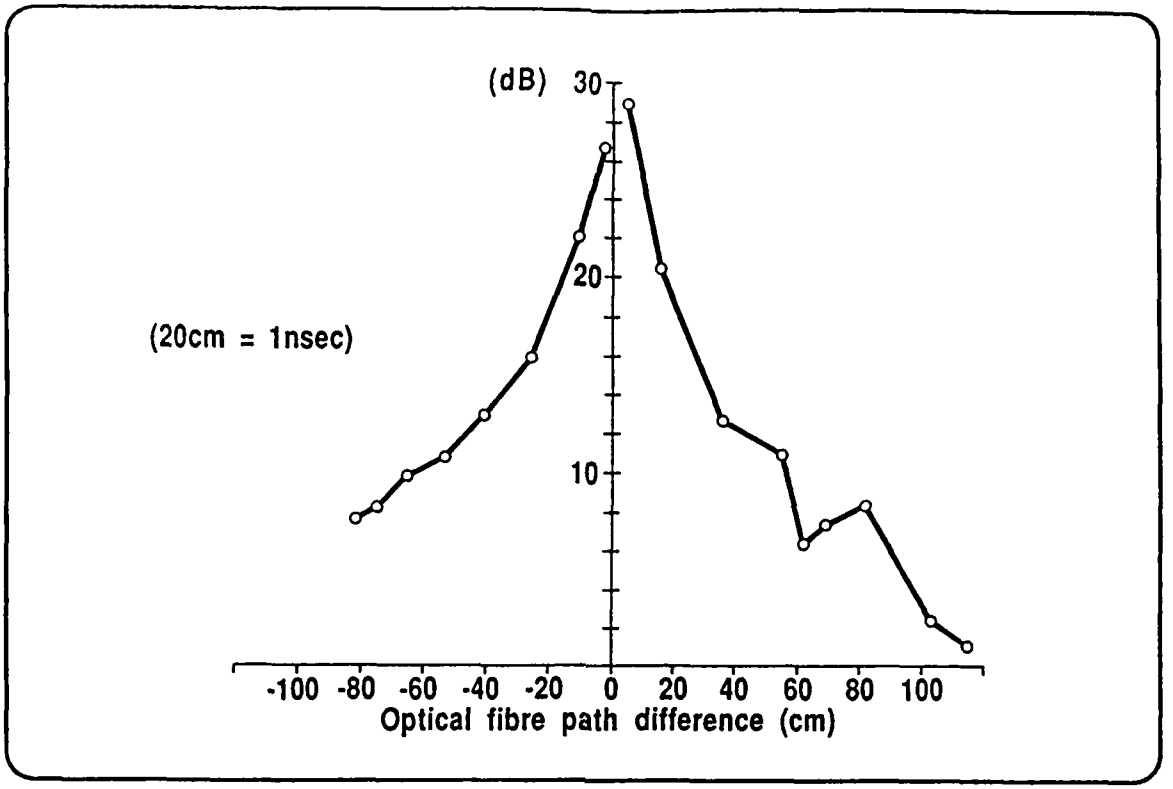

Figure 6.3 RATIO OF PEAK AMPLITUDES OF DELTA FUNCTION AND LORENTZIAN COMPONENTS OF CARRIER AS A FUNCTION OF PATH DIFFERENCE

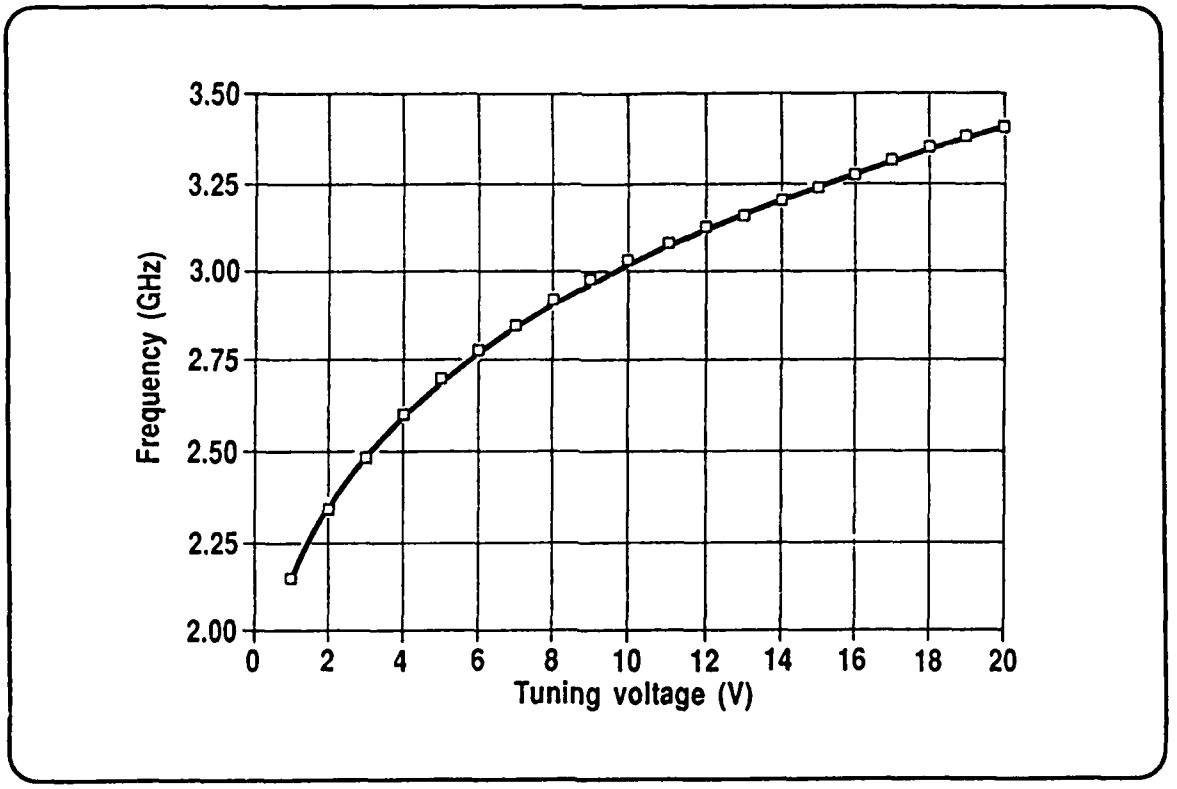

Figure 6.4 VCO TUNING CHARACTERISTICS

receiver approach require an optical phase-locked loop to provide phase and frequency control between the signal and local oscillator lasers. Consequently for an analog coherent system, use of a self-homodyne/ heterodyne optical arrangement offers some advantages in terms of relaxing the linewidth requirements of the laser source, and in terms of maintaining a constant phase/frequency relationship between signal and local oscillator sources. In a self-homodyne/ heterodyne system, a laser of relatively large linewidth of the order of 30MHz may be used as the basic source, and requires frequency stabilisation of only a few megaHertz to avoid phase noise to amplitude noise conversion due to any mismatch in the path lengths of the interferometer.

6.1.3 Path Matching

Path matching of the two arms of the interferometer, configured as represented in Figure 6.1, is necessary to minimise the effective linewidth of the laser source, and to minimise any differential phase/polarisation changes that may occur e.g. due to a change in ambient temperature.

Considering the short lengths of fibre used in the system, initial path matching can be done by measuring the lengths of fibre in the two arms. However the signal arm has a phase modulator in it and the different refractive index of the lithium-niobate from the optical fibre must be taken into account when comparing the two path lengths. Matching of the path lengths to within 1 cm is possible with this technique.

For more accurate matching, optical techniques must be used. The simplest and perhaps most accurate of these is to modulate the frequency of the laser and observe any phase to amplitude conversion at the output due to any path mismatch. By adjusting the path lengths until no observable conversion occurs the path mismatch can be minimised. Using this technique accuracy of 1 mm can be achieved [1].

6.2 SYSTEM CONSTRUCTION

6.2.1 Modulating electrical input signal

The modulating input is used to frequency modulate the voltage controlled oscillator (VCO) is such that an output signal from the VCO is at an average frequency of 3 GHz with ±100 MHz frequency modulation bandwidth. The modulating input is of a nominal frequency of 10 kHz.

A signal source with a d.c. offset of approximately 10V, and an a.c. component of 5 V peak to peak is required as the input to the system. If such a signal source is not available then the d.c. and the a.c. component may be applied separately by using a bias-tee.

6.2.2 VCO

The voltage controlled oscillator (VCO) is supplied by Avantek and has the part number VTO-8240. It has a tuning range of 2.2 GHz to 3.5 GHz, as shown in Figure 6.4. It has output power of -10 dBm as shown in Figure 6.5. Figure 6.5 also shows that the output of the unmodulated VCO has sidebands at ±25MHz from the main output. However since these are 40 dB down on the central peak, they were found to have negligable effect on the performance of the system.

Figure 6.4 shows that the modulating characteristic of the VCO is non-linear and will degrade system performance. It might be possible to insert a preamplifier in the system to counteract this non-linearity, but this has not been implemented.

By modulating the bias voltage of the VCO, the output of the VCO is frequency modulated. Though the modulating input is limited to relatively

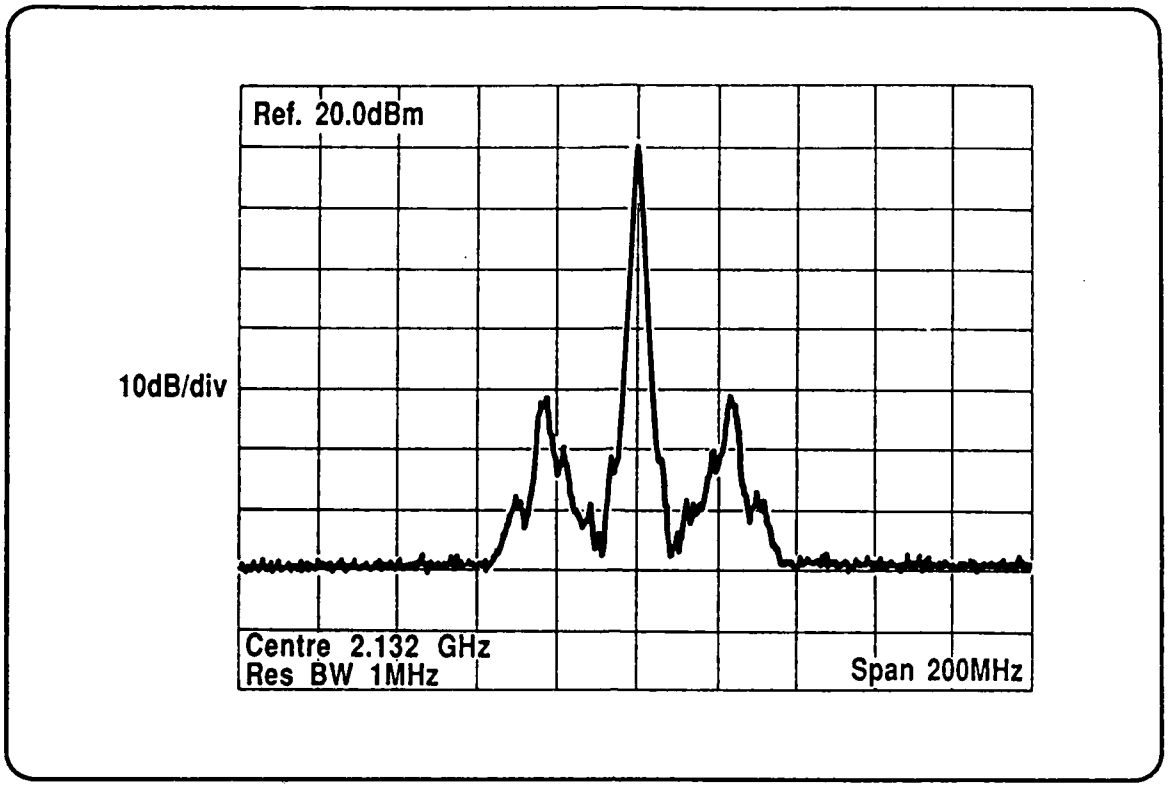

Figure 6.5 VCC OUTPUT AT 2.132GHz

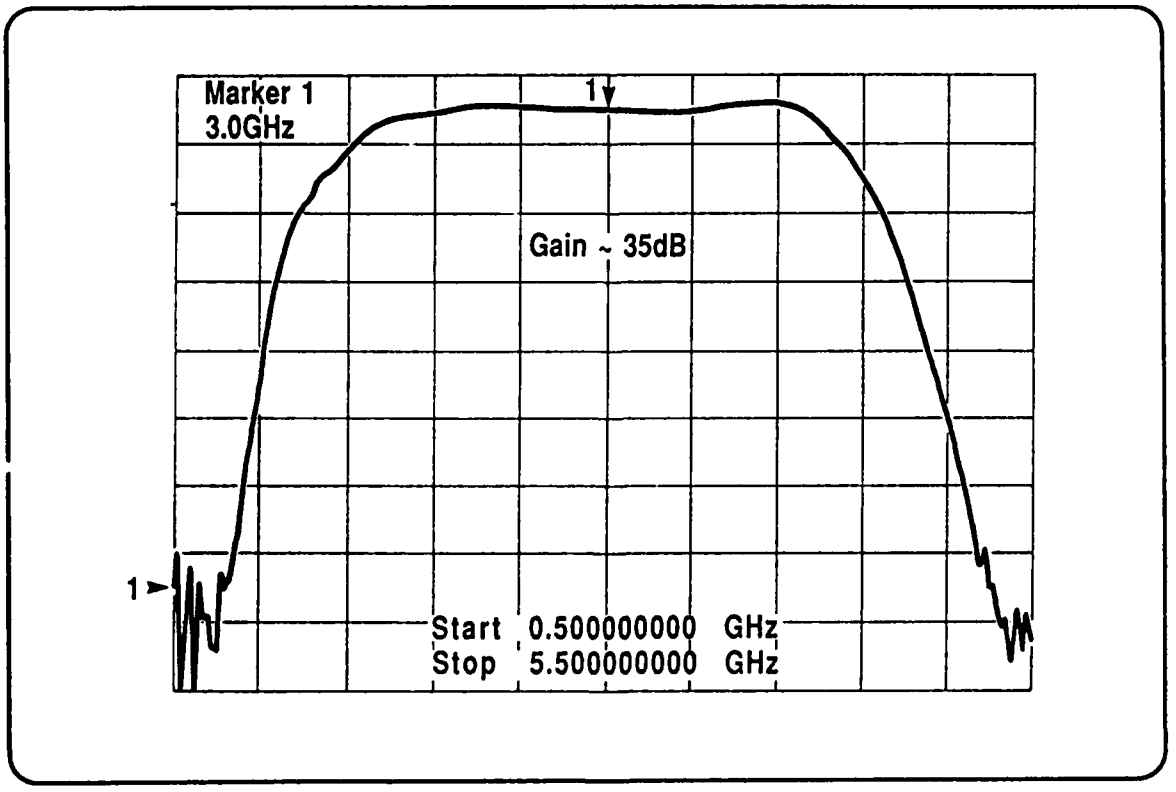

Figure 6.6 GAIN RESPONSE OF 4074 POWER AMPLIFIER

low frequencies, e.g. 10 kHz, the output of the VCO can yield a modulated spectrum of typically 100 MHz bandwidth.

6.2.3 Power Amplifier

The power amplifier is used to drive the phase modulator. The amplifier used was the APT-4074 from Avantek. The amplifier has a nominal bandwidth of 2 GHz, and a gain of 35 dB. The gain and phase response of the amplifier used is shown in Figures 6.6 and 6.7. The 1 dB compression point was measured to be 34 dB as in Figure 6.8. The input impedance of the phase modulator is 50 W, and the voltage required to modulate the optical phase by π radians is 14 V. Therefore to obtain $\pm\pi/10$ phase modulation, the output of the power amplifier is arranged to be 15 dBm by inserting a 20 dB attenuator between the VCO and the power amplifier. The attenuator also serves to isolate the VCO. Since the output of the amplifier was approximately 15 dBm, the output of the amplifier should have minimal harmonic content. The input and output impedance of the amplifier is 50 ohms.

The VCO/Power amplifier combination has an output as a function of frequency as in Figure 6.9. The frequency response is reasonably flat over the entire frequency range of interest.

6.2.4 Laser source

The laser used in the analog system is the one used in the digital system. This is a Plessey, 1.55 μm distributed feedback (DFB) laser, pig-tailed with monomode optical fibre. The laser is mounted on a ceramic substrate onto a two-stage thermocooler. It has a nominal linewidth of 30 MHz.

Exact frequency stabilisation of the laser is not strictly required for the self-homodyne system since drift is common to both signal and local oscillator. However because of the Fabry-Perot cavity of the phase

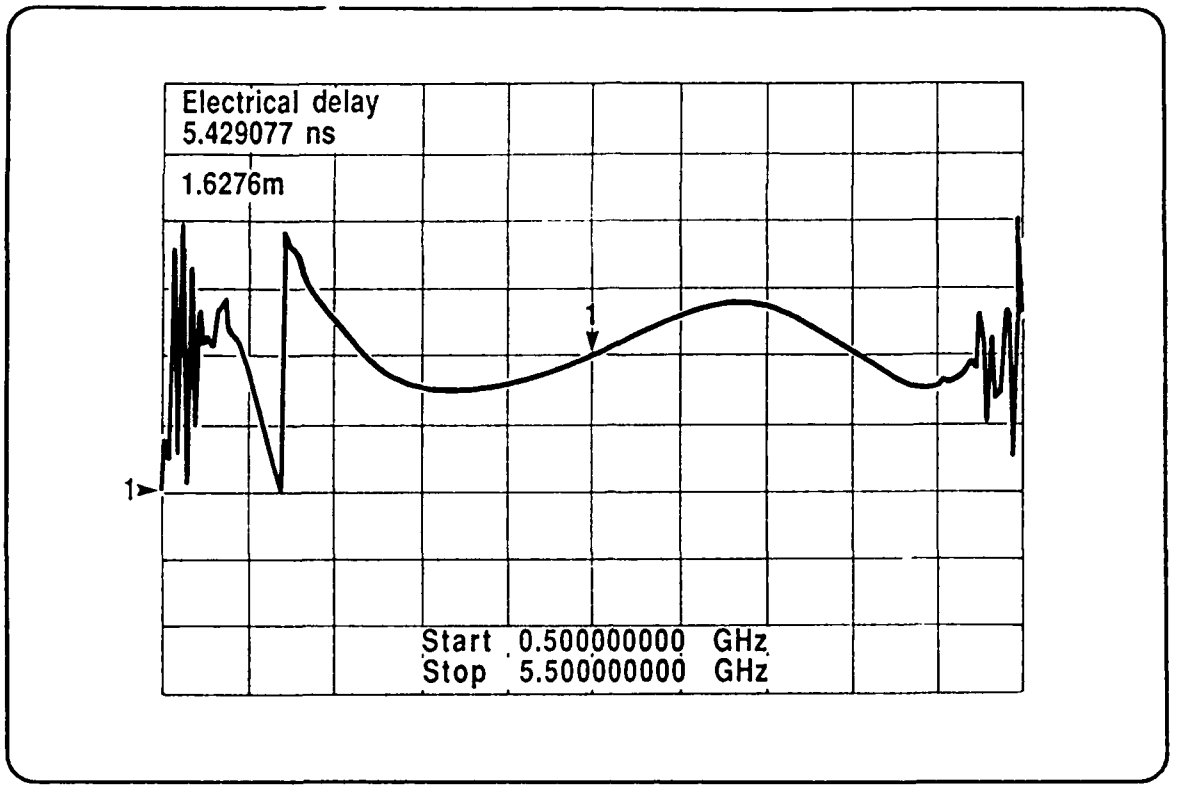

Figure 6.7 PHASE RESPONSE OF 4074 POWER AMPLIFIER

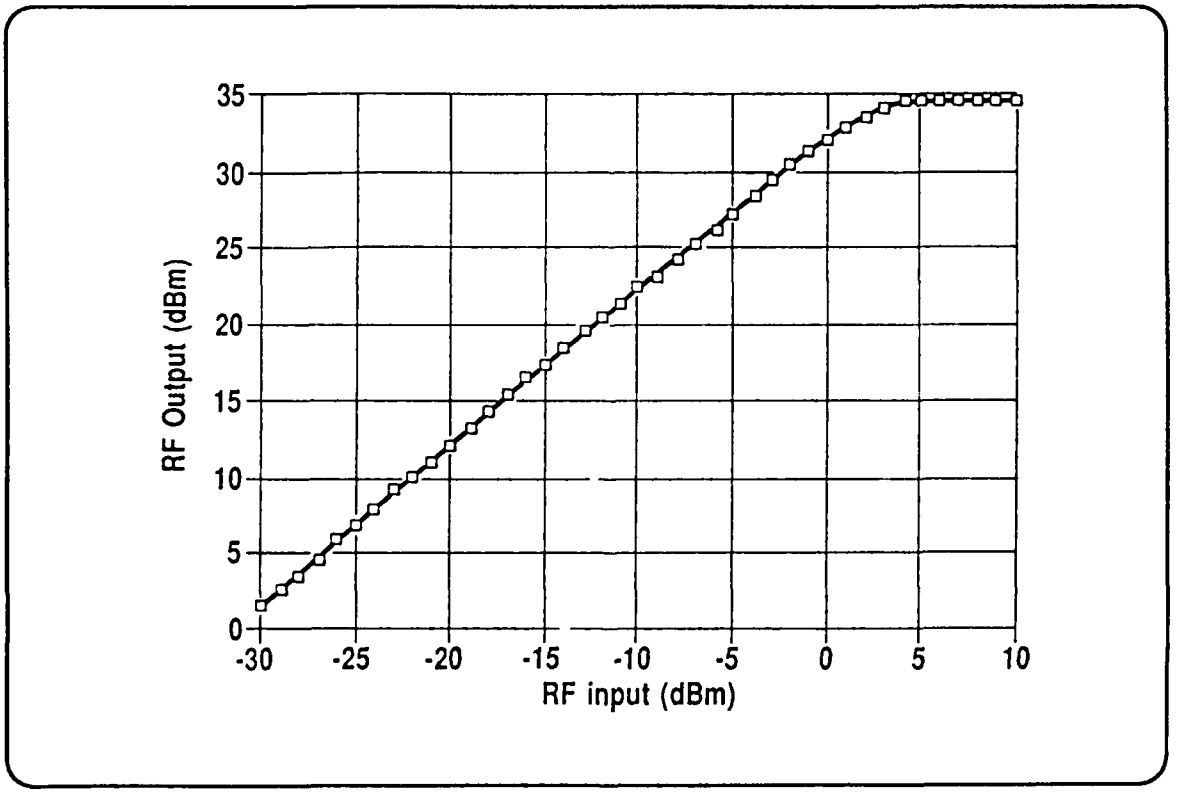

Figure 6.8 4074 POWER AMPLIFIER OUTPUT POWER AS A FUNCTION OF INPUT POWER

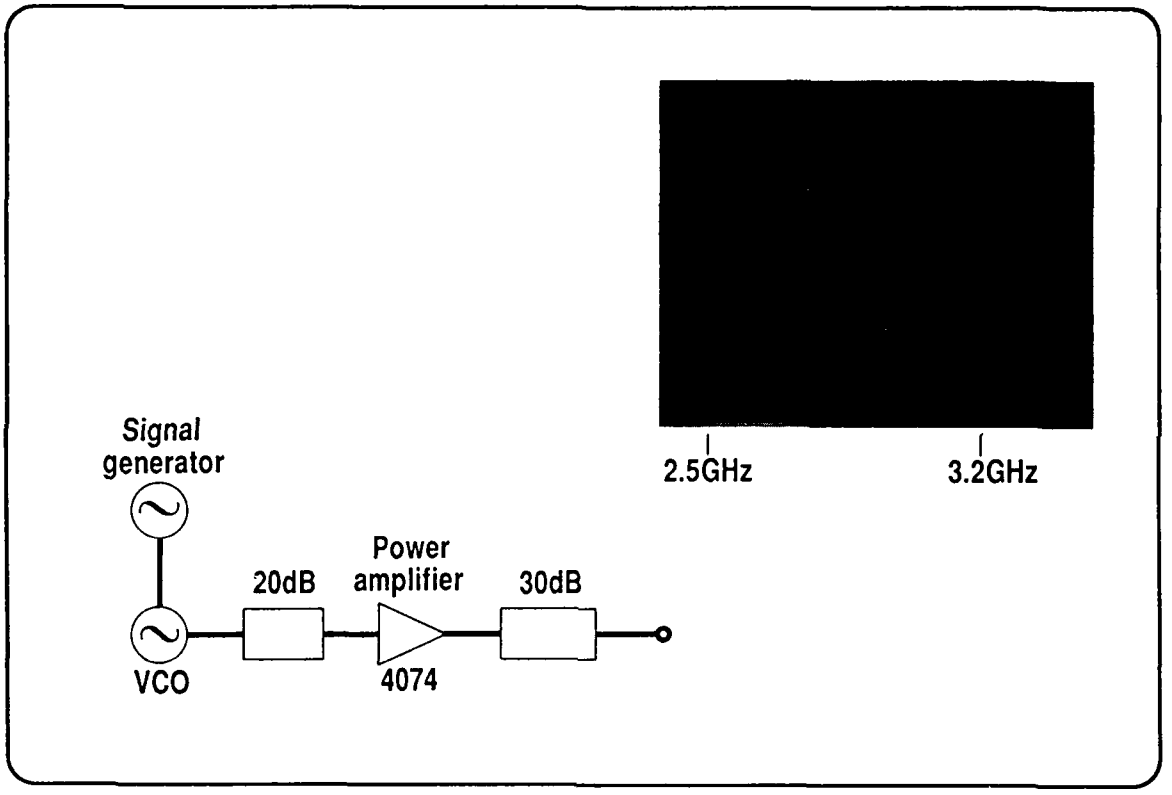

Figure 6.9 VCO/POWER AMPLIFIER OUTPUT AS A FUNCTION OF FREQUENCY, AND THE EXPERIMENTAL ARRANGEMENT

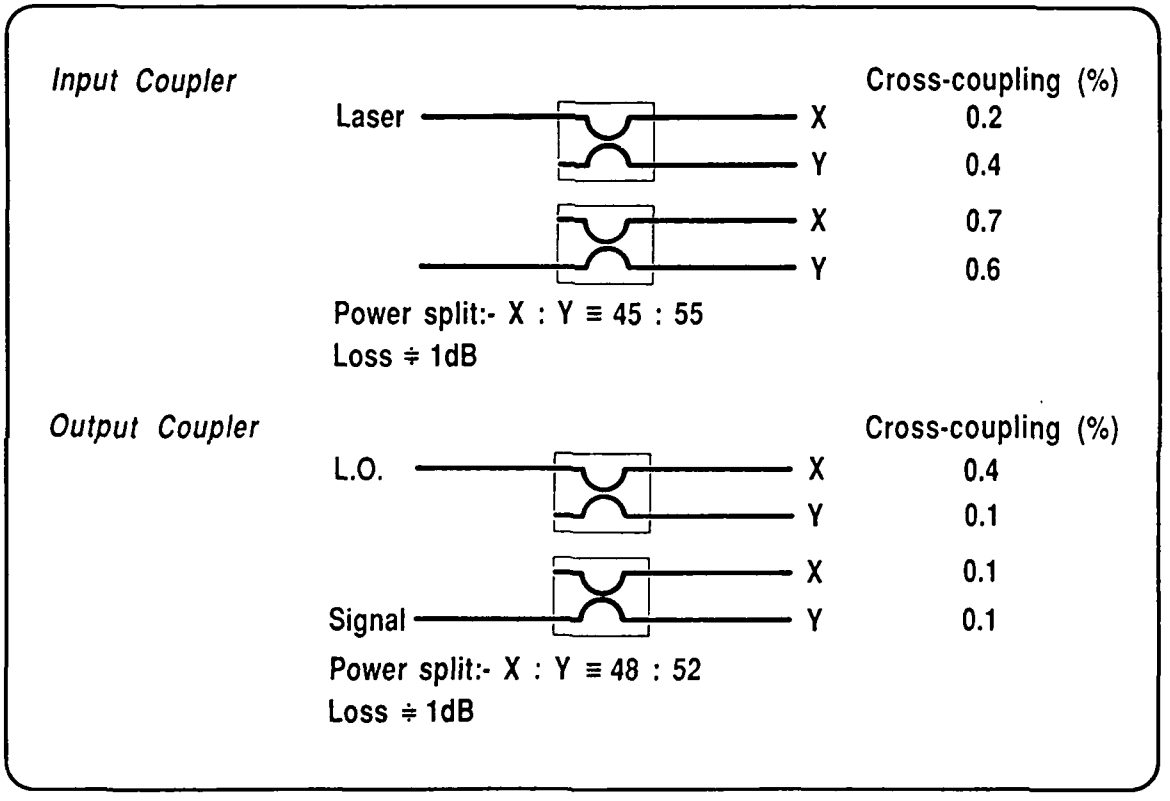

Figure 6.10 HIGH-BIREFRINGENT COUPLERS CHARACTERISTICS

modulator, and because of any mismatch of path length, frequency drift of the laser will result in amplitude fluctuations of the output and hence degrade the performance of the system. The temperature and bias control circuitry of the digital system is used to control the laser. This circuitry will stabilise the frequency of the laser to within 100 MHz.

6.2.5 High-birefringent couplers

High-birefringent couplers were used in the system for two reasons. The first of these is that the phase modulator has high- birefringent fibre pig-tails, so that use of a similar fibre in the remainder of the system would minimise insertion loss, including polarisation mismatch, for the phase modulator. The second, and perhaps more important reason for the use of high-birefringent couplers was that this would eliminate any problems due to polarisation drift of either the signal or local oscillator. Use of high-birefringent fibre for all optical components of the interferometer was possible because of the short lengths of fibre used.

All other optical components, i.e. the pig-tailed laser, and the two photo-detectors, did not use high-birefringent fibre. For the two photodetectors high-birefringent fibre was unnecessary since polarisation of the detected optical signal was immaterial. It would have been beneficial to use high-birefringent fibre for the laser. However the laser to be used in the system was that used in the digital system which had a standard monomode fibre pigtail.

The properties of the high-birefringent couplers used in the interferometer are summarised in Figure 6.10. The couplers were supplied by Canadian Instruments, and were constructed of York high-birefringent fibre. The extinction ratios of the output polarisation state of both output fibres were measured to be less than 1%. These figures were obtained by rotating the polarisation state of the optical input to the coupler. The couplers

had insertion losses measured to be less than 1 dB by the cut-back method. The power split of the couplers was approximately 50:50.

The fibre tails to be spliced to the phase modulator, were connectorised with a keyed connector supplied by Radiall. Use of a keyed connector ensured that joining the couplers to the phase modulator would maintain the appropriate polarisation, i.e. aligned to the major axis of the high-birefringent fibre.

6.2.6 Polarisation control

Polarisation control was necessary to match the polarisation of the output of the laser with the appropiate axis of the high-birefringent fibre used in the input coupler. Once this has been achieved, the polarisation preserving properties of the fibre will ensure that the local oscillator and signal are matched in polarisation upon recombination.

The polarisation controllers are similar to construction to those used in the digital system. They consist of two fibre squeezers orientated at 45 degrees to each other. The amount of squeezing applied to the fibre is controlled by solenoids. The squeezing induces polarisation changes in the fibre because of stress induced birefringence.

Polarisation matching is best acheived in the following manner. The input polarisation should be adjusted until maximum light is passed by the phase modulator. This is best done by disconnecting the local oscillator arm. With the local oscillator arm reconnected, the phase of the signal should be modulated at a low frequency, e.g. 1 kHz, and the output of the power monitor photodetector monitored on an oscilloscope. Use of phase modulation helps to distinguish between changes in detected optical power due to polarisation changes and due to phase changes. The local oscillator connection can then be manipulated until maximum output voltage swing is

obtained. When this has been done, the local oscillator arm can be set permanently. For this purpose, the local oscillator arm uses a conventional glass splice that can be UV set. From then on the input polarisation need only be adjusted for maximum detected optical power, since the polarisation should be maintained by the high-birefringent fibre used.

6.2.7 Phase modulator

Phase modulation is induced about the quadrature point of the interferometer. If the maximum phase deviation is limited to $\pi/10$, then the phase modulation of the system is quasi-linear. The sinusoidal phase response of the interferometer can be approximated by:

$$\sin(x) = x \qquad \text{for small } x \qquad 6.2$$

Expanding sin(x) in full;

$$\sin(x) = x - \frac{x^3}{3!} + \frac{x^5}{5!} \ldots \qquad 6.3$$

For $x \leq \pm\pi/10$, third-order rejection of 18 dB is obtained. This is sufficient not to degrade the performance of the system significantly.

The phase modulator used was supplied by Crystal Technology. A summary of its characteristics is shown in Figure 6.11. The phase modulator has pig-tails of high-birefringent, York, bow-tie fibre. The alignment of the pig-tails with respect to the phase modulator is 5 degrees for the input, and 0.5 degrees for the output. Both input and output fibres were connectorised with keyed connectors supplied by Radiall. These mated with the connectors on the input and output fibre couplers.

Loss: 3.5dB

3dB Phase modulator response: 3.25GHz

V_π : 14volts

On chip polariser extinction $\frac{TM}{TE}$ = -30dB

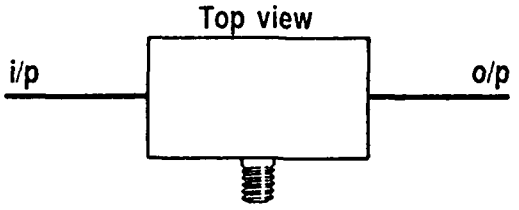

Alignment of Hi -Bi pigtails with respect to chip

i/p = 5° o/p = 0.5°

NB *Phase modulation gives intensity modulation of the guided light of -13dB max. This is due to formation of a Fabry-Perot cavity between the two fibre/chip interfaces*

Figure 6.11 PHASE MODULATOR CHARACTERISTICS

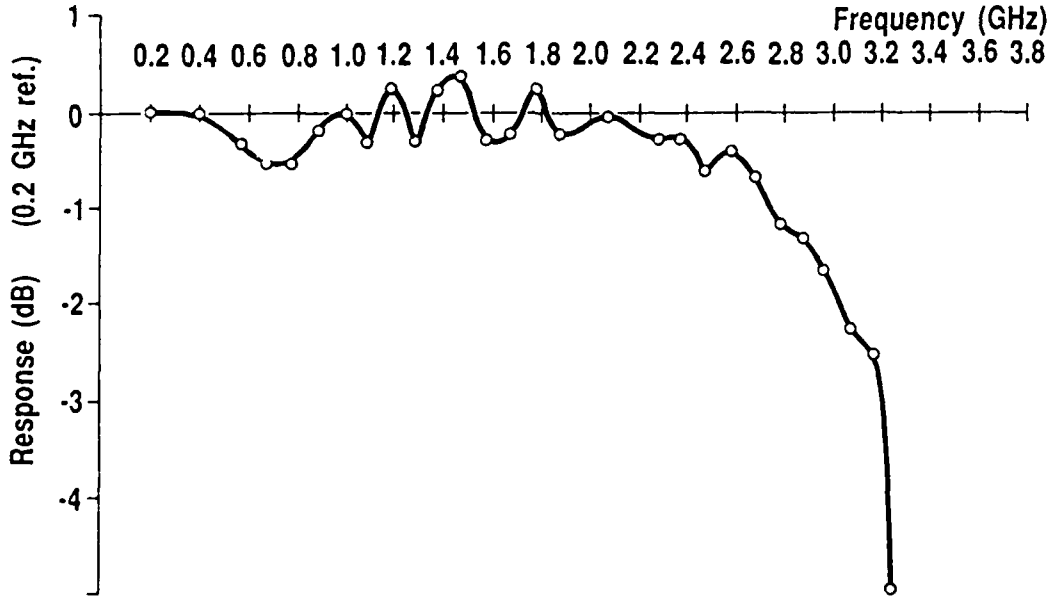

Figure 6.12 PHASE MODULATOR FREQUENCY RESPONSE

The insertion loss of the phase modulator was measured to be 3.5 dB. This figure was obtained by the cut-back method where, after establishing a satisfactory launch power into the input fibre, the output power is measured. The input fibre is then cleaved a few inches along its length and the light emerging from this will be measured using the same apparatus as before. The ratio of these two measurements yields the insertion loss of the phase modulator.

The polarisation extinction of the phase modulator was measured to be approximately 30 dB. This was obtained by rotating the polarisation of the optical input, and measuring the ratio of the maximum to minimum output power.

The phase modulator had a measured -3 dB frequency bandwidth of 3.25 GHz as in Figure 6.12. This was obtained by examining the phase modulation sidebands using an optical spectrum analyser (scanning a Fabry-Perot interferometer), while monitoring the r.f. drive power incident on the phase modulator using a calibrated directional coupler and detector. This technique also gives the voltage necessary to induce a phase change of π radians to be 14 V.

The output of the power amplifier was limited to 15 dBM. Taking into account the phase modulator frequency response at 3 GHz of -1.8 dB, and the load impedance of 50 ohms, the peak voltage applied to the phase modulator is 1.45V. This corresponds to phase modulation of $\pm\pi/10$ radians. This is summarised in Figure 6.13.

The -3 dB bandwidth of the phase modulator is 3.25 GHz. Therefore using a carrier frequency of 3 GHz with ±100 MHz modulation bandwidth will result in some distortion. Use of a lower carrier frequency will reduce this effect.

Power amplifier output at 3GHz = 15dBm

Phase modulator response at 3GHz = -1.8dB

Phase modulator input impedance = 50Ω

Peak voltage applied to phase modulator = 1.45V

Figure 6.13 PHASE MODULATOR PROPERTIES

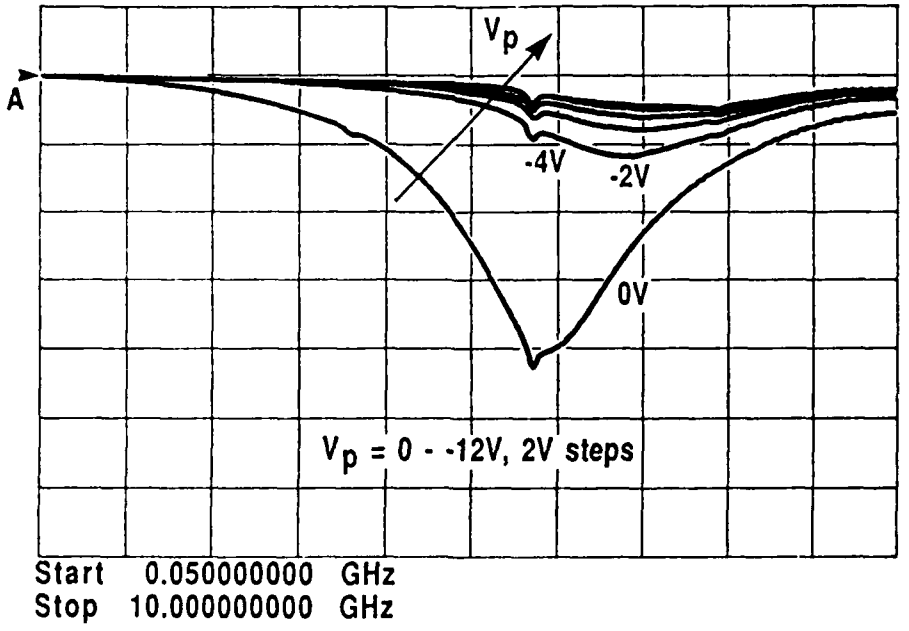

Figure 6.14 HIGH-SPEED PHOTO-DETECTORS FREQUENCY RESPONSE FOR SEVERAL VALUES OF REVERSE BIAS

The interfaces between the fibre pig-tails and the lithium-niobate chip formed a Fabry-Perot cavity. The effect of this was to convert any phase fluctuations of the laser, including frequency drift, to amplitude fluctuations of the output. This will degrade the performance of the system.

6.2.8 High-speed detector

The high-speed detector is a Plessey substrate entry PIN mounted on a ceramic block. It has a total capacitance of 0.15 pF. The package has a SMA bulkhead connector on the rear, and a fibre pig-tail of single-mode fibre.

The responsitivity of the photodetector is 0.62 A/W. This is the product of the quantum efficiency of the photodetector, the energy of the received photons, and the fibre alignment efficiency. This was measured using a similar method to the cut-back method, but now the detected photocurrent is compared to that of a calibrated reference photodetector.

The frequency response of the photodetector, taken to be s_{11}, is shown in Figure 6.14 as a function of the bias voltage. A nearly flat frequency response at 3 GHz is obtained for reverse bias voltages of more than 4 V, with less than 0.2 dB variation across the frequency band of interest (2.5 GHz to 3.5 GHz). Even less variation is obtainable by increasing the magnitude of the bias voltage. Measurement of s_{11} will not include any photoelectron transit time effects in the detecting junction, but since these are known to be insignificant below frequencies of 10 GHz to 12 GHz at bias voltages greater than 4V, s_{11} is a good approximation to the true frequency response of the photodetector.

6.2.9 Power monitor detector

The purpose of the power monitor detector is to indicate the optical power detectable at the output of the system. It is also used in setting up the system, e.g. matching of local oscillator and signal polarisation. The power monitor photodetector is made by Plessey. The properties of the photodetector are summarised in Figure 6.15. It has a recommended bias voltage of -5 V, and the reponsitivity of the photodetector was measured to be approximately 0.5 A/W.

6.2.10 Signal amplifier

The signal amplifier used was the AMT-4054 supplied by Avantek. It has a nominal bandwidth of 2 GHz, and a gain at 3GHz of 55 dB. Figures 6.16 and 6.17 shows the gain and phase response of the amplifier used. The input and output impedance of the amplifier was 50 Ω.

6.2.11 FM demodulator

Demodulation of the detected FM electrical signal could be acheived in a number of ways, e.g. phase-locked loop, stagger-tuned circuit, or phase discriminator. Because of the limited time scale the stagger-tuned circuit was not considered.

The operation of the phase-locked loop can be understood by considering Figure 6.18. The modulated signal is mixed with a reference signal in a phase comparator. Any change in frequency of the signal causes a change in the output of the phase comparator such that the frequency of the reference signal is adjusted to be the same as that of the input signal. Consequently, the output of the phase comparator is linearly related to the input frequency, and hence represents the demodulated output. A loop filter is included to limit the frequency fluctuations of the output.

Type N°. LR1526

Serial Nø. 0139
Nominal Wavelength of
Peak Responsivity 1.6μm

Fibre type: 100/140μm, 0.3NA
step index silica

Active area Dia. 100μm

Responsivity at 1.3μm. 0.50A/W

Leakage current at 5V. 1.0 nA

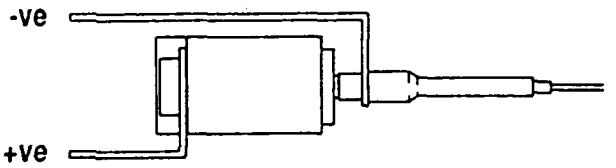

Recommended bias voltage. 5V

Maximum bias voltage. 10V

Under normal operating conditions the diode is reverse biased. The device is not intended to be forward biased, and the forward current should not be allowed to exceed 50mA.

Figure 6.15 POWER MONITOR PHOTO-DETECTORS CHARACTERISTICS

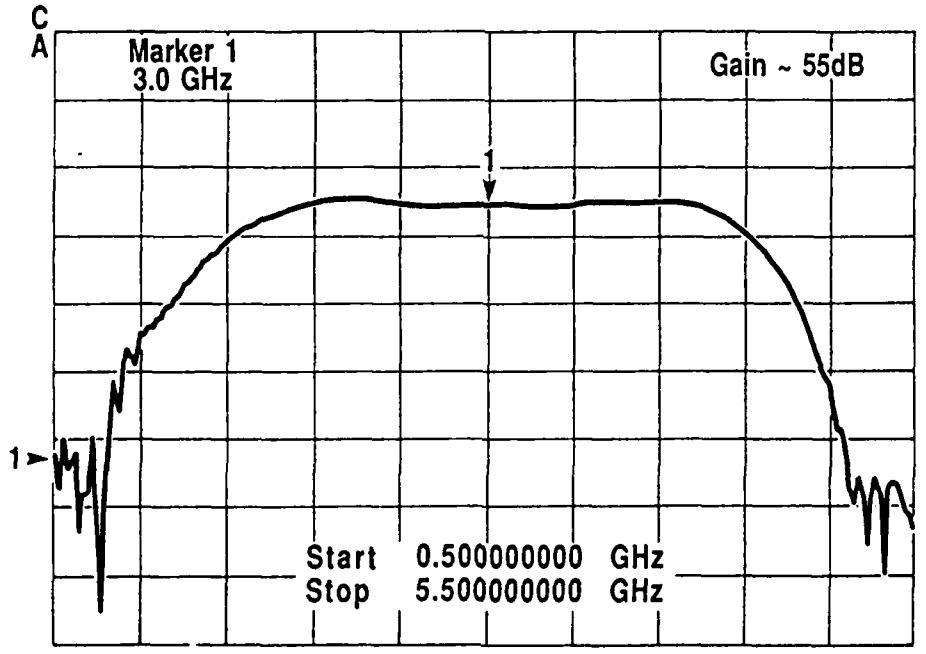

Figure 6.16 GAIN RESPONSE OF 4054 SIGNAL AMPLIFIER

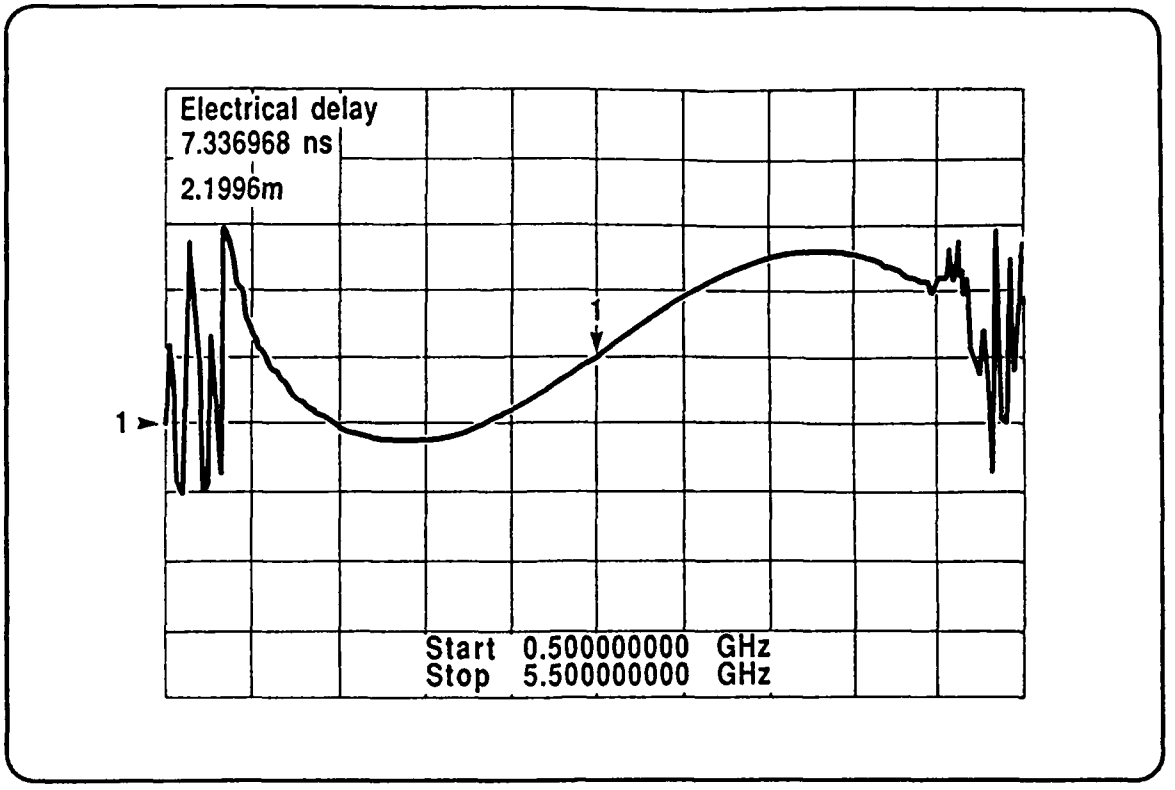

Figure 6.17 PHASE RESPONSE OF 4054 SIGNAL AMPLIFIER

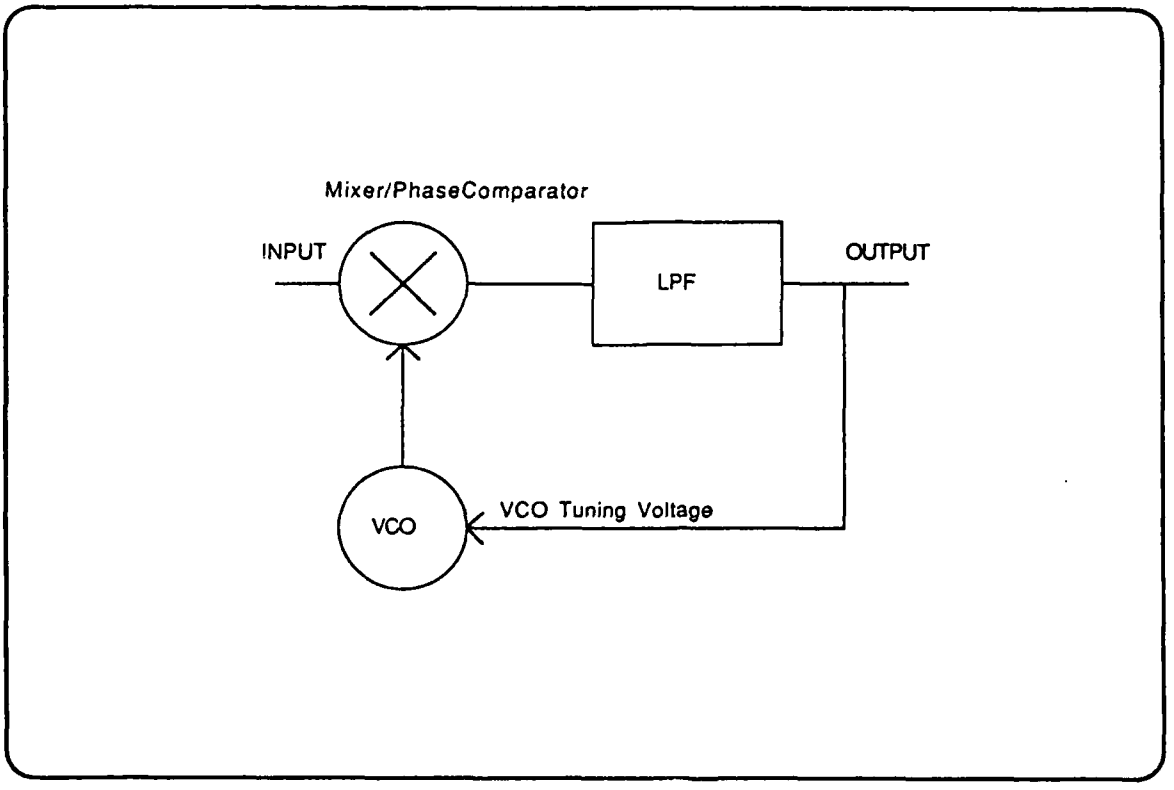

Figure 6.18 PHASE-LOCKED LOOP FM DEMODULATOR

It was found that this method did not perform well in the system. This was because the frequencies of the two VCOs used exhibited fluctuations in the frequency of their output of up to 4 MHz. Since we were using a relatively low modulating frequency of 10 kHz, it was found difficult to produce a demodulated output.

The second approach, that of using a delay-line phase discriminator overcame the problems found in the phase-locked loop approach. The operation of the delay-line demodulator can be understood by considering Figure 6.19. The input is divided equally by a resistive splitter. One half of the signal is applied to one port of the phase comparator directly, whilst the other half is delayed by use of a delay line, in this case a length of coaxial cable. The phase difference between the two halves of the signal is then proportional to the path difference, and is also proportional to the frequency. Thus frequency changes are transfomed into amplitude changes by the phase comparator.

The phase comparator was a double-balanced mixer, the WJ-M1H, supplied by Watkins-Johnson. The incoming electrical power is split into two using a power splitter, a d.c. to 18 GHz, 50 Ω splitter supplied by Suhner. Before recombination in the mixer, one half of the incoming power is delayed in time by passing it through a 300 mm length of coaxial cable. Electrical padding was necessary to ensure that reflections do not degrade the performance of the demodulator. The frequency response of the demodulator is shown in Figure 6.20.

6.2.12 System housing

The system is housed in two 19 inch rack systems supplied by Schroff (UK) Ltd. The electronics (except the two photodetectors) are housed in a 3U-84HP rack. Power supply requirements are +18V 2A, ±7V 1A, for which there are appropiately labelled 4 mm sockets at the rear of the rack. The

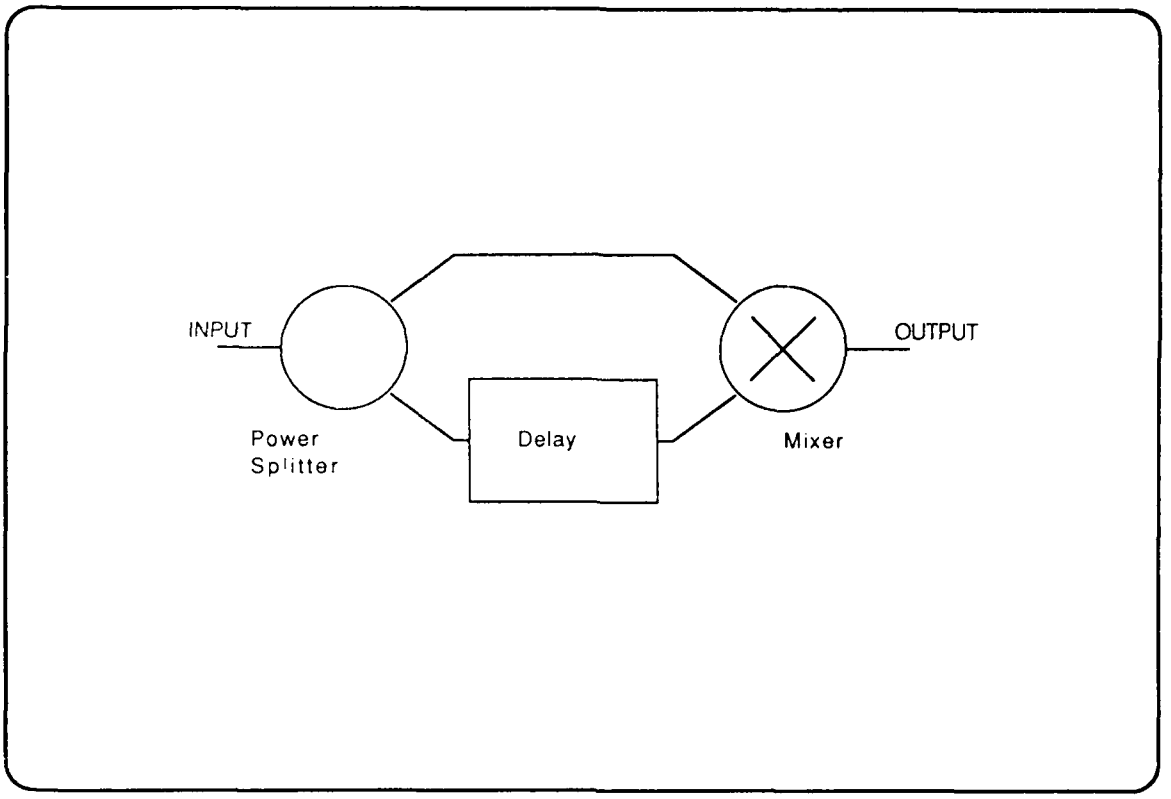

Figure 6.19 DELAY-LINE FM DEMODULATOR

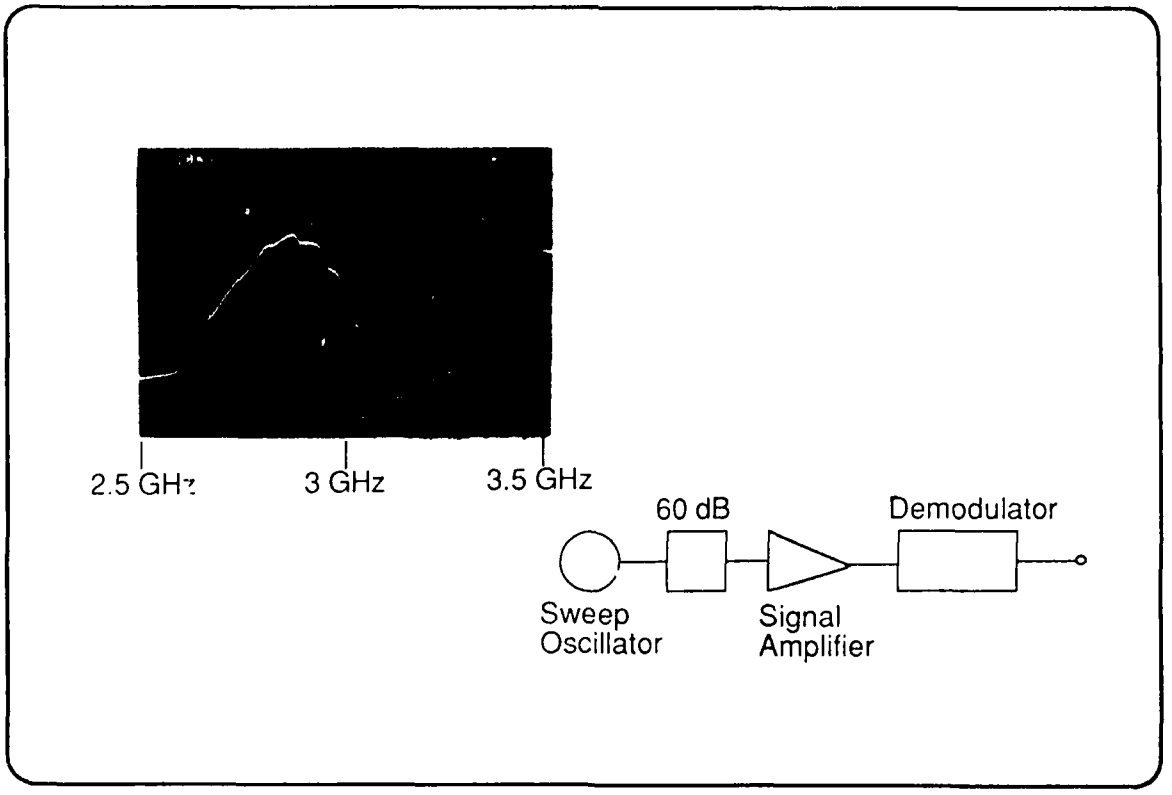

Figure 6.20 FM DEMODULATOR FREQUENCY RESPONSE AND THE EXPERIMENTAL ARRANGEMENT

power supply is derived from the digital system power supply. All other necessary power supplies are provided by the electronics rack, and there are suitable connectors for these links.

All optical components are housed in a 6U-84HP rack system. The bottom half contains the interferometer, whilst the top half contains the polarisation controller, and the two photodetectors. The interferometer is mounted on a sheet of aluminium to maintain a constant temperature for all the optical components and optical fibre in the interferometer. To further minimise the effects of temperature fluctuations and vibrations, the interferometer is encased in foam.

Figure 6.21 shows the construction of the racks, and indicates the appropiate conections. All connecting cable has been supplied with the racks to RADC.

6.3 TEST RESULTS

The system has been characterised according to the analog test plan "Test plan for a narrow band analog coherent fibre optic link", CDRL A004, October 1988. Much of the component characterisation has been discussed in section 6.2. The following test results are related to the testing of the system as a whole, or do not fall easily into any previous section.

6.3.1 System frequency response

The frequency response of the system will determine the frequencies at which it is possible to modulate the phase modulator. The measured gain and phase response of the system is shown in Figures 6.22 and 6.23. Referring to Figure 6.1, the frequency response was measured between the input to the power amplifier and the output of the signal amplifier, with the interferometer set in the quadrature condition for maximum sensitivity

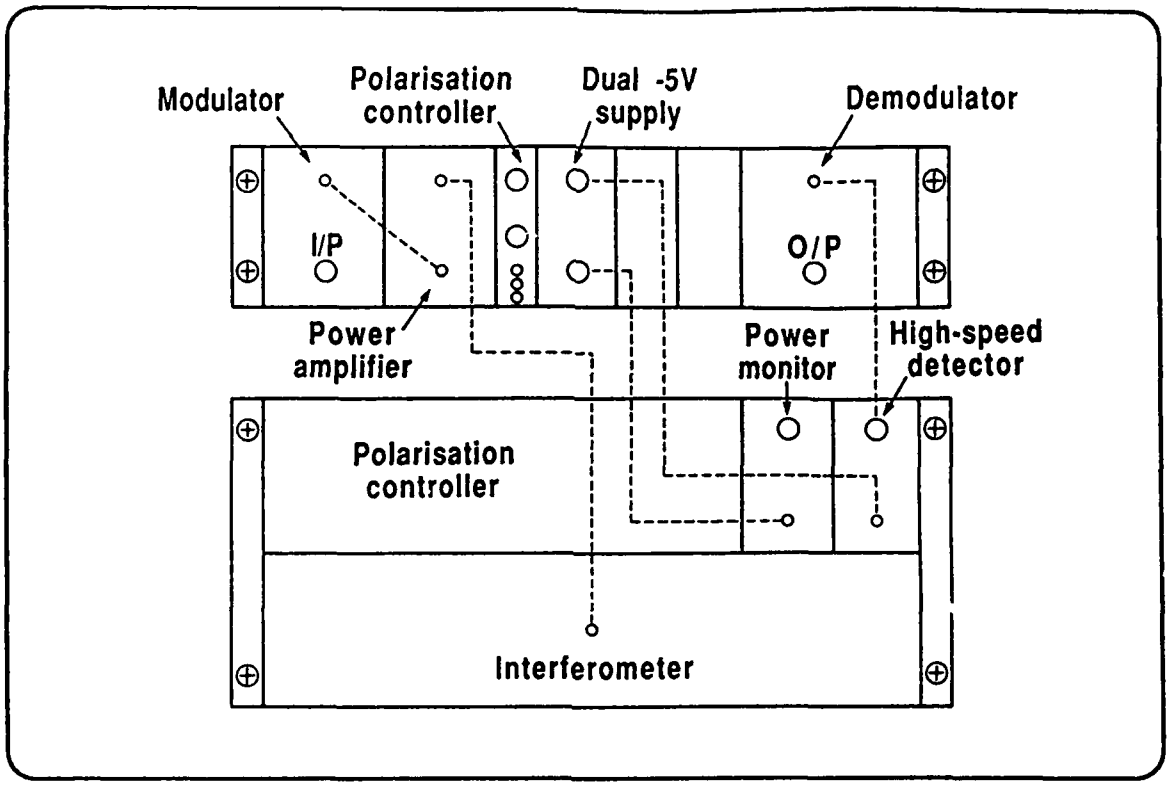

Figure 6.21 SYSTEM CONFIGURATION IN 19" RACKS

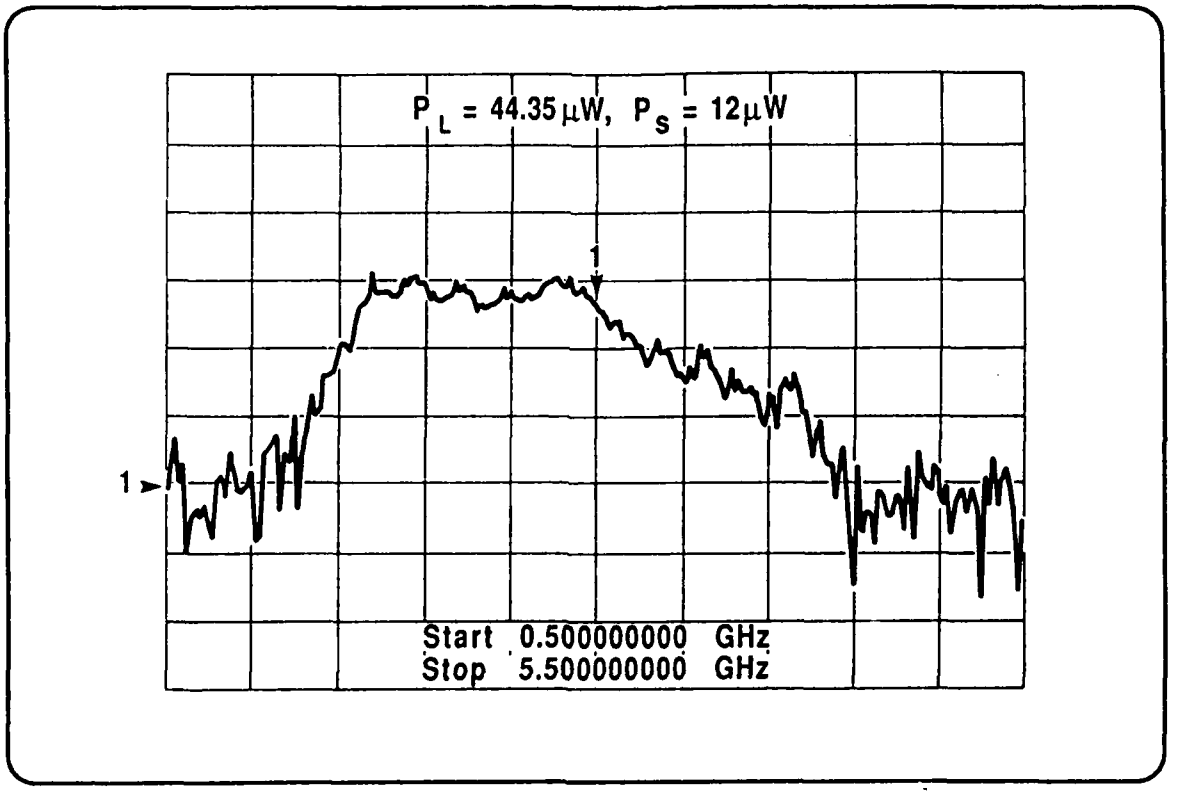

Figure 6.22 GAIN RESPONSE OF SYSTEM (excluding FM demodulator)

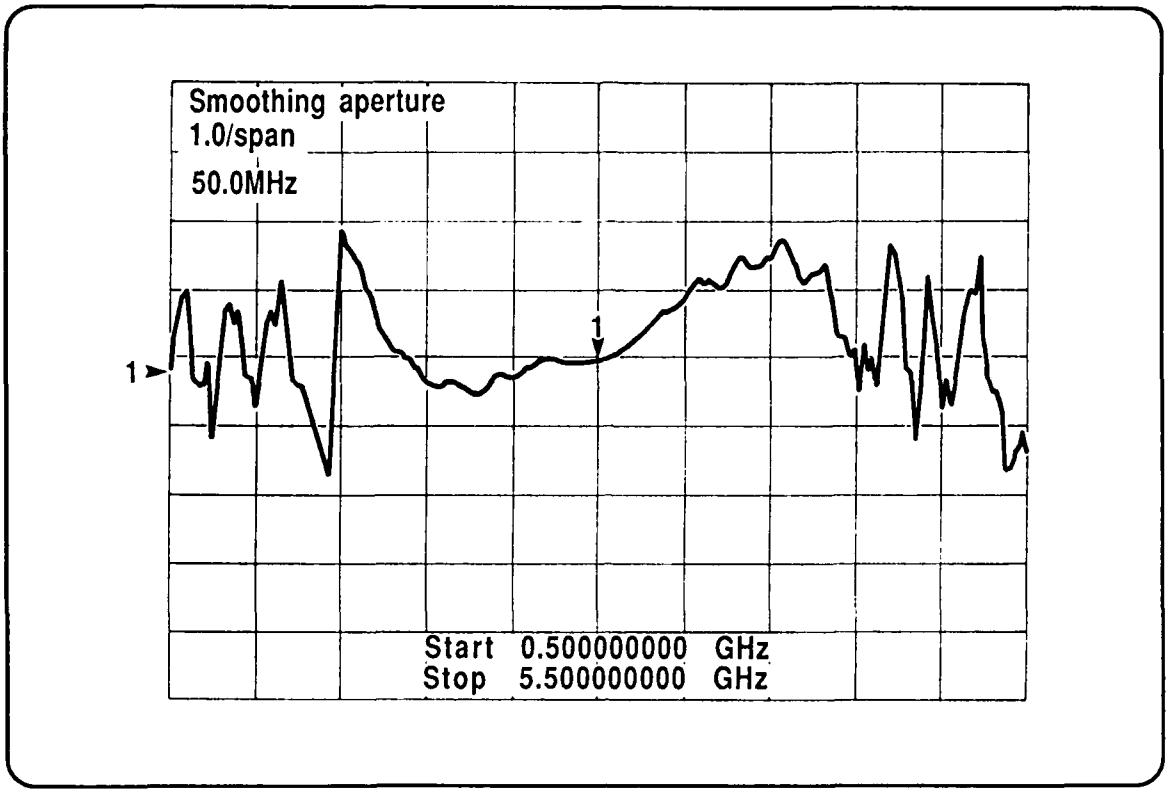

Figure 6.23 PHASE RESPONSE OF SYSTEM (excluding FM demodulator)

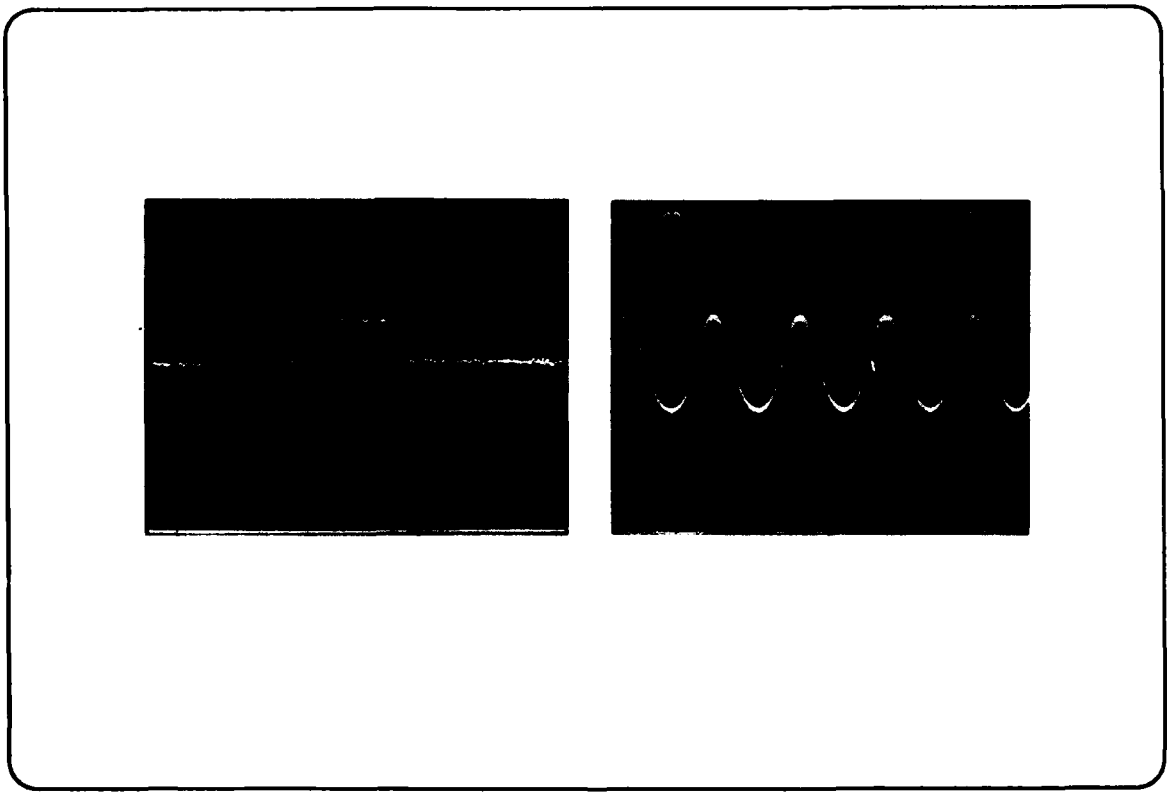

Figure 6.24 DEMODULATED OUTPUT AT 2.26GHz

and linearity. The input level to the power amplifier was sufficiently small to ensure that the non-linearity of the optical phase modulation (sinusoidal in nature) had negligable effect.

The low frequency end of the gain response is due to the bandwidth limitations of the two amplifiers used in the system. The high-frequency roll-off is primarily due to the phase modulator which has a -3 dB bandwidth of 3.25 GHz. This limits the range of carrier frequencies and modulation bandwidths that can be used with the system to lie within 1.7 GHz and 3 GHz. If any transmitted frequencies lie outside this range, system performance will degrade.

6.3.2 Theoretical comparison

Using parameters chosen to match experimental conditions, the performance of the system can be predicted. The signal to noise ratio penalty for the phase noise floor is given by:

$$SNR_{pn} = \frac{k_\theta^2 B}{4\pi\Delta V_{if}} \qquad 6.4$$

where k_θ is the phase modulation index ($\pi/10$), B is the receiver bandwidth (2.5 GHz), and ΔV_{if} is the effective linewidth. From equation 6.1, the effective linewidth of the laser in the system is 5.4 MHz, assuming path matching to within 0.5 ns, and a true laser linewidth of 30 MHz. Therefore the phase noise floor penalty is 5.6 dB.

The local oscillator penalty is given by:

$$\text{Penalty (LO)} = 1 + \frac{2kTF}{eR_d P_L R} \qquad 6.5$$

where P_L is the received local oscillator power (16.12 mW), F is the signal amplifier noise figure (2), R_d is the detector responsitivity (0.62 A/W), e is the electronic charge, and R is the input impedance of the signal amplifier (50 Ω). Therefore, the local oscillator penalty is 26.2 dB.

The SNR is given by:

$$SNR = \frac{RP_r k_\theta^2}{eB} \qquad 6.6$$

where P_r is the received optical signal power (0.8 mW). Therefore the signal to noise ratio is 20.8 dB, but taking into account the local oscillator penalty, the true SNR is -5.4 dB. For the optical powers used, P_r = 0.8 μW and P_L = 16.12 μW, the measured value of 5.5 dB at these power levels corresponds well with the theoretical prediction.

6.3.3 Demodulated output

The output of the system (after demodulation) is shown for three different carrier frequencies, though with ±10% frequency modulation for all three frequencies, in Figures 6.24, 6.25, 6.26. The output is more non-linear for higher carrier frequencies. This is because the VCO tuning characteristic is more non-linear at higher carrier frequencies, and the phase modulator response begins to roll-off at higher frequencies. This indicates that if possible lower carrier frequencies should be used. However in the present system, the FM demodulator determines the optimum carrier frequency (as being the frequency in the centre of the linear portion of the demodulator response as in Figure 6.20). The sinusoidal demodulator response means that there are more than one such optimum operating points (though sensitivity may be reduced). Therefore, for optimum system performance, the lowest carrier frequency should be used that is within the 1.7 GHz to 3.25 GHz bandwidth of the system, that

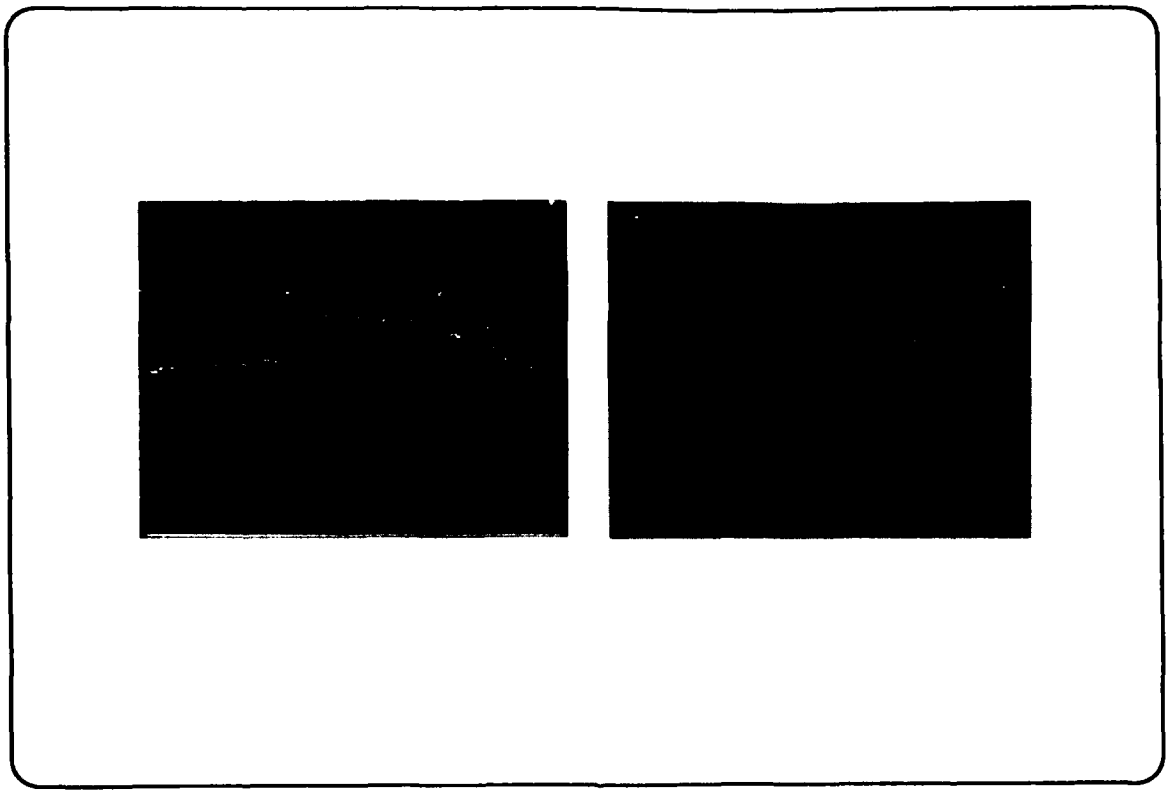

Figure 6.25 DEMODULATED OUTPUT AT 2.63GHz

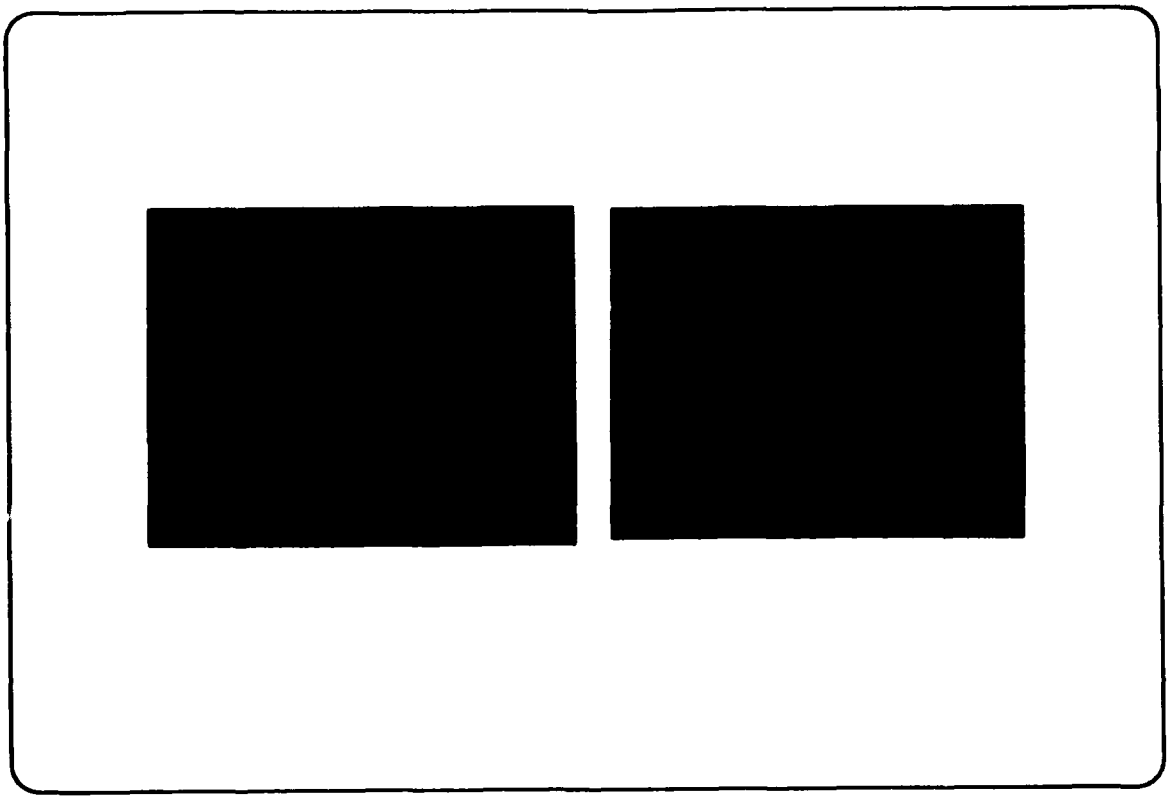

Figure 6.26 DEMODULATED OUTPUT AT 3GHz

corresponds to maximum demodulator linearity, should be used. The harmonic content of the demodulated output is shown in Figure 6.27 for a carrier frequency of 3 GHz. The second harmonic is 15 dB down on the signal.

6.3.4 System stability

The stabilty of the system was measured by observing the output of the system over a period of one hour. No long-term drift was observed, though short term amplitude fluctuations occurred. These amplitude fluctuations could be due to phase noise to amplitude noise conversion by the Fabry-Perot cavity formed within the phase modulator, or due to any mismatch in path length.

6.4 SUMMARY AND DISCUSSION

An analog transmission system using coherent optical techniques has been constructed and extensively characterised. Analog transmission using electrical FM, and optical phase modulation, has been demonstrated using a carrier frequency of 3 GHz, with a modulation bandwidth of ±100 MHz. A self-homodyne optical system was used to allow control of the effective linewidth of the laser source. The effective linewidth of the detected electrical signal was far less than the linewidth in heterodyne system using two lasers. This is because the phase noise of the modulated and unmodulated optical signals are partly correlated (if their relative delay is less than the coherence time of the laser source), and so phase noise cancellation occurs at the receiver. Reduction of effective detected linewidth according to equation 6.1 is achieved, i.e. for short delays, the effective linewidth is less than that of the laser source.

The self-homodyne technique for a coherent system allows assessment of the performance of an analog phase modulated link without the need for extensively engineered highly stabilised, narrow linewidth optical sources

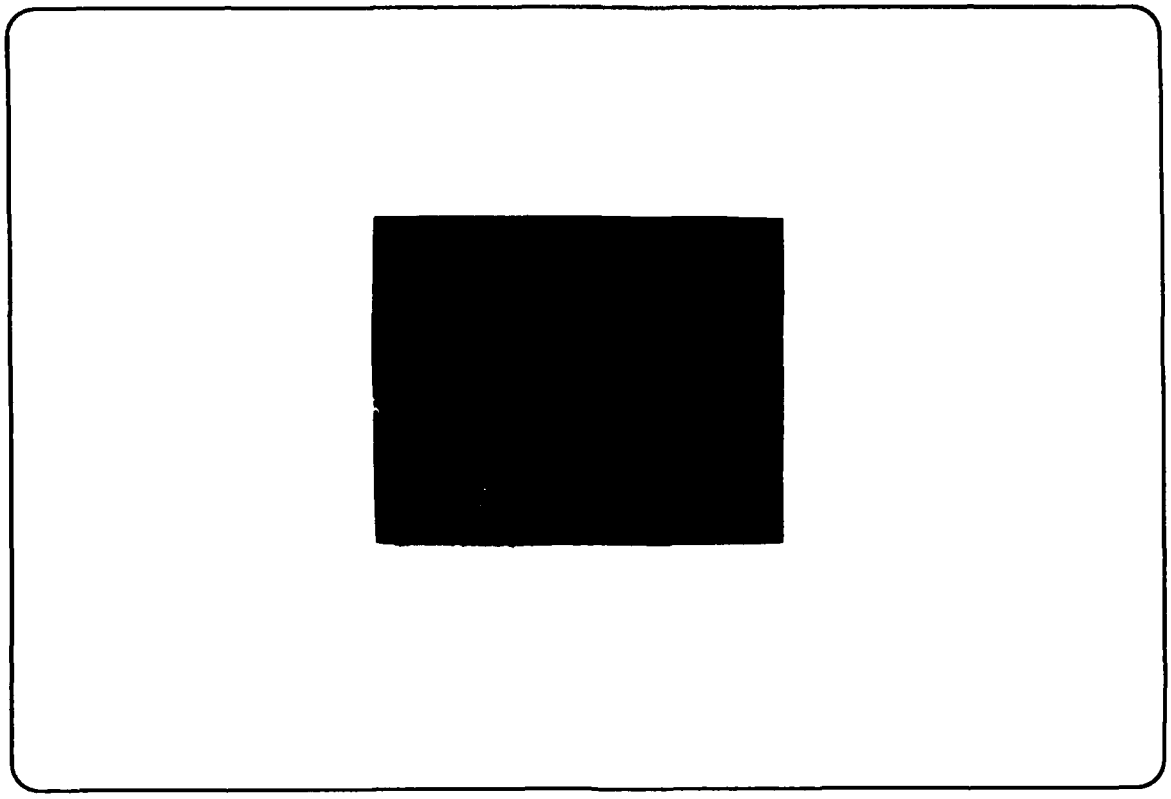

Figure 6.27 HARMONIC CONTENT OF DEMODULATED OUTPUT AT 3GHz

and control of optical frequency and phase. We have demonstrated that the effect of laser phase noise can be controlled and therefore minimised in such a system.

This technique would be useful if a full transmission system was set up. There it may be required to use a single optical fibre as the transmission medium. Extension of this system would then involve transmitting a pilot tone, i.e. an unmodulated optical signal, as well as the modulated signal. This would allow phase noise cancellation at the receiver.

Assessment of the system as a whole and as a complete system has allowed determination of those components that degrade the performance of the system significantly. Recommendations for improvements to these components or the problems they introduce are discussed below.

Comparison of the coherent detection link with an equivalent, in terms of signal power, direct detection link have indicated the advantages of coherent detection, particularly for weak optical signals. There is good agreement between experimental results and the theoretical predctions for CNR in the coherent analog link.

Various modifications could be made to the system as it now stands to improve its performance, particularly its linearity. The first of these would be to linearise the VCO tuning characteristic by use of a pre-amplifier with a suitable voltage shaping response. This would then produce an output frequency from the VCO that had a linear relationship to the tuning voltage.

The second improvement that could be made would be to improve the linearity of the demodulator. This could be acheived by using a stagger-tuned frequency discriminator. The greater number of design parameters in this approach would allow a more linear frequency response to be obtained.

Another improvement would be to provide a feedback loop to the phase modulator to ensure that the interferometer maintained the quadrature condition.

Another would be to use a band-pass filter, centred on 3 GHz, and with a bandwidth encompassing the bandwith of the detected signal. This would improve the carrier to noise ratios of the system.

A practical analog homodyne/heterodyne communication system using just a single fibre for transmission could be developed by transmitting a pilot tone for phase noise cancellation. What this would mean is that as well as the modulated optical signal, an unmodulated optical signal could also be sent along the same fibre to allow phase noise cancellation at the receiver.

REFERENCES

[1] G. Beheim: Electronic Letters, Jan. 1985, Vol. 21, No. 3.

7. CONCLUSIONS AND RECOMMENDATIONS

The studies and theoretical analysis of coherent fiber optic communication systems conducted within this programme has provided a comprehensive survey of the technical issues and systems options for this emerging transmission technology. These studies also led to the recommendations for the experimental models of digital and analog coherent systems to be constructed within this programme in order to adequately demonstrate the features and advantages of the technology.

A digital 140 Mb/s FSK system was successfully built and tested and achieved a performance close to that predicted. As implemented, this demonstrated a coherent detection sensitivity advantage of 7dB compared with direct detection. The-50.6dBm receiver sensitivity at 140Mb/s and a BER of 10^{-9} is approximately 8dB from the theoretical shot noise limit, which leaves scope for improvement. Specific recommendations for further work discussed in Section 5 are:

- Improved polarisation control. The existing implementation is manual polarisation control via a pair of electro-mechanical fibre squeezers. Two additional squeezer stages and microprocessor control could provide a fully automatic polarisation control system.

- The implementation of electrical equalisation of the transmitter laser FM response and biphase coding in order to eliminate dependence on data word pattern.

- Optimisation of filtering appropriate to the data rate.

Other possibilities which could yield improved sensitivity include higher specification lasers, in terms of narrower linewidth, flatter FM response and higher power, and the use of double sideband detection via a frequency discriminator in the data demodulation stage. The latter would also necessitate a wider bandwidth receiver front-end.

The benefits and desirability of the recommendations described above depend upon the future directions for coherent transmission envisaged by RADC. Whether for single channel or multichannel application within point-to-point or point-to-multipoint architectures high sensitivity is an important and desirable feature. In this context the points discussed above, for FSK systems, as well as the exploration of higher sensitivity techniques such as DPSK and CPFSK should be addressed. If the possibilities of multi-channel systems of potentialy huge capacity within LAN type networks are seen as important, then in addition another set of technical issues need to be addressed, which includes polarisation handling schemes, multichannel transmitter stabilisation, and modulation techniques for spectral efficiency. These are areas currently being explored in broad terms within telecommunications laboratories with the view to application of coherent multichannel techniques within future broadband subscriber networks.

For analog signal transmission a system was constructed which represented a valuable tool in assessing the performance of coherent detection analog links. The phase modulated system which was realised demonstrated a performance in close agreement with theoretical predictions which gave confidence in the theoretical framework and analysis established on this programme and confirmed the signal to noise ratio detection advantage of coherent detection in the weak signal case. However, as a general conclusion it was recognised that for very short transmission links where the received optical power is high coherent detection offers little, if

any, signal to noise ratio advantage compared with direct detection. This issue was discussed fully in Section 4.

The PM system configuration is not necessarily the most optimum from the point of view of linearity. Our studies suggest that optical FM is potentially the most attractive format in this respect, but component constraints mean that it is difficult to realise at the present time. This technique warrants more extensive consideration at an experimental level in order to determine the most optimum implementation. This includes assessment of direct FM modulation of the laser, the impact of non-uniform FM response and frequency discriminator non-linearities, and options for the use of external modulators. Within the analog system as it presently exists we would recommend some modifications in order to improve its linearity. These should focus on linearisation of the VCO tuning characteristics and improving the linearity of the frequency discriminator.

During the last year coherent detection techniques applied to the transmission of analog signals have started to receive significant attention as evidenced in the scientific literature. The main emphasis at present is in the transmission of electrical subcarrier multiplexed signals for CATV, where the receiver sensitivity is seen as offering advantages over direct detection. Nevertheless, useful lessons can be learned from this work. Most significant is the concept of transmitting a pilot carrier together with the signals which then acts as a phase reference to be used in laser phase noise cancellation. The concept is essentially the electrical domain equivalent of the technique implemented in the optical domain within the PM system constructed for this programme. This principle could be adopted in future systems work in order to reduce the stringent laser linewidth requirements for analog signal transmission.

8.0 APPENDICES

A. Technical Note: Self Heterodyne/Homodyne Analogue Link

B. Analysis of Effective Linewidths in Self-Homodyning Configuration

C. Publications

APPENDIX A

TECHNICAL NOTE

SELF HETERODYNE/HOMODYNE ANALOGUE LINK

CONTRACT: COHERENT FIBRE OPTIC LINKS

1 October 1987

BACKGROUND

The concept of a self-heterodyning and homodyning system configuration relates to the situation where the transmitter source and local oscillator source are derived from the same laser. The output from the laser is split into two, one part of which is modulated and subsequently recombined with the other part, representintg the local oscillator, at the receiver. The local oscillator 'source' can be frequency shifted using an acousto-optic modulator to represent a heterodyning configuration, or remain unshifted in frequency thus simulating a homodyning configuration. The advantage of this approach is that the need to deal with the laser stabilisation and receiver IF tracking issues is removed and system experiments can be performed more readily. Indeed these configurations were adopted in the early coherent optical communications experiments in order to demonstrate basic concepts, advantages and parameter dependencies before the laser source and control electronics development had reached the level to permit experiments with independent transmit and local oscillator lasers.

Other than the points made above a major advantage in adopting the self heterodyning or homodyning configuration for the analogue link is that it will permit the capability to control the effective linewidth of the laser source. This arises out of the ability to match the path lengths between the laser source and receiver for both the transmitter and local oscillator arms and thus correlate the combined signals. In this way laser phase noise levels can be partially cancelled thus reducing the effective IF spectral width. The worst case situation is clearly where the two arms are uncorrelated in which case the IF spectral width will be twice the source laser linewidth. The problem of the degree of phase noise reduction achievable by the technique of path length matching is one which we are not aware of having been addressed in the literature. Some analysis has been carried out to determine the linewidth reduction achievable in practice in order to assess the type of laser source necessary to implement a self heterodyne/homodyne analogue link.

Effective Laser Linewidth

Analysis of the laser phase noise statistics leads to a simple identity for the effective IF spectral width FIF. We find

$$FIF = FL \times TD \times B$$

where : FL = true linewidth of the laser source
TD = time delay between two signal arms
B = signal (receiver) bandwidth

The expression for FIF can be rewritten as:

$$FIF\ (Hz) = FL(Hz) \times DL(mm) \times B(GHz) \times 0.003$$

where : DL = path difference between signal arms

If we now make some reasonable assumptions for the magnitude of parameters in the equation we can assess the magnitude of FIF. We assume:

(1) A DFB laser with FL = 15 MHz
(2) B = 1 GHz, corresponding to transmission and full recovery of a signal on a 1 GHz carrier.

This result in,

$$FIF \doteq DL(mm) \times 45\ KHz$$

Based on these results we conclude that an effective linewidth of approximately 10 KHz should be achievable with a DFB laser as the primary source. This is very encouraging in that it permits a self heterodyning/homodyning configuration to yield results otherwise only achievable with sophisticated external cavity lasers.

System Configuration

Based on the results of the previous section it becomes clear that these magnitudes of effective laser linewidth permit an analogue link to be realised using a DFB semiconductor laser and which will demonstrate a good performance. We would recommend a self-homodyning phase modulation system. The self-heterodyning configuration requires a frequency shifting element and will be 3dB poorer in SNR than homodyning. The PM system offers good performance and is fairly straightforward to implement using an external lithium niobate phase modulator. The carrier frequency will be determined from the bandwidth of available phase modulators and receivers. The available low noise receivers would be marginal in bandwidth for a 1 GHz carrier so that the optimum approach would appear to be to use a detector and 50 ohm amplifier with a carrier frequency of approximately 2 GHz.

Path delay matching is an important aspect of this configuration and we propose to implement this by mounting fibre ends of the transmitter or local oscillator arm on adjustable micropositioning equipment with micron accuracy.

System Performance

The self-homodyning configuration should be regarded as a vehicle for demonstrating a coherent analogue link which will permit the investigation of performance as a function of receiver signal power, local oscillator power and laser linewidth. The performance should be compared with an intensity modulation/direct detection link for the same received optical power.

The actual performance which can be achieved with a PM self-homodyning link is highly dependent on the details of the implementation, e.g. received signal power, L.O. power, linewidth, signal bandwidth and receiver type.

What we will do here is give an indication of projected performance based on calculations assuming reasonable parameter values. We will give two examples.

Example 1

Assumptions:

- received signal power 1uW
- L.O. power 100uW
- signal carrier frequency of 2 GHz with full carrier recovery at receiver
- path matching DL = 0.1mm
- modulation index pi/2

Results:

Coherent SNR (phase noise floor) = 49dB
Coherent SNR (realisable) = 25dB
IM/DD SNR (realisable) = -6dB

Example 2

Assumptions:

- received signal power 10uW
- L.O. power 100uW
- other assumptions as above

Results:

Coherent SNR (phase noise floor) = 49dB)
Coherent SNR (realisable) = 35dB
IM/DD SNR (realisable) = 14dB

In neither case is the coherent SNR phase noise limited. The main limitation is due to the low L.O. power.

The results in the examples above give an indication of the SNR performance advantage which can be realised using a PM self-homodyne configuration.

Clearly these are example calculations which give a good idea of the relative coherent advantage, but further calculations based on the analysis of specific system design configuration would be necessary to quantify the performance more fully.

Merits of Self-Homodyne Approach

The self-homodyne approach for demonstrating an analogue coherent link has a number of interesting features and advantages compared with the use of independent transmit and L.O. lasers. This configuration allows a very narrow effective laser linewidth to be achieved and thus establish a link with a peformance which is not laser phase noise dominated. The real bonus in the approach is that this situation can be constructed using a standard DFB laser without an external cavity and the concomittant engineering and stability issues.

This link configuration permits the investigaton of the PM homodyne system performance as a function of received signal power, local oscillator power, and laser linewidth. In particular the range of laser linewidth accessible through adjusting the path differences is very large and probably represents a unique way of achieving such a broad linewidth range. This approach will therefore allow experiments to be made to compare results with the theoretical linewidth analysis carried out on this programme.

Thinking more broadly than the present programme, this configuration could also be a useful vehicle for investigating aspects of multichannel system

behaviour, without the need to address the problems of multitransmitter stabilisation. The laser transmitter output could be split and each component frequency shifted and independently modulated using integrated optic components. The channel frequency spacings would be well defined and stable having been derived from the same source and thus issues concerned with the detection and channel spacing in a multichannel coherent system could be investigated in a much more stable configuration. The spectral properties and hence channel spacing for such a configuration would be identical to the case of using independent transmitter lasers. Moreover, because of the significant technical difficulties in stabilising the channel spacing in an array of independent lasers, the approach of using a single source, perhaps with subsequent optical amplifiers, could represent a better technical approach for a multichannel transmitter configuration.

Our present assessment of this technical approach to the analogue link is that it falls within the scope of the engineering resource of the current programme. There could be a requirement to increase the materials allocation for this part of the programme dependent on the detailed technical approach, in particular with regard to the laser source, but in all events this would be fairly small.

B T Debney
1/10/87

APPENDIX B

ANALYSIS OF EFFECTIVE LASER LINEWIDTH IN SELF-HOMODYNING CONFIGURATION

Laser phase noise can be characterised in terms of a probability density function (pdf) for the phase fluctuations $\Delta\phi$. This generally takes the form of a gaussian function with the result that the pdf for the phase fluctuations in the signal spectrum of a heterodyning/homodyning system using two uncorrelated laser sources takes the form

$$P(\Delta\phi) = \frac{1}{\sqrt{4\pi^2\Delta\nu_s\tau}} \exp\left(-\frac{\Delta\phi^2}{4\pi\Delta\nu_s\tau}\right) \qquad (1)$$

In this expression $\Delta\nu_s$ represent the sum of the linewidth of transmitter and local oscillator lasers, and τ is the characteristics measurement time over which the phase fluctuations are measured.

A similar approach can be taken to characterising the phase noise in a self-homodyne configuration. In this case the two 'sources' are correlated, the extent of which depends on the relative time delay spitting and recombining. Because the 'sources' are correlated the maximum time over which phase fluctuations can occur is the delay time τ_D. The probability density function therefore takes the form,

$$P(\Delta\phi) = \frac{1}{\sqrt{4\pi^2\Delta\nu\tau_D}} \exp\left(-\frac{\Delta\phi^2}{4\pi\Delta\nu\tau_D}\right) \qquad (2)$$

In this case $\Delta\nu$ is the true linewidth of the single laser source, since the phase fluctuations are acquired by one effective laser source relative to the other over the delay period.

From the receiver point of view it will observe phase noise which is attributable to effective transmitter and local oscillator laser sources, which can be represented via $\Delta\nu_s^{eff}$. The effective laser linewidth in the self-homodyne configuration can be determined from the equivalence between

the descriptions in equations 1 and 2. Therefore we find,

$$\Delta\nu_s{}^{eff}\tau \equiv \Delta\nu\tau_D$$

The characteristic measurement time τ is related to the receiver bandwidth, R_B, and so we can write,

$$\tau = 1/R_B$$

Therefore,

$$\Delta\nu_s{}^{eff} = \Delta\nu\tau_D R_B$$

Alternatively, expressing τ_D in terms of the equivalent path delay ΔL, we find

$$\Delta\nu_s{}^{eff} = \frac{\Delta L}{C_m} R_B \Delta\nu$$

where C_m is the velocity of light in the appropriate medium.

APPENDIX C:

PUBLICATIONS

The following publications have to date arisen from this programme. Copies are attached.

B Chen and B Debney
'Design considerations for a 140 Mb/s FSK heterodyne communication system', SPIE Vol. 841, Fiber Optic Networks & Coherent Technology in Fiber Optic Systems II, San Diego, 1987.

B Debney and J Metcalfe
'Coherent analog fiber optic links',
SPIE, Boston, 1988.

J Hankey, C Park, N Wood, B Debney and B Chen
'An engineered rack mounted coherent transmission system',
SPIE, Coherent Lightwave Communications, Boston, 1989 (accepted).

MISSION
of
Rome Air Development Center

RADC plans and executes research, development, test and selected acquisition programs in support of Command, Control, Communications and Intelligence (C^3I) activities. Technical and engineering support within areas of competence is provided to ESD Program Offices (POs) and other ESD elements to perform effective acquisition of C^3I systems. The areas of technical competence include communications, command and control, battle management information processing, surveillance sensors, intelligence data collection and handling, solid state sciences, electromagnetics, and propagation, and electronic reliability/maintainability and compatibility.